社会人教育プログラム：第２回共通特別講義
［日時］2月7日（金）　19:30～21:00
大阪大学・文理融合型研究棟セミナー室（オンライン）

カーボンニュートラル・水素社会に貢献する材料の創出

近藤 剛弘

筑波大学 数理物質系物質工学域
筑波大学 数理物質系エネルギー物質科学研究センター
筑波大学ゼロCO_2エミッション機能性材料開発研究センター
東北大学材料科学高等研究所

Acknowledgements

Univ. Tsukuba : Mr. H. Nishino
Univ. Tsukuba : Mr. T. Fujimori
Univ. Tsukuba : Mr. A. Fujino
Univ. Tsukuba : Mr. R. Ishibiki
Univ. Tsukuba : Mr. T. Goto
Univ. Tsukuba : Ms. Linghui Li
Univ. Tsukuba : Mr. R. Kawamura
Univ. Tsukuba : Mr. H. Kusaka
Univ. Tsukuba : Mr. K. Goto
Univ. Tsukuba : Ms. H. Yoshioka
Univ. Tsukuba : Mr. N. Watanabe
Univ. Tsukuba : Ms. N. Noguchi
Univ. Tsukuba : Dr. S. L. Shinde
Univ. Tsukuba : Ms. M. Hikichi
Univ. Tsukuba : Dr. S. Ito
Univ. Tsukuba : Prof. J. Nakamura
Univ. Tsukuba : Prof. E. Nishibori
Univ. Tsukuba : Prof. T. Sakurai
Univ. Tsukuba : Prof. S. Okada
Univ. Tsukuba : Prof. M. Otani
Univ. Tsukuba : Dr. S. Hagiwara
TUAT. : Prof. A. Yamamoto
Nagoya Univ. : Dr. T. Tokunaga
Tohoku Univ. : Prof. T. Fujita
Tohoku Univ. : Prof. A. Hirata
Tohoku Univ. : Prof. S. Orimo

NIMS : Dr. T. Taniguch
NIMS : Dr. M. Miyakawa
NIMS : Dr. K. Watanabe
NIMS : Dr. S. Tominaka
NIMS : Dr. N. T. Cuong
NIMS : Dr. N. Umezawa
NIMS : Dr. T. Masuda
NIMS : Dr. T. Mori
NIMS : Dr. T. Aizawa
AIST : Dr. T. Fujitani
Osaka Univ. : Prof. I. Hamada
CSIC : Dr. Josep M Oliva-Enrich
Tokyo Univ. : Prof. I. Matsuda
KEK : Dr. K. Horiba
Tokyo Tech. : Mr. R. Kawamura
Tokyo Tech. : Mr. T. Hirabayashi
Tokyo Tech. : Ms. C. Shimada
Tokyo Tech. : Mr. K. Miyazaki
Tokyo Tech. : Dr. Y. Fujimoto
Tokyo Tech. : Dr. S. Iimura
Tokyo Tech. : Dr. A. Yamaguchi
Tokyo Tech. : Prof. M. Toyoda
Tokyo Tech. : Prof. J. Nomura
Tokyo Tech. : Prof. S. Saito
Tokyo Tech. : Prof. M. Miyauchi
Tokyo Tech. : Prof. H. Hosono

Kondo Laboratory Member

Fundings

This work was supported by the JST-PRESTO. TIES, KAKENHI (Grant-in-Aid for Scientific Research (S, A, B), Challenging Research (Pioneering), Science of Atomic Layers (SATL), Hydrogeno- mics, Murata-fund, Samuko-fund, Ogasawara-fund, and Kumagai-fund, amd MHI Innovation Accelerator LLC, NEDO, JST(CREST)

Outline

1. 自己紹介

2. カーボンニュートラルの必要性と材料開発の重要性

3. 水素製造に貢献する材料開発
典型元素を利用した高活性アルカリ水電解触媒

(1) 硫化ホウ素(r-BS)の合成と評価

(2) r-BSとグラフェンの混合物が示す
高いOER触媒特性

(3) r-BSの活性点（MoS_2のHER活性点との比較）

(4) r-BS＋グラフェンOER触媒の高耐久性化

4. 水素利用に貢献する材料開発

5. 水素吸蔵に貢献する材料開発

自己紹介（略歴）

近藤剛弘（こんどう たかひろ）
1976年9月に東京で生まれる（48歳）：

1999年3月　筑波大学第三学群基礎工学類 卒業
2003年3月　筑波大学大学院 工学研究科博士課程 物理工学専攻
博士（工学）取得
博士論文：超音速分子線技術を用いた表面化学反応の制御に関する研究
指導教官：山本恵彦教授
2003年4月　独）理化学研究所 中央研究所 基礎科学特別研究員
（川合眞紀主任研究員:川合表面科学研究室）
2006年4月　独）理化学研究所 川合表面化学研究室 協力研究員
（川合眞紀主任研究員:川合表面科学研究室）
2007年4月　筑波大学（テニュアトラック助教）
（中村潤児教授：中村研究室）
2011年10月　筑波大学 数理物質系 物質工学域 講師
（中村潤児教授：中村研究室）
2015年1月　筑波大学 数理物質系 物質工学域 准教授
（中村潤児教授：中村・近藤研究室 3年間）
2018年4月より独立研究室運営：触媒表面化学グループ 近藤研究室
2022年4月　筑波大学 ゼロCO_2エミッション機能性材料開発研究センター
センター長（兼任）
2022年12月　筑波大学 数理物質系 物質工学域 教授（現在に至る）

Outline

1. 自己紹介

2. カーボンニュートラルの必要性と材料開発の重要性

3. 水素製造に貢献する材料開発
典型元素を利用した高活性アルカリ水電解触媒

(1) 硫化ホウ素(r-BS)の合成と評価

(2) r-BSとグラフェンの混合物が示す
高いOER触媒特性

(3) r-BSの活性点（MoS_2のHER活性点との比較）

(4) r-BS＋グラフェンOER触媒の高耐久性化

4. 水素利用に貢献する材料開発

5. 水素吸蔵に貢献する材料開発

カーボンニュートラルの必要性

IOP Publishing Environ. Res. Lett. 16 (2021) 114005 https://doi.org/10.1088/1748-9326/ac2966

ENVIRONMENTAL RESEARCH
LETTERS

コーネル大学の研究者による88125件の査読付き論文の精査：
人間が引き起こした現代の気候変動に関する科学的コンセンサスは査読済学術論文の 99% を超えていると結論

CrossMark

OPEN ACCESS

RECEIVED
7 June 2021

REVISED
21 September 2021

ACCEPTED FOR PUBLICATION
23 September 2021

PUBLISHED
19 October 2021

LETTER

Greater than 99% consensus on human caused climate change in the peer-reviewed scientific literature

Mark Lynas[1,*], Benjamin Z Houlton[2] and Simon Perry[3]

[1] Visiting Fellow, Cornell University, Global Development, Alliance for Science, B75 Mann Library, Ithaca, NY 14850, United States of America
[2] Cornell University, Department of Ecology and Evolutionary Biology and Department of Global Development, Cornell University, Ithaca, NY 14850, United States of America
[3] Alliance for Science, Ithaca, NY 14850, United States of America
[*] Author to whom any correspondence should be addressed.

E-mail: ml866@cornell.edu

Keywords: global warming, climate change, scientific consensus

Supplementary material for this article is available online

Abstract

While controls over the Earth's climate system have undergone rigorous hypothesis-testing since the 1800s, questions over the scientific consensus of the role of human activities in modern climate change continue to arise in public settings. We update previous efforts to quantify the scientific consensus on climate change by searching the recent literature for papers sceptical of anthropogenic-caused global warming. From a dataset of 88125 climate-related papers published since 2012, when this question was last addressed comprehensively, we examine a randomized subset of 3000 such publications. We also use a second sample-weighted approach that was specifically biased with keywords to help identify any sceptical peer-reviewed papers in the whole dataset. We identify four sceptical papers out of the sub-set of 3000, as evidenced by abstracts that were rated as implicitly or explicitly sceptical of human-caused global warming. In our sample utilizing pre-identified sceptical keywords we found 28 papers that were implicitly or explicitly sceptical. We conclude with high statistical confidence that the scientific consensus on human-caused contemporary climate change—expressed as a proportion of the total publications—exceeds 99% in the peer reviewed scientific literature.

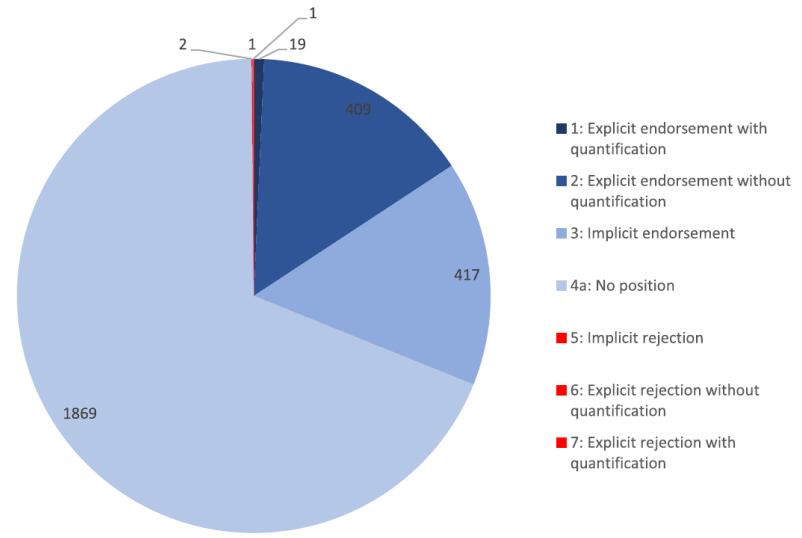

Figure 1. Ratings and categorizations given to 2718 randomly-sampled climate abstracts.

1951 年から 1980 年までの長期平均と比較した地球表面温度の変化

Global Temperature

LATEST ANNUAL AVERAGE ANOMALY: 2023

1.17 °C | 2.11 °F

Download Data

地球の気温の長期記録が「地球温暖化」を示している

GLOBAL LAND-OCEAN TEMPERATURE INDEX

Data source: NASA's Goddard Institute for Space Studies (GISS). Credit: NASA/GISS

https://climate.nasa.gov/vital-signs/global-temperature/?intent=121

source: NASA/GISS

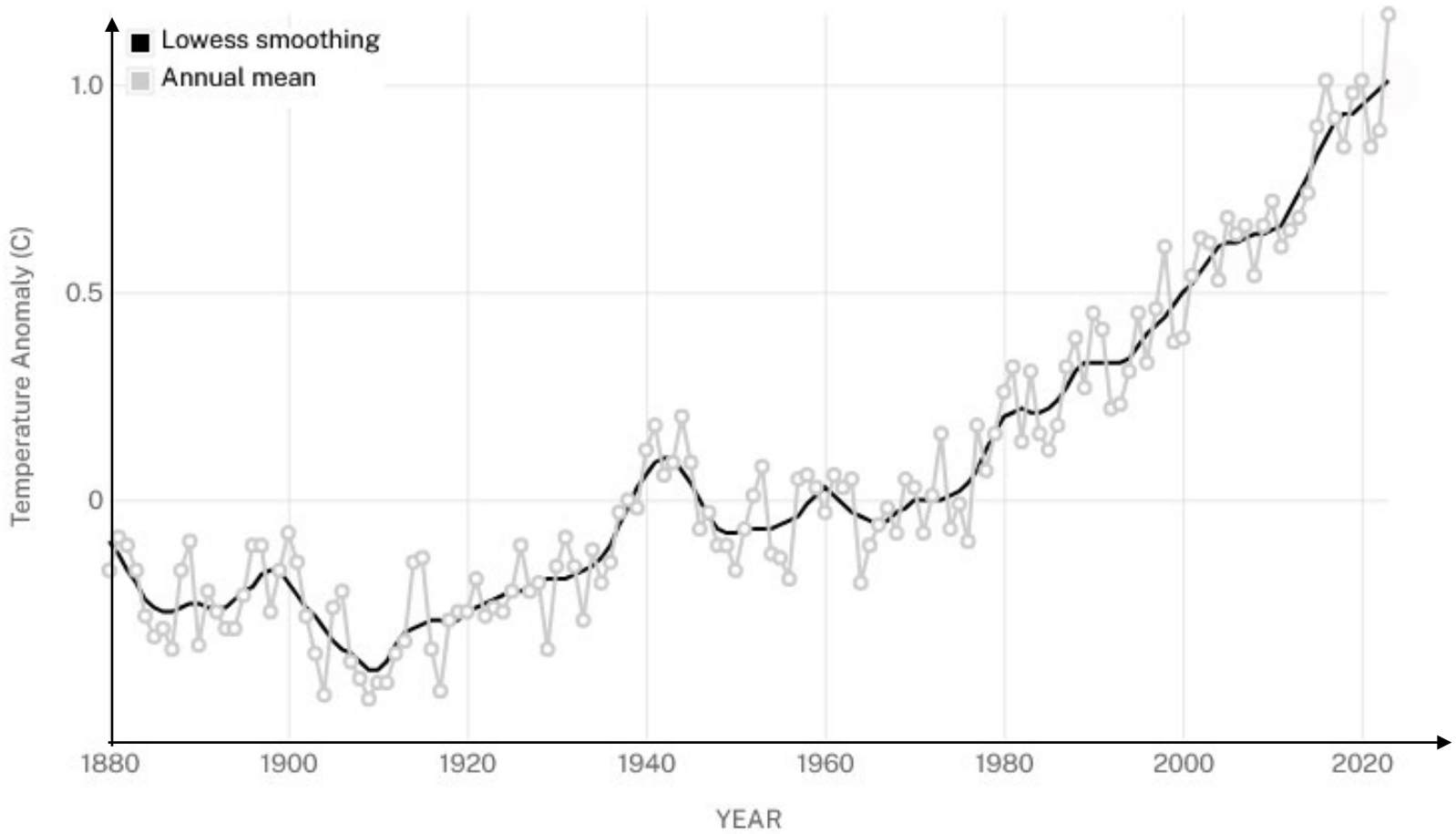

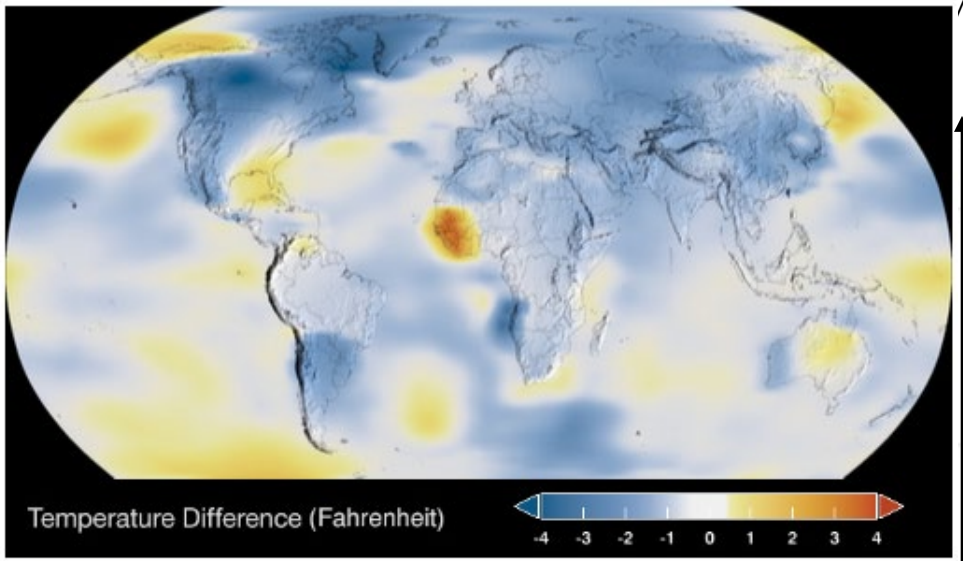

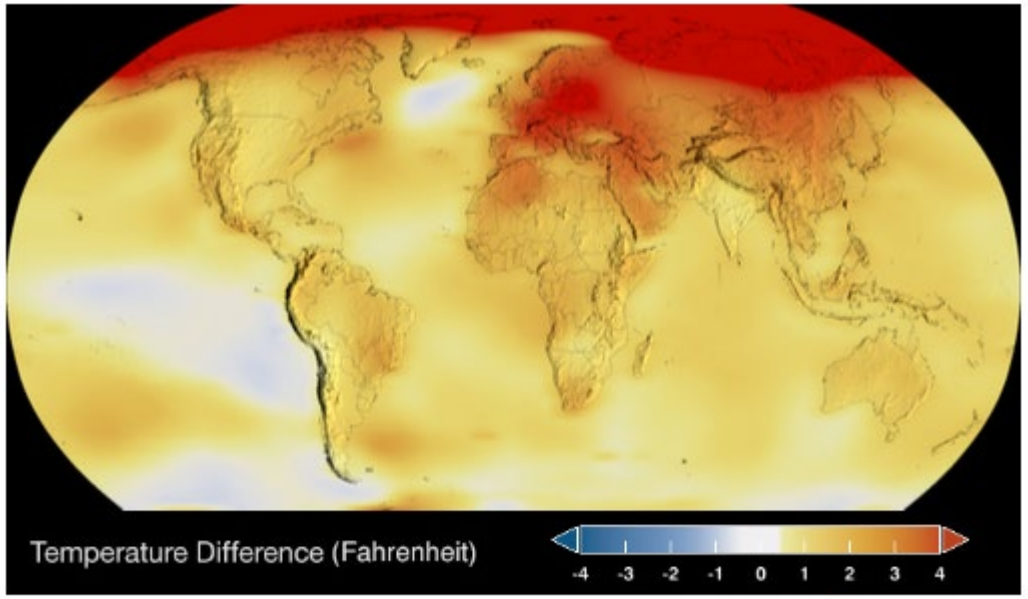

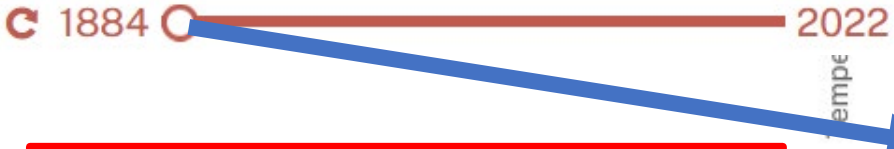

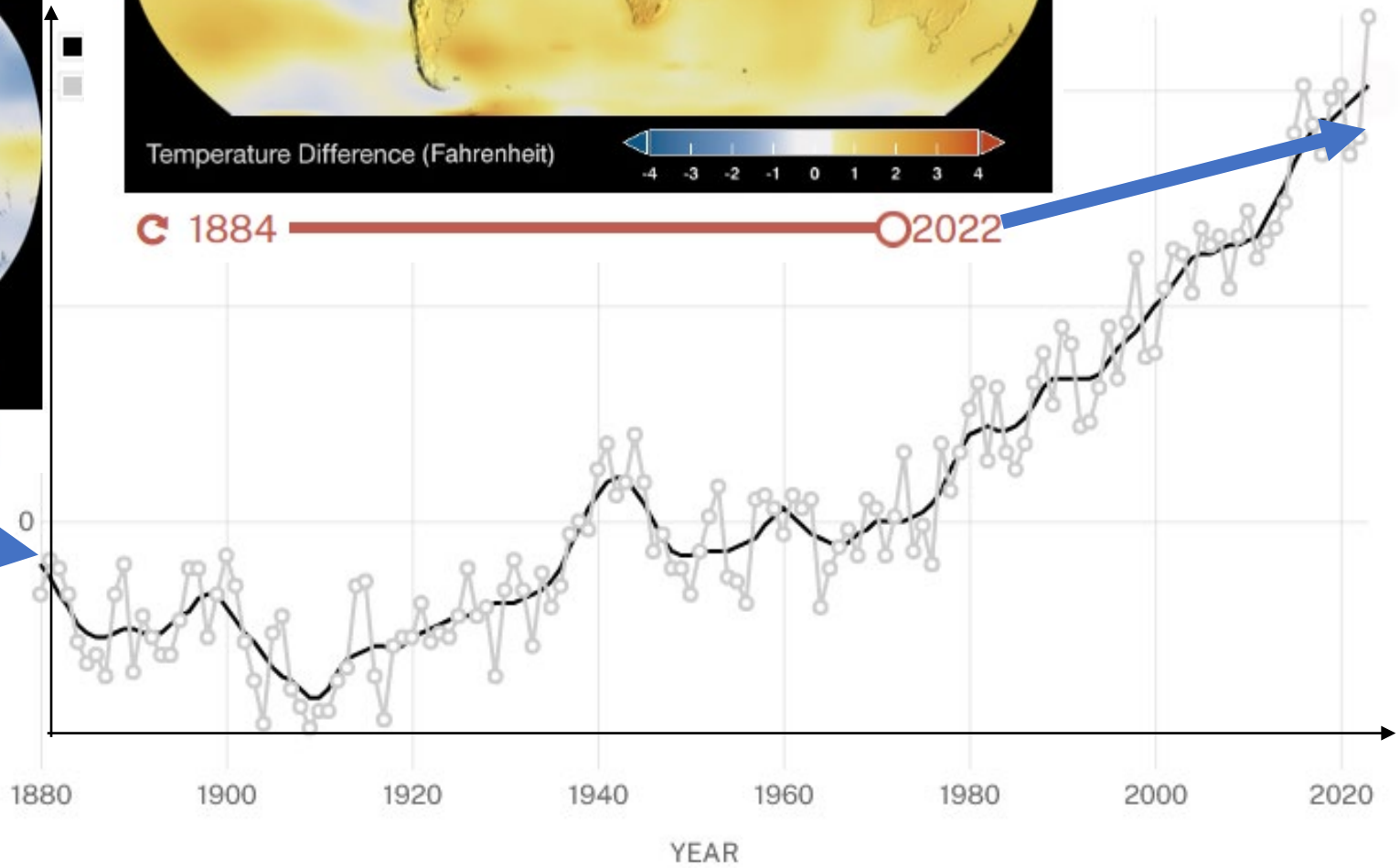

地球の気温の長期記録が
「地球温暖化」を示している

CO_2 levels measured by NOAA at Mauna Loa Observatory, Hawaii
https://climate.nasa.gov/vital-signs/carbon-dioxide/?intent=121

Carbon Dioxide

LATEST MEASUREMENT: July 2024

426 ppm

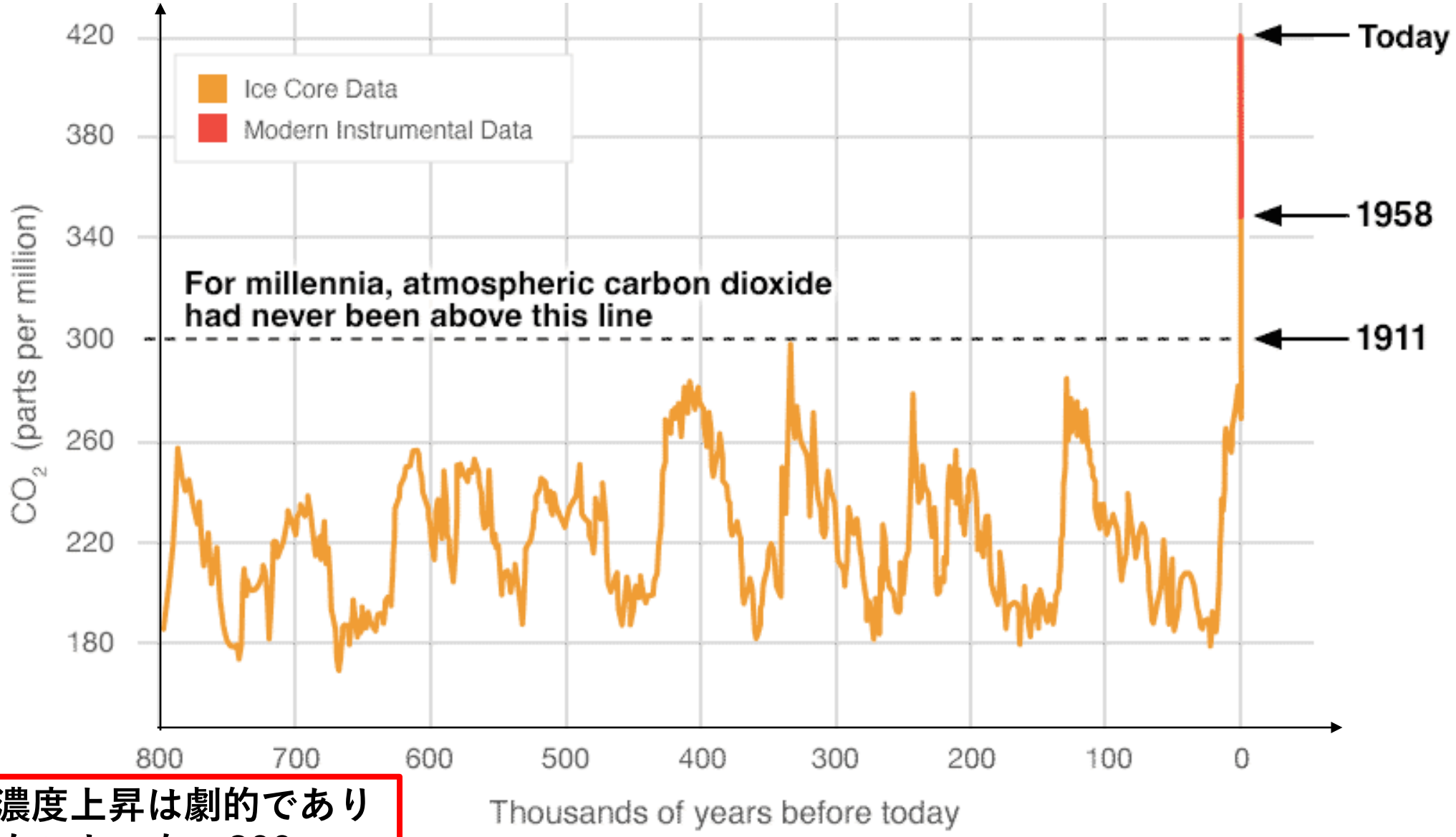

この100年のCO_2濃度上昇は劇的であり過去800年で超えたことのない300ppmを超えて40%増の426 ppm

Carbon Dioxide

LATEST MEASUREMENT: July 2024

426 ppm

CO_2 levels measured by NOAA at Mauna Loa Observatory, Hawaii

https://climate.nasa.gov/vital-signs/carbon-dioxide/?intent=121

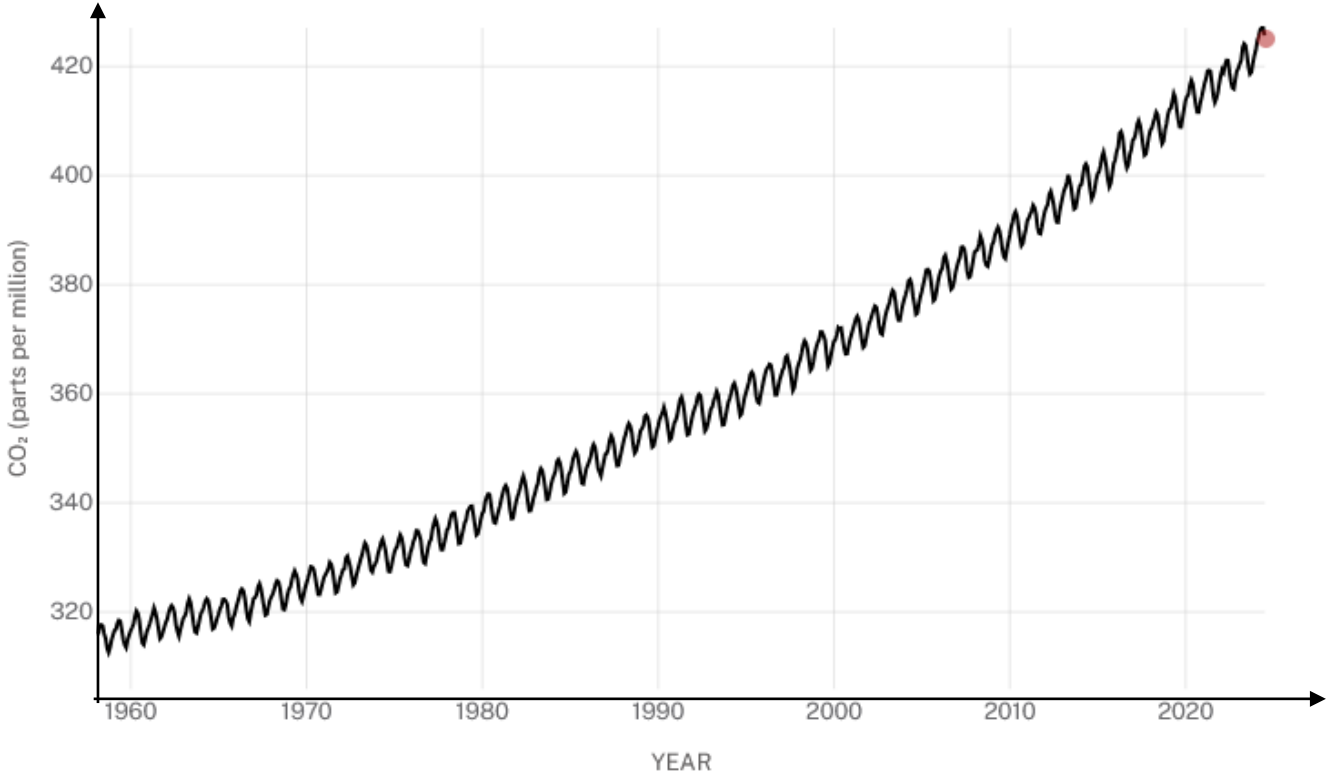

大気中の二酸化炭素含有量が単調に増加し続けている

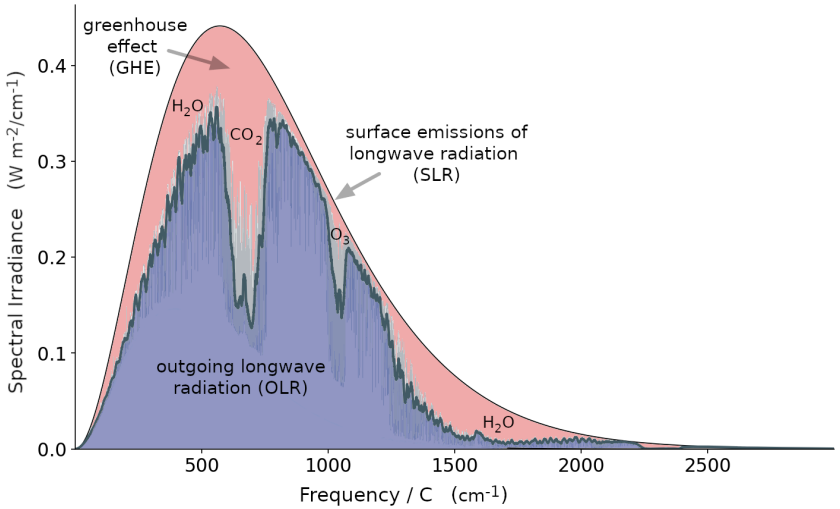

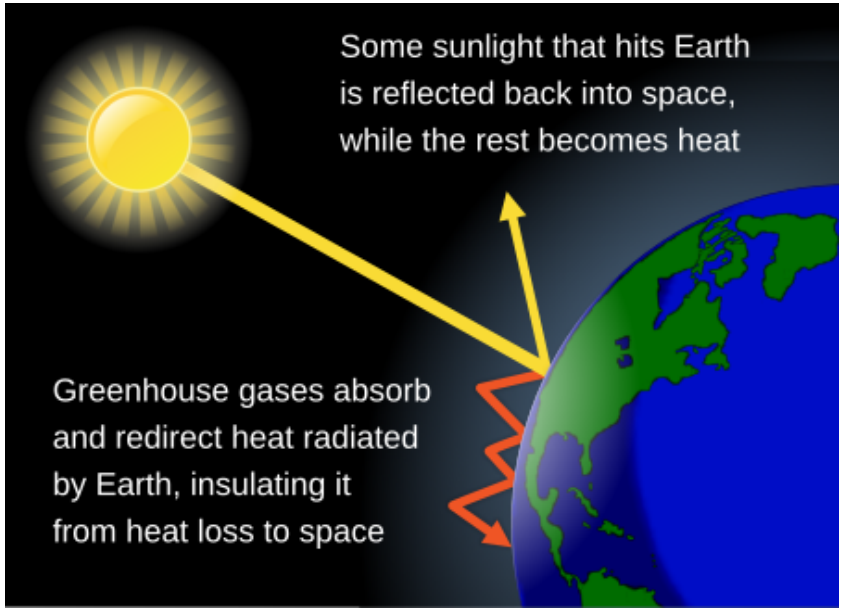

https://en.wikipedia.org/wiki/Greenhouse_effect

二酸化炭素は温室効果ガスと呼ばれるガスであり
地表からの熱放出が大気中で吸収されてしまい放出され
なくなってしまうことで温暖化の原因となっている

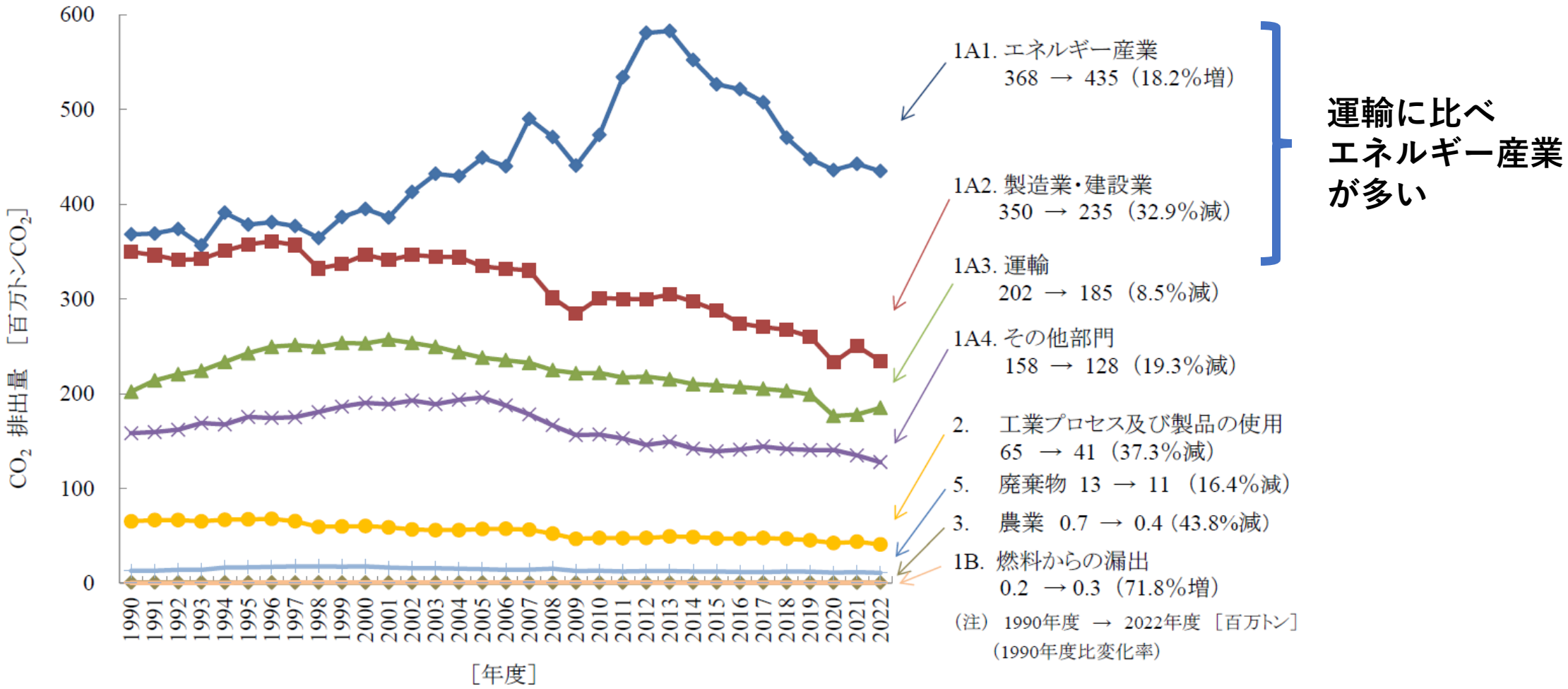

図 2-3　各部門の CO_2 排出量の推移

（注）括弧内の数値は 1990 年度比

日本国温室効果ガスインベントリ報告書（国立研究開発法人国立環境研究所2024年4月版）より

カーボンニュートラルが求められている

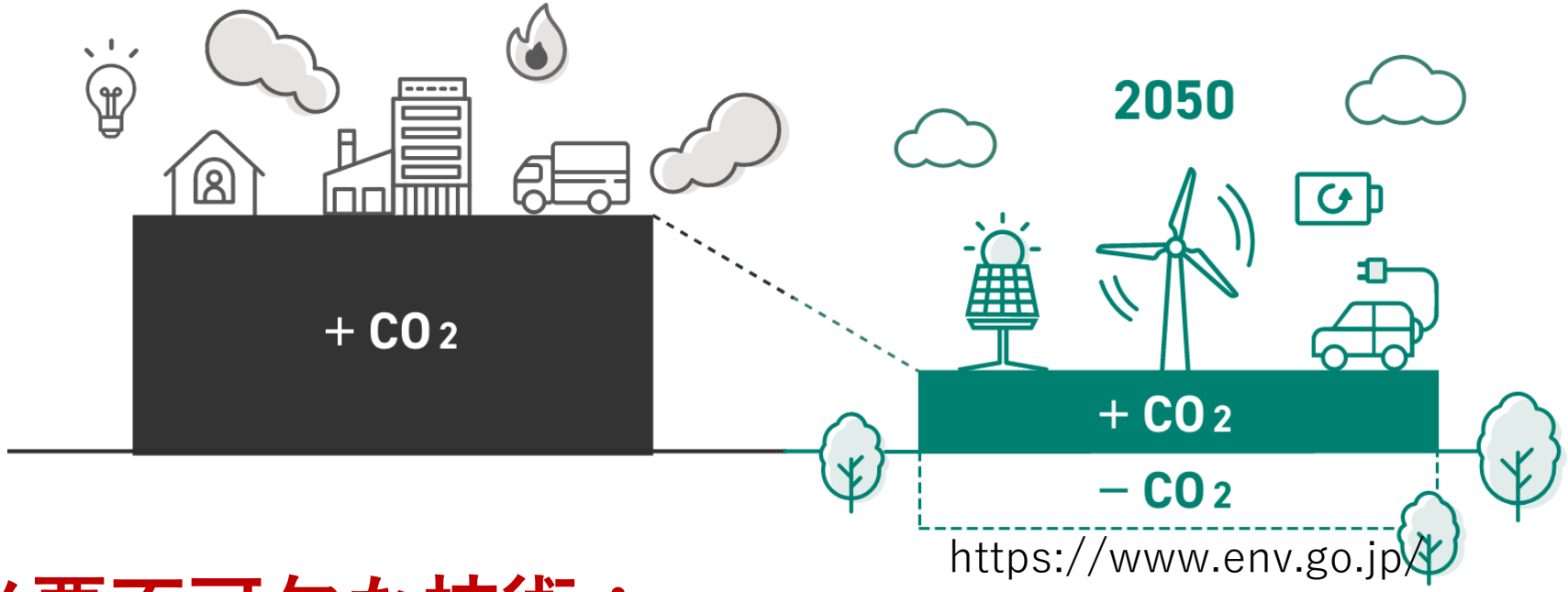

https://www.env.go.jp/

必要不可欠な技術：

(1) 水素(H_2)を燃料として利活用する技術

$2H_2 + O_2 \rightarrow 2H_2O$ ：この時に発電　(発電時にzero CO_2)

(2) 二酸化炭素（CO_2）を有用な物質に変換する技術

$CO_2 + 3H_2 \rightarrow CH_3OH + H_2O$　(- CO_2)

Grey hydrogen

Source: Natural gas
Process: steam reforming

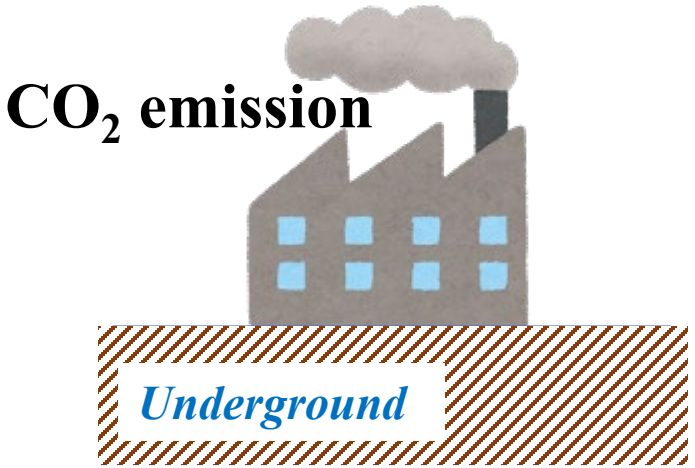

Blue hydrogen

Source: Natural gas
Process: steam reforming with carbon capture

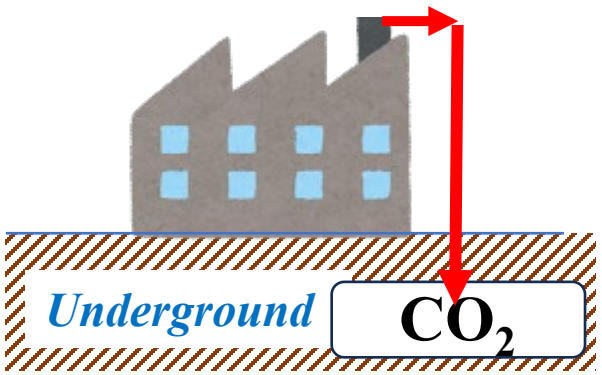

Green hydrogen

Source: Electrolysis
Process: Renewable energies

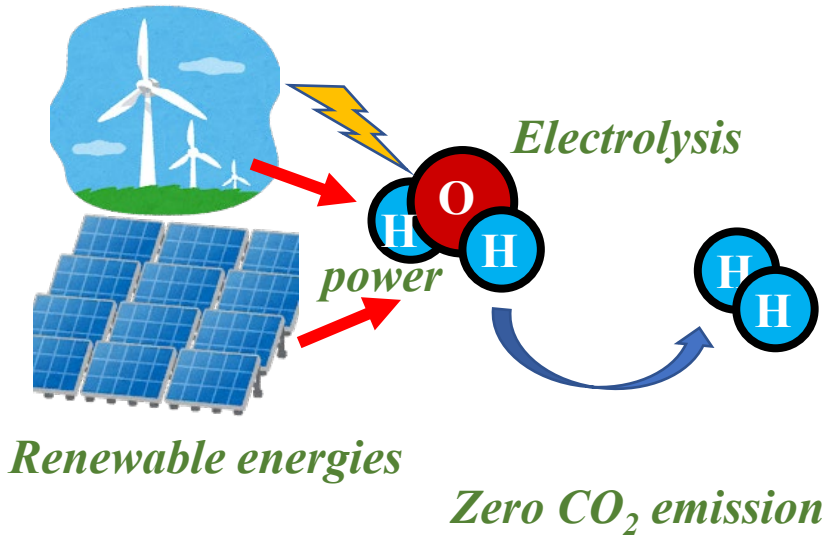

水素の利活用全体においてCO_2を出さないことが重要

ENERGY earthshots
U.S. DEPARTMENT OF ENERGY

Hydrogen

1 Dollar

1 Kilogram

1 Decade

https://www.energy.gov/eere/fuelcells/hydrogen-shot

米国エネルギー省は10年で1kgの水素を1ドルにする
１，１，１政策を開始

水素(H_2)を燃料として利活用する技術

$2H_2 + O_2 \rightarrow 2H_2O$ ：この時に発電　(発電時にzero CO_2)

水素社会のイメージ

現状の課題

水素を作る

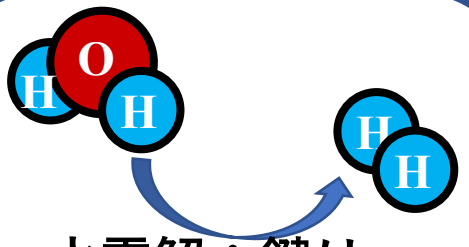

水電解：鍵は
電極触媒材料
現行の貴金属触媒は
高価で埋蔵量が少ない

水素をためる

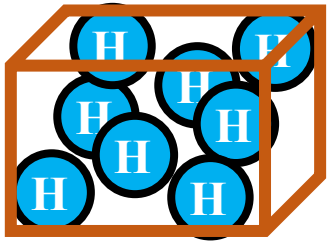

水素貯蔵材料が鍵
安価で安全に高密度の
貯蔵ができる材料が必要

水素を使う

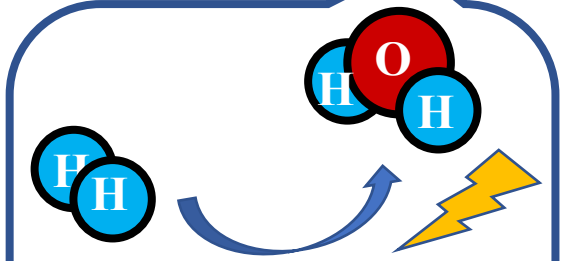

燃料電池：鍵は
電極触媒材料
現行の貴金属触媒は
高価で埋蔵量が少ない

鍵は材料開発！

水素社会のイメージ

水素を作る

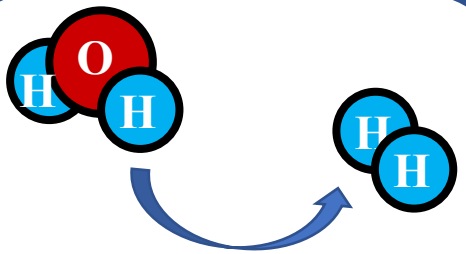

水電解：鍵は
電極触媒材料

現行の貴金属触媒は
高価で埋蔵量が少ない

水素をためる・運ぶ

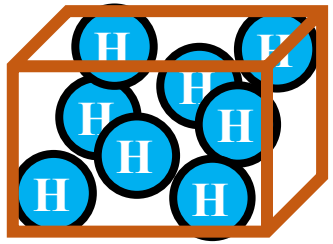

水素貯蔵材料が鍵

安価で安全に高密度の
貯蔵ができる材料が必要

水素を使う

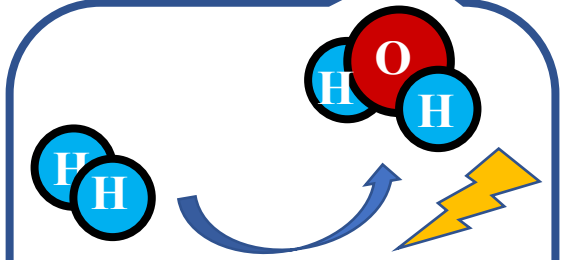

燃料電池：鍵は
電極触媒材料

現行の貴金属触媒は
高価で埋蔵量が少ない

現状の課題

我々の研究成果

新しい触媒材料の
硫化ホウ素を開発
（非金属世界最高活性！）

- *J. Mate. Chem. A (2021)*
- *Nano Letters (2023)*
- *Chem. Eng. J. (2023)*
- *ACS Appl. Mater. Int. (2023)*
- *Sci. Tech. Adv. Mate. (2023)*
- *Sci. Rep. (2023)*

新しい水素含有物質
のホウ化水素シート
を世界で初めて合成

- *J. Am. Chem. Soc. (2017)*
- *Nature Commun. (2019)*
- *Chem (2020)*
- *Commun. Mate. (2021)*
- *Commun. Chem. (2022)*
- *Adv. Mate. Int. (2023)*
- *Small (2024), Adv. Sci (2024), Small (2024)*

貴金属触媒に代わる
最有力候補の窒素
ドープ炭素の活性点
を世界で初めて解明

- *Science (2016)*
  (4009 citations)
- *ChemSusChem (2018)*

SDGs
に貢献！

Outline

1. 自己紹介

2. カーボンニュートラルの必要性と材料開発の重要性

3. 水素製造に貢献する材料開発
典型元素を利用した高活性アルカリ水電解触媒

(1) 硫化ホウ素(r-BS)の合成と評価

(2) r-BSとグラフェンの混合物が示す
高いOER触媒特性

(3) r-BSの活性点（MoS_2のHER活性点との比較）

(4) r-BS＋グラフェンOER触媒の高耐久性化

4. 水素利用に貢献する材料開発

5. 水素吸蔵に貢献する材料開発

菱面体硫化ホウ素の背景

r-BS：菱面体硫化ホウ素

Rhombohedral boron monosulfide

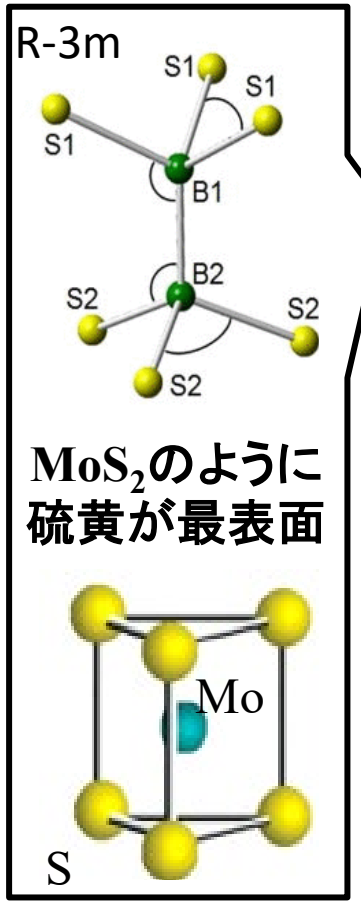

MoS_2のように硫黄が最表面

高温高圧条件で合成

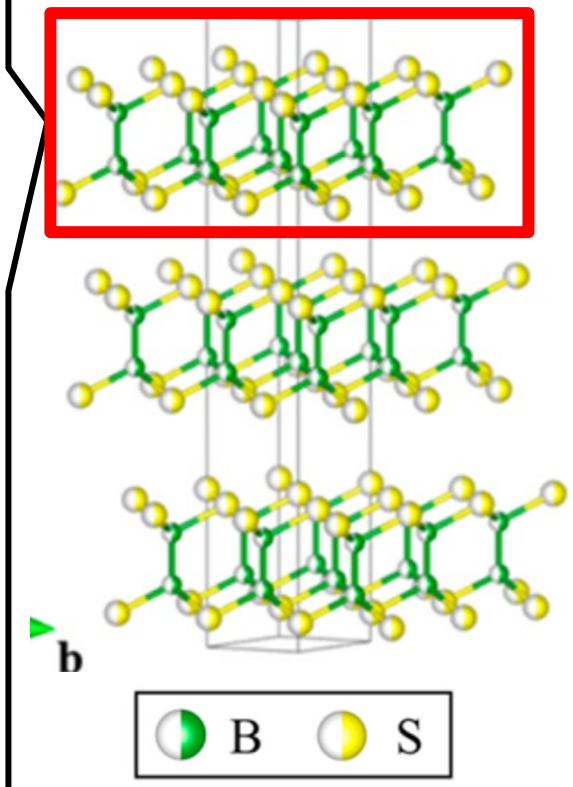

実験では2グループが報告
Phys. Stat. Sol. 223, 29 (2001).
J. Appl. Phys. 117, 185904 (2015).

硫化ホウ素ナノシートの理論予測

- 4種類の安定な結晶構造が理論予測
  (Appl. Phys. Lett. 117, 013103 (2020) .)

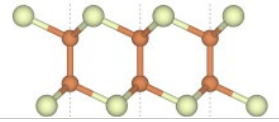

- 優れた熱電特性 ZT ≒ 1 が理論予測
  (Sustain. Energy Fuels, 4, 2363 (2020).)

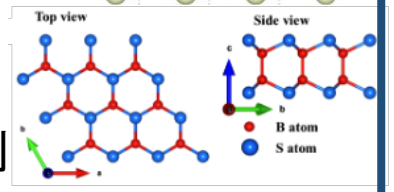

- 水素吸蔵材料としての可能性が理論予測
  (J. Appl. Phys. 127, 184305 (2020).)
- 超伝導(Tc : 約22 K)が理論予測
  (Appl. Phys. Lett. 117, 013103 (2020))

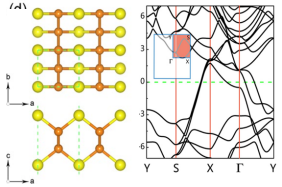

- SiCとBSの組み合わせ
  → 優れた水分解に対する光触媒特性
  (Phys. Lett. A, 410, 127514 (2021).)

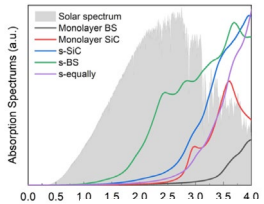

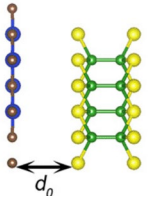

- MoS_2とBSの組み合わせ
  → スピン操作が可能
  (J. Mate. Chem. C. 10, 312 (2022).)

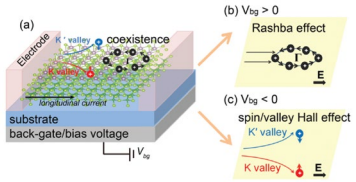

我々は層状物質 r-BSを劈開することで
BSシートの生成に成功した（2021）

Methods

By Prof. Yamamoto in Tokyo Agriculture and technology

With NIMS Dr. Miyakawa and Dr. Taniguchi

- Amorphous boron 99.9% (B_2H_6 decomposition)
- Sulfur 99%, Wako

➢ **B:S = 1 : 1 powder was mixed**
➢ **Pellet was sealed in capsule**
➢ **High pressure and high temperature**

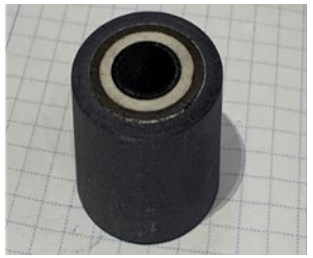

Temperature Program

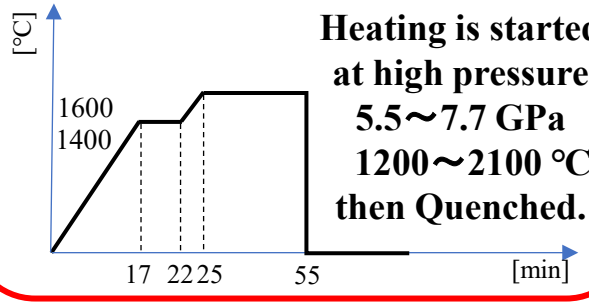

Heating is started at high pressure 5.5～7.7 GPa 1200～2100 °C then Quenched.

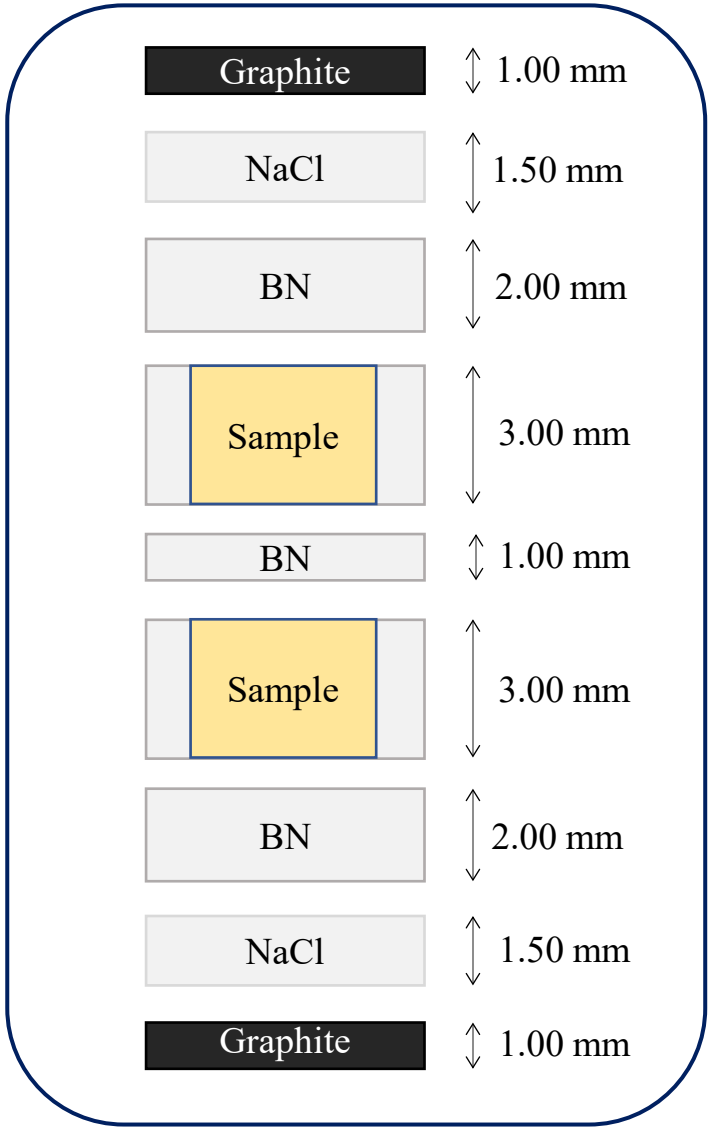

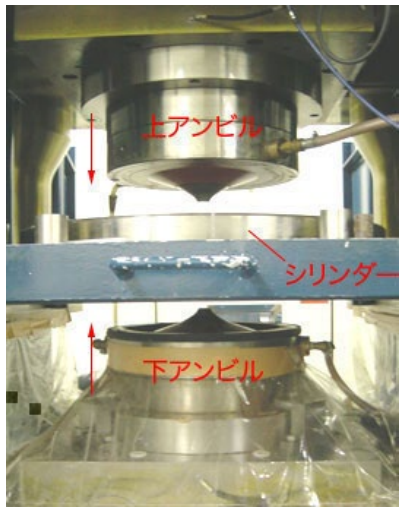

石引くん
(2020 卒)

日下くん
(2022卒)

As synthesized (capsule)

r-BS

BN wall

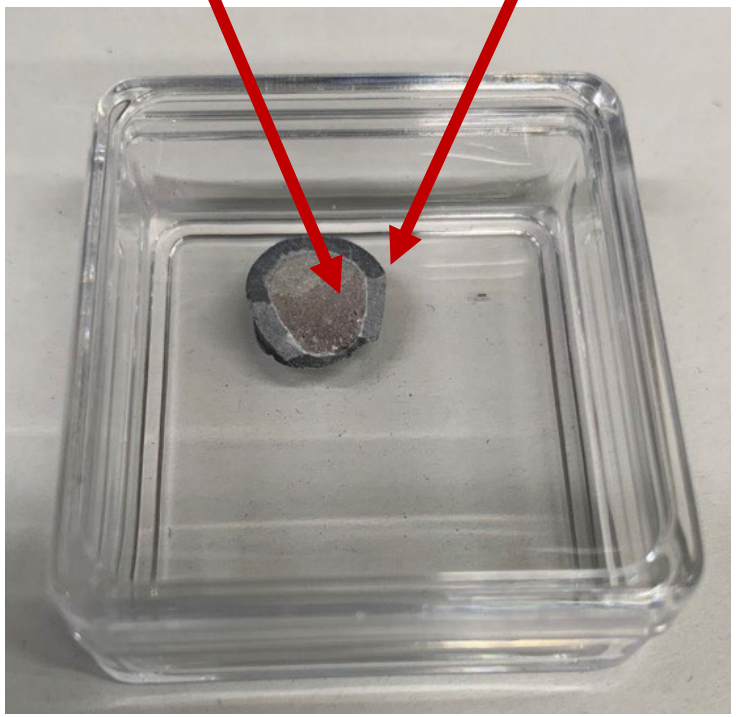

Scanning electron microscopy (SEM) of r-BS

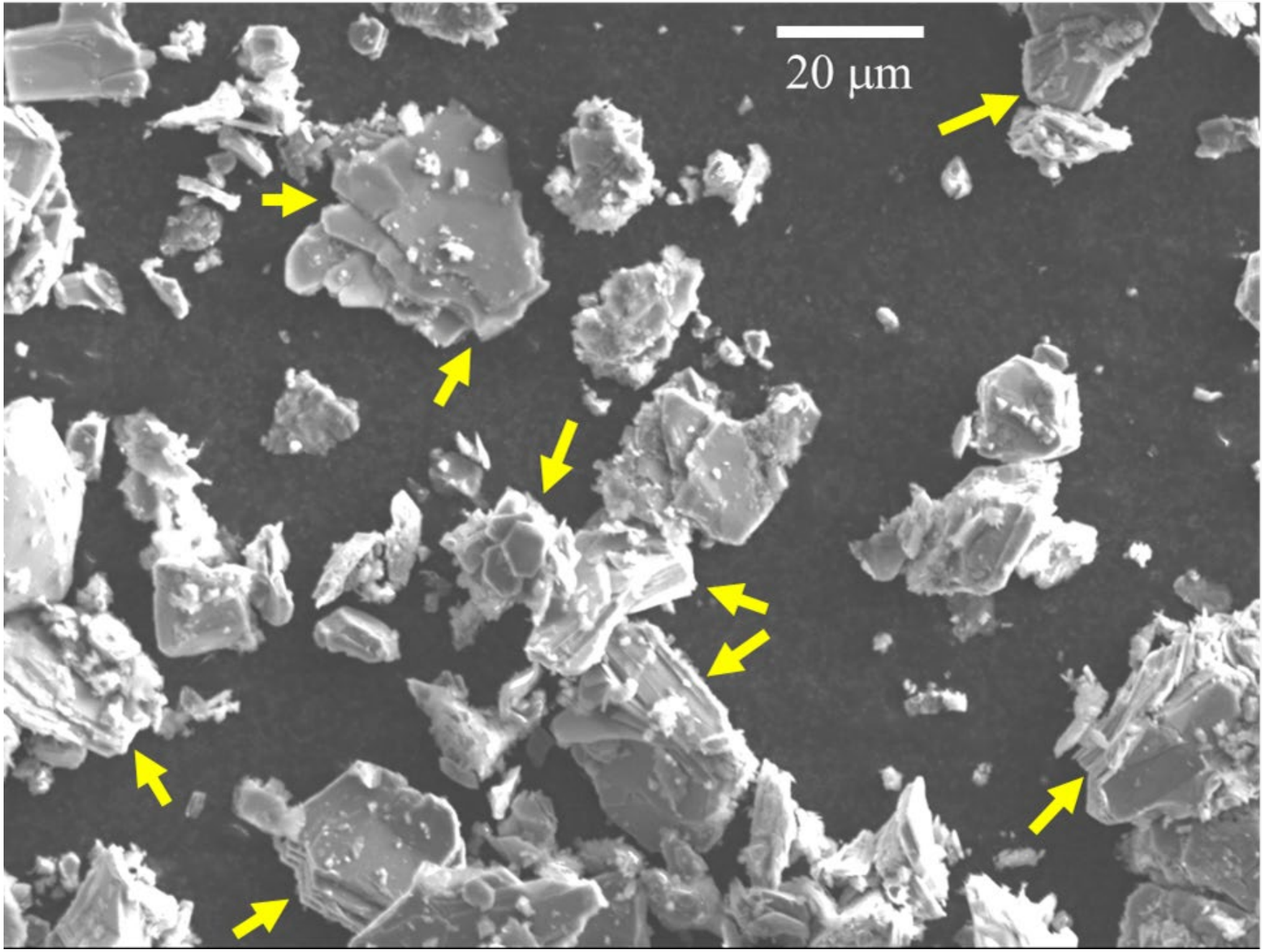

Scanning electron microscopy (SEM) and Electron Probe Micro Analyzer (EPMA) of r-BS

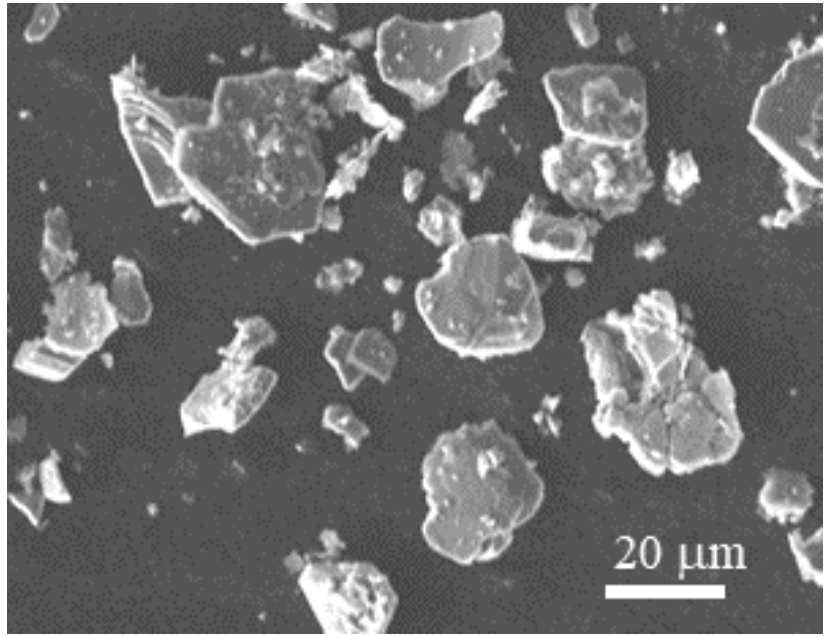

All of them shows uniform B and S intensity

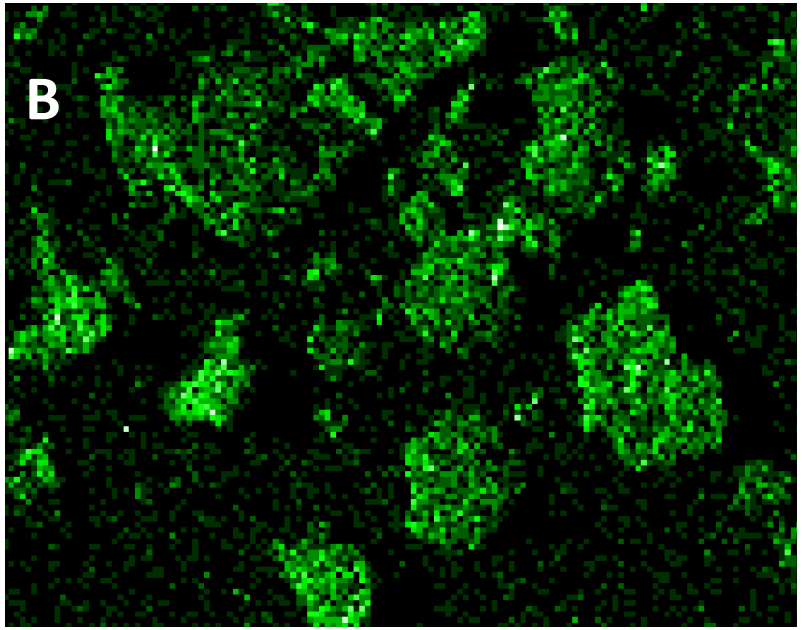

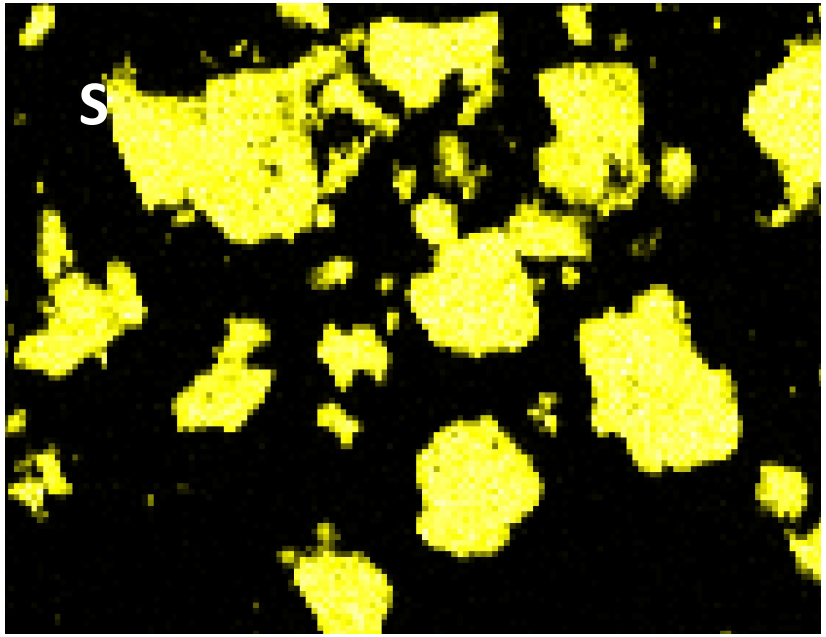

Scanning electron microscopy (SEM) and Electron Probe Micro Analyzer (EPMA) of r-BS

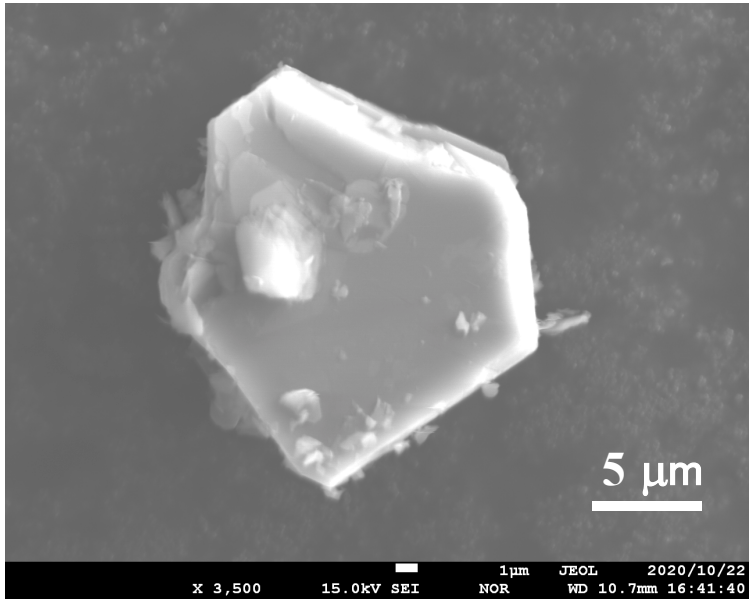

~15 µm size r-BS was observed

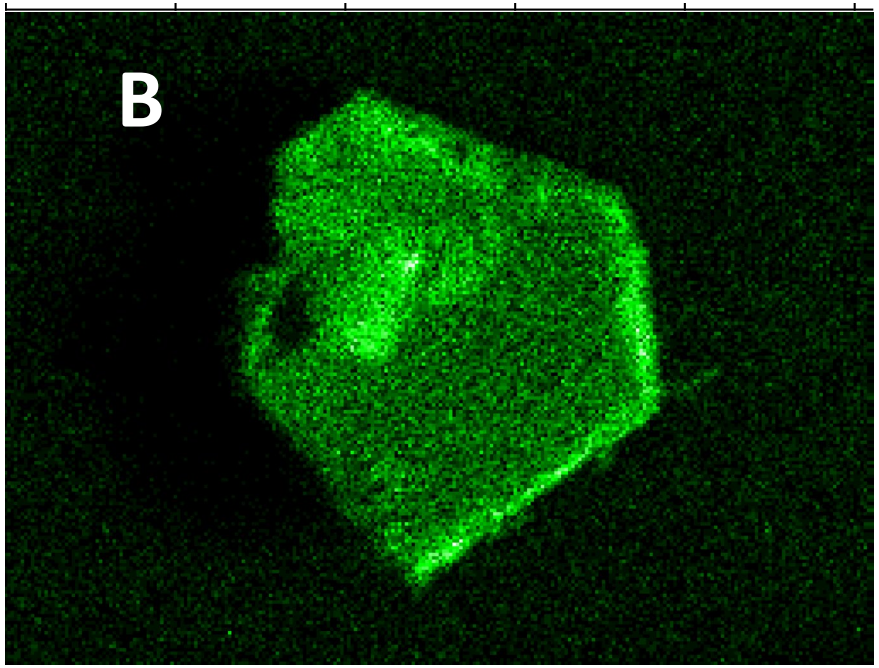

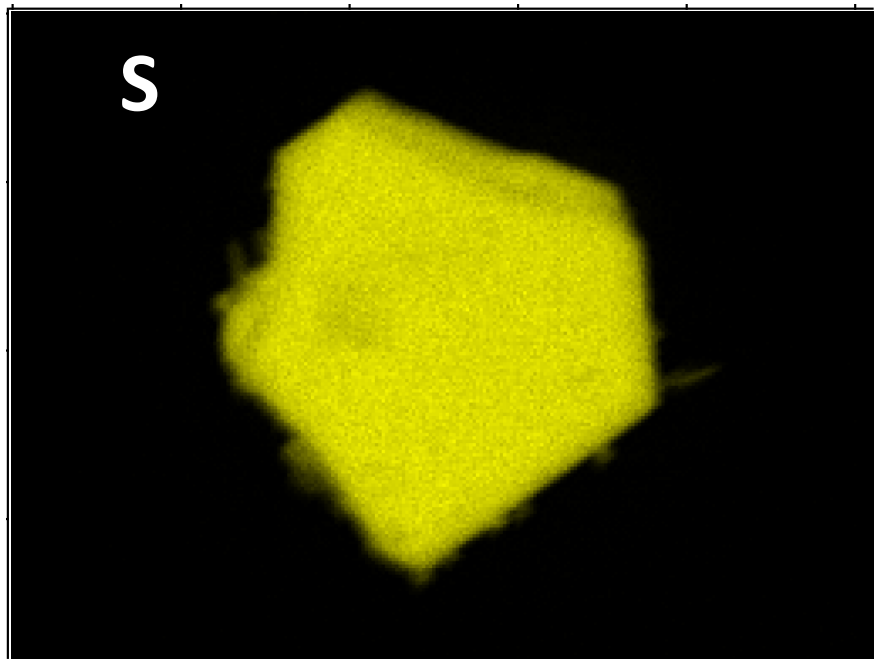

XRD of r-BS (synthesized at 5.5 GPa and 1873 K)

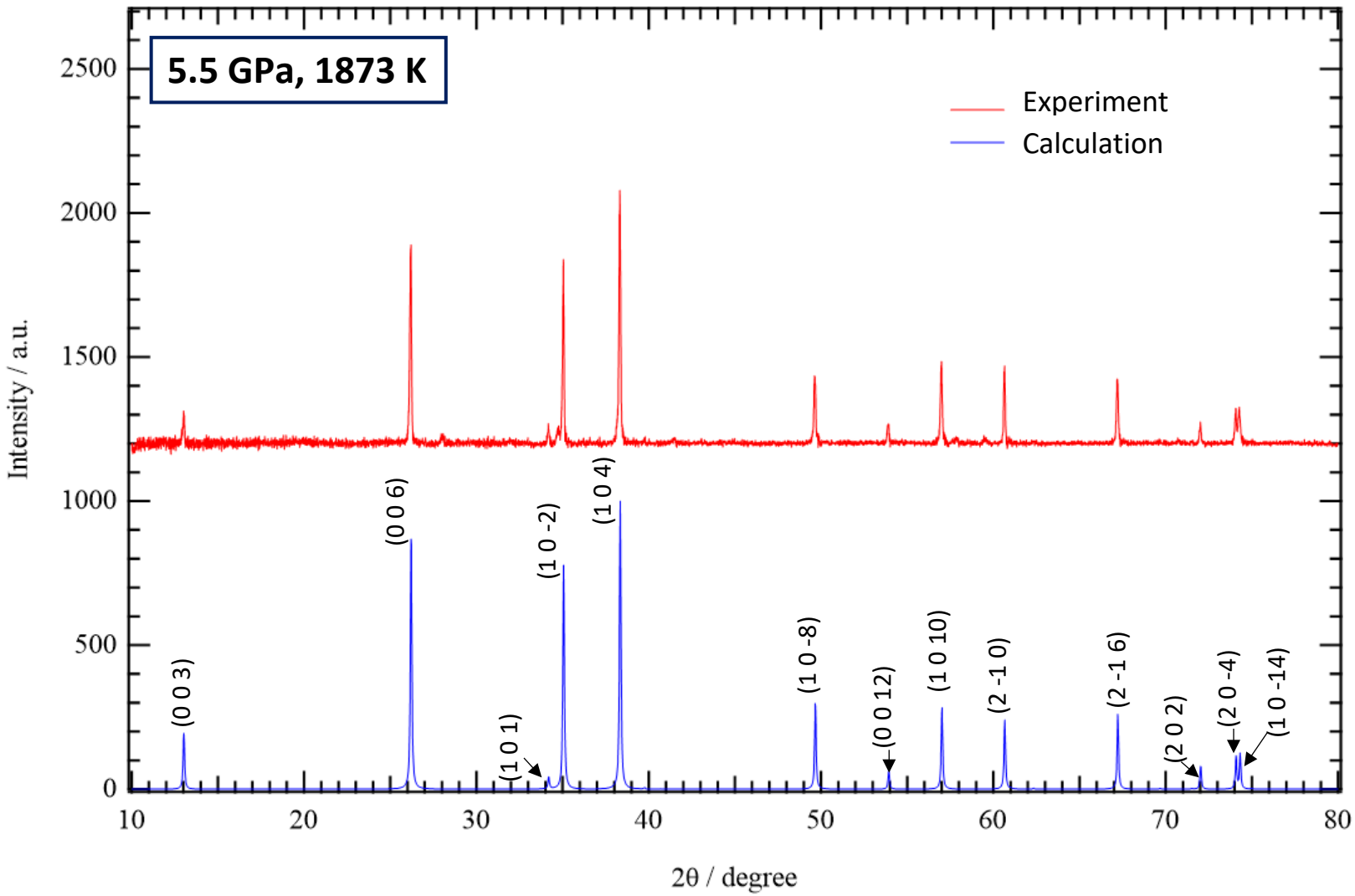

XRD indicates that r-BS is synthesized as single phase.

H. Kusaka, T. Kondo* et al., J. Mater. Chem. A 9 (2021) 24631-24640

Rietveld analysis of XRD measured at SPring-8 (Prof. Eiji Nishibori)

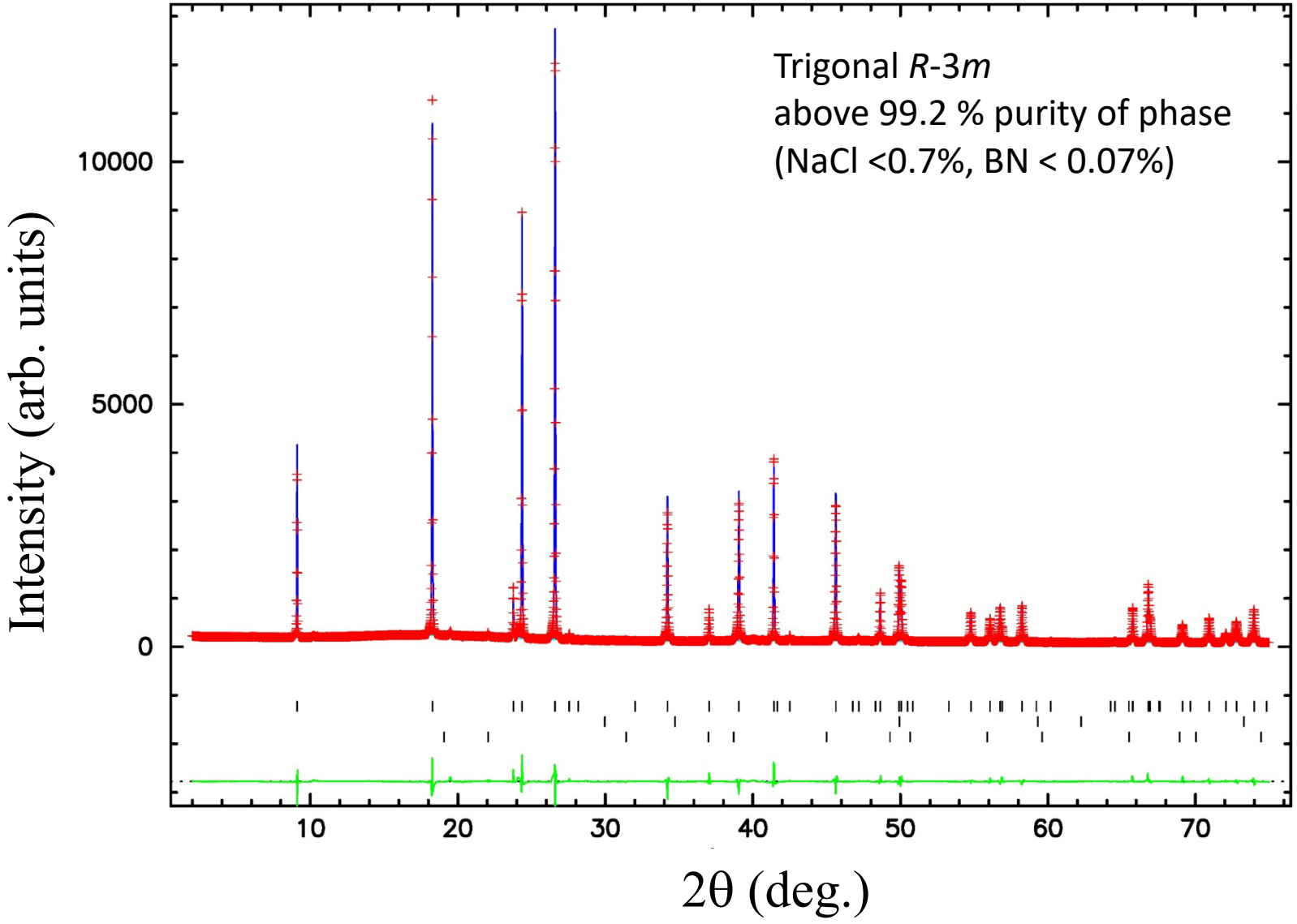

Prof. Eiji Nishibori

Single phase (above 99.2 % purity of phase) was achieved

H. Kusaka, T. Kondo* et al., J. Mater. Chem. A 9 (2021) 24631-24640

B-B bond

Derived data by Rietveld analysis of XRD measured at SPring-8 (Prof. Eiji Nishibori)

Crystal data	
Crystal system, space group	Trigonal, $R\bar{3}m$
Temperature (K)	300
a, c (Å)	3.05070, 20.3846 (1)
V (Å^3)	164.30 (1)
Z	3
Radiation type	Synchrotron, λ = 1.07900 Å
Selected bond lengths (Å) B—B	1.6756 (1)

Fractional atomic coordinates (x, y, z (Å)) and isotropic or equivalent isotropic displacement parameters (U_{iso} (Å^2))

	x	y	z	U_{iso}
S	0.00000	0.00000	0.54110(8)	0.0055(5)
B	0.00000	0.00000	0.24969(3)	0.0055(5)

B-B bond **1.6756 Å**

先行文献で報告されているB-B間距離

B-B single bond : 1.72 Å
Y. Shoji, et al., *J. Am. Chem. Soc.*, 2010, **132**, 8258.

B=B double : 1.560 Å
Y. Wang, et al., *J. Am. Chem. Soc.*, 2007, **129**, 12412.

B≡B triple bond : 1.455-1.504 Å
S.-D. Li et al., *J. Am. Chem. Soc.*, 2008, **130**, 2573

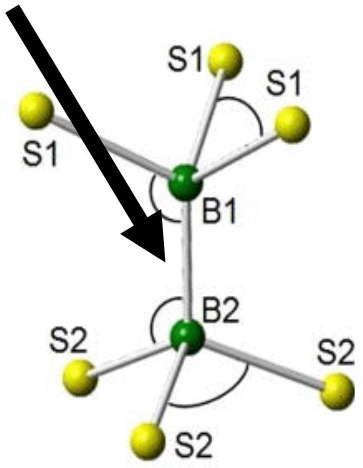

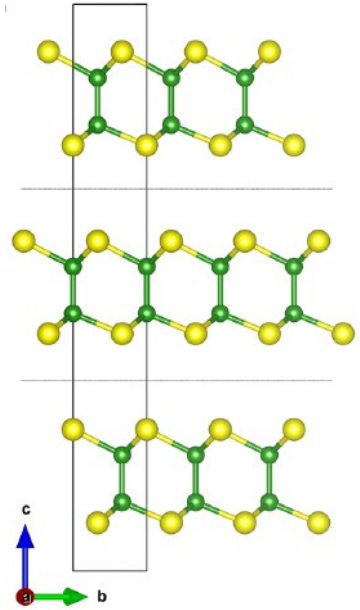

B-B bond corresponds single bond

H. Kusaka, T. Kondo* et al., J. Mater. Chem. A 9 (2021) 24631-24640

XPS of r-BS powder on Au surface

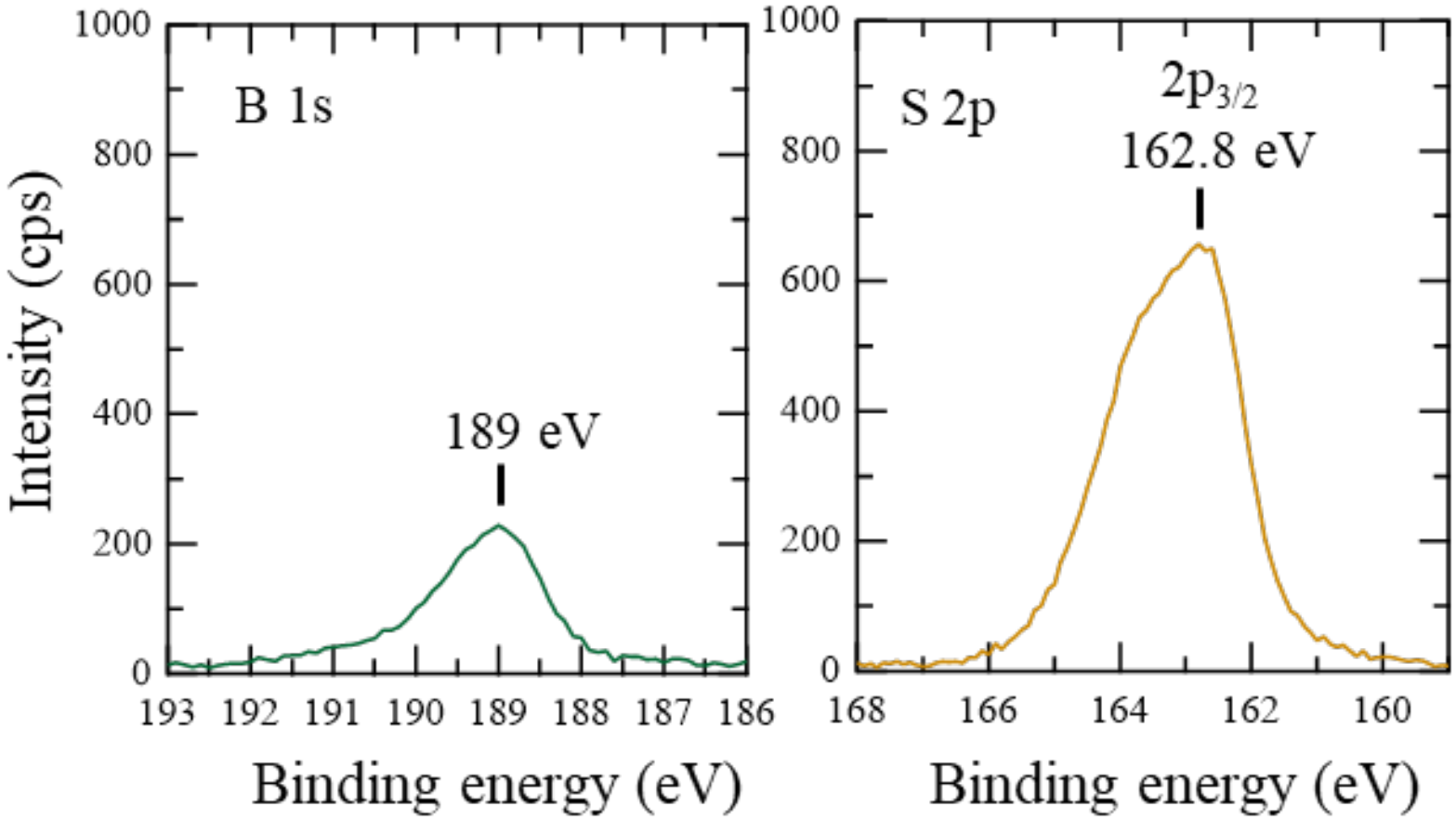

AlKα (1486.6 eV)

XPS Sensitivity
B : 2.102, S: 7.186

B : S = 1.0 ±0.2 : 1.0 ±0.2

Consistent with original starting amount (1:1)
(Sulfur was not lost during heating)

H. Kusaka, T. Kondo* et al., J. Mater. Chem. A 9 (2021) 24631-24640

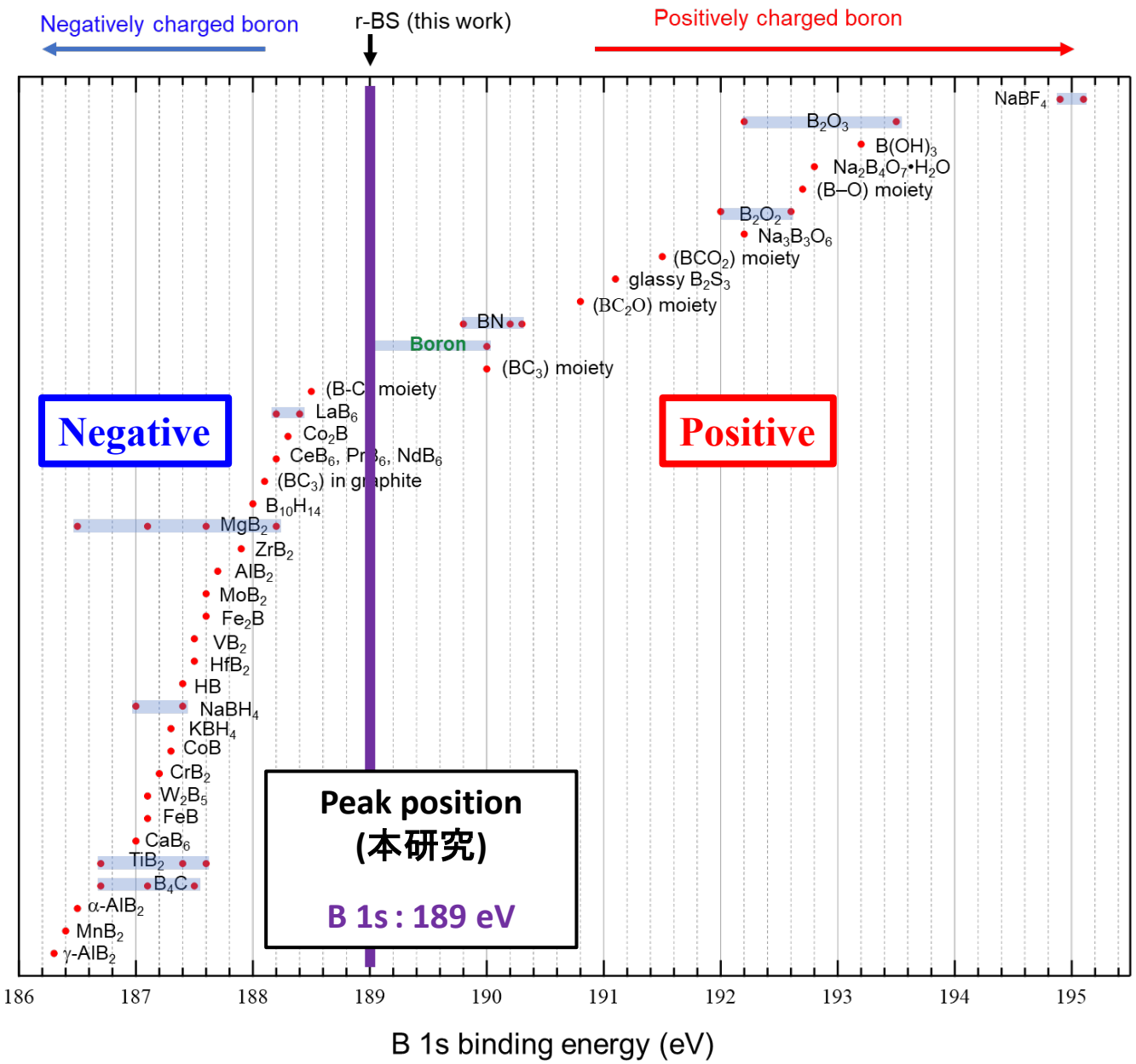

報告されているホウ化物のピーク位置

BE (eV)	Species	Reference
202.8	BF_3(vapor)	[1]
199.8	BCl_3(vapor)	[1]
199.0	BBr_3(vapor)	[1]
197.8	BI_3(vapor)	[1]
196.5	B_2H_6(vapor)	[1]
194.9-195.1	$NaBF_4$	[2,3]
192.2-193.5	B_2O_3	[3,4]
193.2	$B(OH)_3$	[2]
192.8	$Na_2B_4O_7 \cdot H_2O$	[2]
192.7	(B–O) moiety	[5,6]
192.0-192.6	B_2O_2	[3,7]
192.2	$Na_3B_3O_6$	[2]
191.5	(BCO_2) moiety	[5]
191.1	glassy B_2S_3	[37]
190.8	(BC_2O) moiety	[5]
190.0	(BC_3) moiety	[6]
189.0-190.0	boron	[3]
189.8-190.3	BN	[2,3]
188.5	(B–C) moiety	[8]
188.2-188.4	LaB_6	[7, 9,10]
188.3	Co_2B	[11]
188.2	CeB_6, PrB_6, NdB_6	[10]
188.1	(BC_3) in graphite	[12]
188.0	$B_{10}H_{14}$	[2]
187.9	ZrB_2	[13]
187.7	AlB_2	[11]
187.6	MoB_2	[11]
187.6	Fe_2B	[11]
187.5	VB_2	[11]
187.5	HfB_2	[11]
187.4	HB	[14]
187.0-187.4	$NaBH_4$	[1,3]
187.3	KBH_4	[38]
187.3	CoB	[11]
187.2	CrB_2	[11]
187.1	W_2B_5	[11]
187.1	FeB	[11]
187.0	CaB_6	[15]
186.7	TiB_2	[11,33-35]
186.5-188.2	MgB_2	[16-18,36]
186.7-187.5	B_4C	[2,8,12]
186.5	α-AlB_2	[11]
186.4	MnB_2	[11]
186.3	γ-AlB_2	[11]

B1s peak position of r-BS corresponds to that of bulk boron

H. Kusaka, T. Kondo* et al., J. Mater. Chem. A 9 (2021) 24631-24640

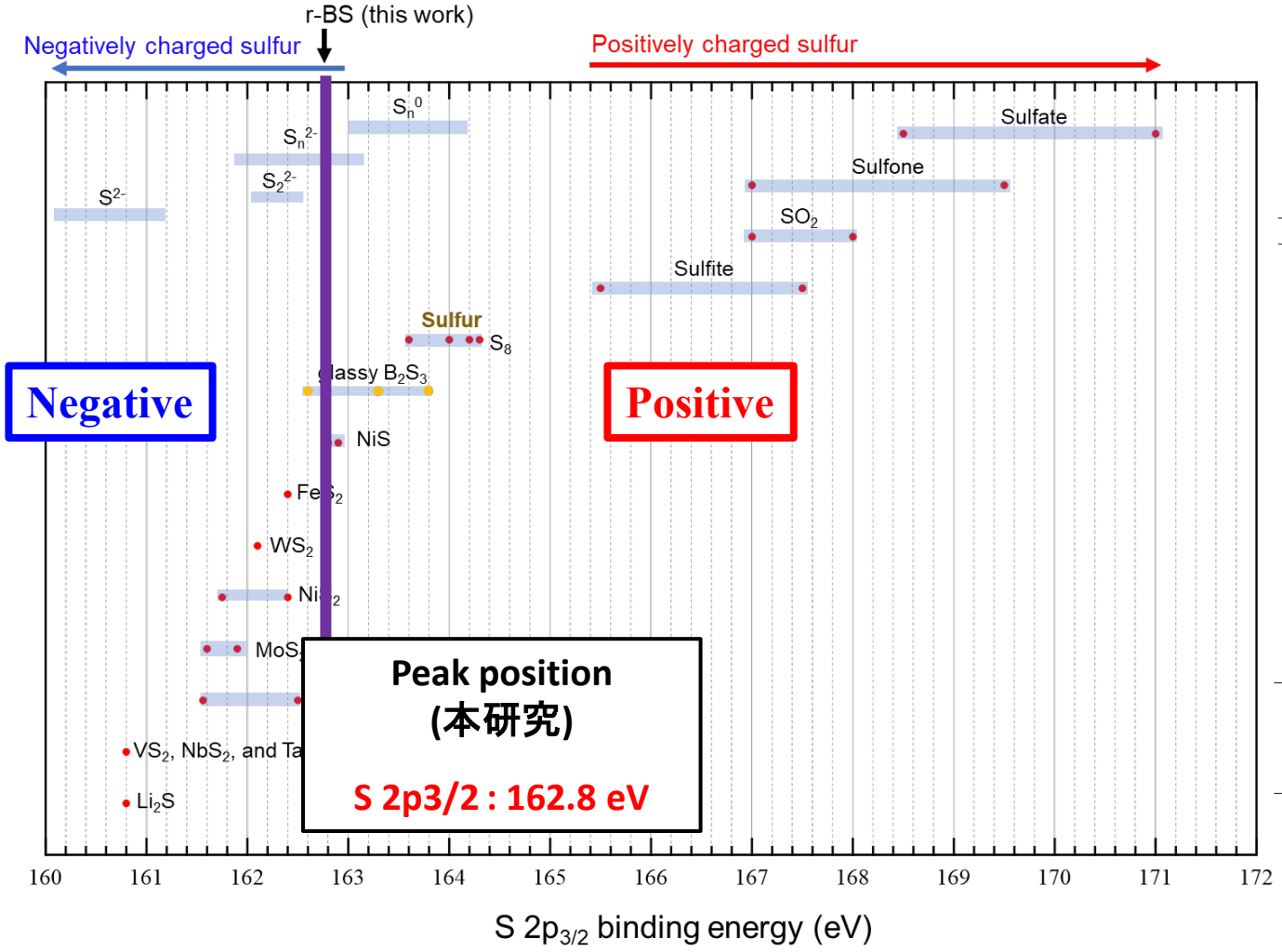

BE (eV)	Species	Reference
174.5-177.0	SF_6	[3]
168.5-171.0	Sulfate	[3,19]
167.0-169.5	Sulfone	[3,19]
167.0-168.0	SO_2	[3,19]
165.5-167.5	Sulfite	[3,19]
163.6-164.3	S_8	[3,19-21]
162.6 163.3 163.8	glassy B_2S_3	[37]
162.8-162.9	NiS	[22]
162.4	FeS_2	[23]
162.1	WS_2	[24]
161.75-162.4	NiS_2	[25,26]
161.6-161.9	MoS_2	[27,28]
161.56-162.5	ReS_2	[29,30]
160.8	VS_2, NbS_2, and TaS_2	[31]
160.8	Li_2S	[32]
160.1-161.2	S^{2-}	[20]
162.1-162.6	S_2^{2-}	[20]
161.9-163.2	S_n^{2-}	[20]
163.0-164.2	S_n^0	[20]

S2p peak position of r-BS locates at slightly negatively charged state

H. Kusaka, T. Kondo* et al., J. Mater. Chem. A 9 (2021) 24631-24640

Calculated electron localization functions (EFLs)

(Prof. M. Toyoda and S. Saito at Tokyo Tech.)

Electron accumulated at p_z orbital of S which causes slightly negative charge of S

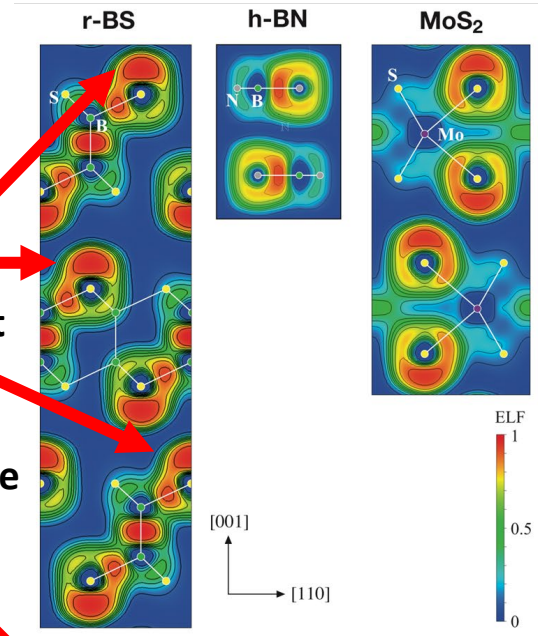

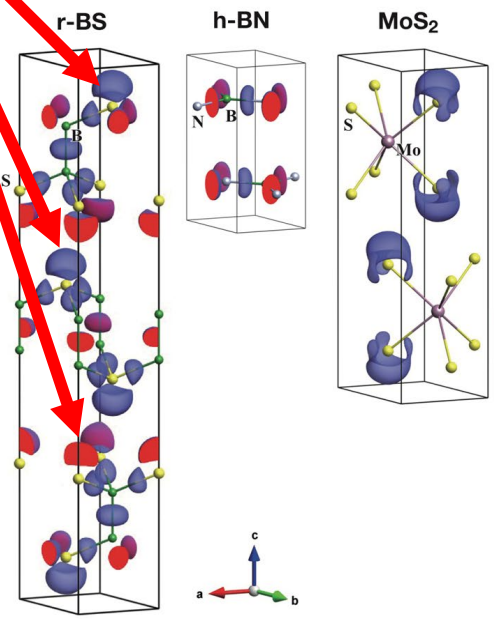

BとSの中間で電荷密度が最大となっている

共有結合的

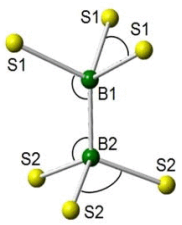

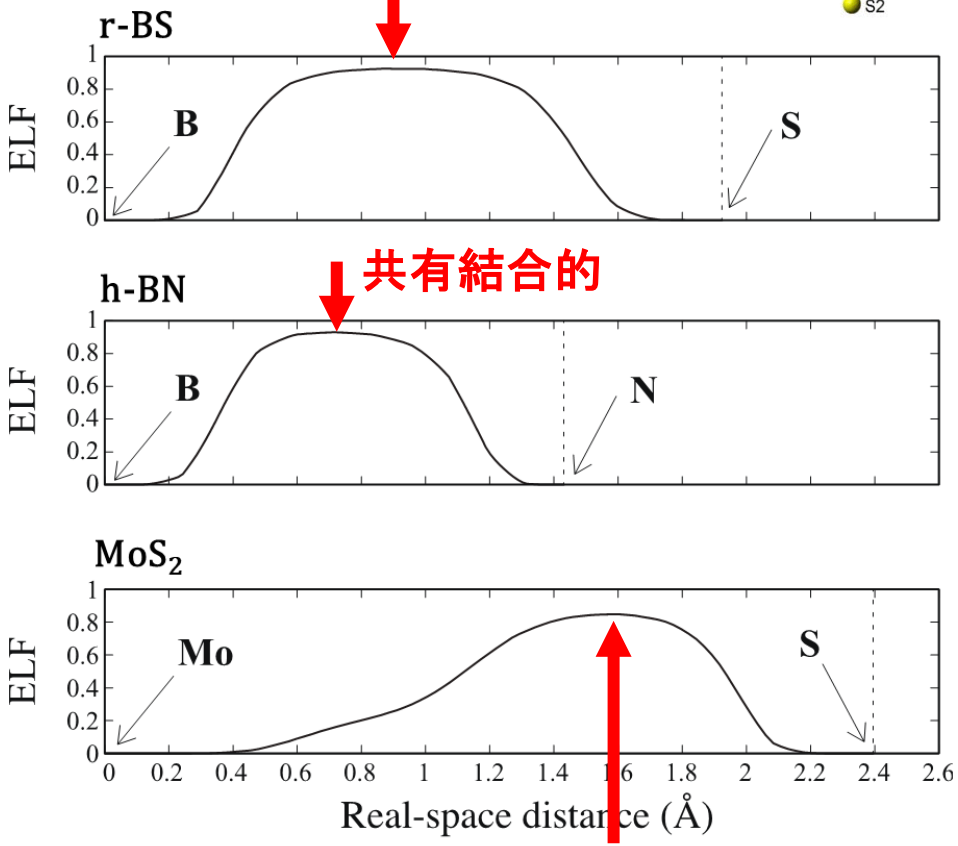

共有結合的

Sに寄った位置で電荷密度が最大となっている

イオン結合的

H. Kusaka, T. Kondo* et al., J. Mater. Chem. A 9 (2021) 24631-24640

Raman Scattering of r-BS

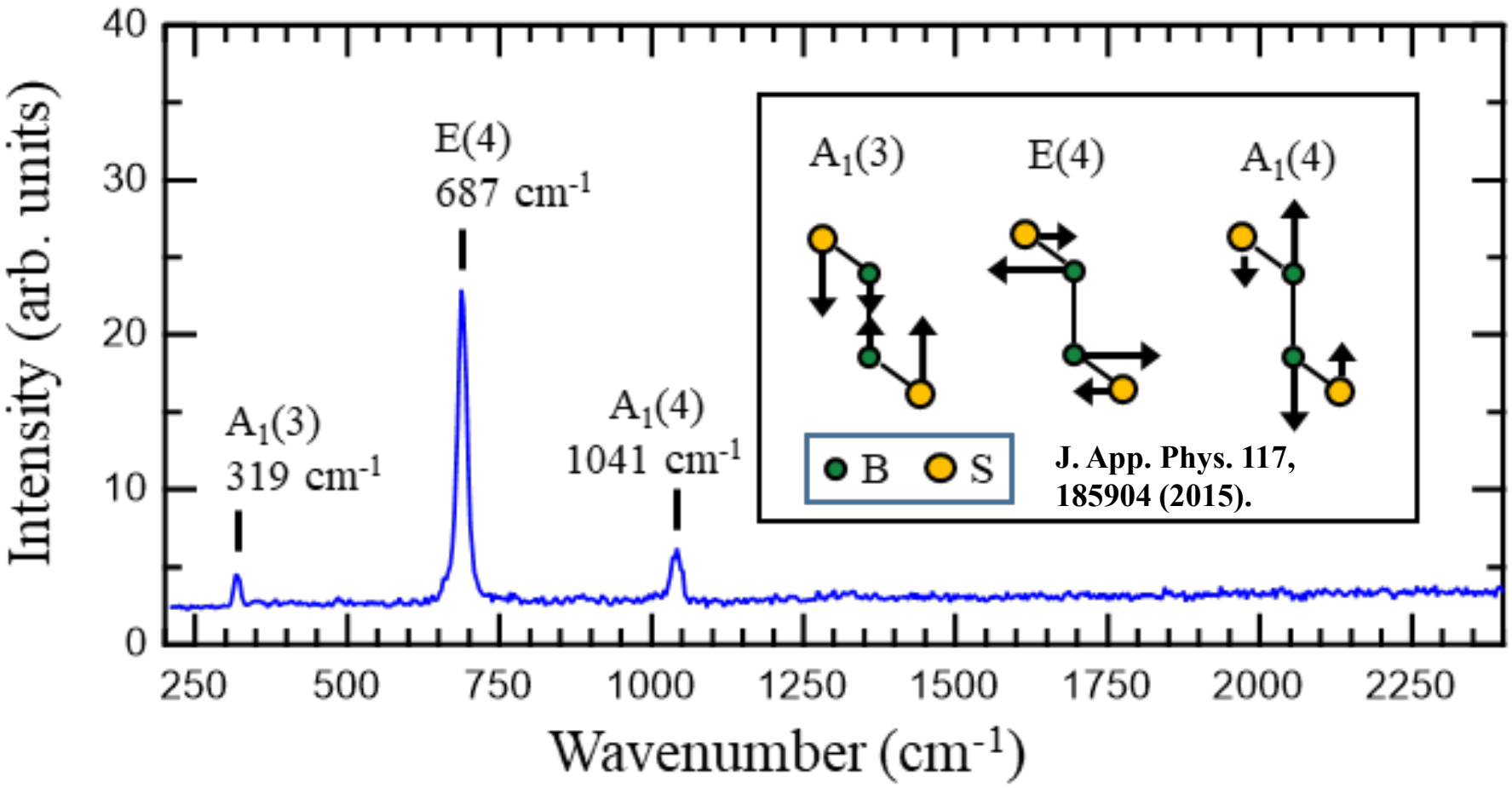

H. Kusaka, T. Kondo* et al., J. Mater. Chem. A 9 (2021) 24631-24640

Thermal stability of r-BS (Thermogravimetric analysis)

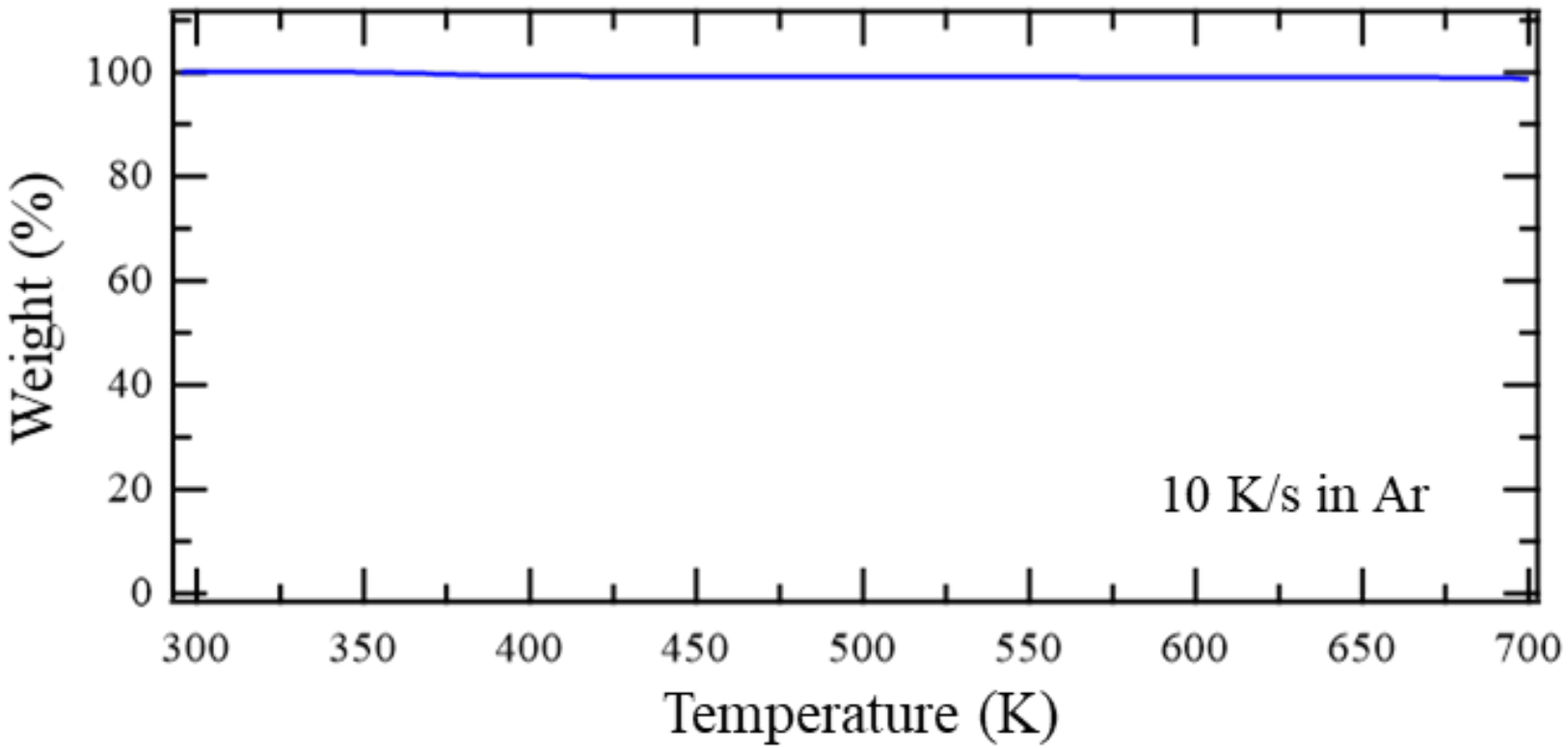

Thermally stable at Ar up to 700 K

H. Kusaka, T. Kondo* et al., J. Mater. Chem. A 9 (2021) 24631-24640

Thermal stability of r-BS (XRD after heating)

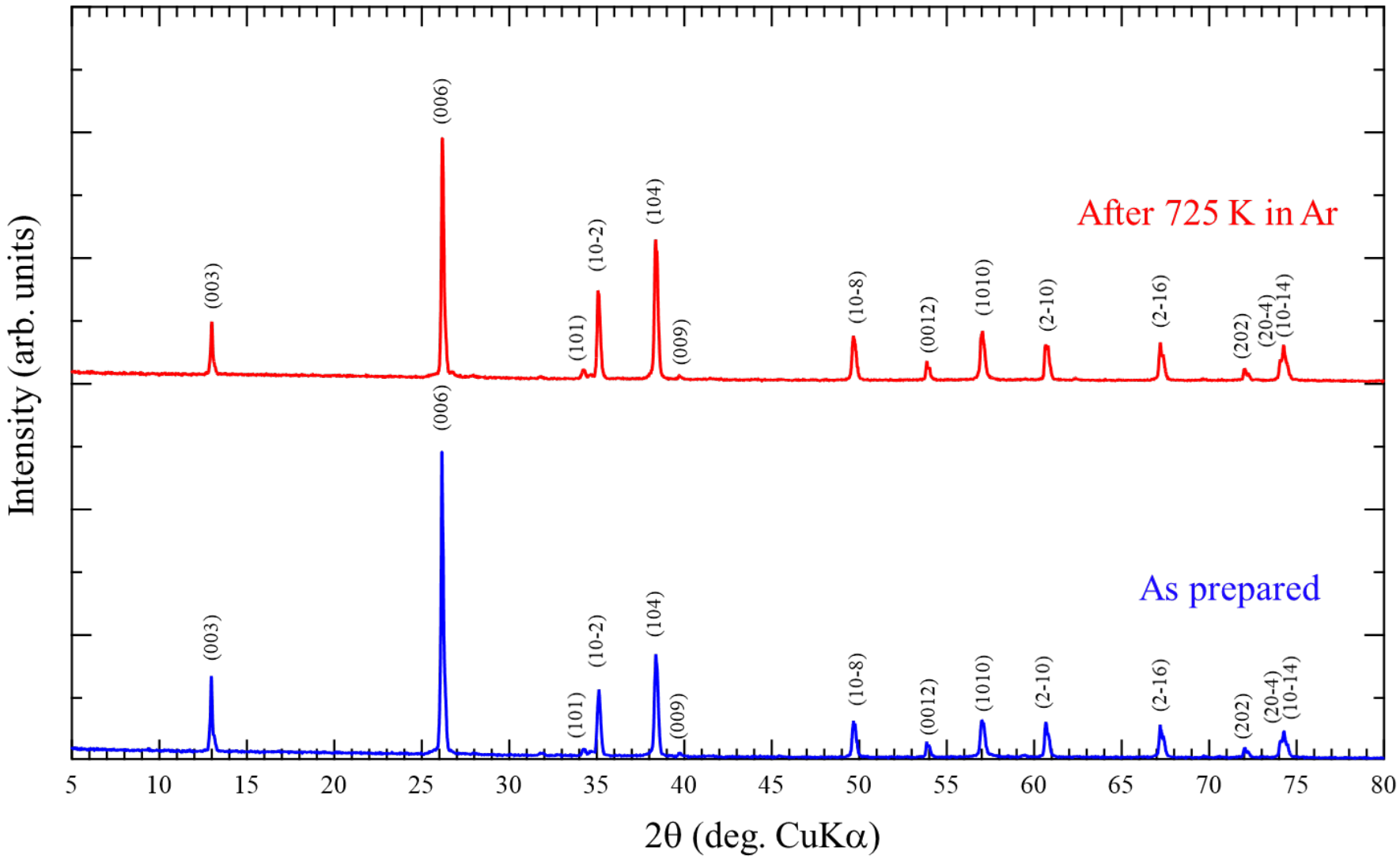

XRD shows the same pattern after 725 K in Ar

H. Kusaka, T. Kondo* et al., J. Mater. Chem. A 9 (2021) 24631-24640

DFT calculation by Prof. S. Saito and Prof. M. Toyoda

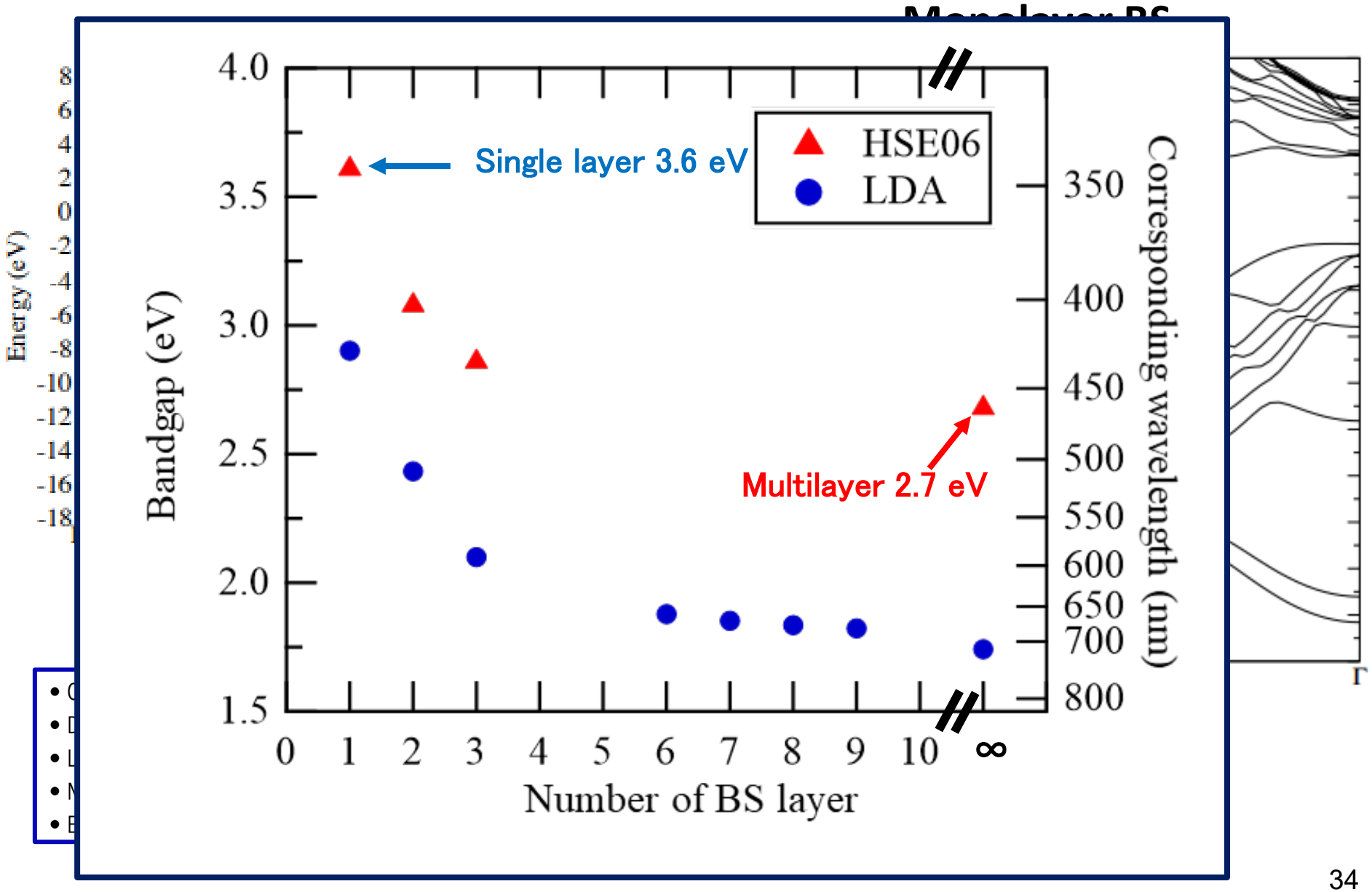

H. Kusaka, T. Kondo* et al., J. Mater. Chem. A 9 (2021) 24631-24640

Why does the bandgap get smaller when the sheets are stacked?

DFT calculation by
Prof. S. Saito and
Prof. M. Toyoda

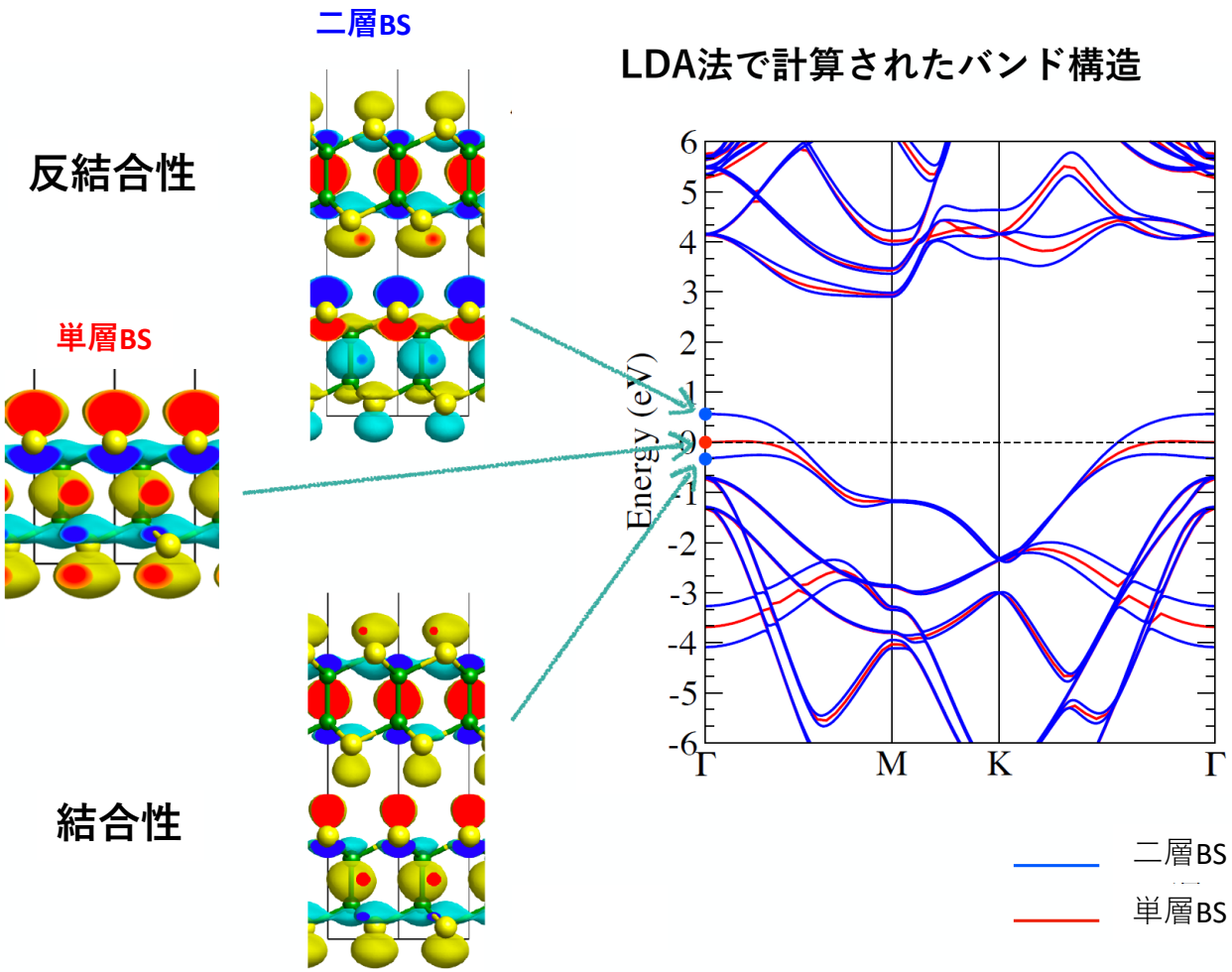

(1) 積層によって、硫黄同士の混成軌道が形成するため価電子帯の電子軌道が分裂
(2) 反結合性軌道によるバンドがバンドギャップ内に生成
(3) 単層と比較して積層することでバンドギャップが狭まる

H. Kusaka, T. Kondo* et al., J. Mater. Chem. A 9 (2021) 24631-24640

Transmission electron microscopy (TEM), Electron energy loss spectroscopy (EELS) and electron diffraction of r-BS

Prof. T. Fujita and T. Tokunaga

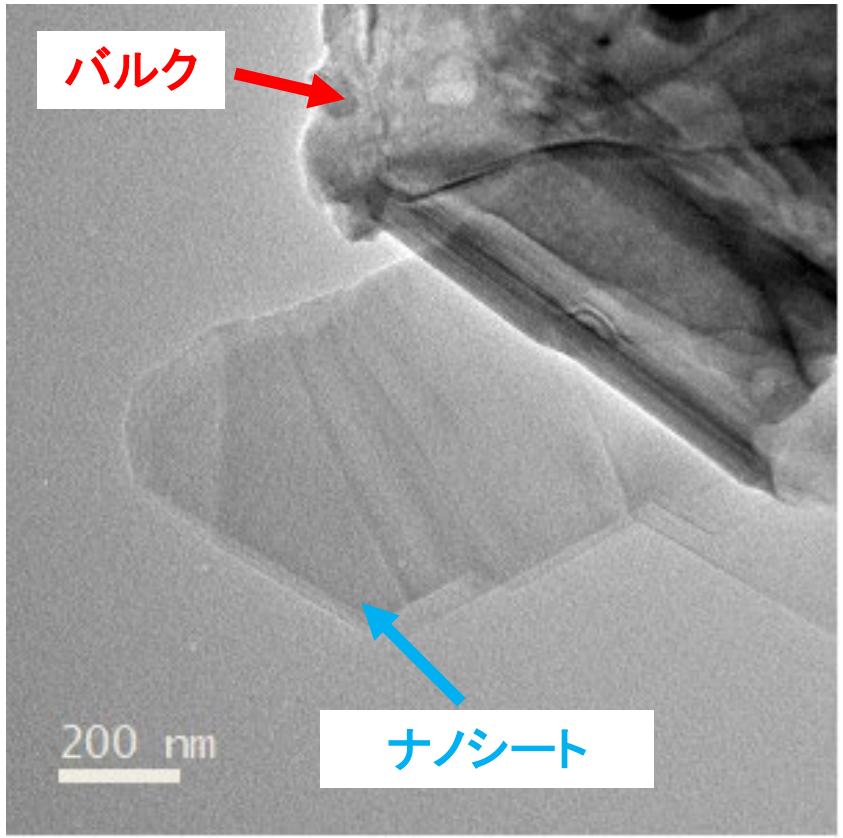

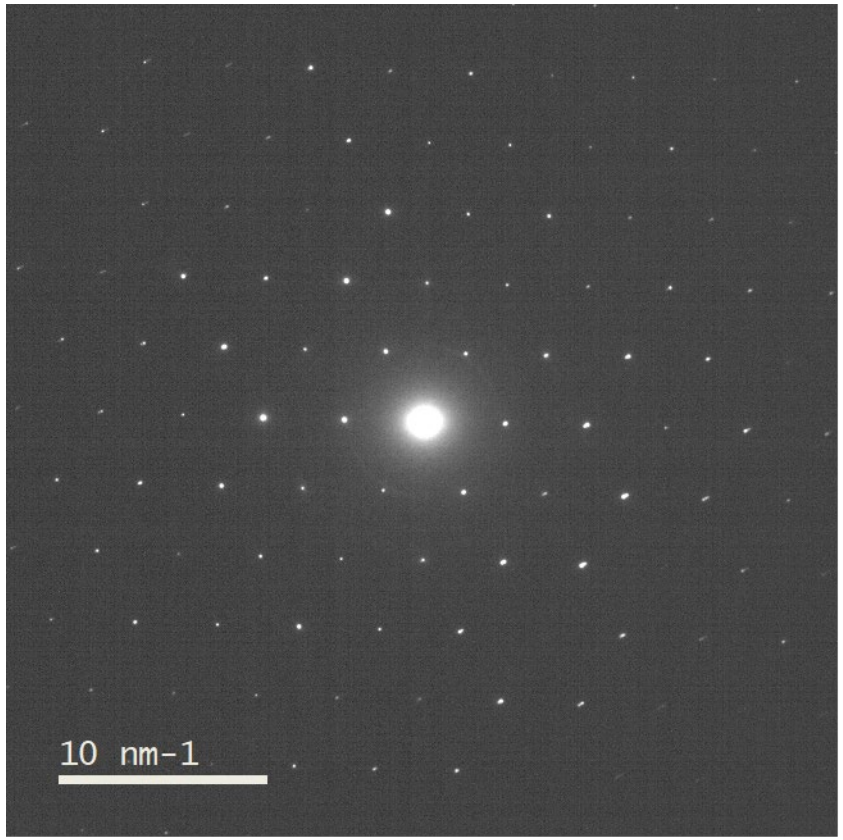

Nanosheets are included in the r-BS sample

H. Kusaka, T. Kondo* et al., J. Mater. Chem. A 9 (2021) 24631-24640

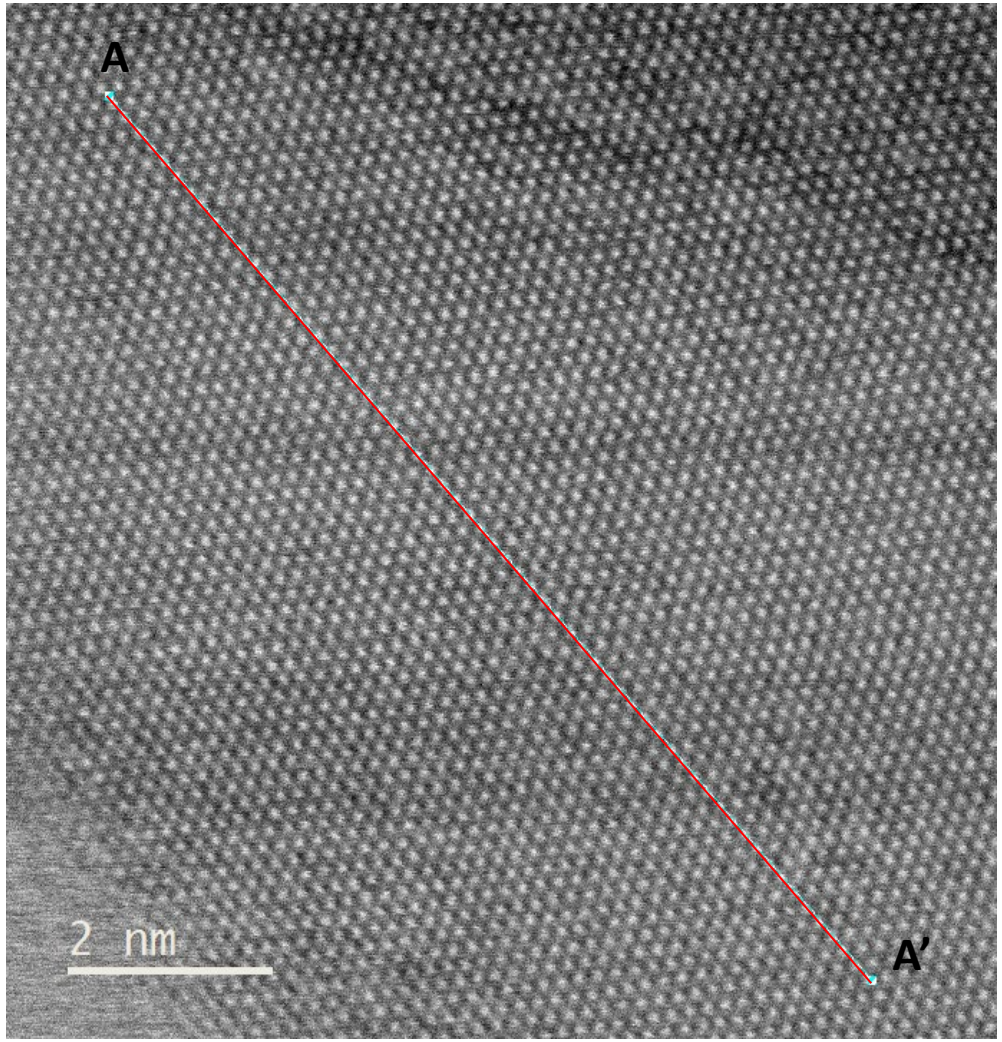

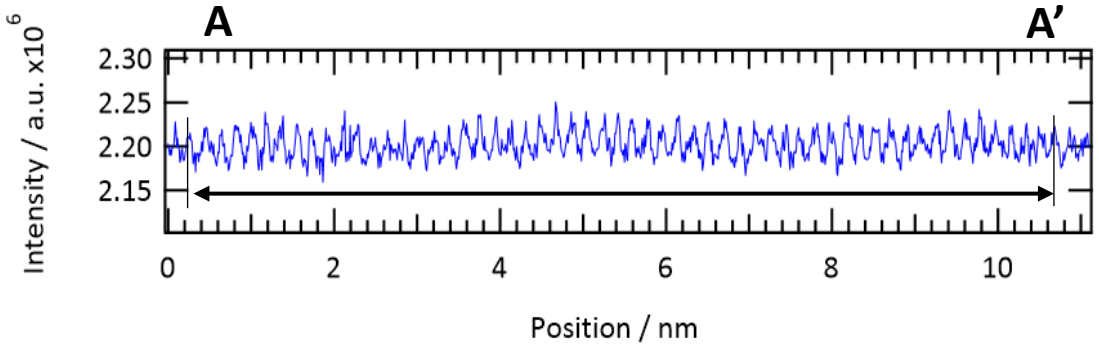

Prof. T. Fujita and T. Tokunaga

1T

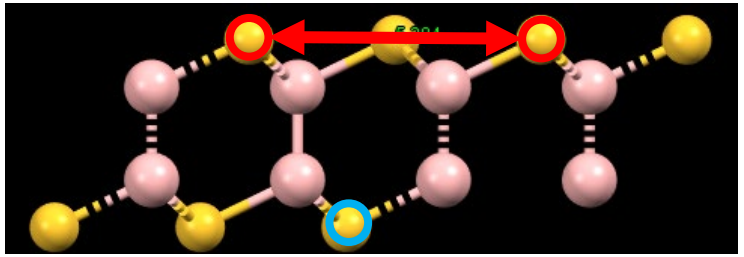

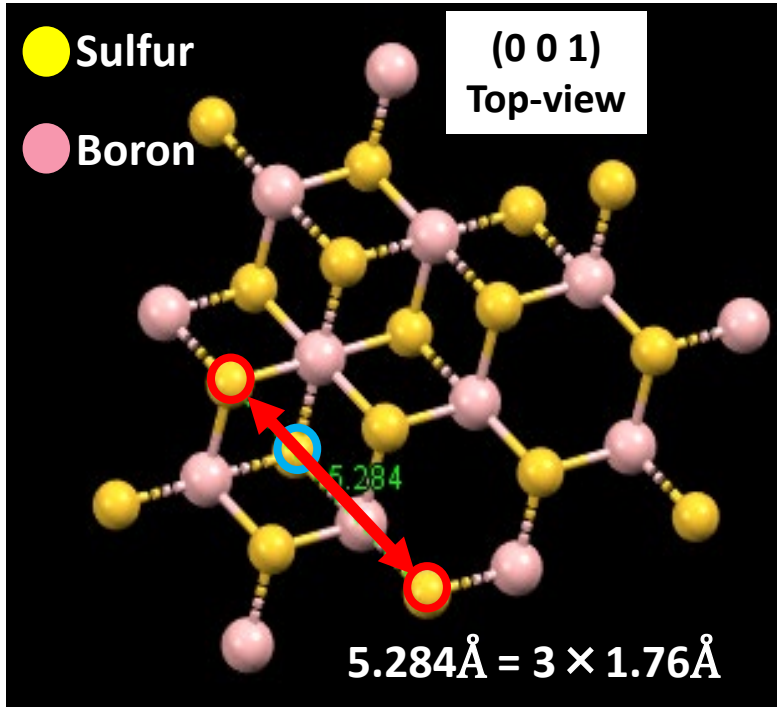

10.42 nm＝57 × 0.182807nm

Atom-atom distance: 0.18 nm

H. Kusaka, T. Kondo* et al., J. Mater. Chem. A 9 (2021) 24631-24640

Excitation Emission Matrix (EEM) of r-BS

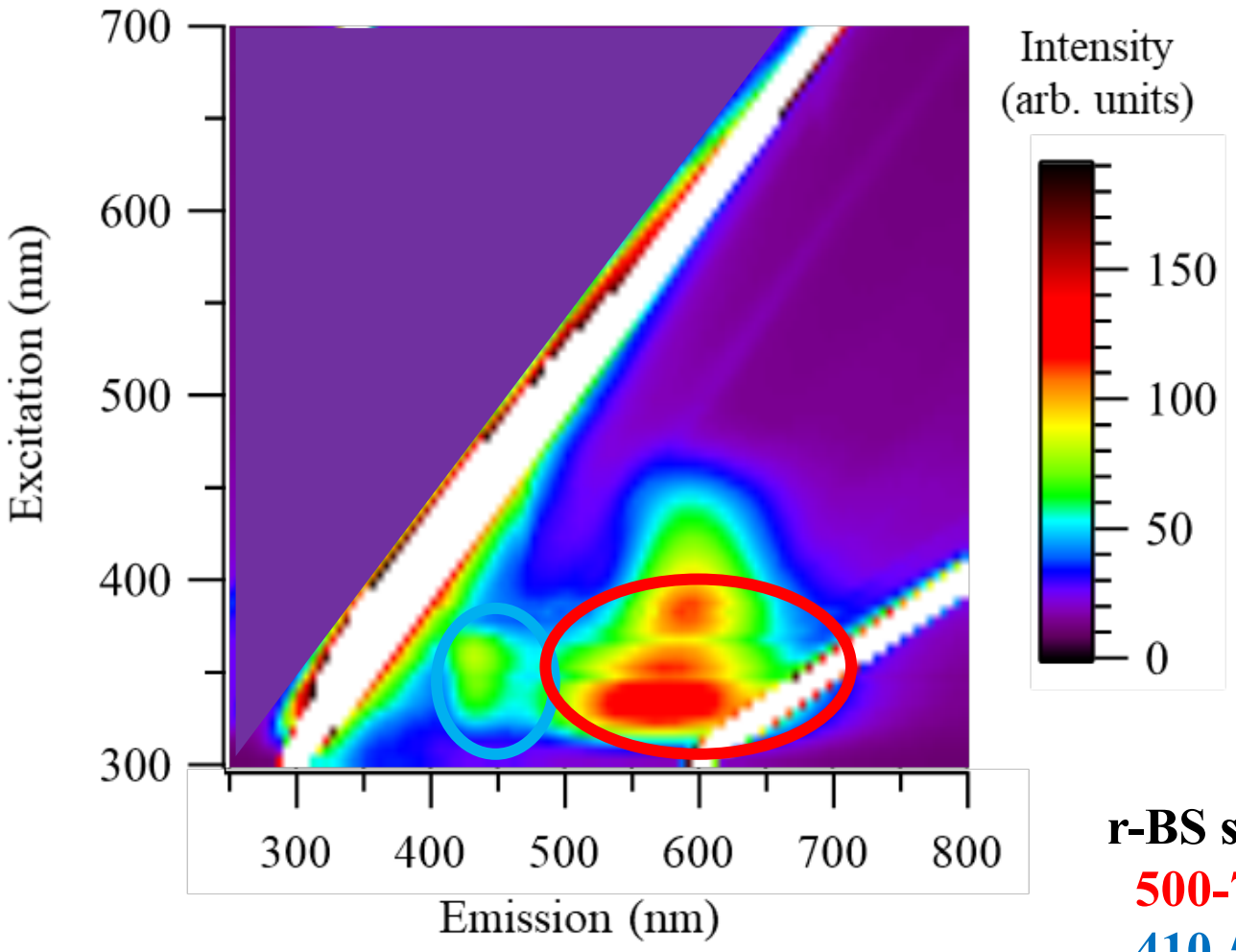

With Prof. M. Miyauchi

Prof. S. Saito and
Prof. M. Toyoda
第一原理計算

Bulk r-BS

E_g = 2.7 [eV] (Z to M)

Monolayer r-BS

E_g = 3.6 [eV] (Γ to M)

r-BS shows

500-700 [nm]（1.77-2.48 eV）

410-500 [nm]（2.48-3.02 eV）

Indicating that nanosheets are included in the material

H. Kusaka, T. Kondo* et al., J. Mater. Chem. A 9 (2021) 24631-24640

層状物質r-BSをスコッチテープ法で劈開することで硫化ホウ素ナノシートの生成を試みた

スコッチテープ法による剥離は30回以上行った

$(\frac{1}{2})^{30} \cong 10^{-9}$ より原理的にはナノメートルに剥離

H. Kusaka, T. Kondo* et al., J. Mater. Chem. A 9 (2021) 24631-24640

After exfoliation

With Dr. T. Masuda

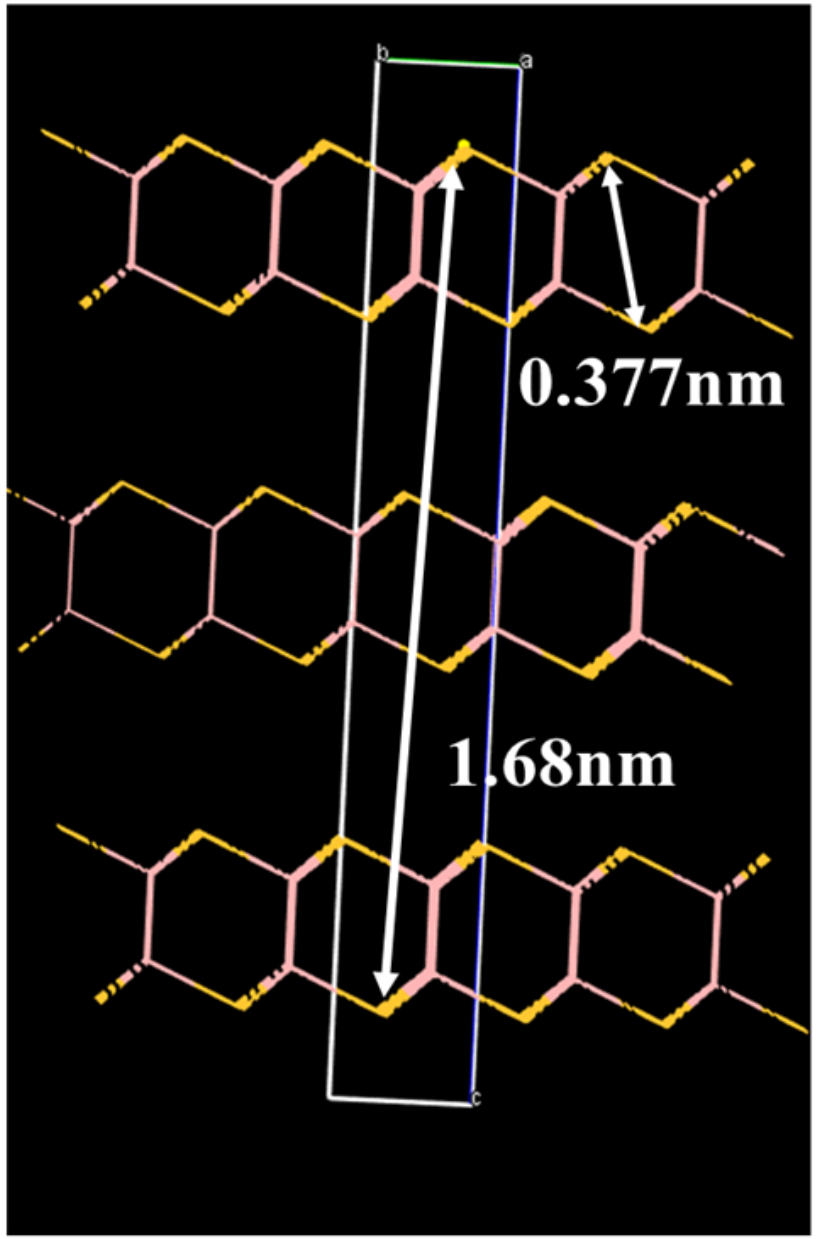

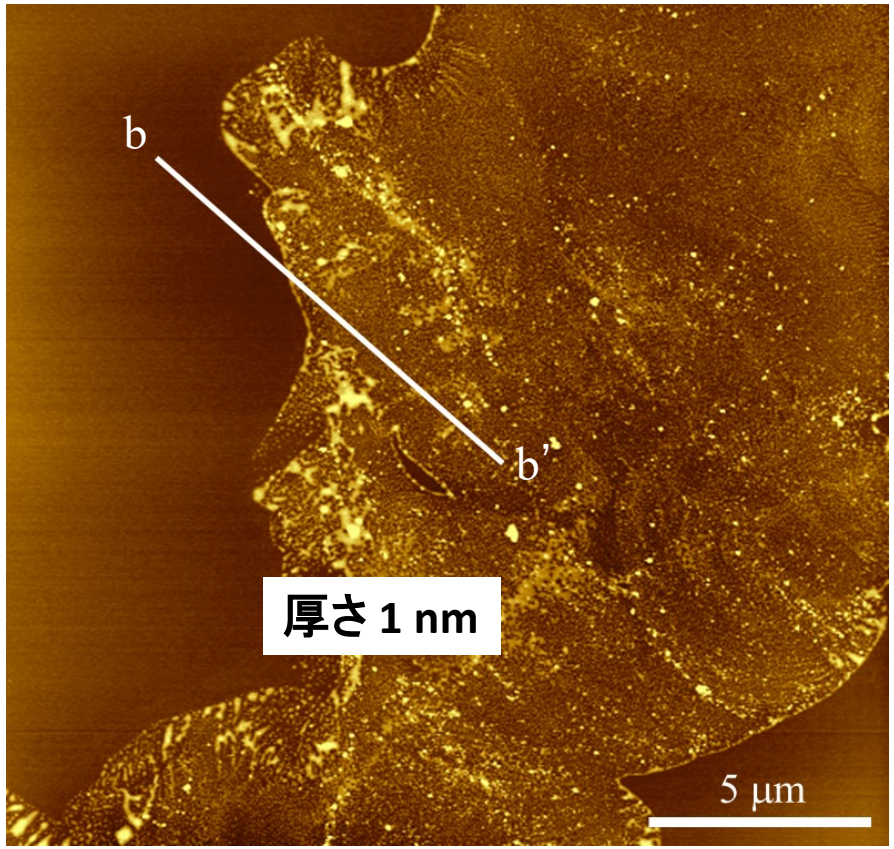

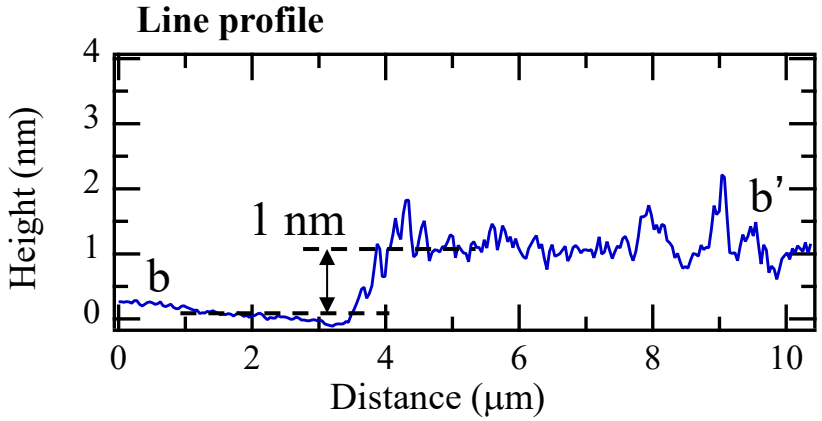

H. Kusaka, T. Kondo* et al., J. Mater. Chem. A 9 (2021) 24631-24640

Cathode luminescence (CL) of r-BS

Dr. K. Watanabe

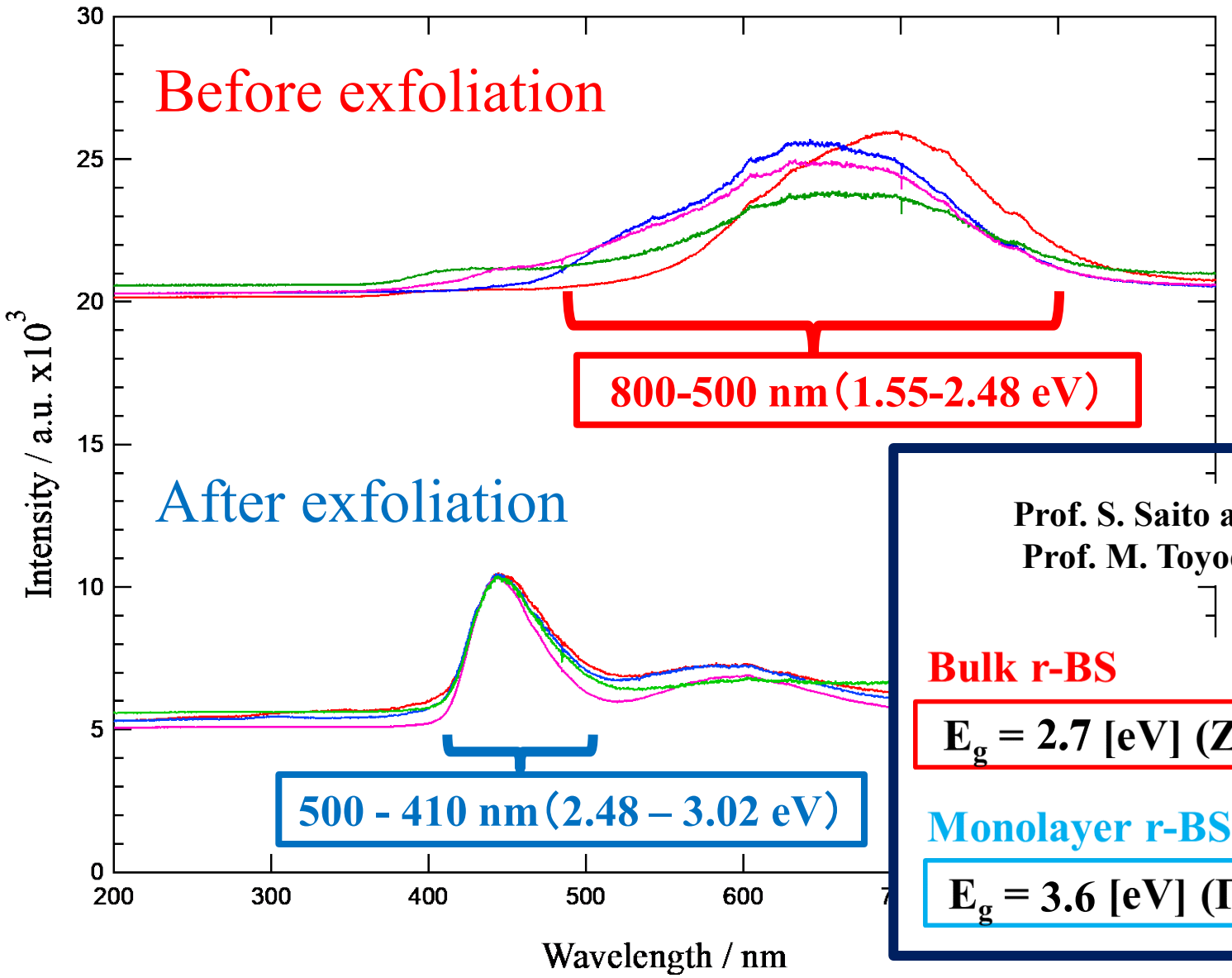

Prof. S. Saito and
Prof. M. Toyoda

Bulk r-BS

E_g = 2.7 [eV] (Z to M)

Monolayer r-BS

E_g = 3.6 [eV] (Γ to M)

H. Kusaka, T. Kondo* et al., J. Mater. Chem. A 9 (2021) 24631-24640

新たに見出した硫化ホウ素ナノシートとr-BSの分離方法

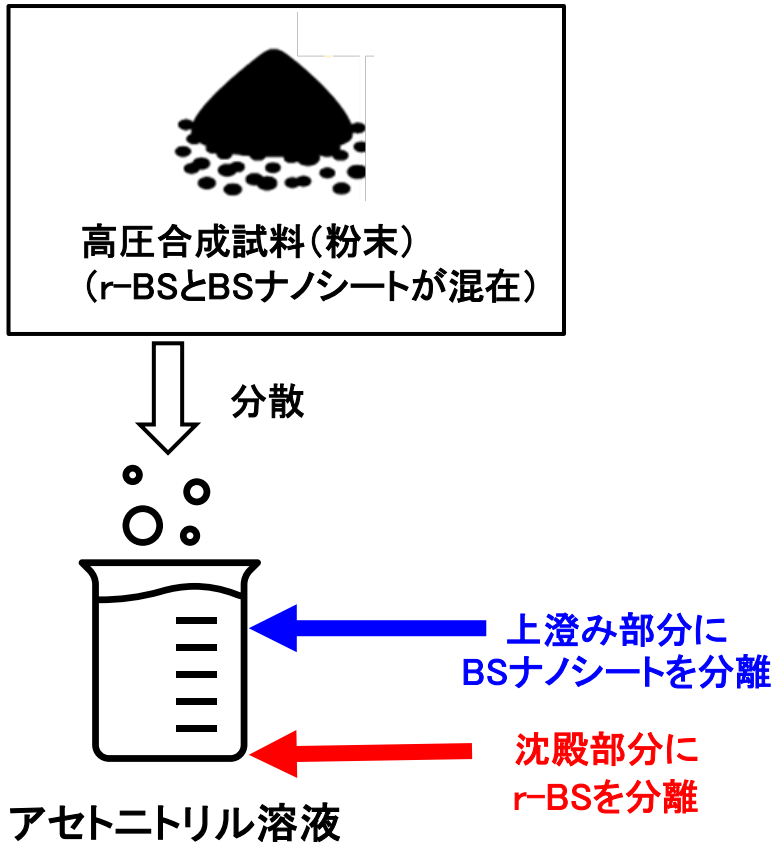

実際の様子

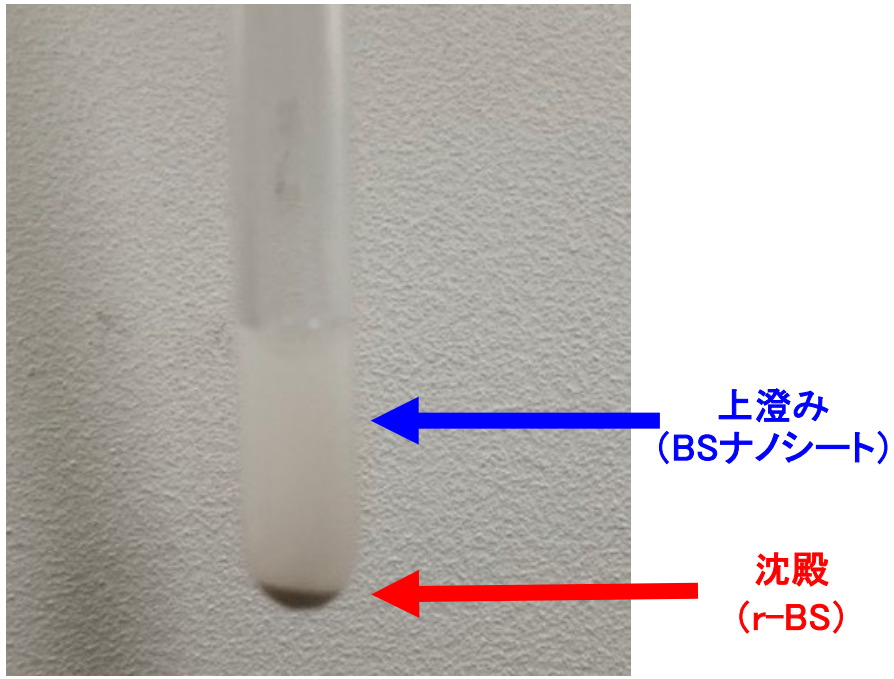

溶液に分散させることで、r-BSと硫化ホウ素ナノシートを分離できる

H. Kusaka, T. Kondo* et al., J. Mater. Chem. A 9 (2021) 24631-24640

EEM of r-BS and BS nanosheets

With Prof. M. Miyauchi

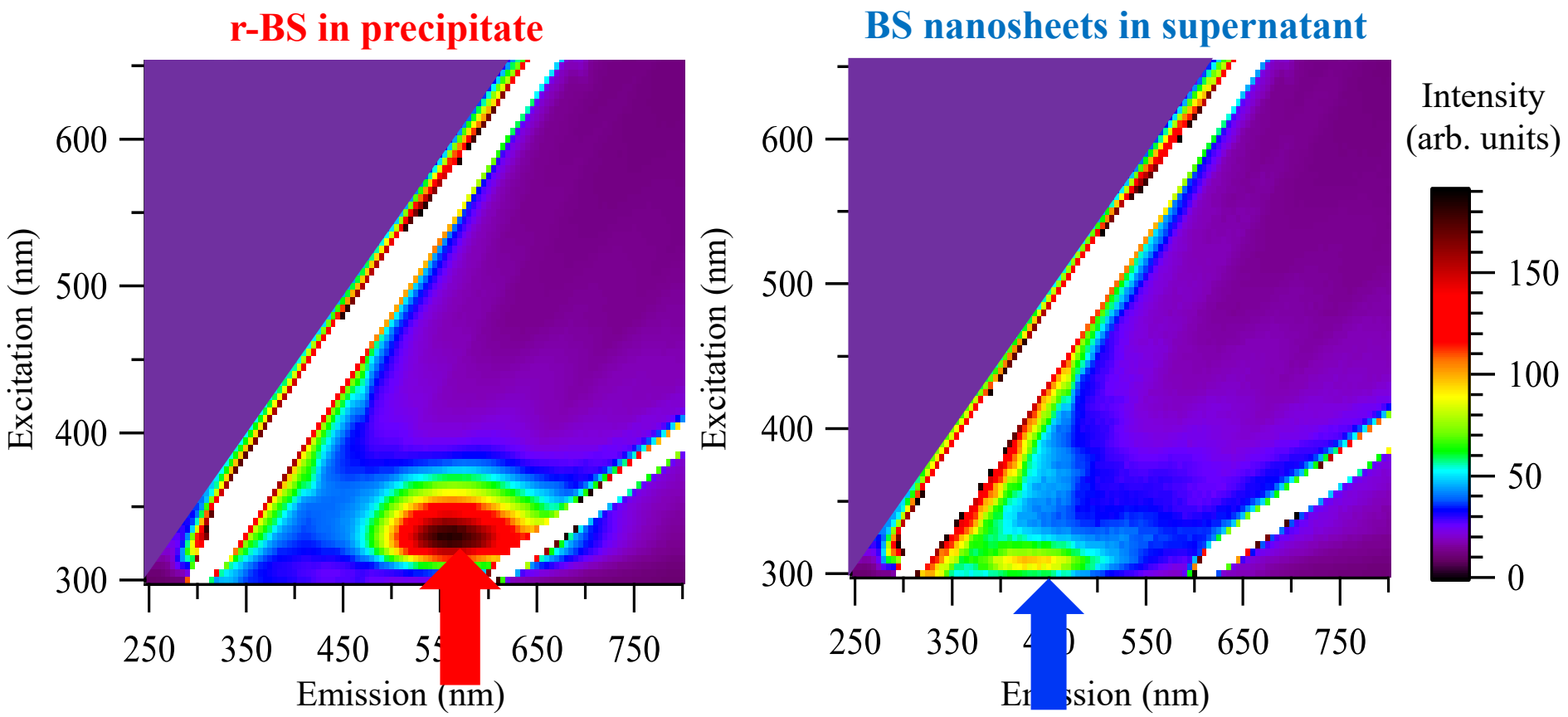

Corresponds to bulk r-BS

500-700 [nm]（1.77-2.48 eV）

Corresponds to 1-2 layers

400-500 [nm]（2.48-3.10 eV）

H. Kusaka, T. Kondo* et al., J. Mater. Chem. A 9 (2021) 24631-24640

SEM of r-BS and BS nanosheets

With Prof. M. Miyauchi

測定はSi上で行った

沈殿部分

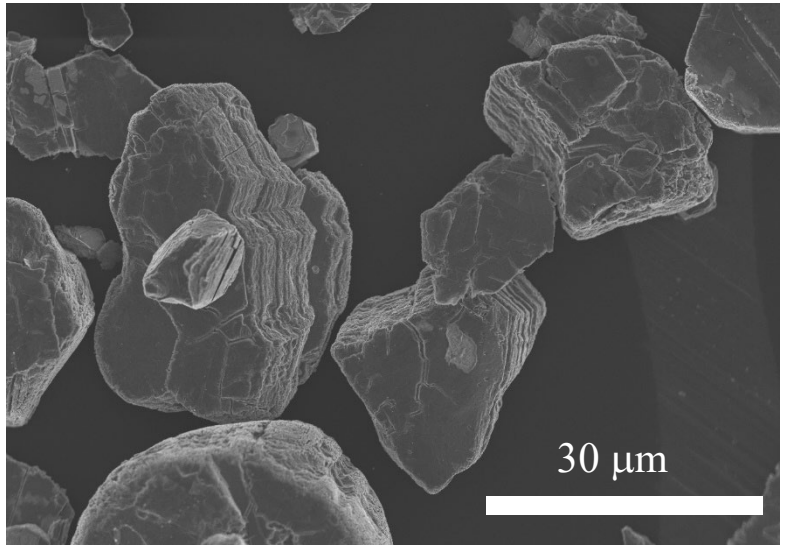

Stacked bulk r-BS

上澄み部分

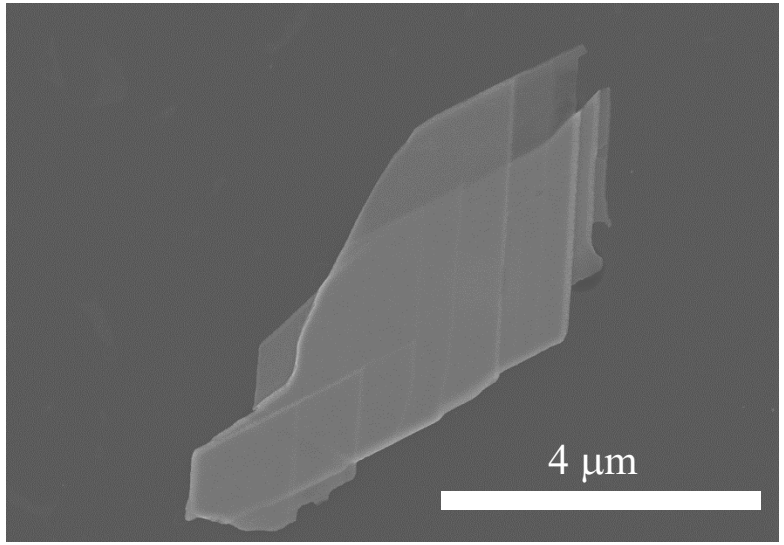

BS nanosheets

蛍光特性と対応して硫化ホウ素ナノシートの分離が示唆された

H. Kusaka, T. Kondo* et al., J. Mater. Chem. A 9 (2021) 24631-24640

AFM of supernatant (BS nanosheets)

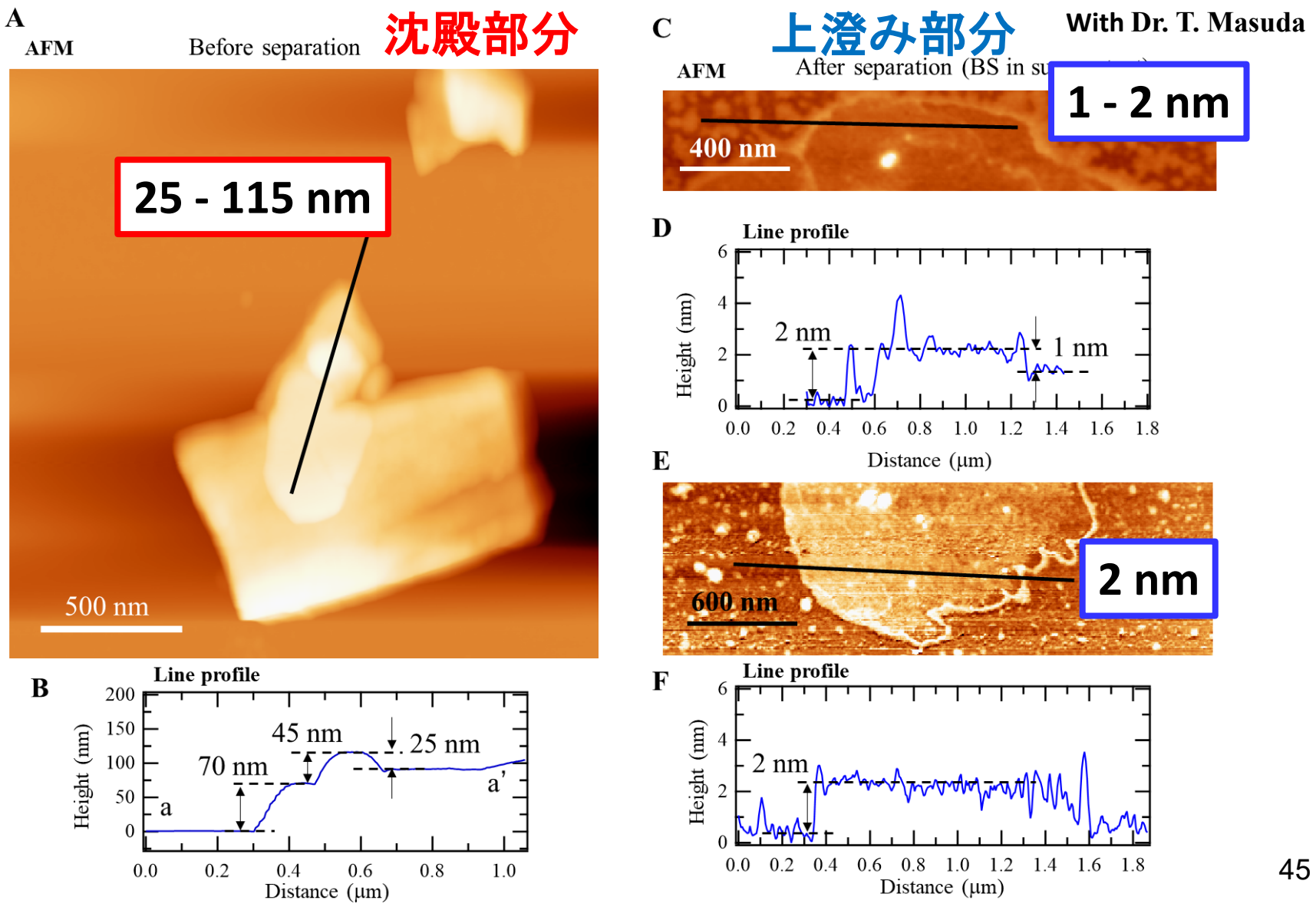

H. Kusaka, T. Kondo* et al., J. Mater. Chem. A 9 (2021) 24631-24640

XPS of supernatant (BS nanosheets) on Au

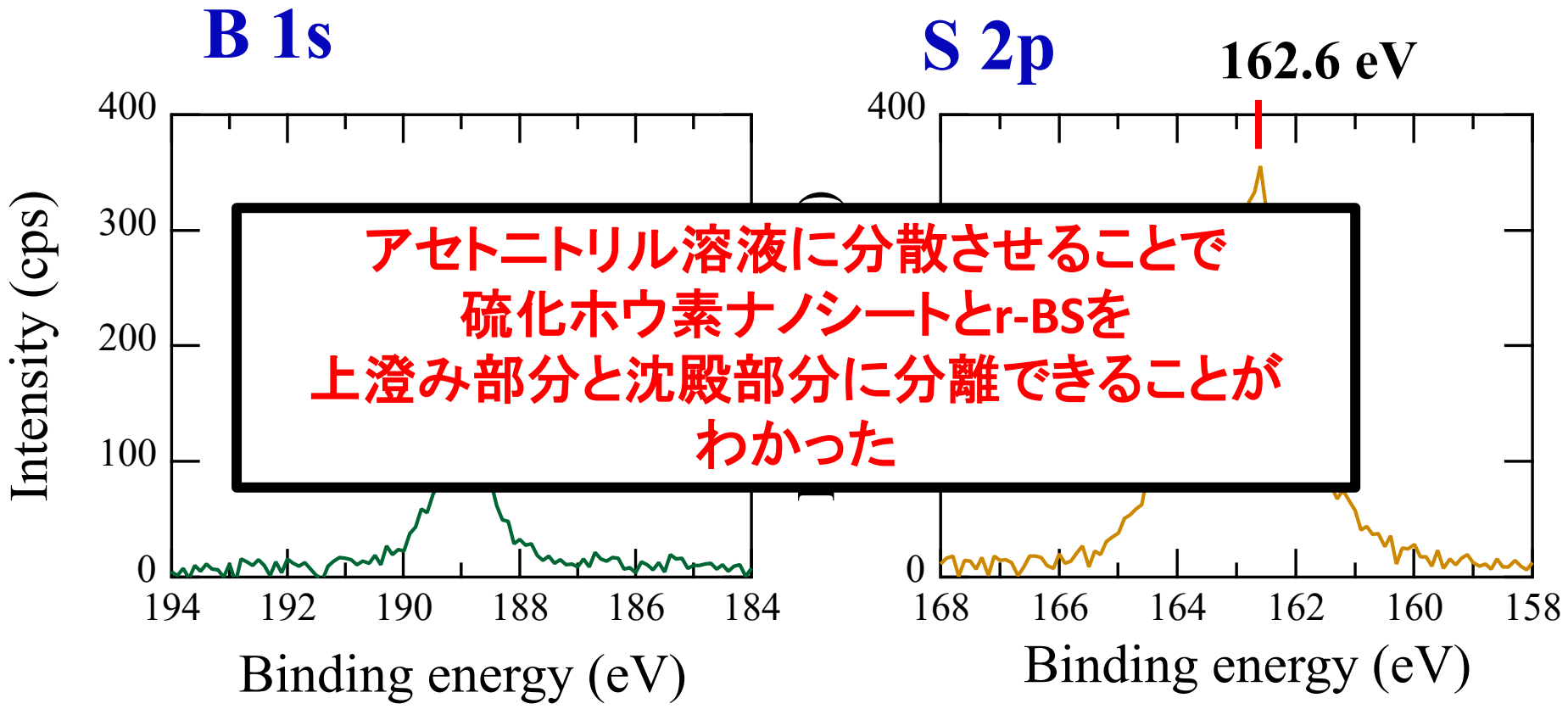

アセトニトリル溶液に分散させることで
硫化ホウ素ナノシートとr-BSを
上澄み部分と沈殿部分に分離できることが
わかった

AlKα (1486.6 eV)

XPS Sensitivity
B : 2.102, S: 7.186

B : S = 1.0 ±0.1 : 1.0 ±0.1

H. Kusaka, T. Kondo* et al., J. Mater. Chem. A 9 (2021) 24631-24640

XPS of BS nanosheets on Carbon with water

BS nanosheets on graphite tape

Distilled water droplet

After exposing to air atmosphere

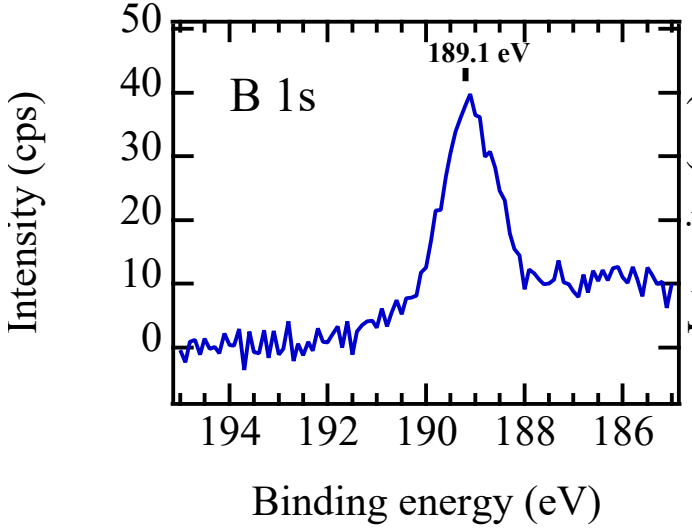

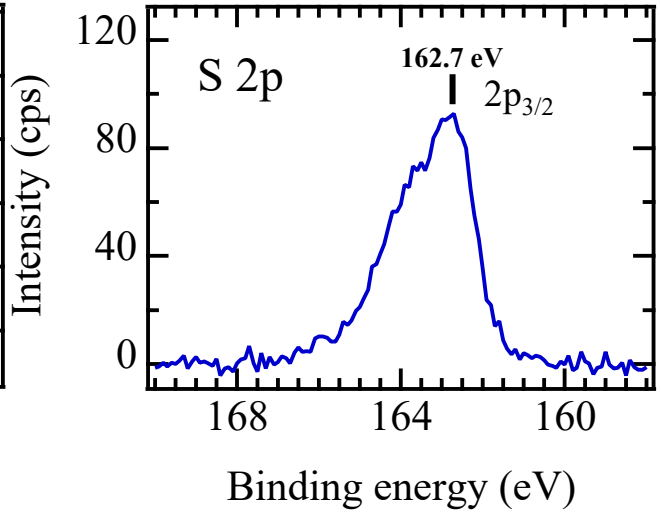

After drying water droplet

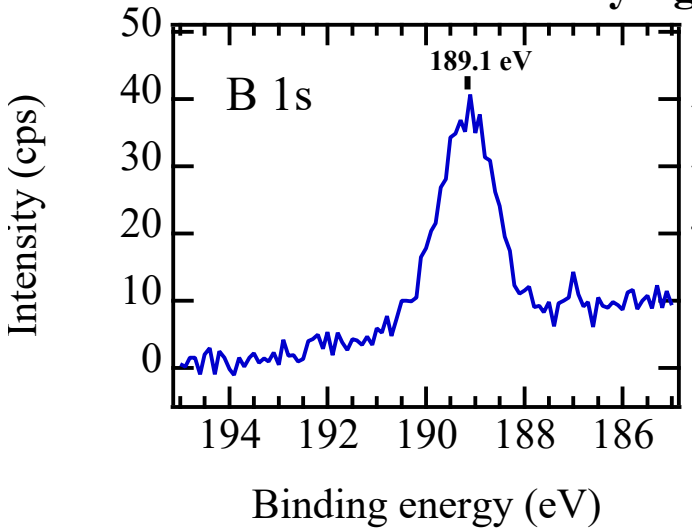

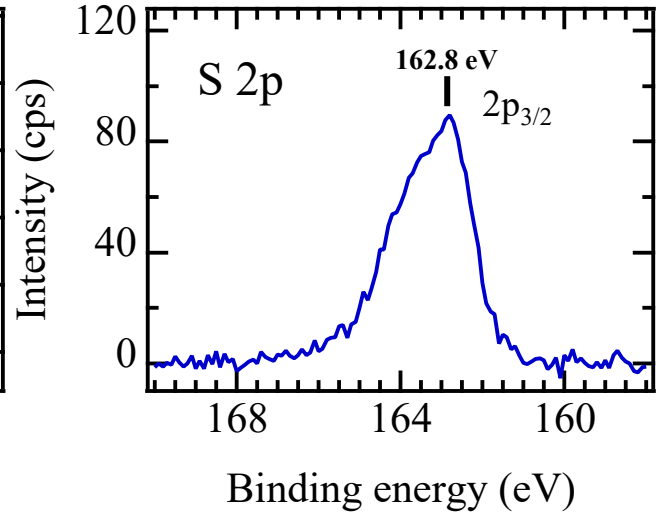

BS nanosheets are environmentally stable

H. Kusaka, T. Kondo* et al., J. Mater. Chem. A 9 (2021) 24631-24640

Synthesized r-BS is p-type semiconductor

Positive seebeck coefficient

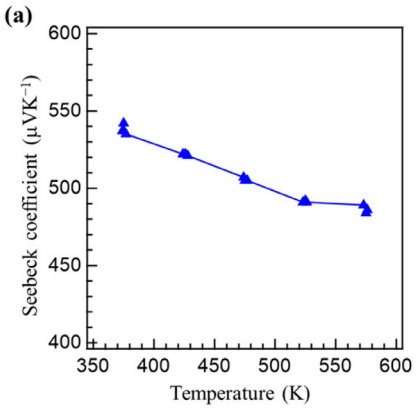

Synthesized r-BS is p-type

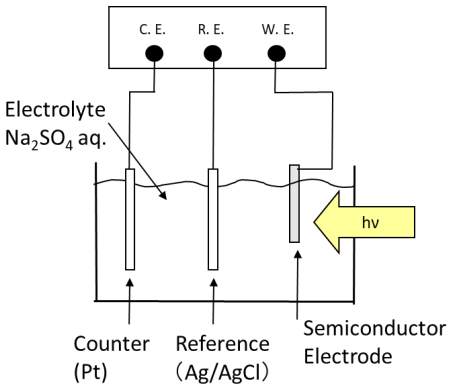

H-type cell
electrolyte : 0.5 M Na_2SO_4 (pH=7)
working: r-BS on carbon (drop cast)
counter : Pt
reference : Ag/AgCl
source: 150 Xe (all light)

Synthesized r-BS is p-type

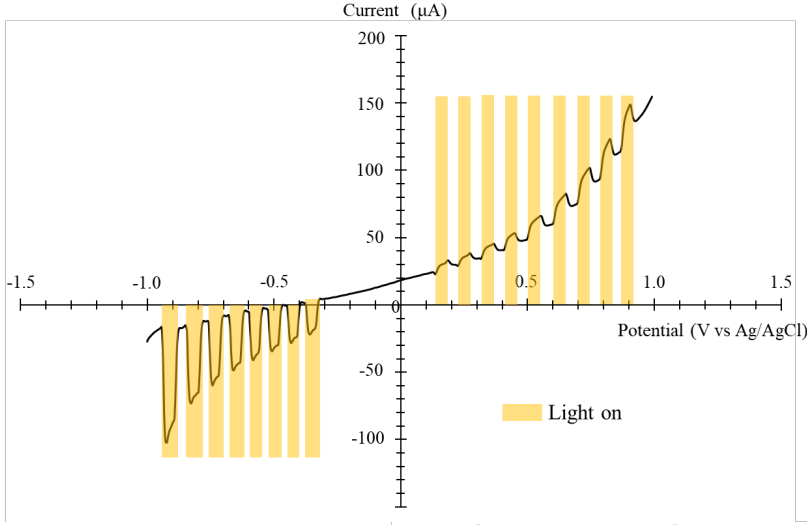

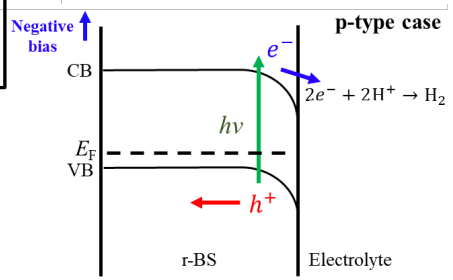

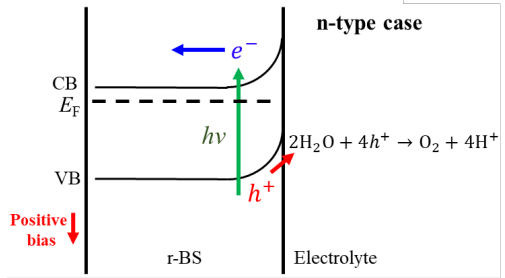

N. Watanabe, K. Miyazaki, M. Toyoda, K. Takeyasu, N. Tsujii, H. Kusaka, A. Yamamoto, S. Saito, M. Miyakawa, T. Taniguchi, T. Aizawa, T. Mori, M. Miyauchi, T. Kondo*
Molecules 28 (2023) 1896. (9 pages)

ARPES also shows p-type nature

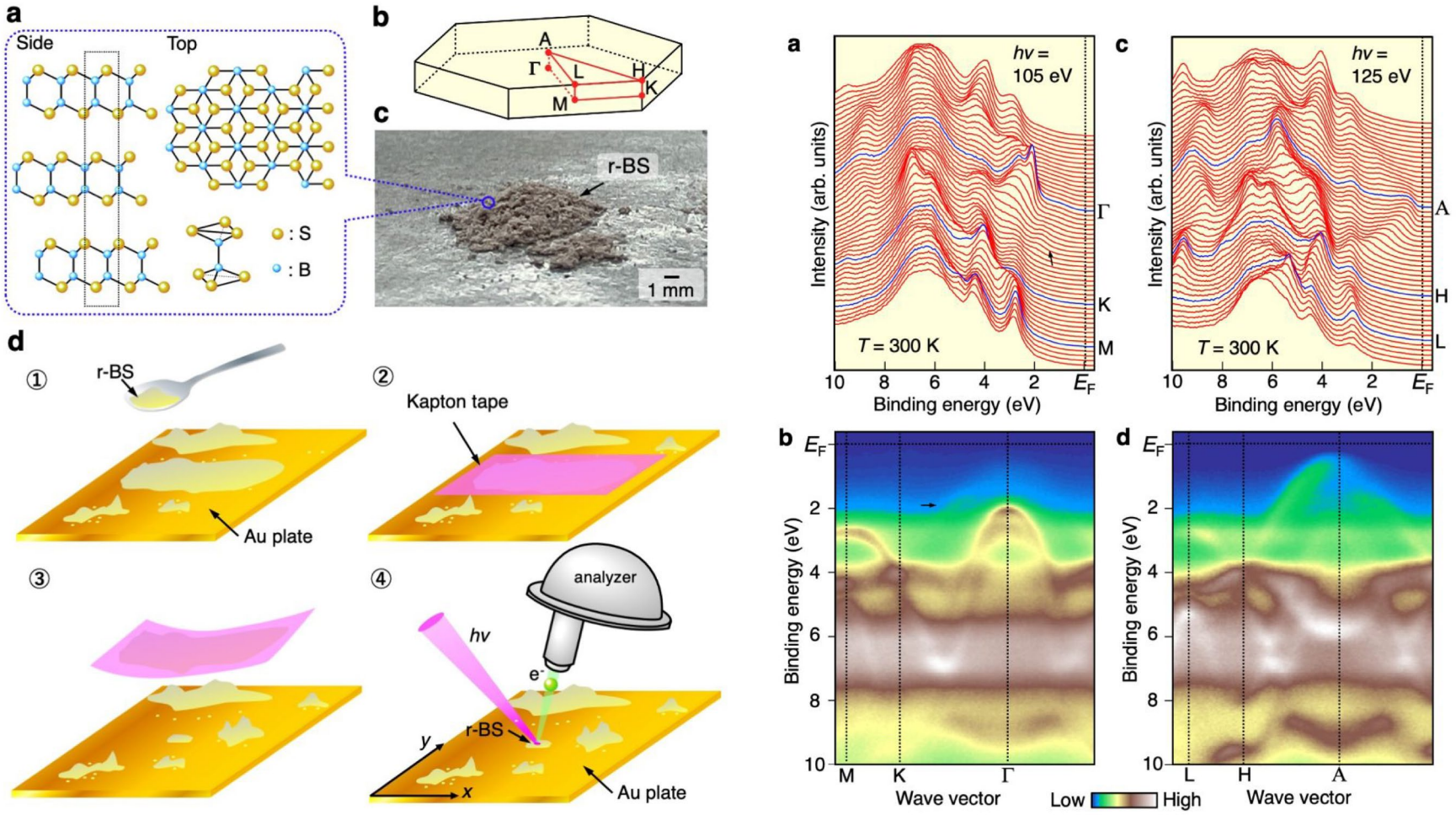

K. Sugawara, H. Kusaka, T. Kawakami, K. Yanagizawa, A. Honma, S. Souma, K. Nakayama, M. Miyakawa, T. Taniguchi, M. Kitamura, K. Horiba, H. Kumigashira, T. Takahashi, S. Orimo, M. Toyoda, S. Saito, T. Kondo, T. Sato, ***Nano Letters*** 23 (2023) 1673

ACS APPLIED MATERIALS & INTERFACES

我々より1年後に中国のグループが
BSナノシートを世界で初めて合成したと報告

www.acsami.org

Research Article

Experimental Realization and Computational Investigations of B_2S_2 as a New 2D Material with Potential Applications

Yibo Zhang, Ming Zhou,* Mingyang Yang, Jianwen Yu, Wenming Li, Xuyin Li, and Shijia Feng

Cite This: *ACS Appl. Mater. Interfaces* 2022, 14, 32330–32340

ABSTRACT: A new two-dimensional material B_2S_2 has been successfully synthesized for the first time and validated using first-principles calculations, with fundamental properties analyzed in detail. B_2S_2 has a similar structure as transition-metal dichalcogenides (TMDs) such as MoS_2, and the experimentally prepared free-standing B_2S_2 nanosheets show a uniform height profile lower than 1 nm. A thickness-modulated and unique oxidation-level dependent band gap of B_2S_2 is revealed by theoretical calculations, and vibration signatures are determined to offer a practical scheme for the characterization of B_2S_2. It is shown that the functionalized B_2S_2 is able to provide favorable sites for lithium adsorption with low diffusion barriers, and the prepared B_2S_2 shows a wide band photoluminescence response. These findings offer a feasible new and lighter member for the TMD-like 2D material family with potential for various aspects of applications, such as an anode material for Li-ion batteries and electronic and optoelectronic devices.

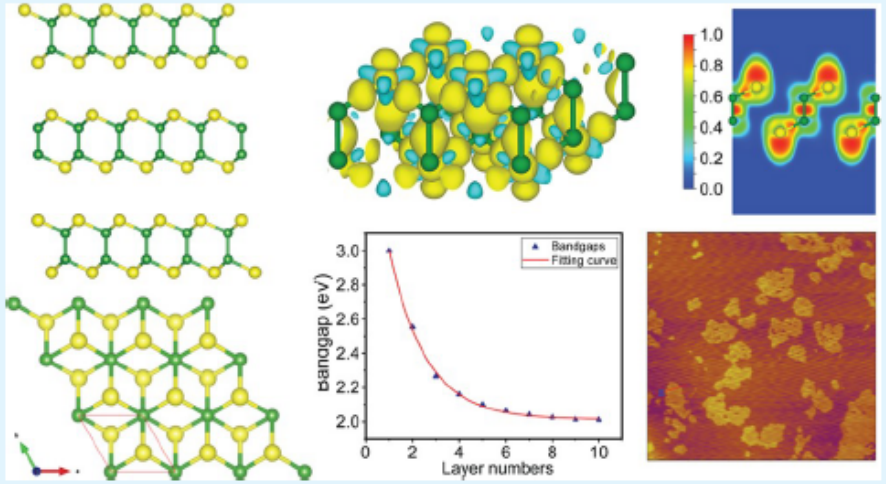

KEYWORDS: *boron disulfide, two-dimensional materials, material synthesis, first-principles calculations, potential applications*

Outline

1. 自己紹介

2. カーボンニュートラルの必要性と材料開発の重要性

3. 水素製造に貢献する材料開発
   典型元素を利用した高活性アルカリ水電解触媒
   - (1) 硫化ホウ素(r-BS)の合成と評価
   - (2) r-BSとグラフェンの混合物が示す高いOER触媒特性
   - (3) r-BSの活性点（MoS_2のHER活性点との比較）
   - (4) r-BS＋グラフェンOER触媒の高耐久性化

4. 水素利用に貢献する材料開発

5. 水素吸蔵に貢献する材料開発

r-BSに関する我々の論文報告 (2021-2023)

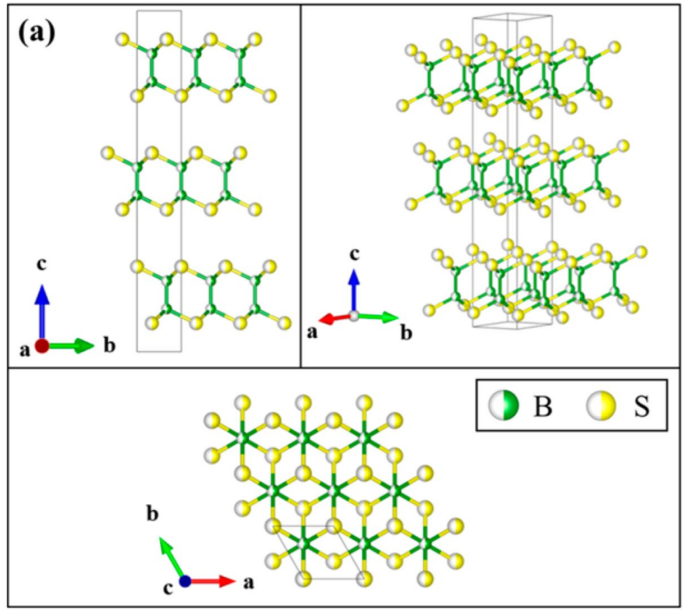

r-BS と BS ナノシートに関する報告

H. Kusaka, R. Ishibiki, T.K.*, et al., ***J. Mater. Chem. A*** 9 (2021) 24631.

合成したr-BS がp型半導体であることを明らかにした報告

N. Watanabe, T.K.*, et al., ***Molecules*** 28 (2023) 1896. (9 pages)

角度分解光電子分光によりr-BSのバンド構造を世界で初めて測定

K. Sugawara, T. K., T. Sato, et al., ***Nano Letters*** 23 (2023) 1673

r-BS とグラフェンの混合で市販RuO_2を上回る世界最高OER活性

L. Li, M. Otani, T. K.* et al., ***Chem. Eng. J.*** 471 (2023) 144489.

r-BS+graphene+Ni で100時間以上のOERの安定性実現

L. Li, T. K.*, et al., ***Sci. Tech. Adv. Mater.*** 24 (2023) 2277681.

r-BSのOERの触媒活性点候補を導出

S. Hagiwara, F. Kuroda, T. K., M. Otani,
ACS Appl. Mater. Interfaces 15 (2023) 50174.

r-BS に光触媒機能もあることを発見

K. Miyazaki, T. K.*, M. Miyauchi*, ***Sci. Rep.*** 13 (2023) 19540.

アルカリ水電解に必要な電極触媒

酸素生成反応
Oxygen evolution reaction (OER) (alakaline)
$4OH^- \rightarrow O_2 + 2H_2O + 4e^-$

水素生成反応
Hydrogen evolution reaction (HER) (alkaline)
$2H_2O + 2e^- \rightarrow H_2 + 2OH^-$

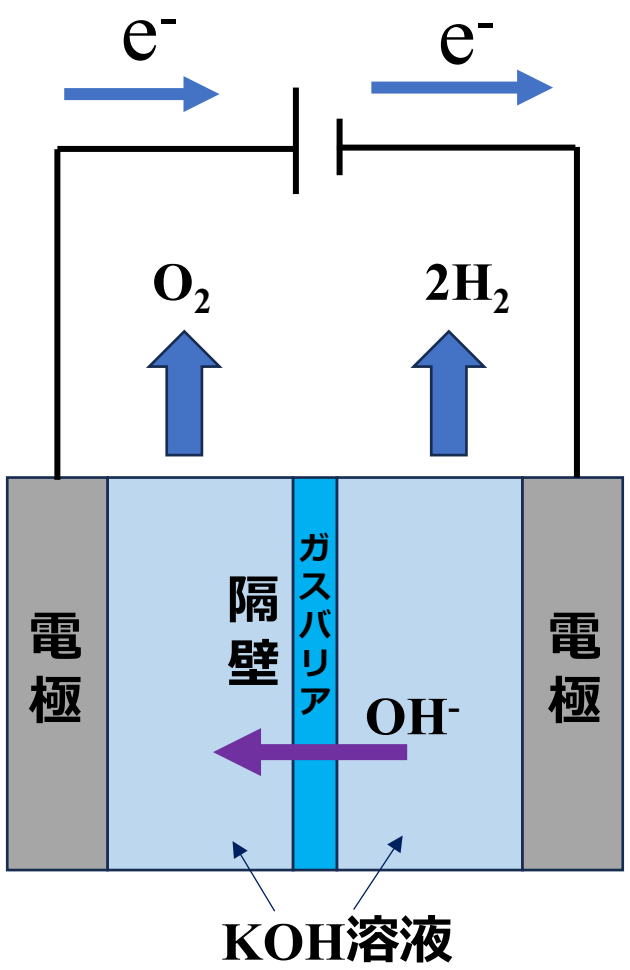

酸化極
アノード

還元極
カソード

触媒として
酸化イリジウム（IrO_2）や
酸化ルテニウム（RuO_2）
が用いられる

触媒として
白金（Pt）
が用いられる

特に4電子が絡む
OERの方で性能が
低いため問題

過電圧（1.23Vよりも余分に必要となってしまう電圧）を下げるために
性能の良い触媒材料を電極とする必要がある。
現在高価で希少なRuやIrやPtが用いられている

Hydrogen and Oxygen Evolution Reactions and Catalysts

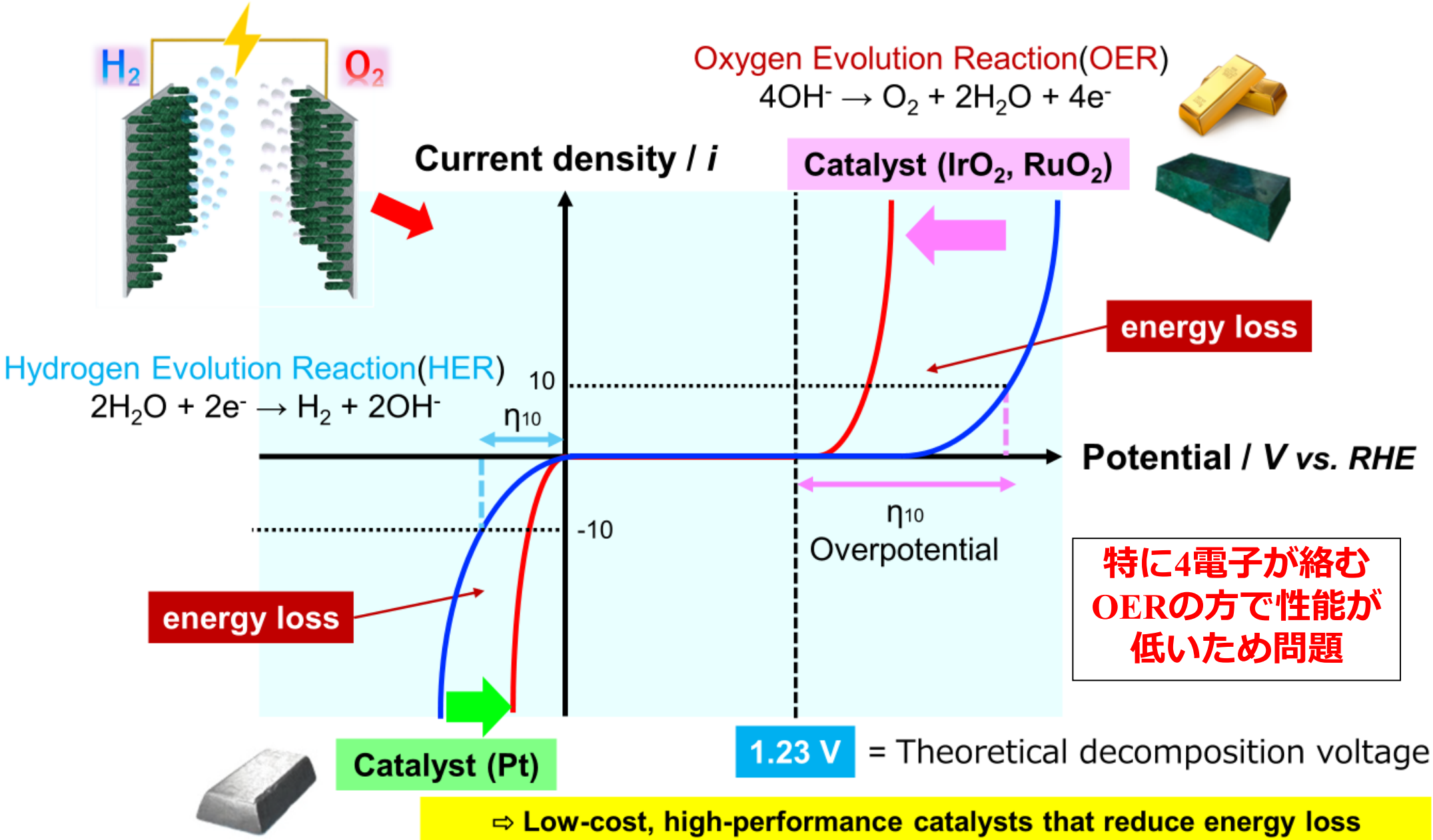

特に4電子が絡む
OERの方で性能が
低いため問題

⇨ **Low-cost, high-performance catalysts that reduce energy loss need to be explored.**

白金族表面はなぜ良い触媒機能を示すのか

酸素還元反応への
触媒活性度が高い

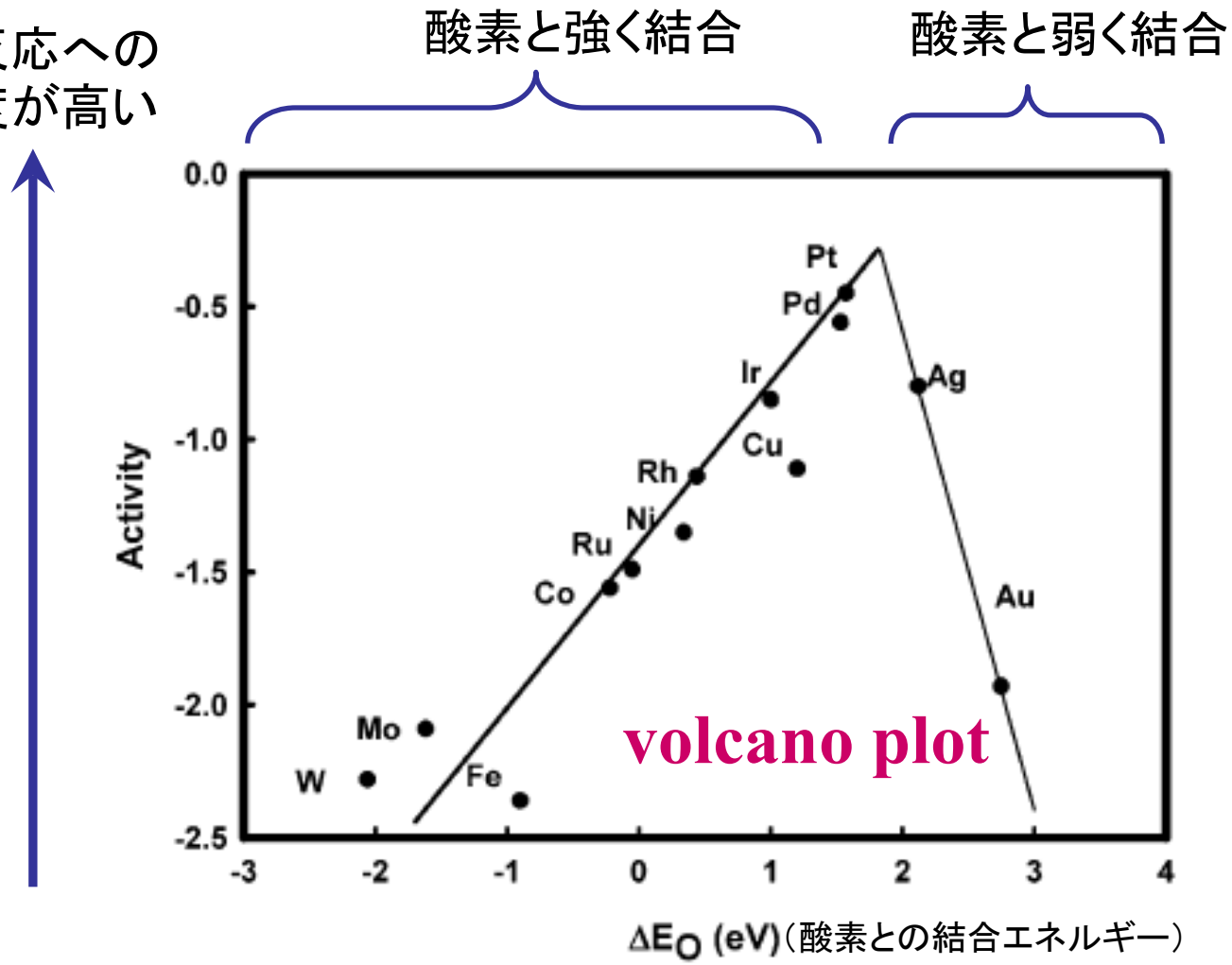

反応分子と弱すぎず強すぎない適度な結合を実現することが大事

（速度論的に好ましい吸着脱離を実現する触媒が高活性な触媒）

J. K. Nørskov et al., J. Phys. Chem. B **108** (2004) 17886

Sabatier principle

Paul Sabatier

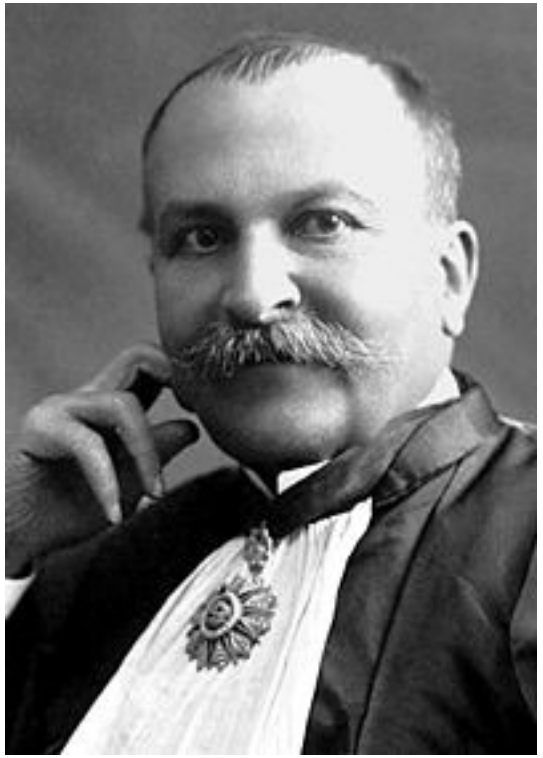

$$CO_2 + 4\,H_2 \xrightarrow[\text{pressure}]{400\ ^\circ C} CH_4 + 2\,H_2O$$

受賞年：1912年
受賞部門：ノーベル化学賞
受賞理由：微細な金属粒子を用いる有機化合物の水素化法の開発

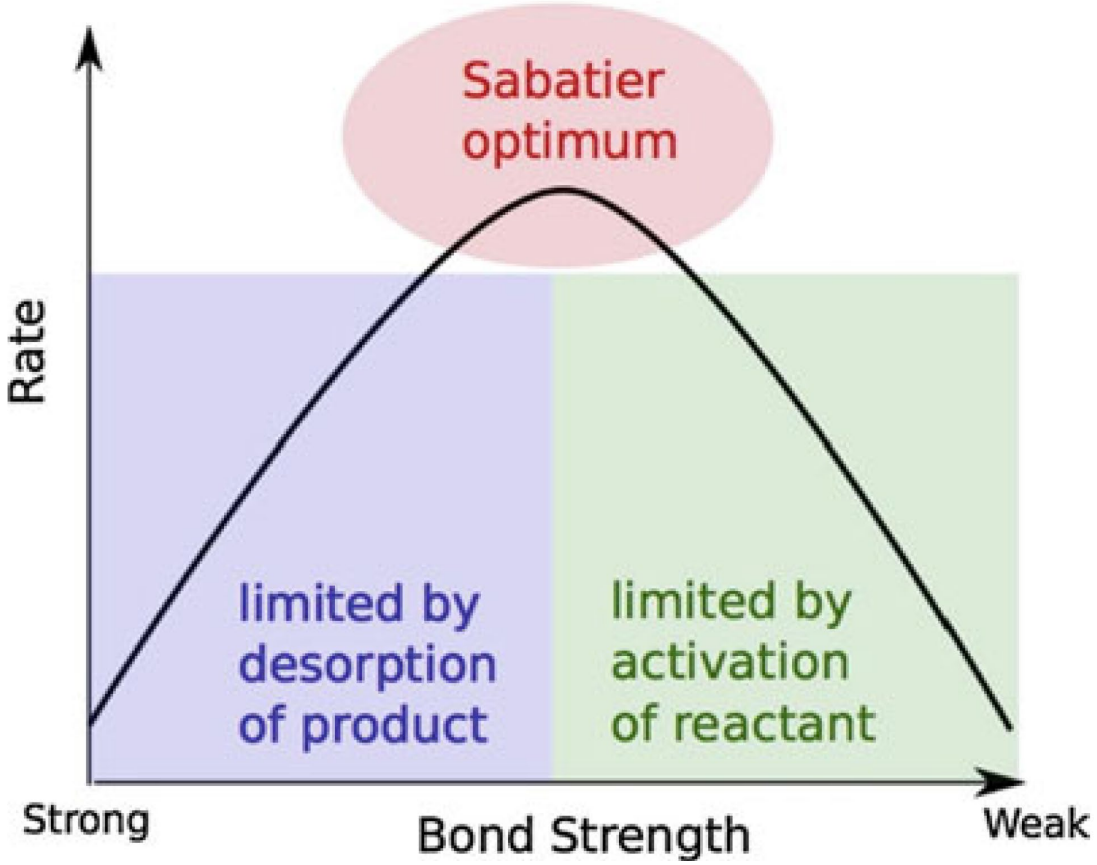

Fig. 3 Representation of the Sabatier principle. (Adapted from Medford et al. (2015))

Handbook of Materials Modeling,
Energy Trends in Adsorption at Surfaces, Springer, 2018

d-band center

d-band center:

Energy at the weighted center in the occupied region of d-band

フェルミエネルギーからd-bandの占有状態の重心位置までのエネルギー

B. Hammer and J. K. Nørskov, Nature **376** (1995) 238.

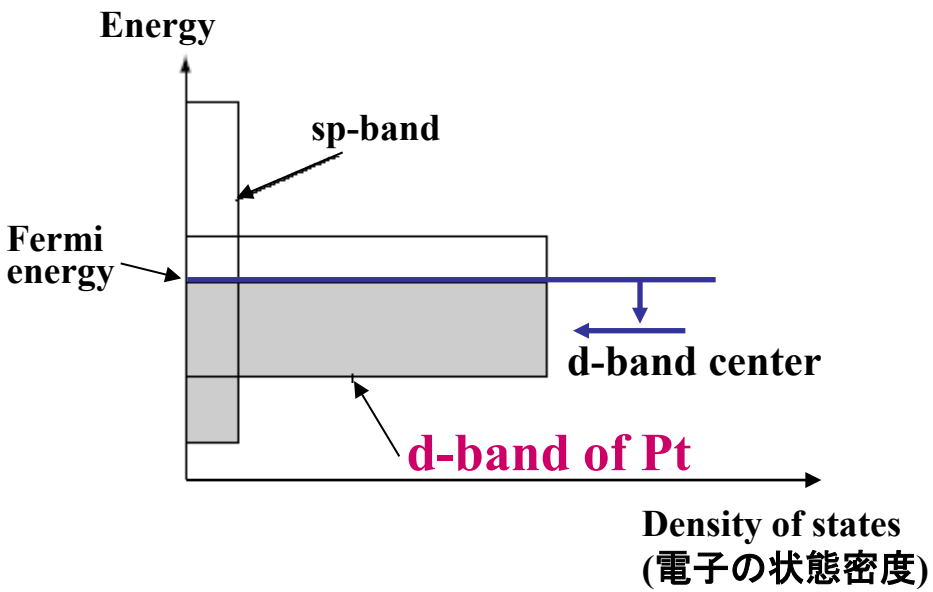

＊要注意

・d-band全体の中心ではなく占有しているところの重心です。

・d-bandという言葉は炭素材料のラマン散乱でも出てきますが全く違う意味なので要注意）

“d-band center” is indicator of adsorption energy and thus indicator of catalytic activity

Why gold is the noblest of all the metals

B. Hammer*† & J. K. Nørskov*

* Centre for Atomic-scale Materials Physics, Physics Department, Technical University of Denmark, DK-2800 Lyngby, Denmark
† Joint Research Center for Atom Technology (JRCAT), 1-1-4 Higashi, Tsukuba, Ibaraki 305, Japan

NATURE · VOL 376 · 20 JULY 1995

THE unique role that gold plays in society is to a large extent related to the fact that it is the most noble of all metals: it is the least reactive metal towards atoms or molecules at the interface with a gas or a liquid. The inertness of gold does not reflect a general inability to form chemical bonds, however—gold forms very stable alloys with many other metals. To understand the nobleness of gold, we have studied a simple surface reaction, the dissociation of H_2 on the surface of gold and of three other metals (copper, nickel and platinum) that lie close to it in the periodic table. We present self-consistent density-functional calculations of the activation barriers and chemisorption energies which clearly illustrate that nobleness is related to two factors: the degree of filling of the antibonding states on adsorption, and the degree of orbital overlap with the adsorbate. These two factors, which determine both the strength of the adsorbate–metal interaction and the energy barrier for dissociation, operate together to the maximal detriment of adsorbate binding and subsequent reactivity on gold.

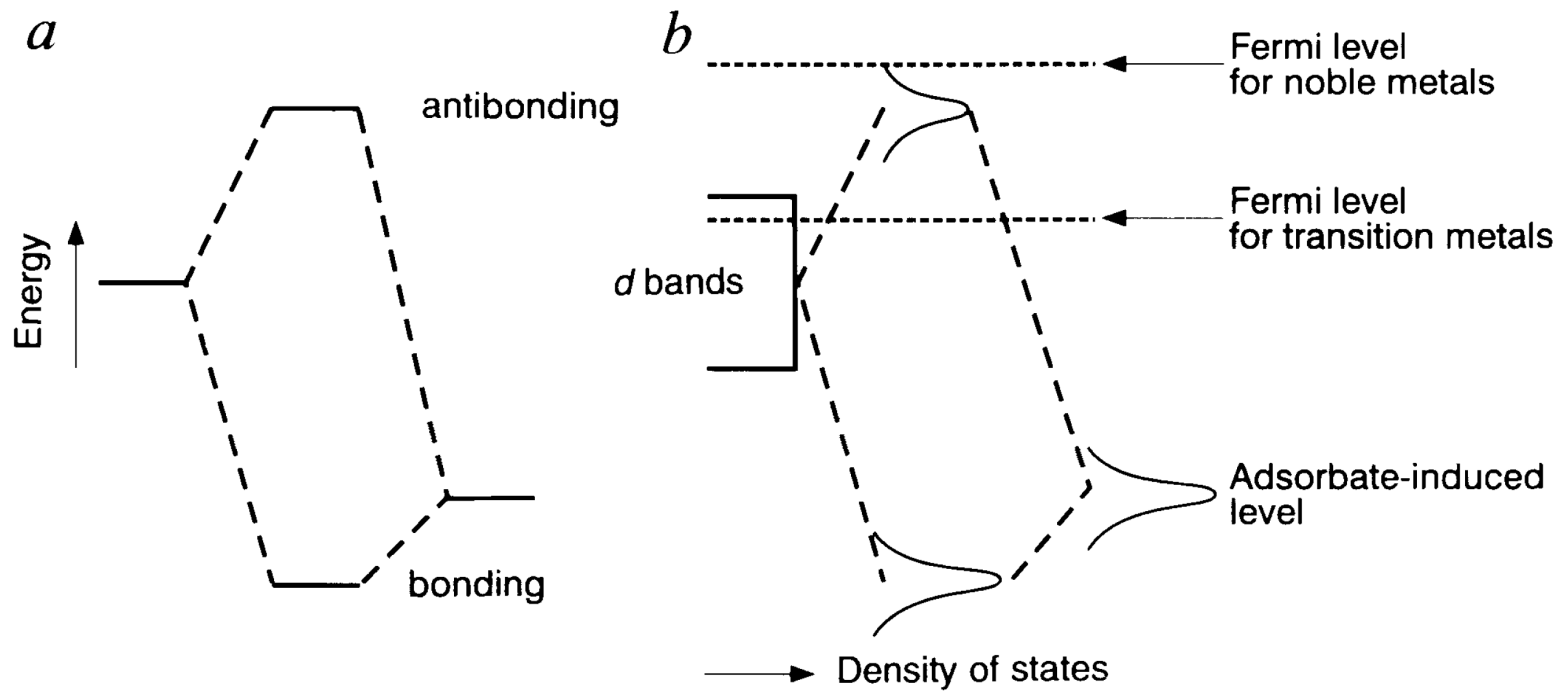

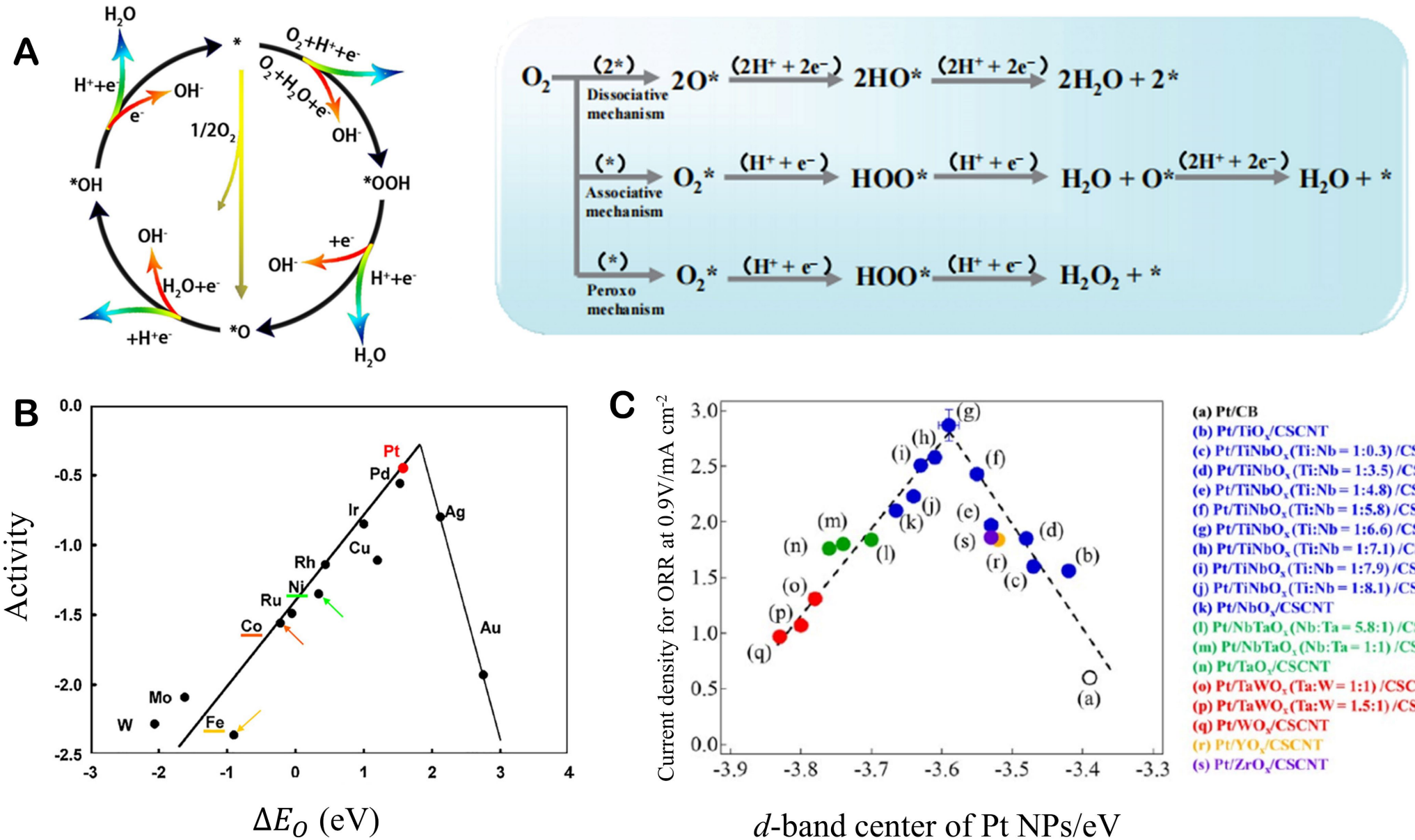

反応分子と弱すぎず強すぎない適度な結合を実現することが大事

d-bandの重心が浅すぎず深すぎないレベルであることに対応

Prog Mater Sci 2021;116:100717.
J Phys Chem B 2004;108:17886-92.
ACS Catal 2021;11:9317-32.
Microstructures 2023;3:2023025.

性能の良い白金族元素は希少金属（レアメタル）

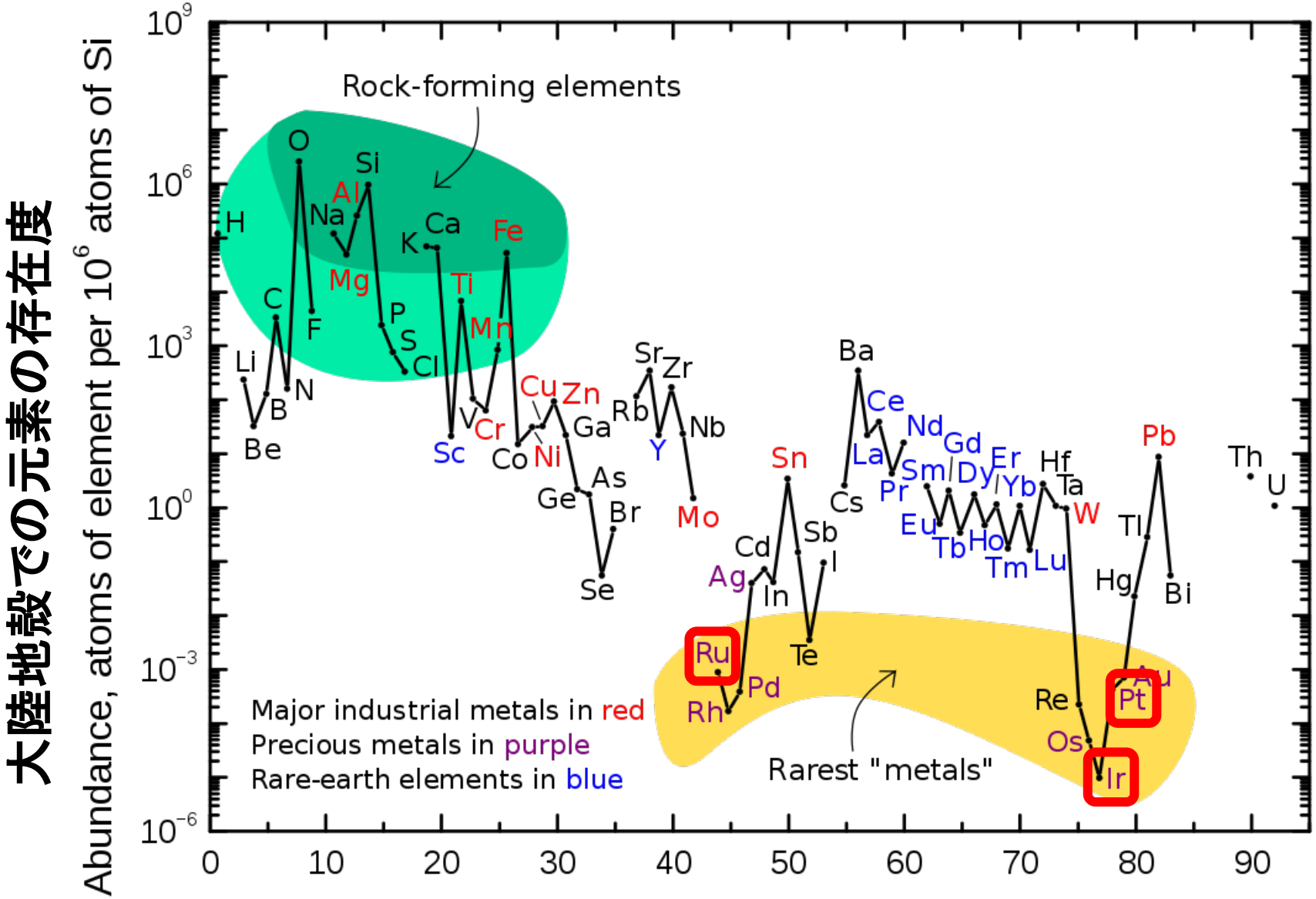

https://ja.wikipedia.org/wiki/地殻中の元素の存在度

白金族以外のOER触媒候補は主に金属材料

Current discussion about OER electrocatalyst basically focuses on
Metal-based materials

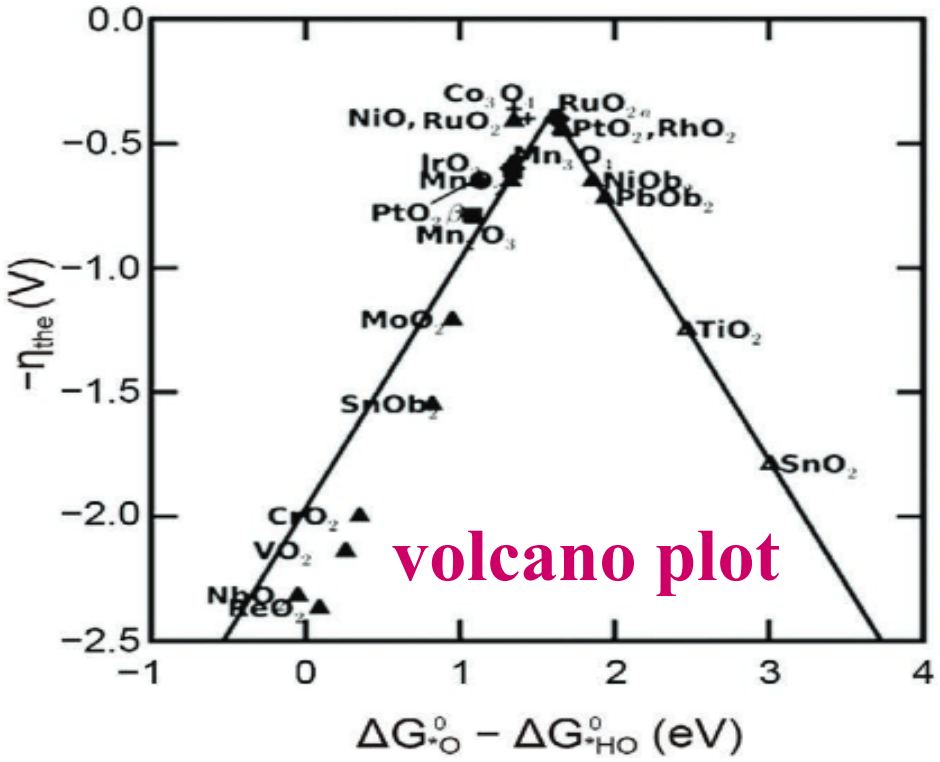

Fig.1 The volcano plot illustrating the relationship between the OER activities against the standard free energy of $\Delta G^0_{*O} - \Delta G^0_{*OH}$, on a set of OER catalysts.

I. C. Man, H. Y. Su, F. Calle-Vallejo, et al. ChemCatChem 2011, 3, 1159.

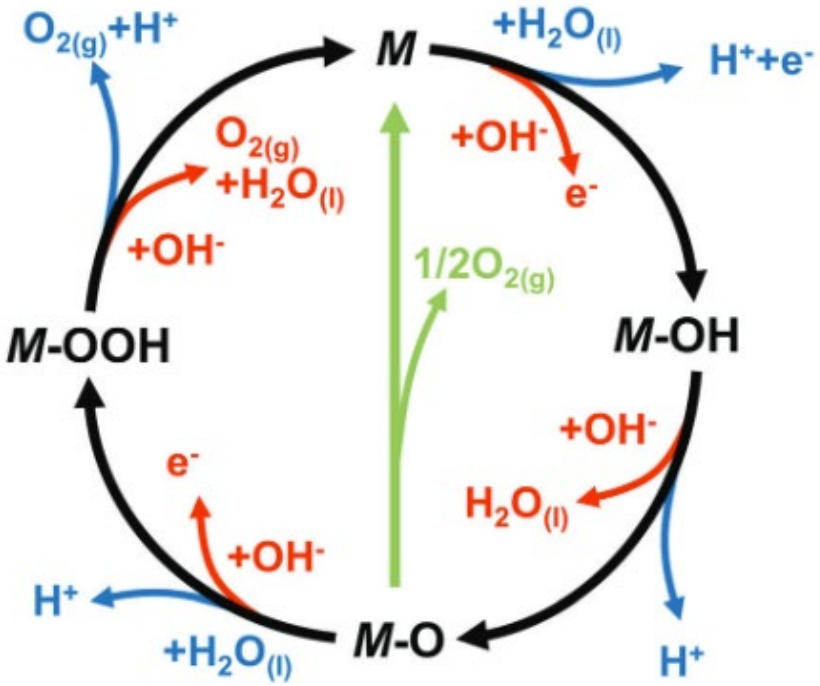

Fig. 2 The OER mechanism for acid (blue line) and alkaline (red line)conditions. The black line indicates that the oxygen evolution involves the formation of a peroxide (M–OOH) intermediate (black line) while another route for direct reaction of two adjacent oxo (M–O) intermediates (green)to produce oxygen is possible as well.

N. T. Suen, S. F. Hung, Q. Quan, et al. Chem. Soc. Rev. 2017, 46, 337-365.

アルカリ水電解に必要な電極触媒の課題

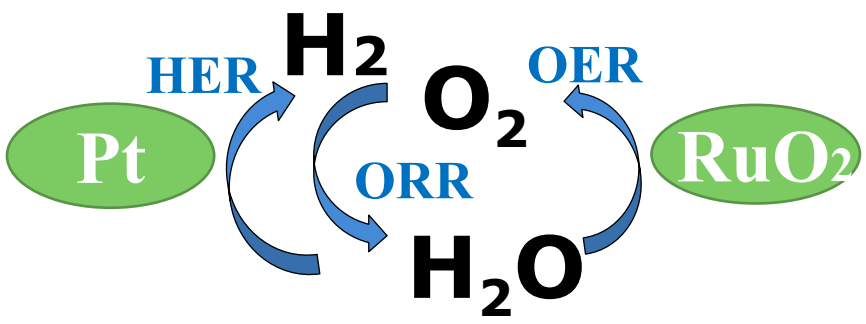

大きな課題:

Low abundance

high prices

poor stability

Designing high activity and low-cost catalysts

Important factors

Structure

methods

High dispersion of active sites

Multilevel channel

Large specific surface area

Efficient utilization of active sites

Components

methods

Metal-free element

Transition metal

High activity and stability

ORR: Oxygen reduction reaction

$O_2 + 2H_2O + 4e^- \rightarrow 4OH^-$

or $O_2 + 2H_2O + 2e^- \rightarrow 2H_2O_2$

現在IrO_2 や RuO_2 を使用
(高くて地球上に少ない物質)

安くて豊富な材料で
高性能な電極触媒が必要

典型元素を利用することに
主眼を置いた材料である
r-BSで解決

水素生成

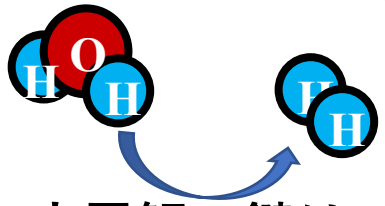

水電解：鍵は
電極触媒材料

Dr. Li-san (Graduated at 2024)

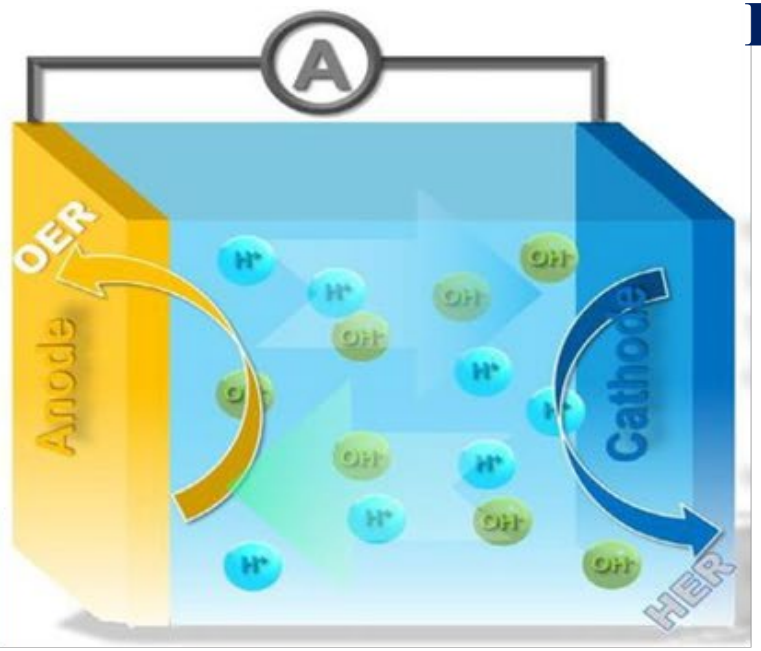

水電解装置

酸素発生反応
(*OER*：Oxygen Evolution Reaction)

OER (alakaline)

$$4OH^- \rightarrow O_2 + 2H_2O + 4e^-$$

水素発生反応
(*HER*：Hydrogen Evolution Reaction)

HER (alkaline)

$$2H_2O + 2e^- \rightarrow H_2 + 2OH^-$$

L. Li, M. Otani, T. K.* et al., *Chem. Eng. J.* 471 (2023) 144489.

BもSも大陸地殻に豊富に存在する元素

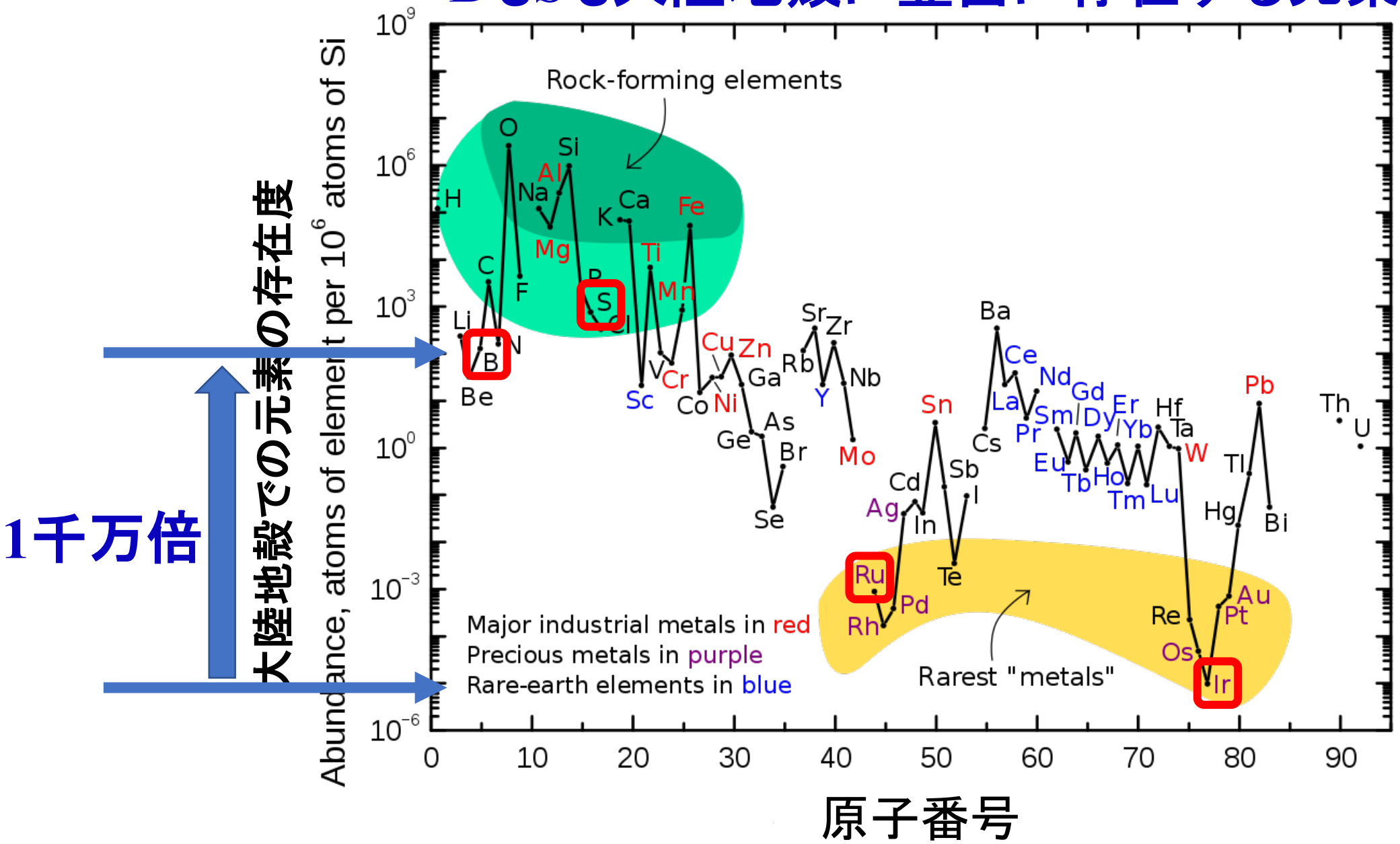

https://ja.wikipedia.org/wiki/地殻中の元素の存在度

r-BS+Gの調製

菱面体硫化ホウ素 (r-BS) に グラフェンを添加 ⇒ r-BS + G

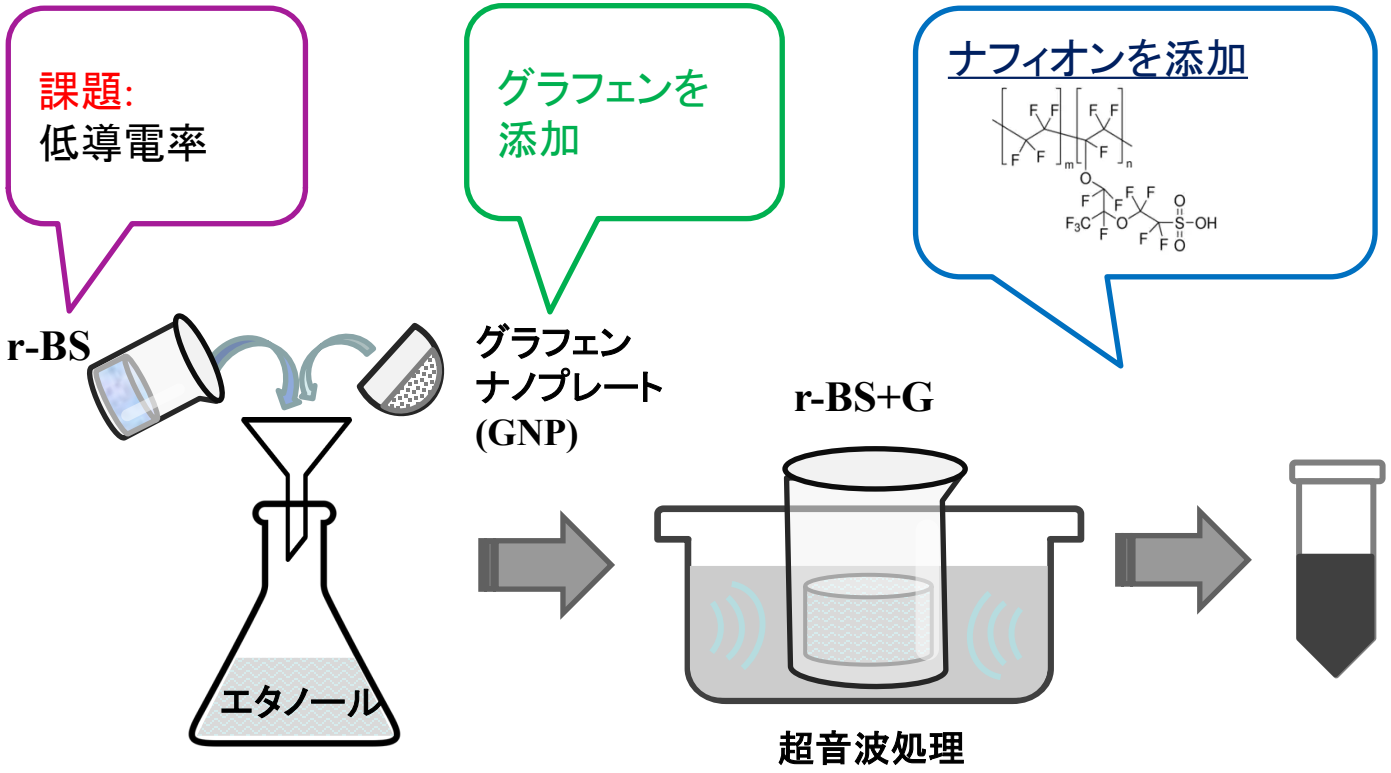

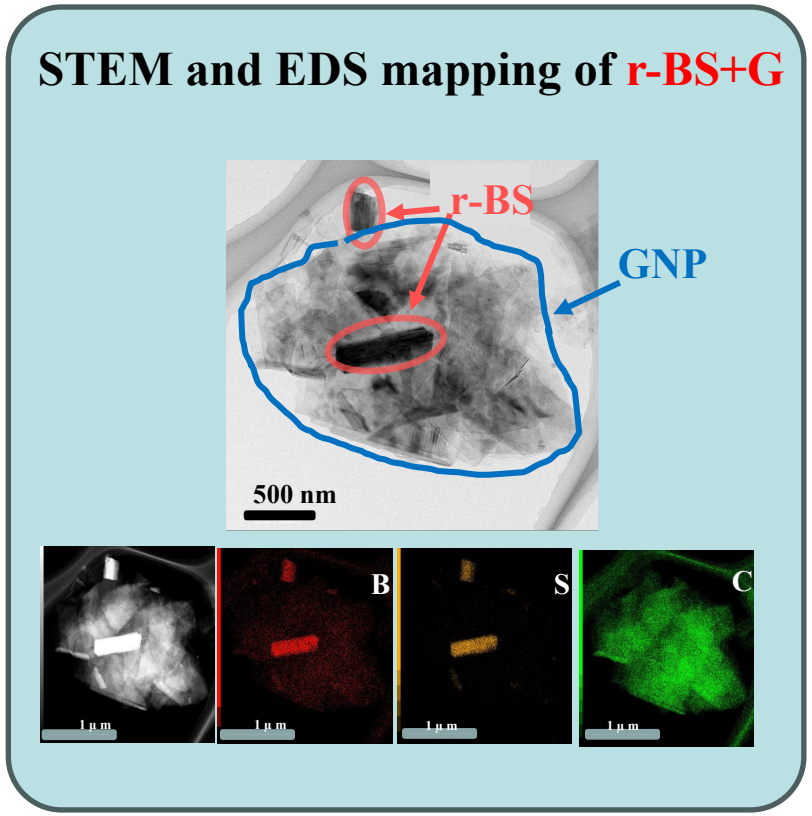

L. Li, T. Kondo, et al. *Chem. Eng. J.* 471, 144489. (2023).

Electronic and atomic coordination structures

X-ray diffraction (**XRD**) patterns of samples

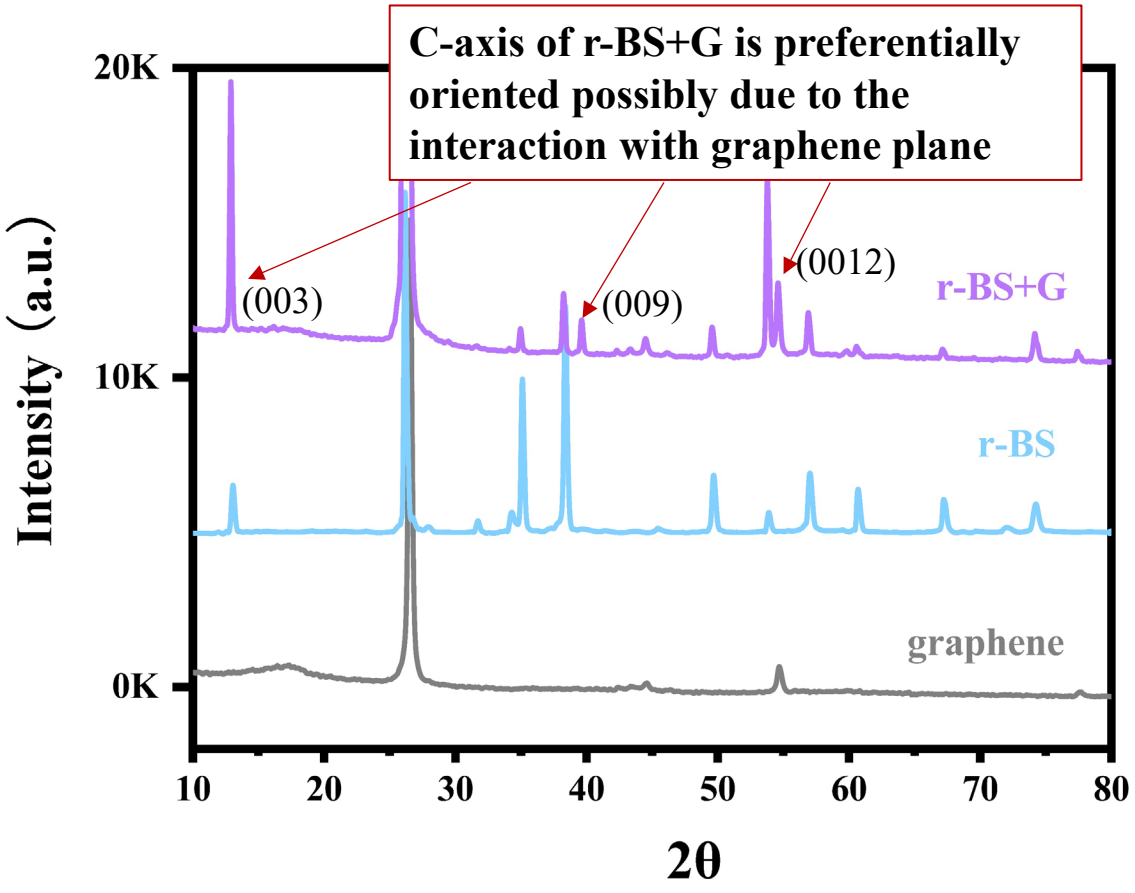

X-ray photoelectron spectroscopy (**XPS**) of **r-BS+G**

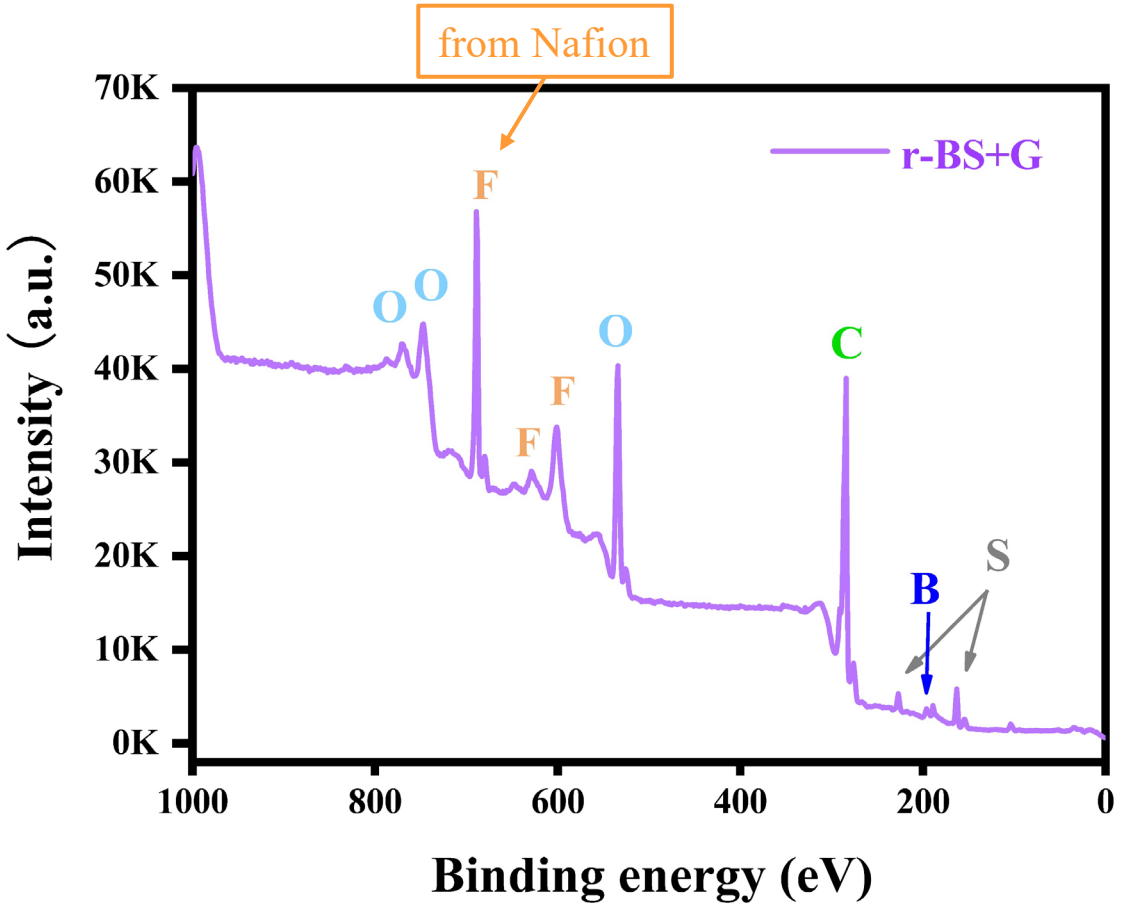

r-BS+G is the mixture of r-BS and GNP, **no reaction, no impurities**.

r-BS+Gの電気化学的特性

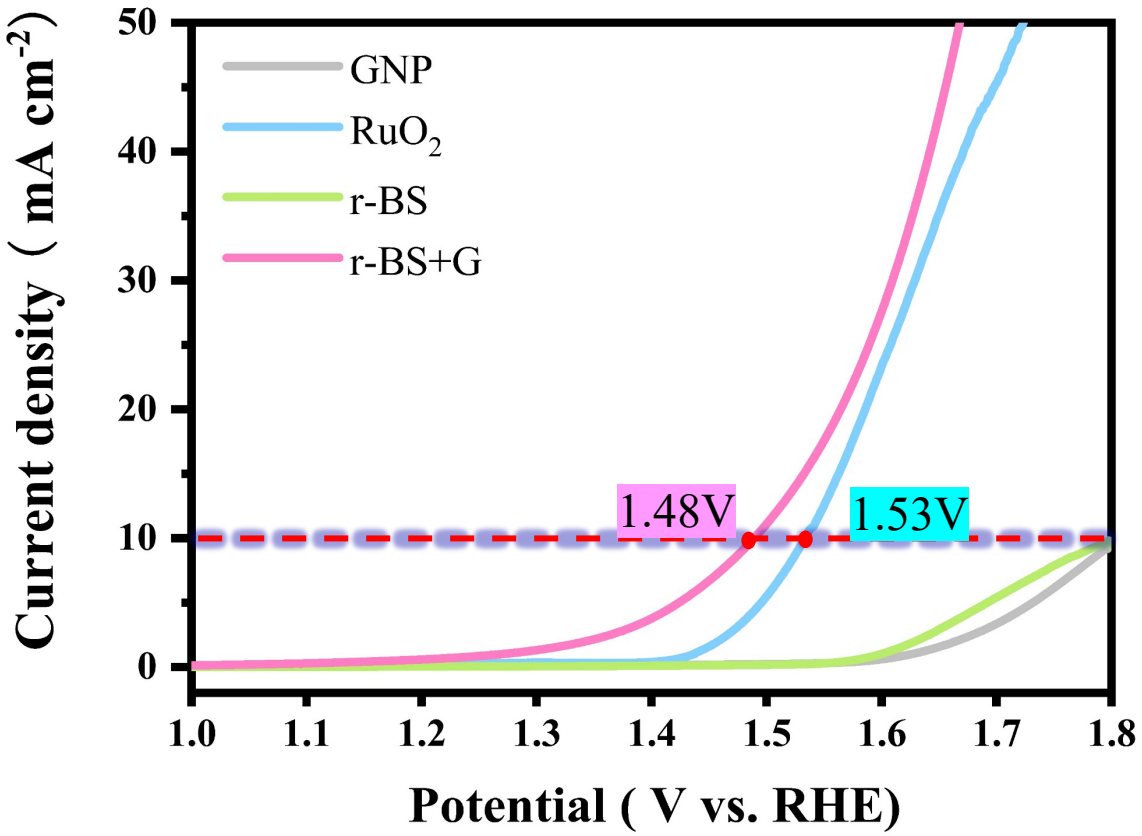

RHE: Reversible Hydrogen Electrode（可逆水素電極）

アルカリ電解質（1M KOH）中のガラス炭素電極（GCE）の3電極システムで測定

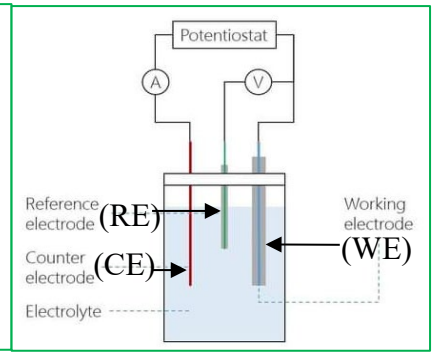

25 ℃
RE: Hg/HgO or Ag/AgCl
1.0 M KOH
LSV 2 mV/s

※ 過電位（Overpotential）
= (実験電位 – 熱力学 (1.23V)) の絶対値

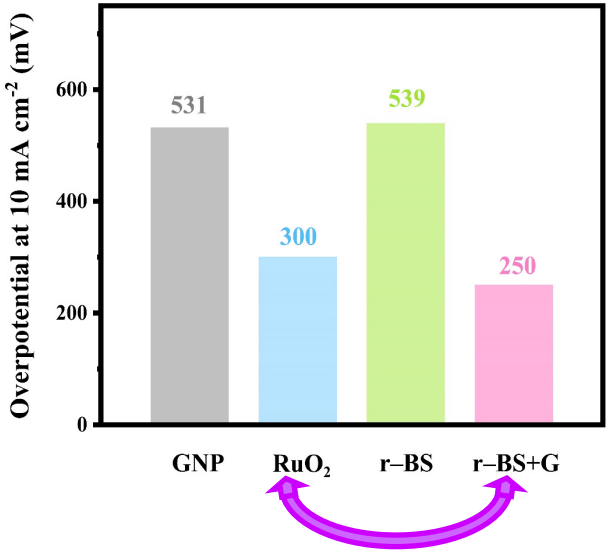

商用のRuO_2より50 mV低い

L. Li, T. Kondo, et al. *Chem. Eng. J.* 471, 144489. (2023).

Electrochemical performance of other samples

25 °C
RE: Hg/HgO or Ag/AgCl
1.0 M KOH
LSV 2 mV/s

LSV curves of **B+S+G** mixture

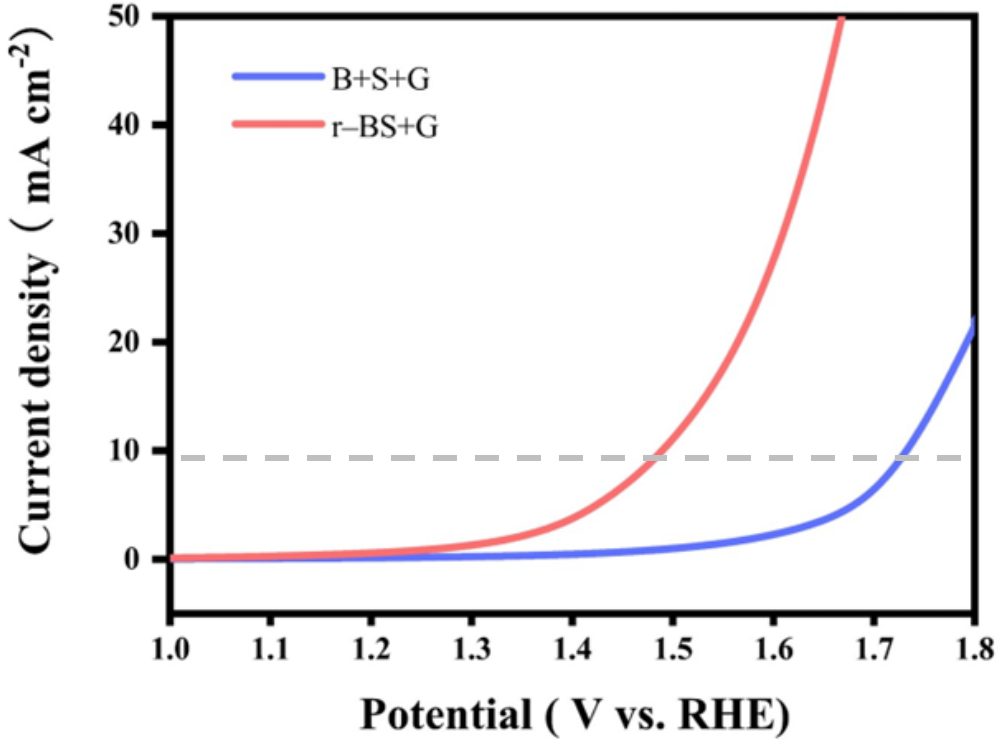

B+S+G mixture: The molar mass ratio of B to S was 1:1, which is the same as that used in r-BS synthesis. The mass ratio of B+S mixture to GNP was 1:2, which is the same as that of r-BS+G, keep the amont of (B+S) is 5 mg.

LSV curves of r-BS+ CB/CNT

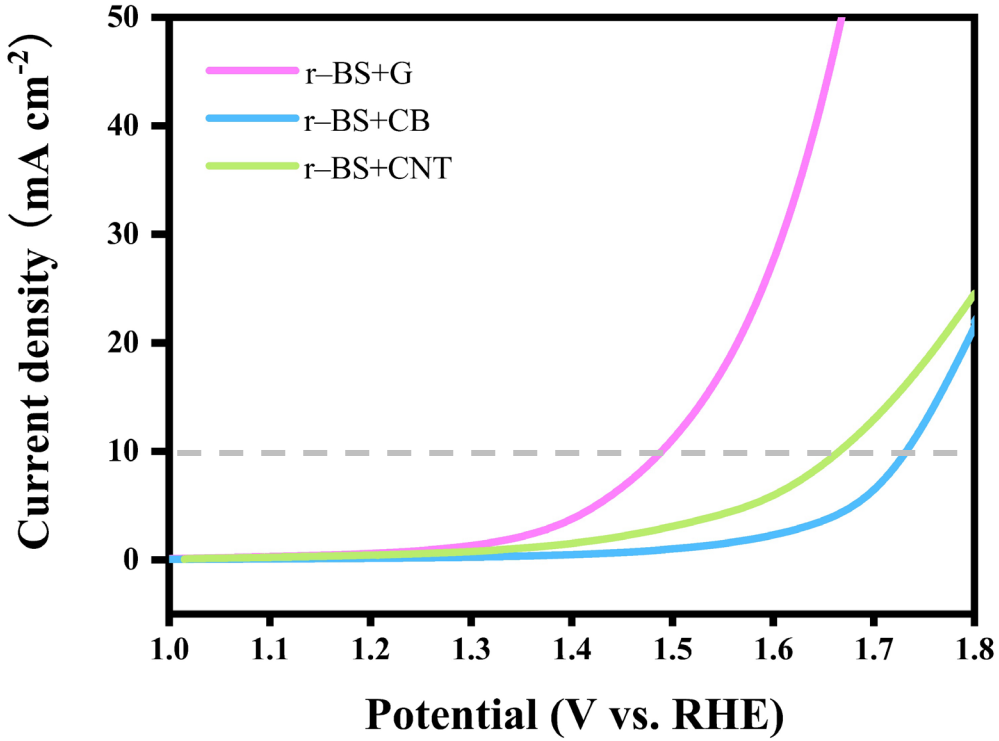

r-BS+carbon black (CB)/ carbon nanotubes (CNT): 5mg r-BS , and 10 mg of CNT/CB were dispersed in 1 mL of ethanol with 25 μL of Nafion, then followed by 1 h sonication

♦Superior electrocatalytic performance of r-BS+G was not produced by a simple mixture of B,S and GNP, indicating **that r-BS is essential** for the high catalytic activity.
♦The **choice of carbon material** also had a huge influence on the properties.

How about the mass ratio?

LSV curves of r-BS mixed with GNP in **different mass ratios**

25 ℃
RE: Hg/HgO or Ag/AgCl
1.0 M KOH
LSV 2 mV/s

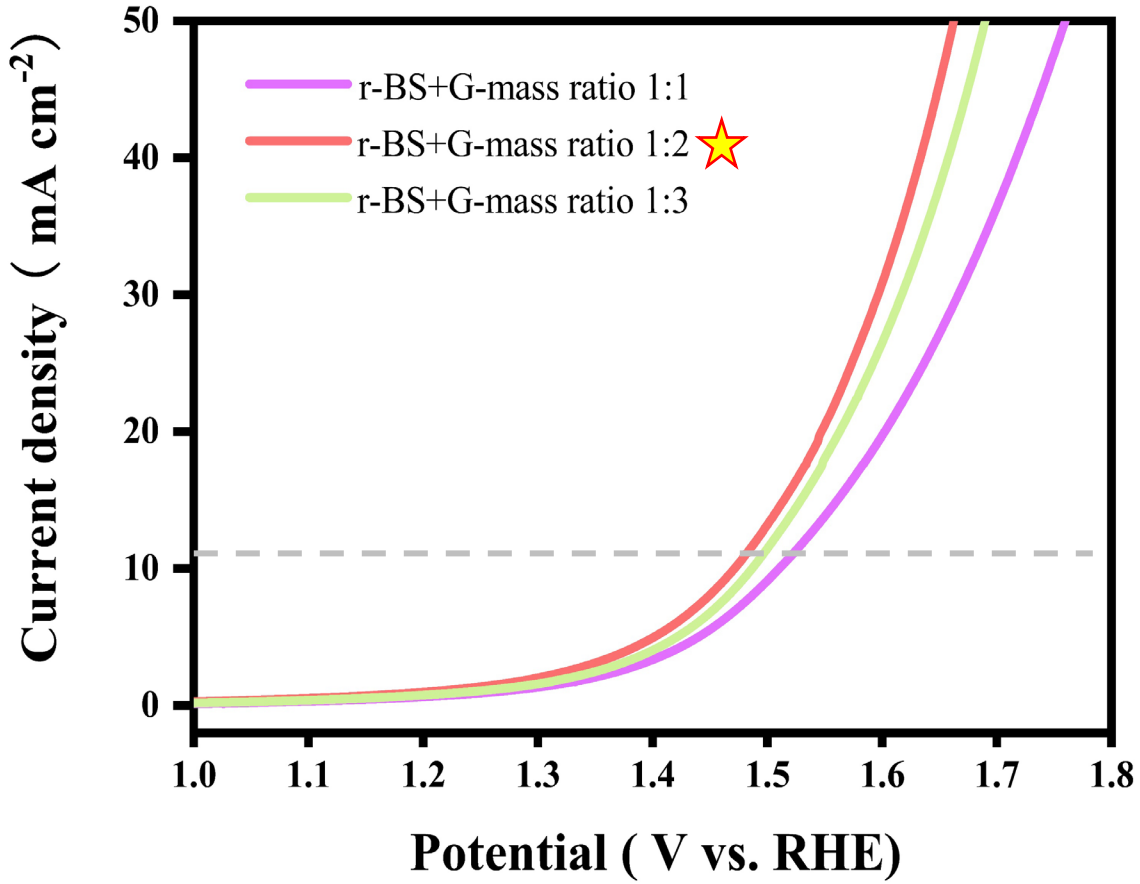

keep the same weight of r-BS (5mg)

SEM images of different mass ratios

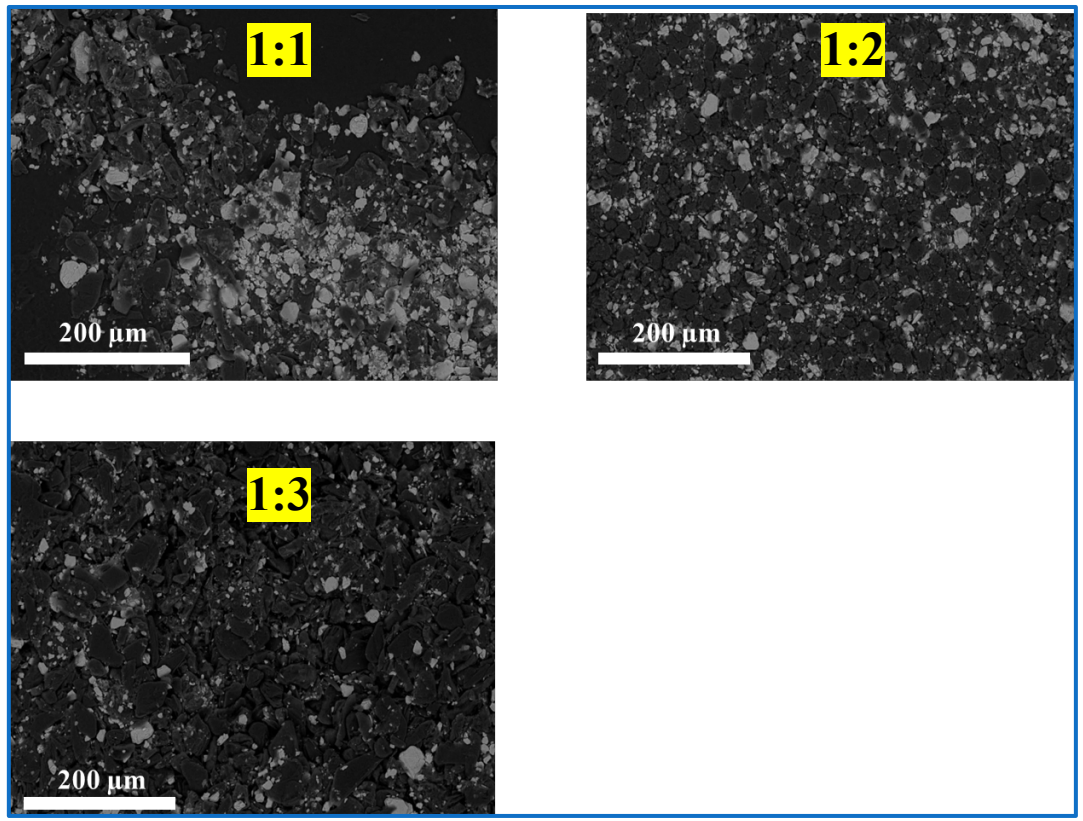

♦An excess of GNP **hides** the performance of r-BS, while a smaller amount of GNP causes **inadequate** conductivity.

The Kinetics of electrode reactions

Electrochemical impedance spectra (**EIS**) of different electrode materials under an applied potential of 1.7 V (*vs.* RHE)

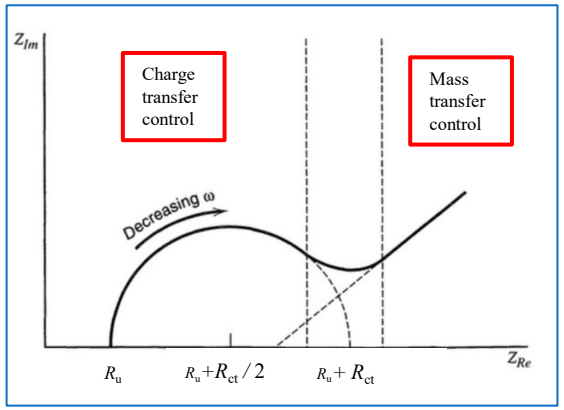

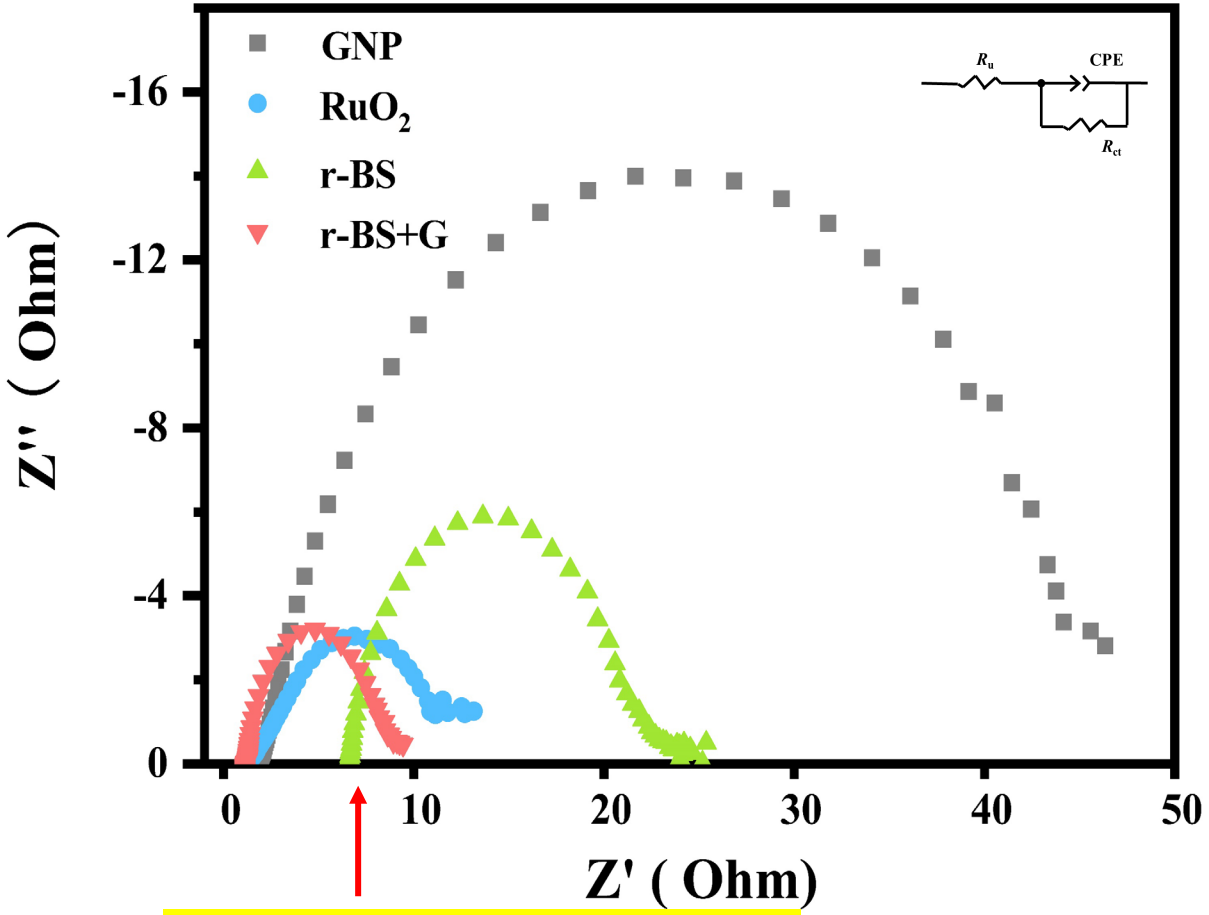

R_u of r-BS is large: poor conductivity

Samples	Solution series resistance (R_u /Ω)	Charge transfer resistance (R_{ct} /Ω)
r-BS+G	1.15	8.40
r-BS	6.58	18.56
RuO_2	1.23	10.87
Graphene	1.85	43.51

For ***Ru***: r-BS >> r-BS+G, indicates the presence of GNP **greatly increased the conductivity.**

For ***Rct***: r-BS+G shows a smaller semicircle, suggesting a **lower activation energy** for the reactions on r-BS+G.

Does electrochemical current originate from the OER?

A rotating ring–disc electrode (**RRDE**) was used, whereby the OER was realized on the disk electrode and the Oxygen Reduction reaction (ORR) proceeded on the ring electrode.

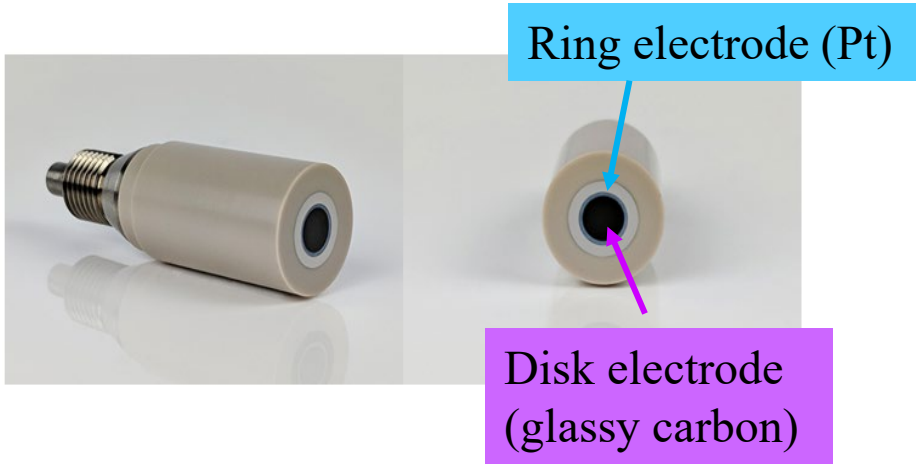

Picture of RRDE

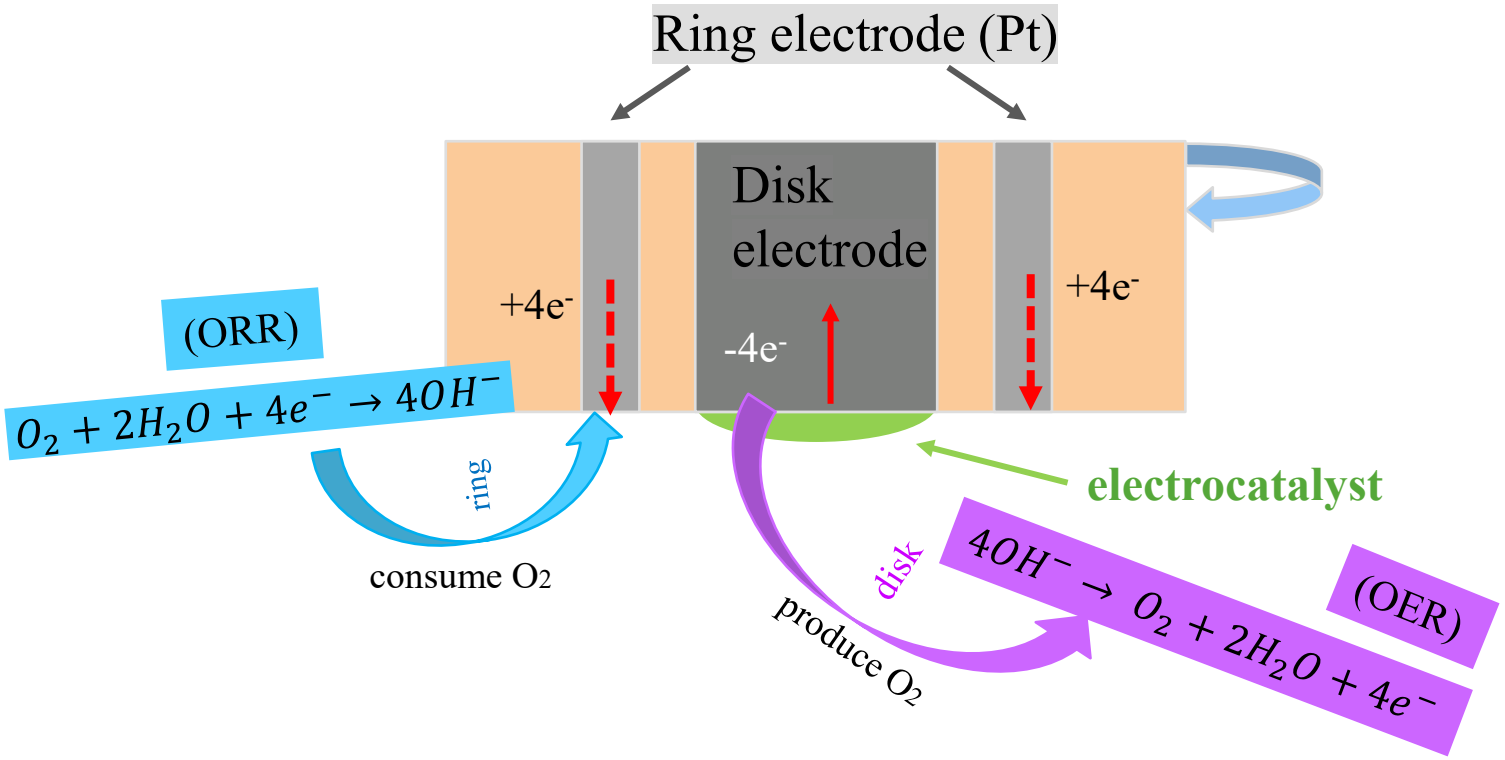

Cross section of RRDE

Electrochemical current originates from the OER

Faradic efficiency (FE):
The proportion of applied current used for a certain electrochemical reaction

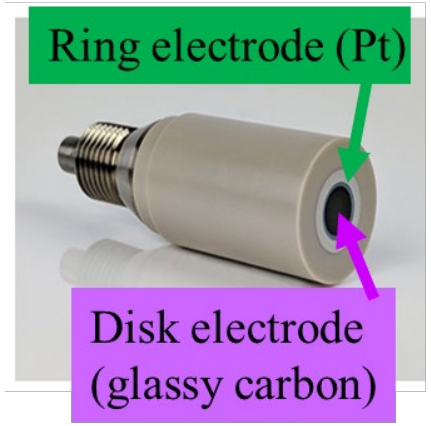

For FE system:

The disk current was set at a constant value of **300 μA** to generate oxygen bubbles in situ. At same time, the formed oxygen was reduced by the ring electrode with an ORR potential of 0.40 V (vs. RHE), then the ring current would be recorded

The Faradaic efficiency (FE) was calculated as:

$$\mathbf{FE} = \frac{I_{\mathbf{ring}}}{C_{\mathbf{e}} \times I_{\mathbf{disc}}}$$

, Ce=0.2

when the applied disk current was set at 300 μA, the detected ring current was approximately **59.3 μA,** corresponding to a Faradaic efficiency of **98.8%,** indicates that **the electrochemical current mainly comes from the OER**

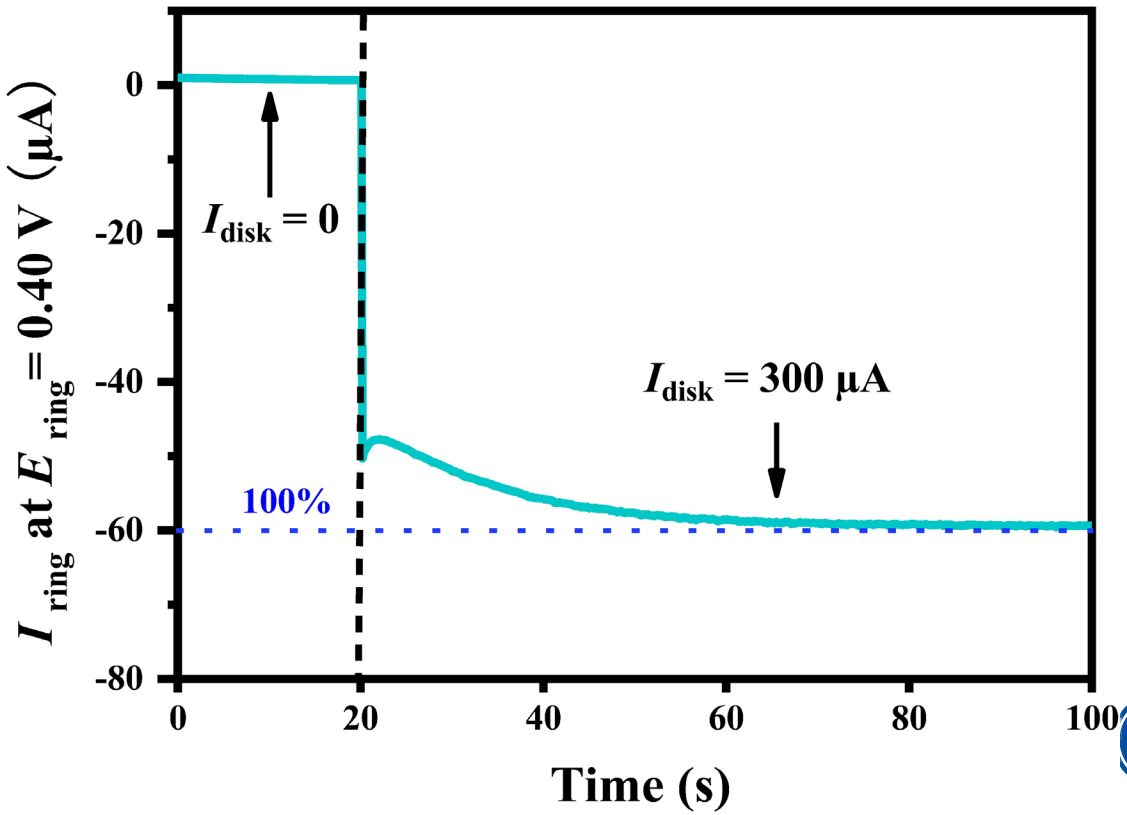

Is the gas generated at the anode oxygen?

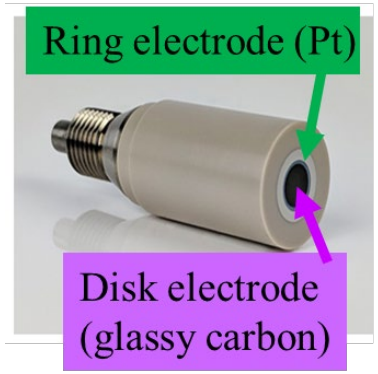

For normal RRDE system:

the potential of the **disk electrode** was scanned over the range identical to that used for the **OER** (1.0 V -1.8 V), where the **ring electrode** was held at a constant **ORR** potential of 0.2 V (vs. RHE), and the ring current and disk current were recorded

When the potential of the disc electrode was swept over **1.48 V,** a marked increase in ring current was observed.

►As this ring current was caused by the **ORR** due to the potential limitation, the bubbles that formed at the disk electrode were attributed to **oxygen gas**.

The electrochemical current whole swept potential range mainly originated from the OER.

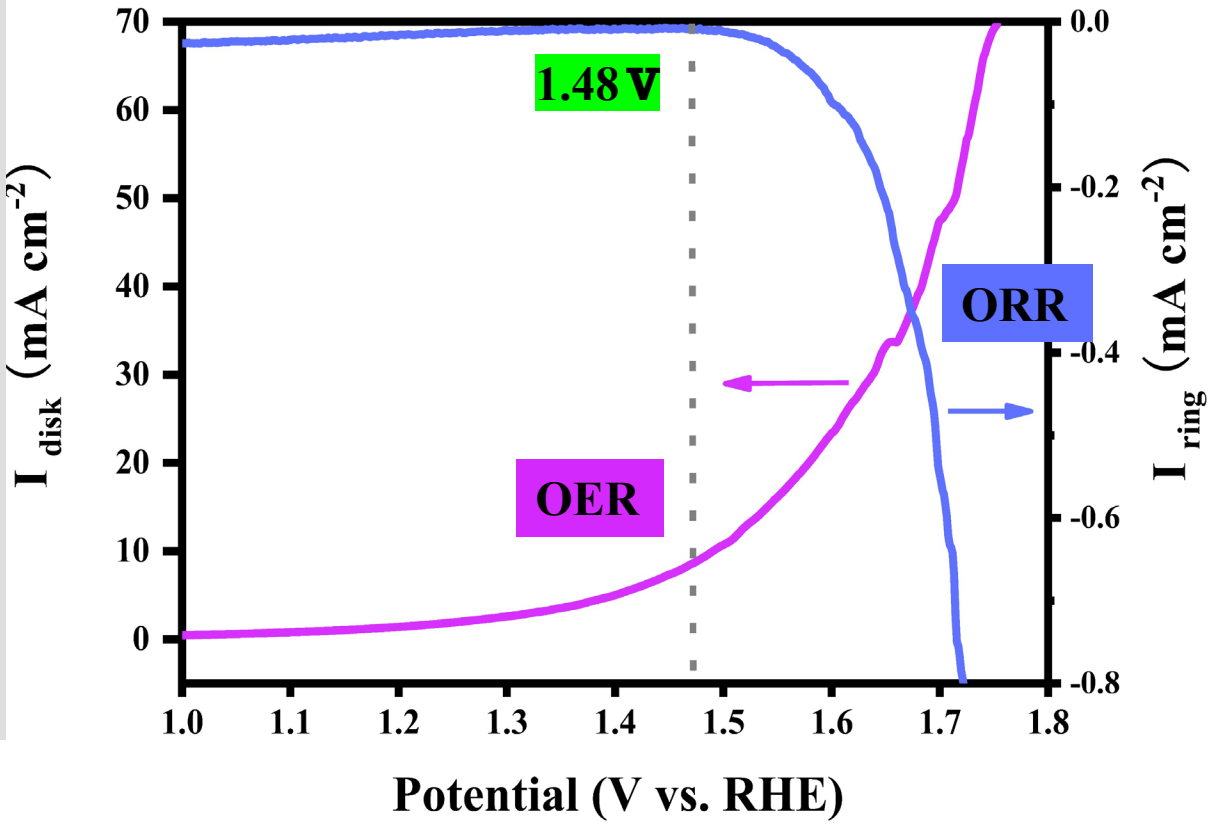

Electrochemical stability of r-BS+G

The stability of r-BS+G was explored using cyclic voltammetry (CV)

LSV curves of r-BS+G before and after 500 CV cycles

(CV cycles: 1.20-1.53 V vs. RHE)

25 °C
RE: Hg/HgO or Ag/AgCl
1.0 M KOH
LSV 2 mV/s

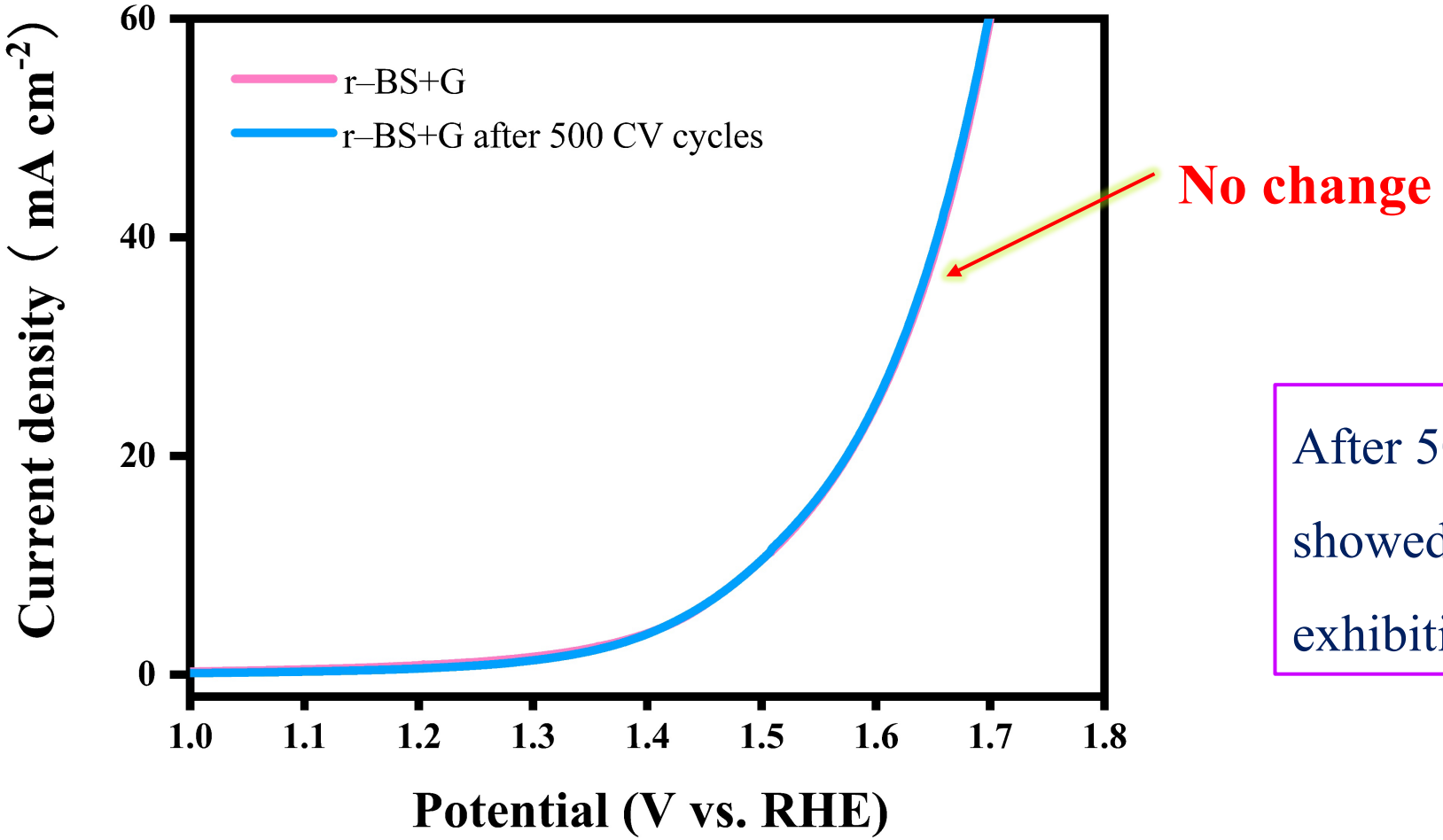

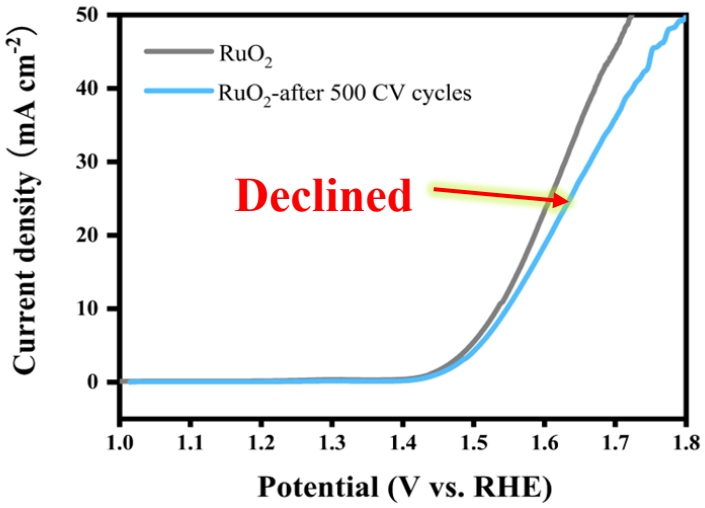

After 500 CV cycles, r-BS+G showed negligible degradation, exhibiting its **good durability**

Morphology stability of r-BS+G

SEM images and corresponding EDS mapping of **r-BS+G**

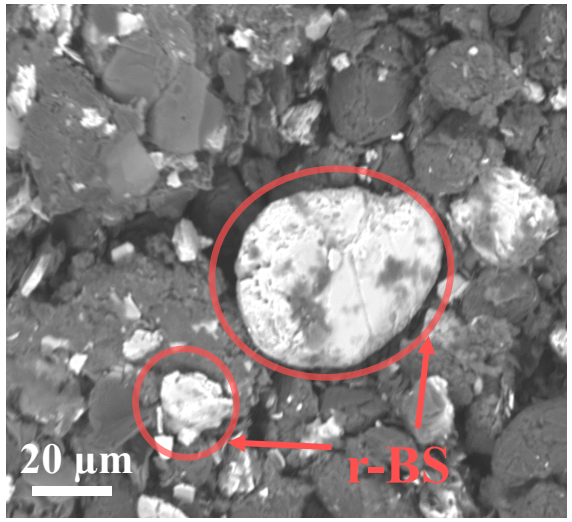

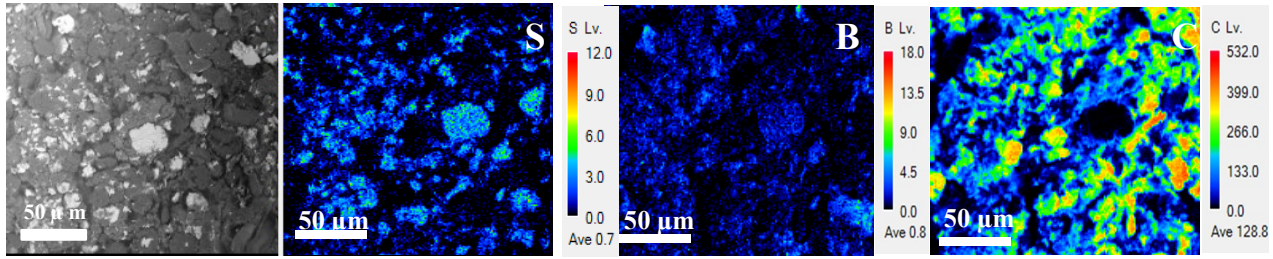

SEM images and corresponding EDS mapping of **r-BS+G after 500 CV cycles**

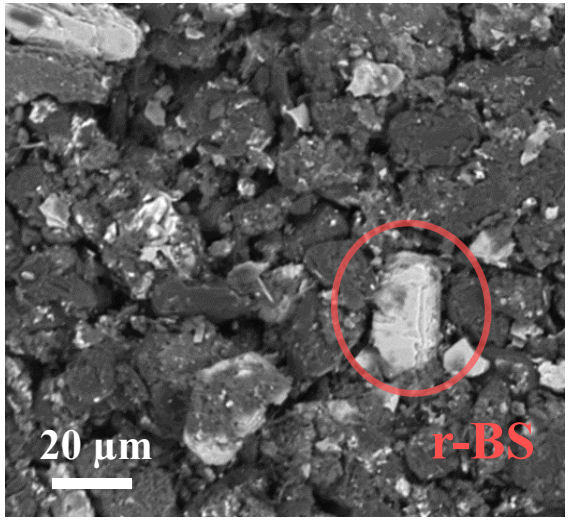

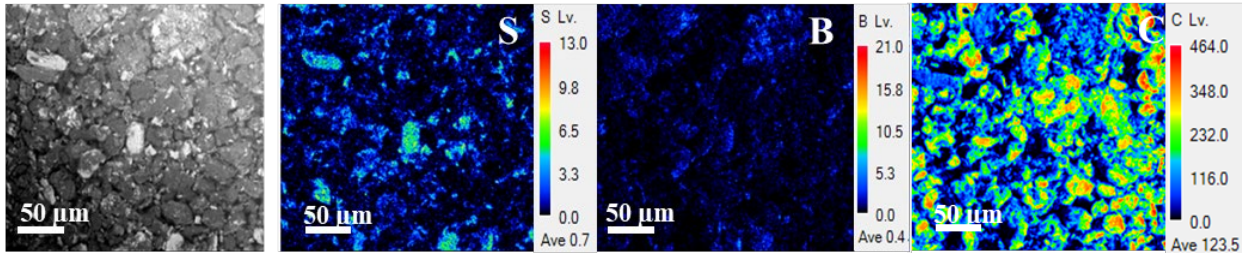

The morphology of r-BS+G showed almost no change after 500 CV cycles

Phase stability of r-BS+G

XRD of **r-BS+G** at different conditions

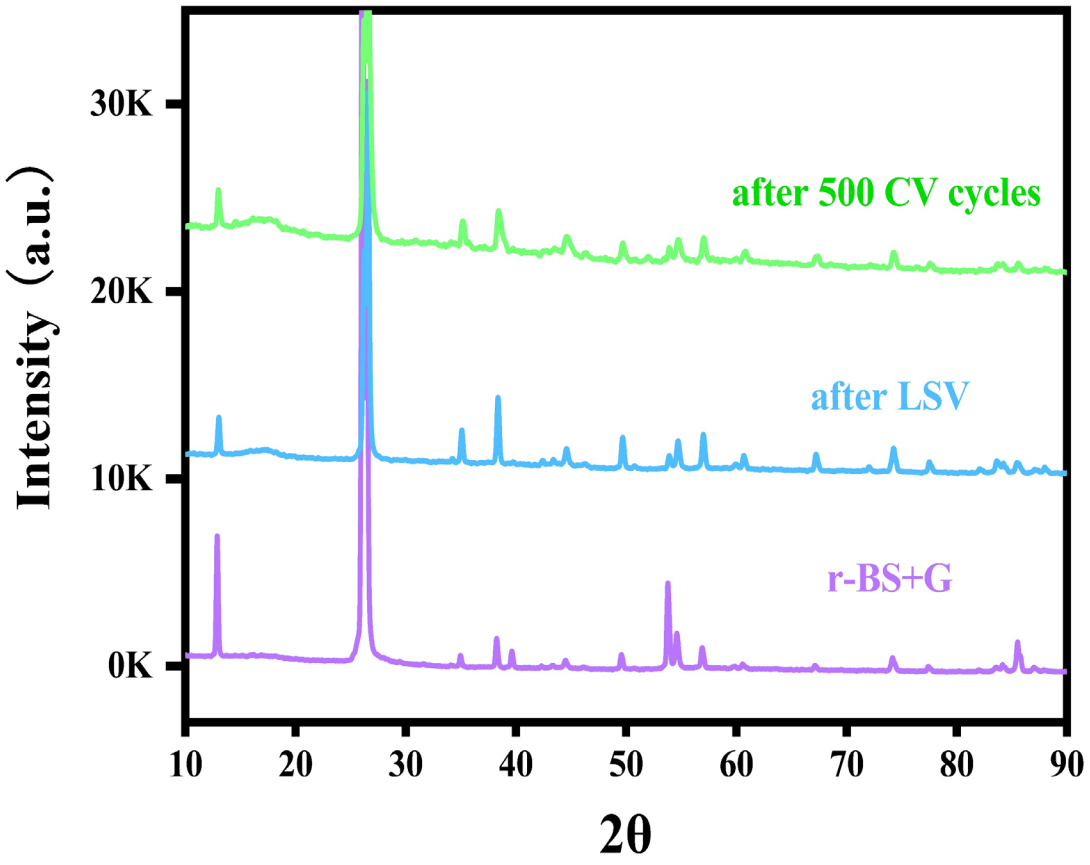

The crystal structure is stable

Full-range XPS of **r-BS+G** at different conditions

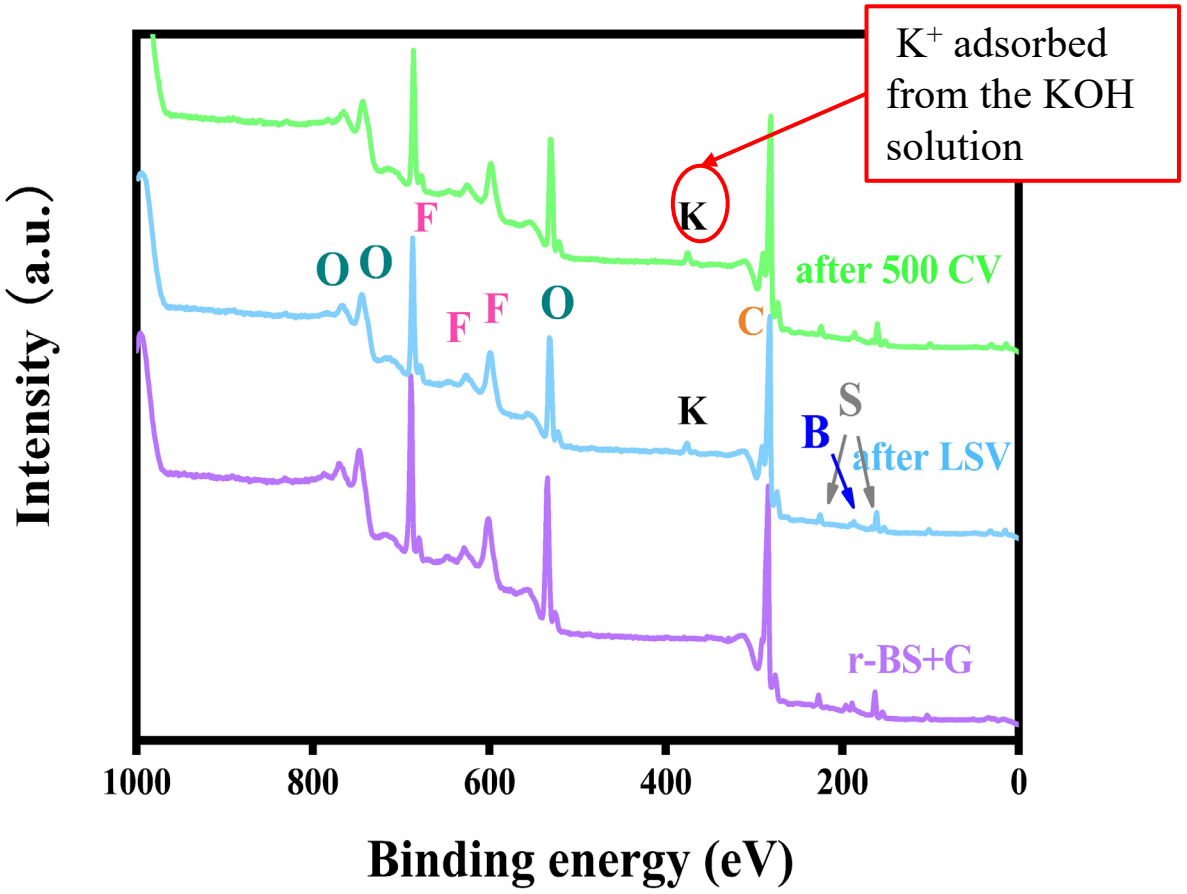

No impurities detected

Phase stability of r-BS+G

XPS of **r-BS+G** at different conditions

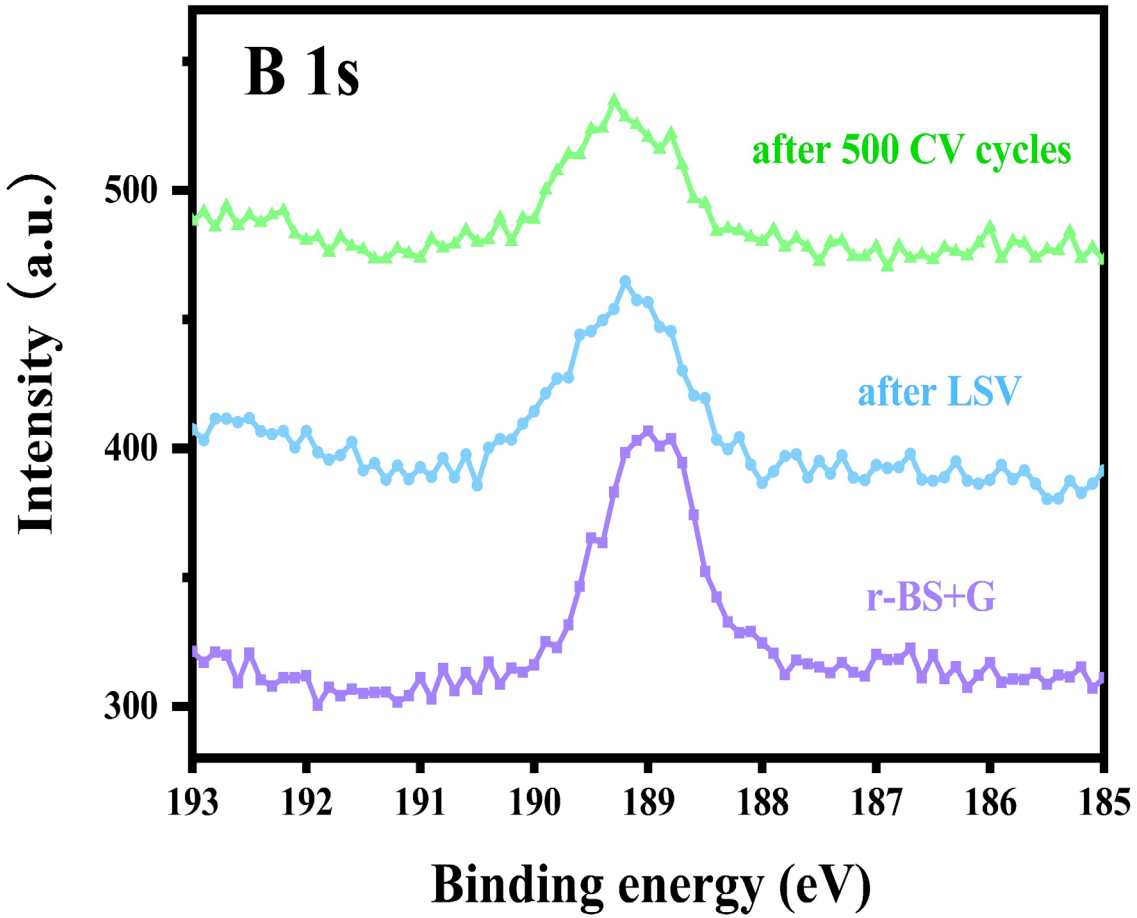

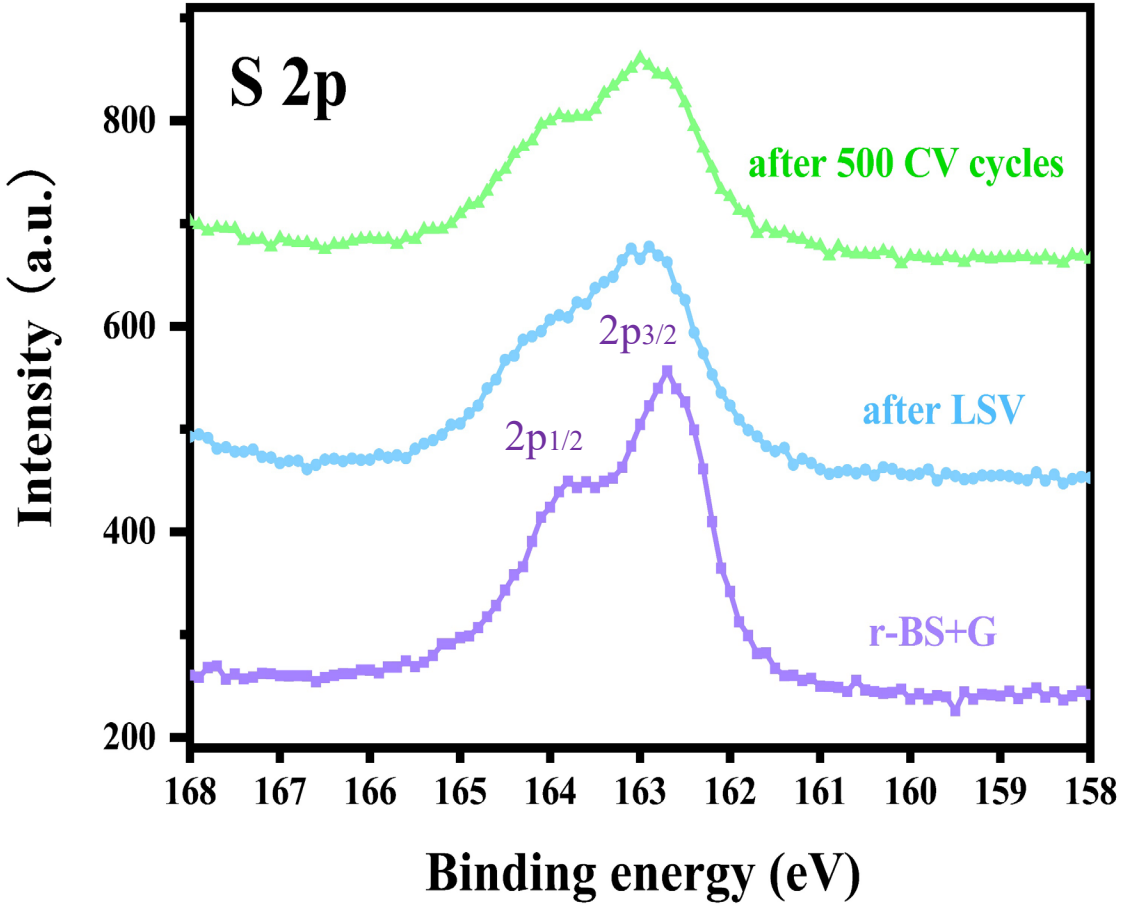

No distinct oxide of boron or sulfur

Phase stability of r-BS+G

Raman of **r-BS+G** at different conditions

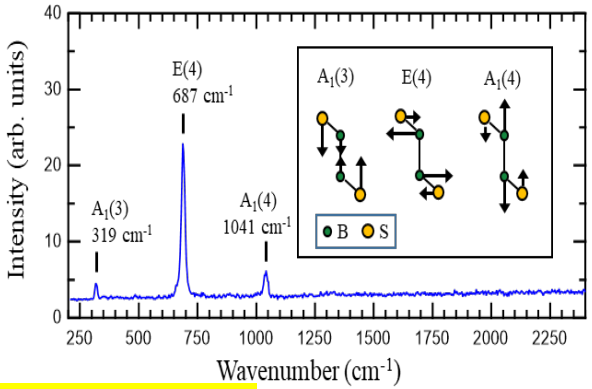

J. App. Phys. 117, 185904 (2015).

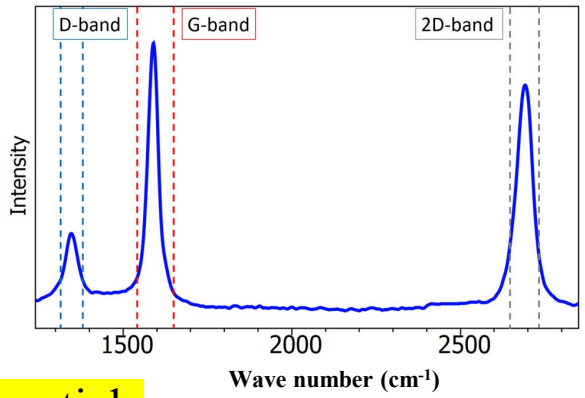

Focus on the r-BS particle

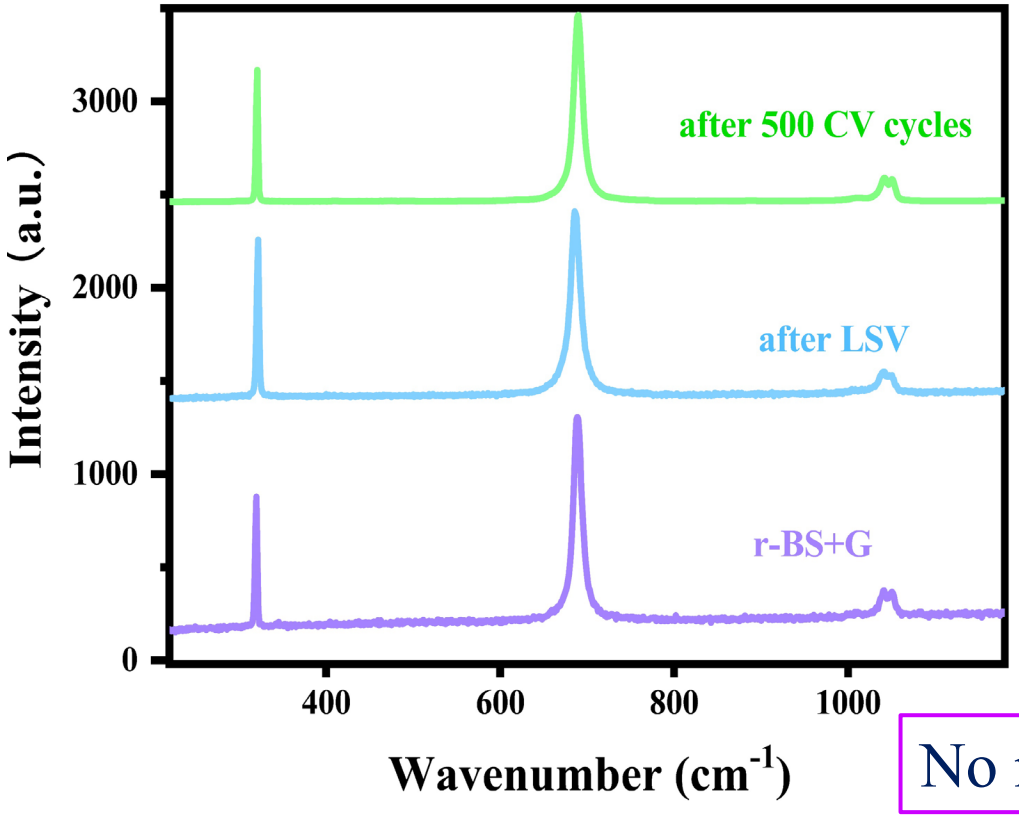

Focus on the graphene particle

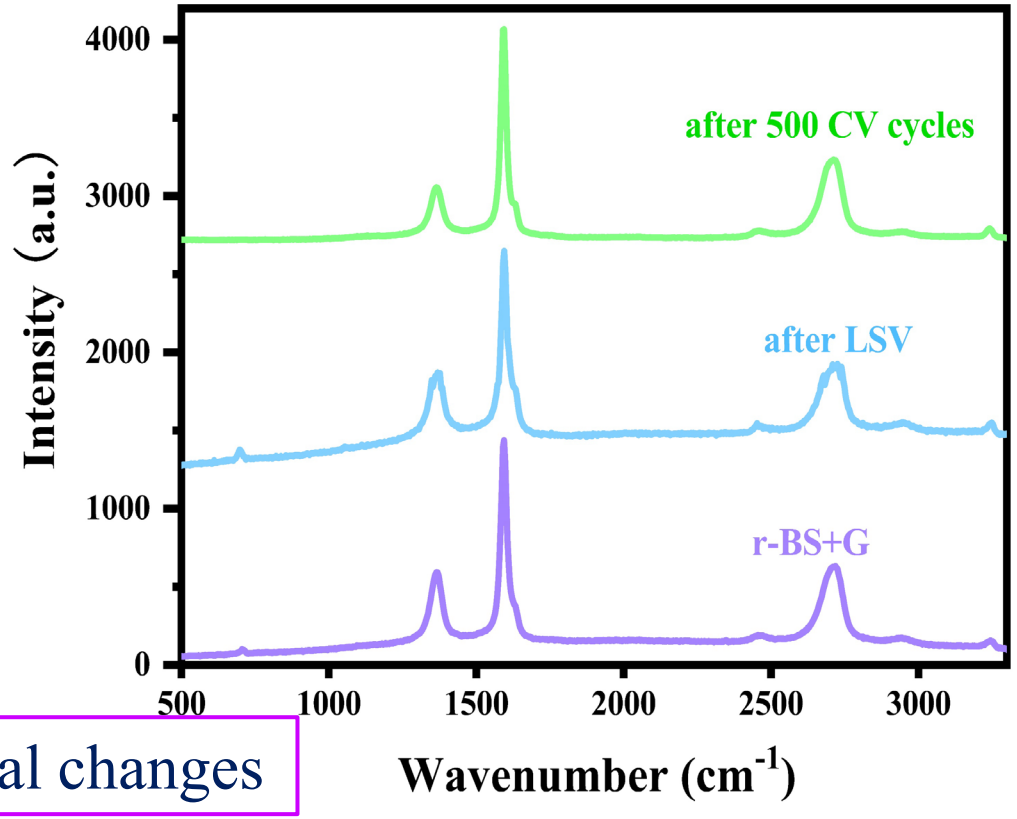

No major spectral changes

Our created rhombohedral boron monosulfide (r-BS) shows top-level catalytic property for oxygen evolution reaction in alkaline media.

Our work: 250 at 10 mA cm^{-2},

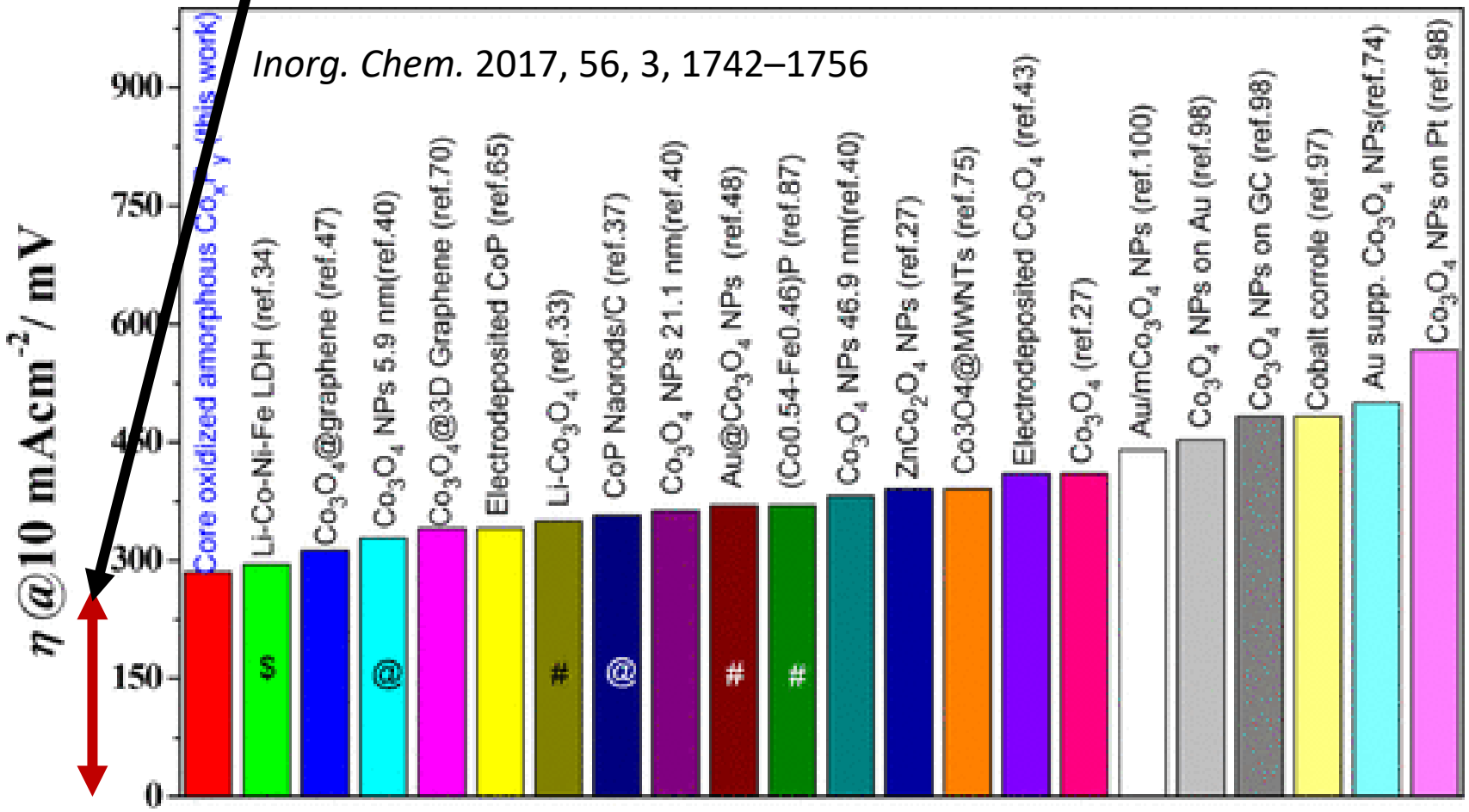

From (*Inorg. Chem*. 2017, 56, 3, 1742–1756)

DFT calculation reproduce experimental finding of OER performance

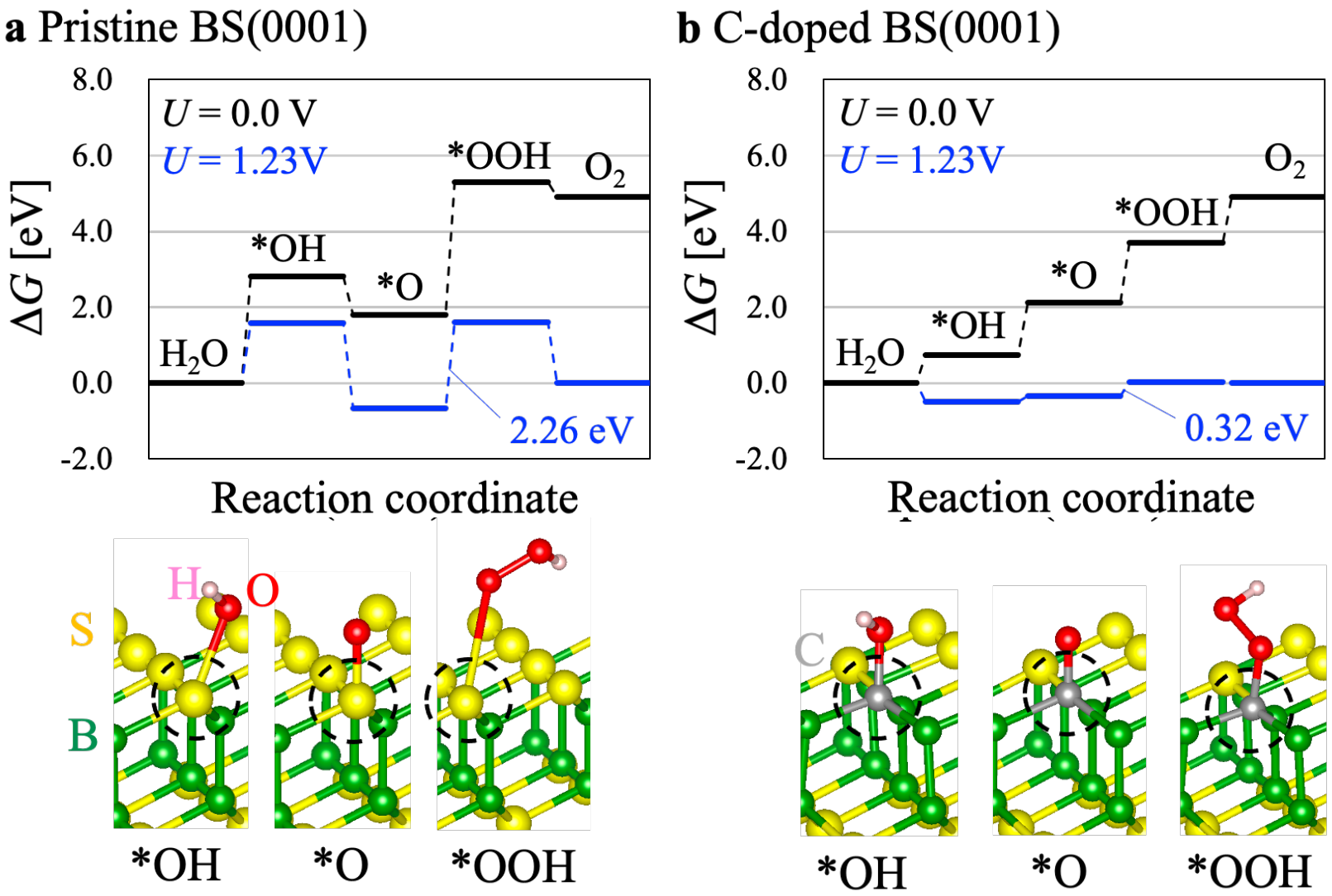

一部の硫黄が炭素と置き換わると高活性となることが示された

L. Li, M. Otani, T. Kondo* et al., *Chem. Eng. J.* 471, 144489. (2023).

DFT calculation reproduce experimental finding of OER performance

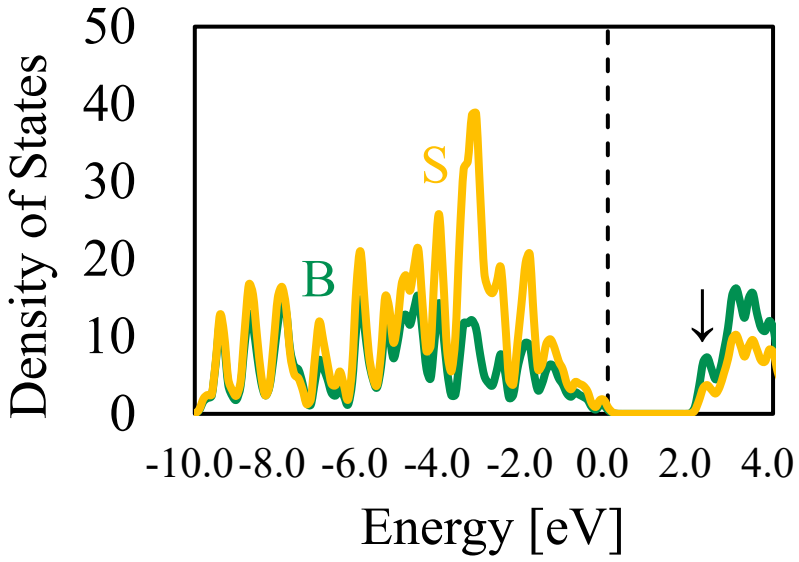

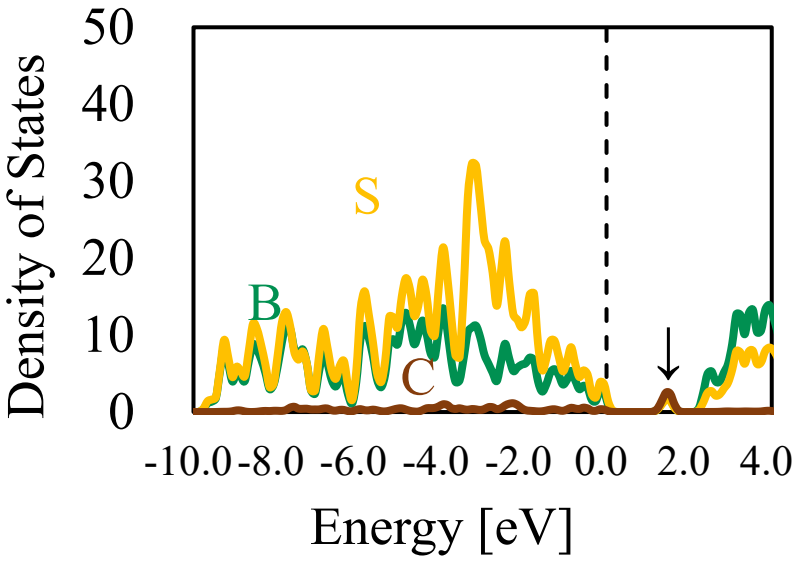

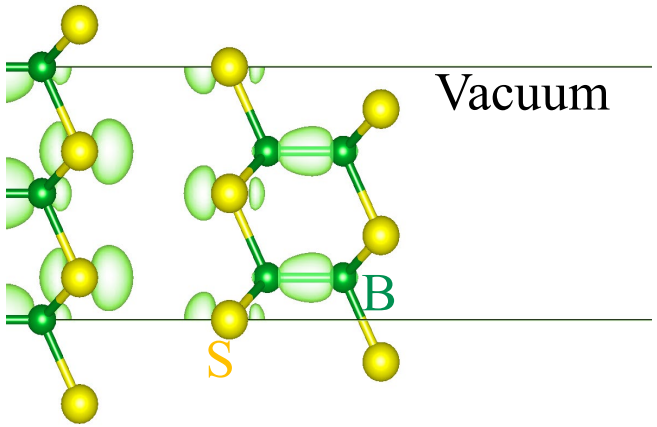

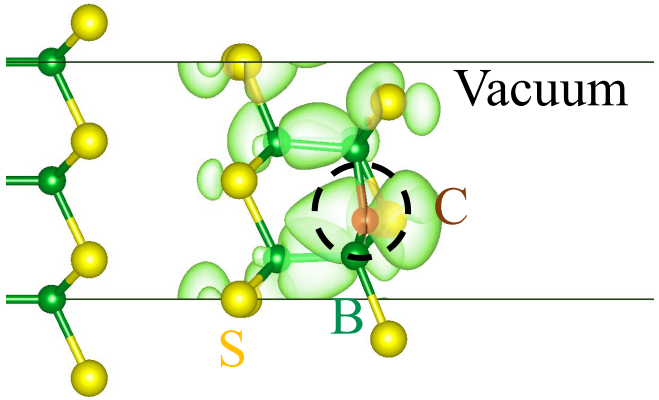

置換炭素近傍でフェルミエネルギー近傍の局在準位が形成：
ここが活性部位となっている可能性が示唆された

L. Li, M. Otani, T. Kondo* et al., *Chem. Eng. J.* 471, 144489. (2023).

ACS APPLIED MATERIALS & INTERFACES

www.acsami.org Research Article

Electrocatalytic Mechanisms for an Oxygen Evolution Reaction at a Rhombohedral Boron Monosulfide Electrode/Alkaline Medium Interface

Satoshi Hagiwara,* Fumiaki Kuroda, Takahiro Kondo, and Minoru Otani*

Cite This: *ACS Appl. Mater. Interfaces* 2023, 15, 50174−50184 Read Online

Theoretically boron vacancy creates active site for OER!

ABSTRACT: Rhombohedral boron monosulfide (r-BS) with a layer stacking structure is a promising electrocatalyst for an oxygen evolution reaction (OER) within an alkaline solution. We investigated the catalytic mechanisms at the r-BS electrode/alkaline medium interface for an OER using hybrid solvation theory based on the first-principles method combined with classical solution theory. In this study, we elucidate the activities of the OER at the outermost r-BS sheet with and without various surface defects. The Gibbs free energies along the OER path indicate that the boron vacancies at the first and second layers of the r-BS surface (V_{B1} and V_{B2}) can promote the OER. However, we found that the V_{B1} is easily occupied by the oxygen atom during the OER, degrading its electrocatalytic performance. In contrast, V_{B2} is suitable for the active site of the OER due to its structure stability. Next, we applied a bias voltage with the OER potential to the r-BS electrode. The bias voltage incorporates the positive excess surface charge into pristine r-BS and V_{B2}, which can be understood by the relationship between the OER potential and potentials of zero charge at the r-BS electrode. Because the OH^- ions are the starting point of the OER, the positively charged surface is kinetically favorable for the electrocatalyst owing to the attractive interaction with the OH^- ions. Finally, we qualitatively discuss the flat-band potential at a semiconductor/alkaline solution interface. It suggests that p-type carrier doping could promote the catalytic performance of r-BS. These results explain the previous measurement of the OER performance with the r-BS-based electrode and provide valuable insights into developing a semiconductor electrode/water interface.

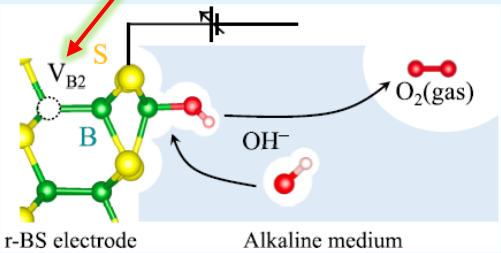

KEYWORDS: *rhombohedral boron monosulfide, oxygen evolution reaction, density functional theory, classical solution theory, semiconductor/water interface*

Summary

In summary, we have developed **a new metal-free electrocatalyst for OER**. Introducing the graphene nanoplates into the r-BS by a very simple method, the mixture (**r-BS+G**) exhibits high electronic performance.

We clarified that the electrochemical current of r-BS+G in the whole swept potential range mainly originated from the OER, and the Faradic efficiency is **98.8%**.

In the experiment, to determine the active sites in r-BS+G, future studies will involve atomic-scale microscopy and further spectroscopy studies on well-defined and defect-controlled model catalysts.

L. Li, T. Kondo, et al. *Chem. Eng. J.* 471, 144489. (2023).

Outline

1. 自己紹介

2. カーボンニュートラルの必要性と材料開発の重要性

3. 水素製造に貢献する材料開発
典型元素を利用した高活性アルカリ水電解触媒

(1) 硫化ホウ素(r-BS)の合成と評価

(2) r-BSとグラフェンの混合物が示す
高いOER触媒特性

(3) r-BSの活性点（MoS_2のHER活性点との比較）

(4) r-BS＋グラフェンOER触媒の高耐久性化

4. 水素利用に貢献する材料開発

5. 水素吸蔵に貢献する材料開発

Investigate the active sites

In addition to the similarity in crystal structure, the electronic structure of r-BS is also similar to that of MoS_2.

MoS_2--the most widely investigated Transitional Metal-Dichalcogenides (TMDs) for HER

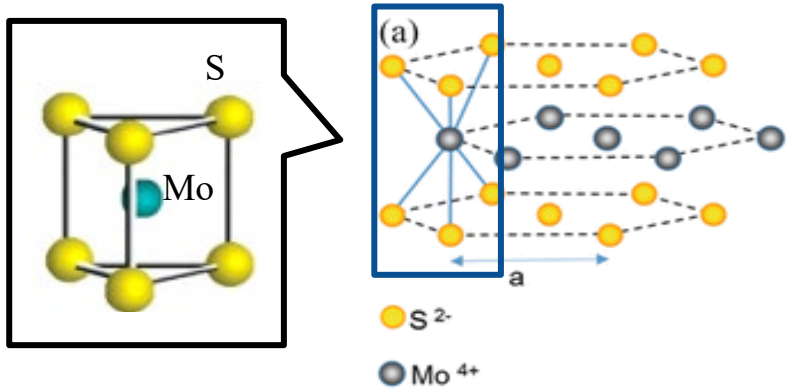

Y. Xu, Y. Peng, T. You, L. Yao, et al. Springer, Cham., 151-191 (2018).

▲HER activity of MoS_2 stemmed on **Mo-edge**

T.F. Jaramillo, K.P. Jorgensen, J. Bonde, et al. *Science* **317**, 100–102 (2007).

Increase the activity

MoS_2 with **more exposed edges**

r-BS

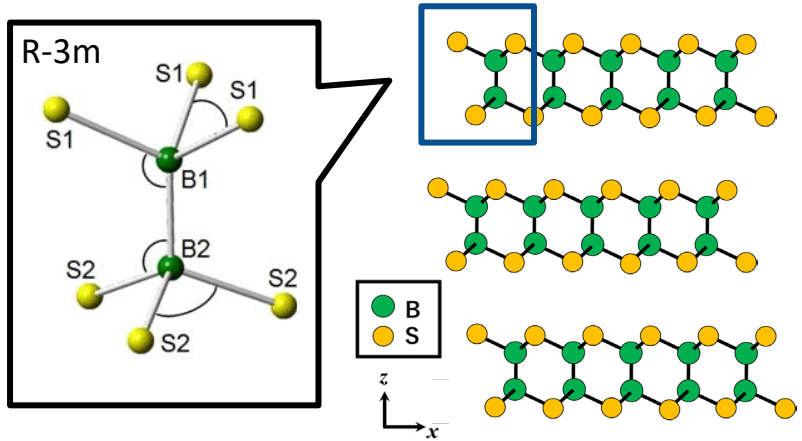

In line with this strategy, we attempted to increase the area of exposed edges in r-BS by decreasing its particle size

In the case of MoS_2 for HER

The synthesize of Size-controlled MoS_2 and the application for HER

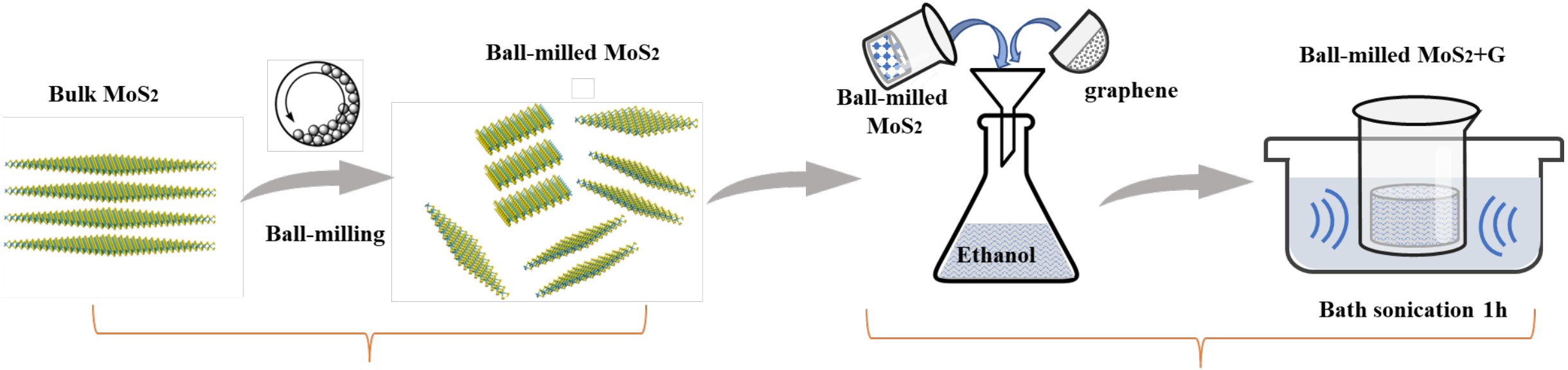

The **size-controlled MoS_2** particles were synthesized by ball-milling, then **introducing graphene** into the ball-milled sample to keep the morphology and increase the electrical conductivity.

L. Li, S. L. Shinde, T. Fujita, T. Kondo*, Science and Technology of Advanced Materials 25 (2024) 2359360. (10 pages)

XRD results of ball-milled MoS_2

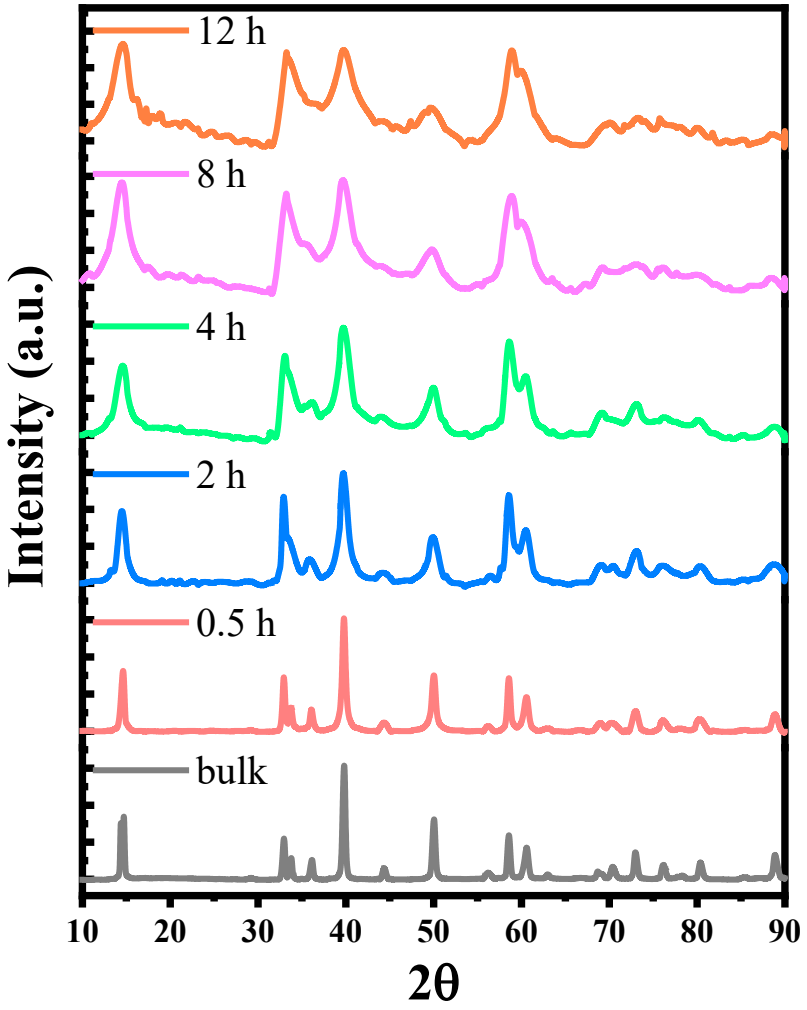

Scherrer equation

$$Crystal\ Size = \frac{k\lambda}{\beta \cos\theta},$$

Table 1. Crystal sizes of MoS_2 samples ball-milled for varying periods, calculated using the Scherrer equation.

Sample	2θ (degree)	FWHM	Crystallite size (nm)
Bulk MoS_2	13.63	0.12	68
MoS_2-15 min	14.05	0.23	35
MoS_2-30 min	14.03	0.30	26
MoS_2-1 h	14.06	0.51	15
MoS_2-2 h	14.05	0.90	8
MoS_2-4 h	14.06	0.98	6
MoS_2-12 h	14.05	1.20	4

♦Based on the Scherrer equation, the corresponding crystal size could be calculated, the crystal size of MoS_2 was gradually reduced from 68 nm to 4 nm by ball-milling.

L. Li, S. L. Shinde, T. Fujita, T. Kondo*, Science and Technology of Advanced Materials 25 (2024) 2359360. (10 pages)

SEM results of ball-milled MoS_2

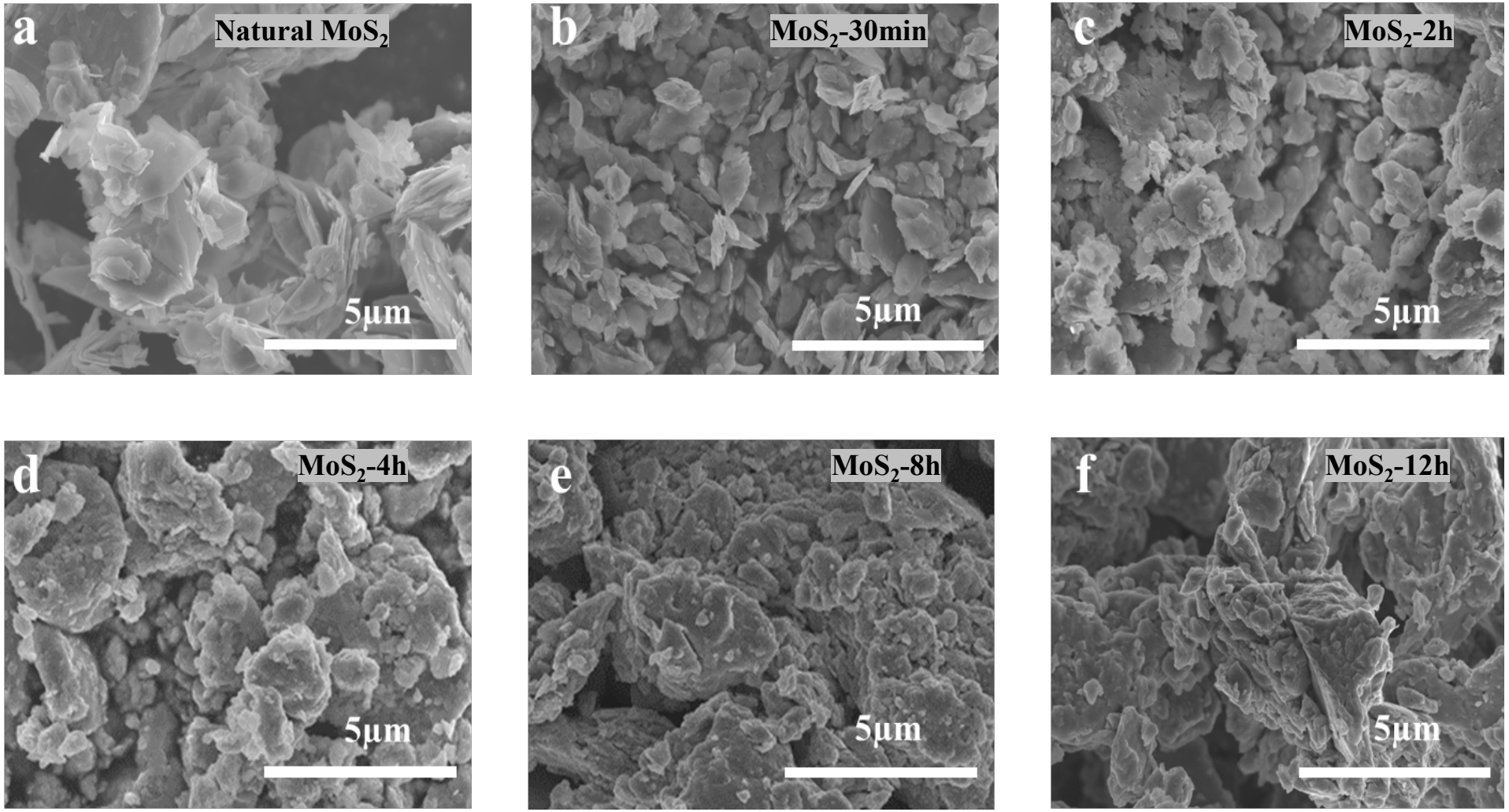

♦The smaller size of MoS_2 particles was produced by ball milling.

L. Li, S. L. Shinde, T. Fujita, T. Kondo*, Science and Technology of Advanced Materials 25 (2024) 2359360. (10 pages)

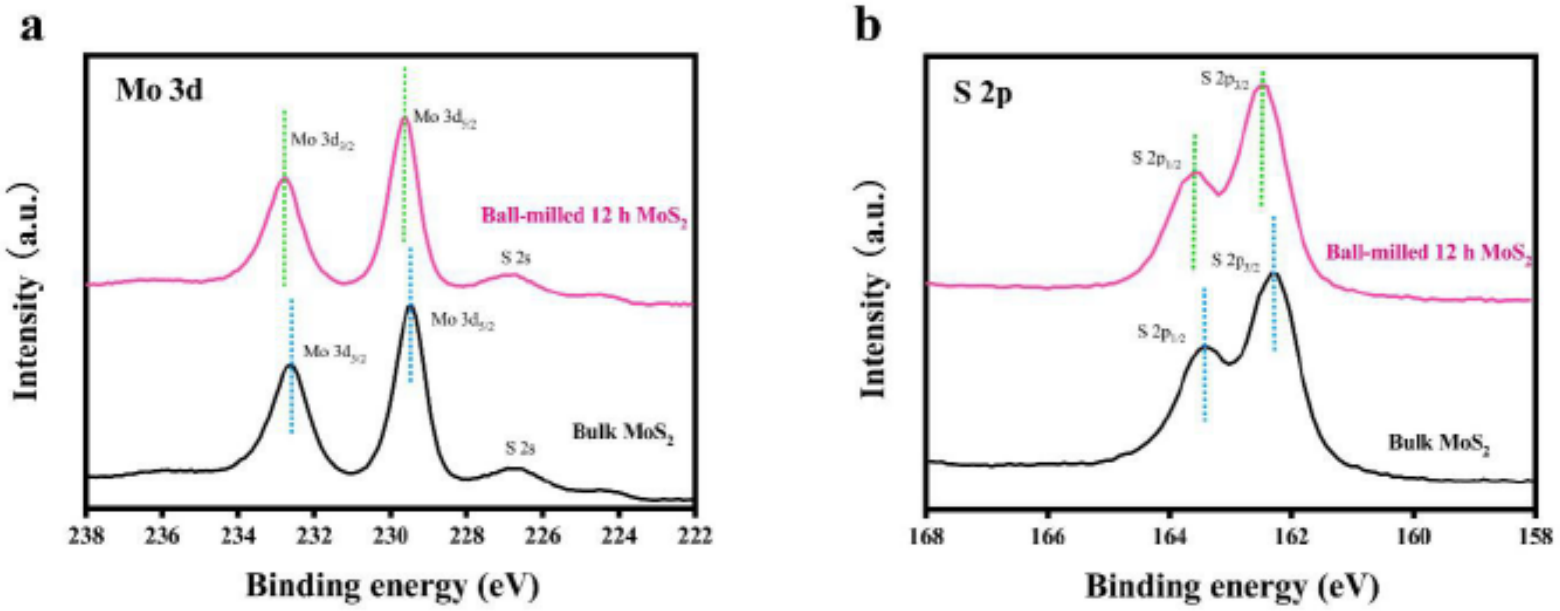

Table 2. Atomic percentages of the main elements detected by XPS for pristine bulk MoS_2 and MoS_2 samples ball-milled for different durations. The values of Mo and S are derived from the areas of the Mo 3d peak and S 2p peaks with sensitivities (Mo 3d5/2:23.52 and S 2p3/2:7.18) determined using SpecSurf software (JEOL Ltd., Japan).

Sample (MoS_2)	Mo (at%)	S (at%)	S/Mo ratio	MoS_2 (S/Mo: 2/1)
Bulk	44.6	55.4	1.24	2.00
Ball-milled 30 min	45.6	54.4	1.19	1.92
Ball-milled 1 h	46.5	53.5	1.15	1.85
Ball-milled 2 h	46.9	53.1	1.13	1.82
Ball-milled 4 h	47.5	52.5	1.10	1.77
Ball-milled 12 h	48.2	51.8	1.07	1.72

Number of S vacancy increased

S vacancy is reported as active sites of MoS_2 for HER

J. Joyner, et al., ***ACS Appl Mater Interfaces*** 12 (2020)12629–12638.

X. Wang, et al., ***J Am Chem Soc.*** 142 (2020) 4298–4308.

Y. Cheng, et al., ***Chem Asian J.*** 15 (2020) 3123–3134.

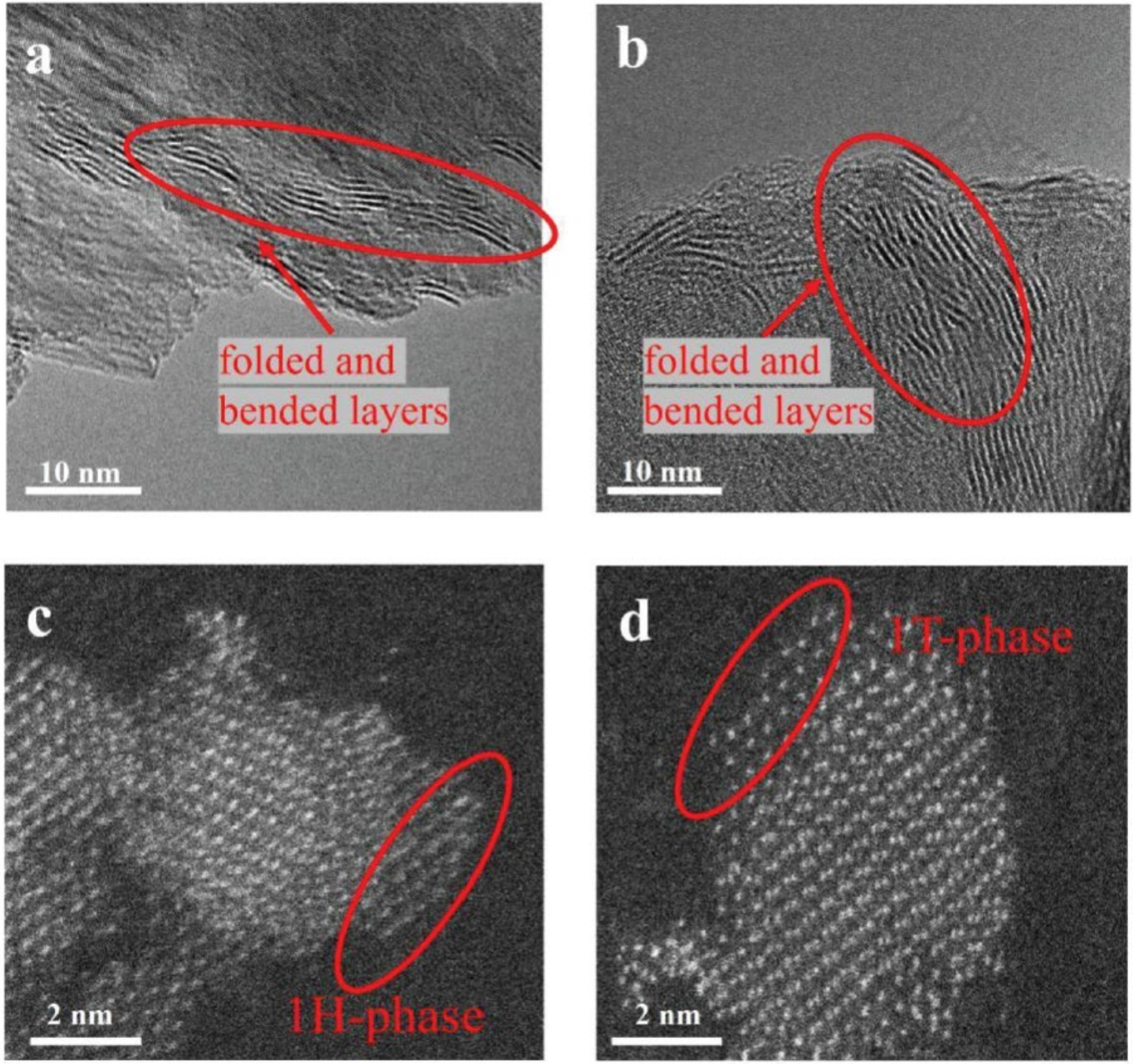

STEM images of (a) MoS_2-30 min and (b – d) MoS_2-12 h.

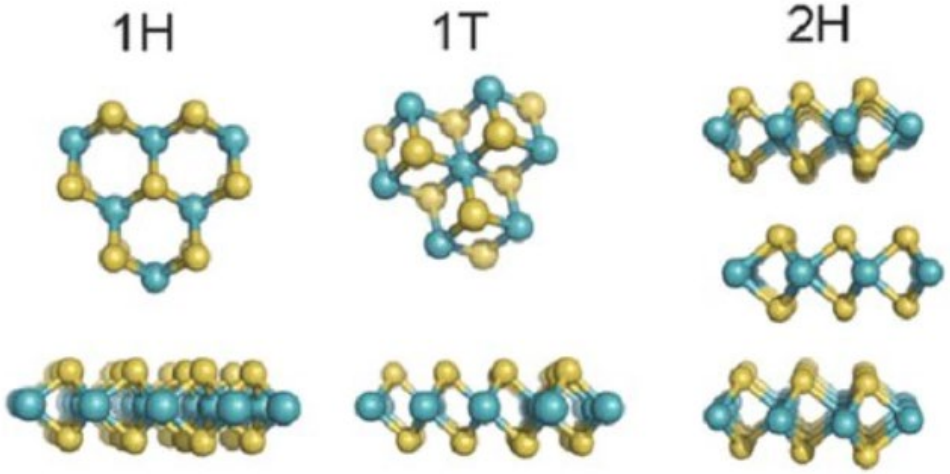

DOI: 10.1039/D2SD00208F

1T phase isreported as active sites of MoS_2 for HER

D. Voiry D, et al. ***Nat Mater.*** 12 (2013) 850–855.

D. Wang, et al. ***J Mater Chem A***. 5 (2017) 2681–2688.

1T phase is observed

Electrochemical activity of ball-milled MoS_2

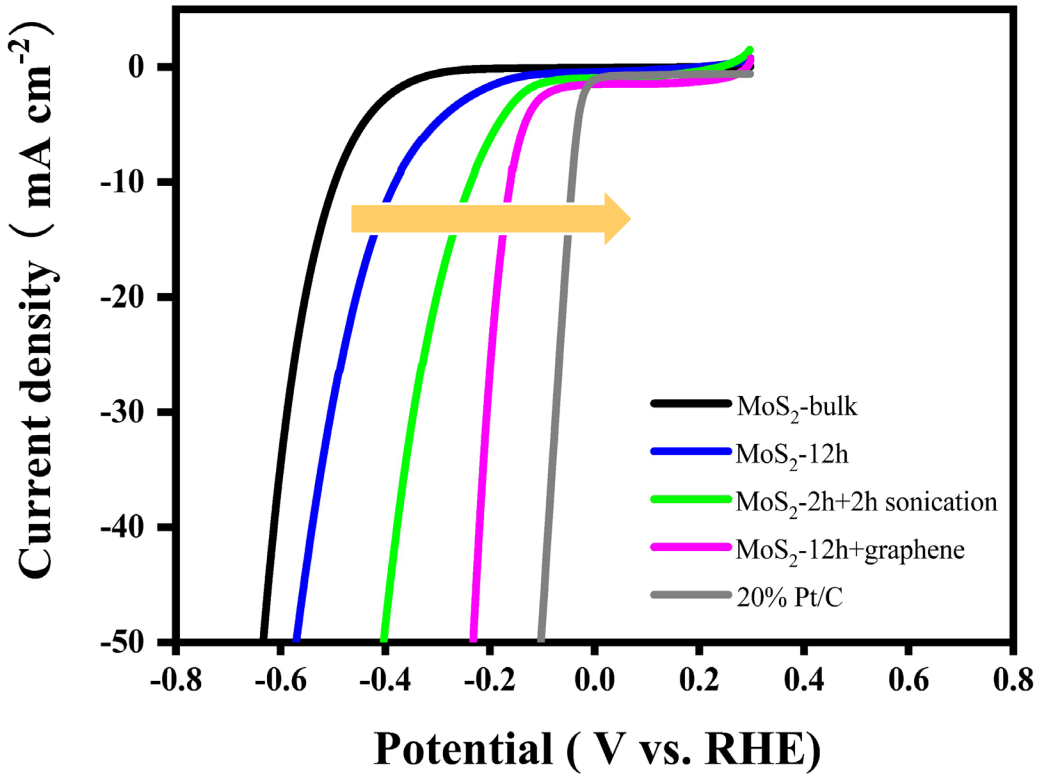

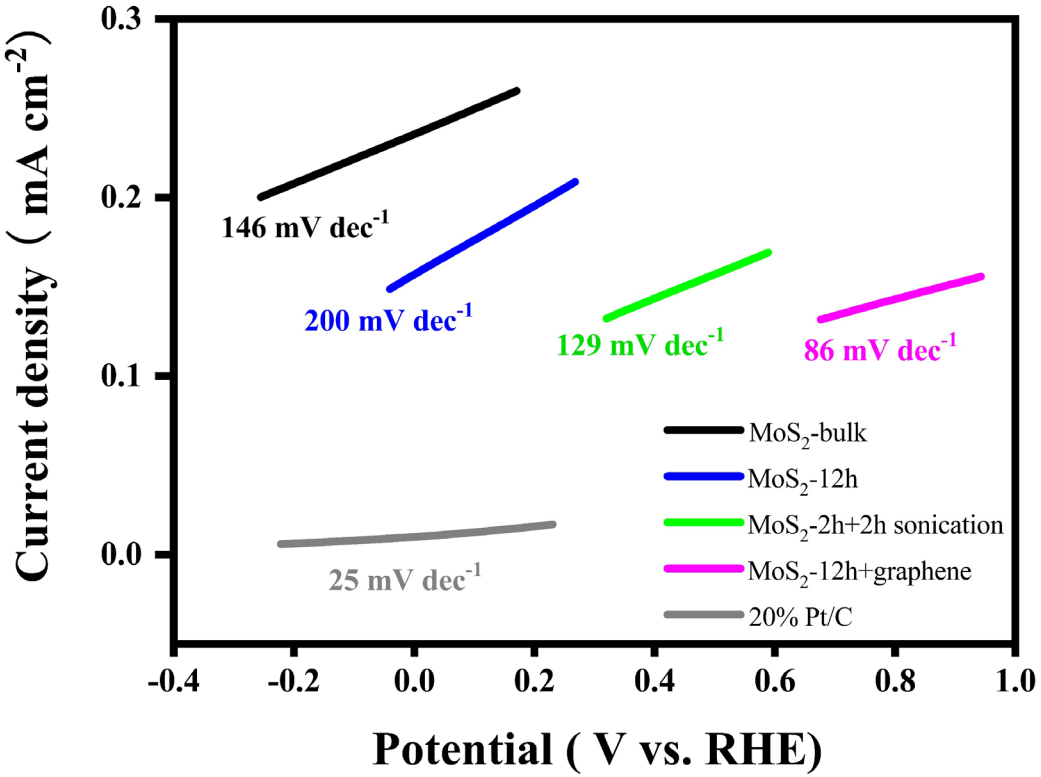

The **size-controlled MoS_2** particles were synthesized by ball-milling, and the as-prepared samples exhibited significantly enhanced electrochemical and catalytic properties than the natural bulk MoS2 material. After **introducing graphene** into the ball-milled sample, the HER activity was further improved. In particular, the **MoS_2-12 h+G** sample exhibited the best performance, showing a more decreased overpotential (**160 mV at 10 mA cm^{-2}**), which is lowered by about 335 mV from natural bulk MoS2.

L. Li, S. L. Shinde, T. Fujita, T. Kondo*, Science and Technology of Advanced Materials 25 (2024) 2359360. (10 pages)

In the case of r-BS for OER

experimentally evaluated the catalytic active sites of r-BS by using ball-milling

Method:
r-BS (100 mg) and six balls were put into the container, and milling was performed at atmospheric pressure, a temperature of ~300 K, and a rotation speed of 400 rpm. Each cycle involved 5 min of rotation followed by a rest time of 30 s (to prevent a temperature rise during long-time operation). Ball-milling was performed for 15 min, 30 min, or 45 min.

XRD

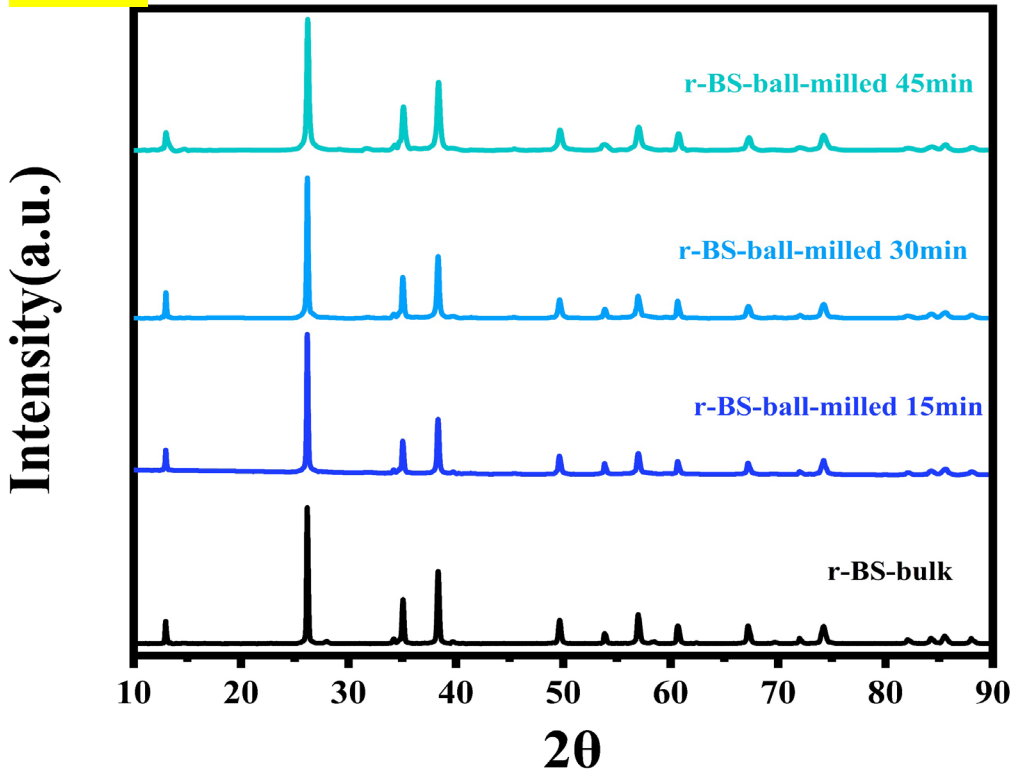

The crystal sizes are calculated based on the Scherrer equation.

XRD peak positions and full widths at half-maxima (FWHMs) as well as calculated crystal sizes of ball-milled r-BS samples

Ball-milling time [min]	2θ [°]	FWHM [°]	Size [nm]
0	26.14	0.24	34
15	26.15	0.26	31
30	26.17	0.30	27
45	26.16	0.31	26

In the case of r-BS for OER

experimentally evaluated the catalytic active sites by using ball-milling

Brunauer–Emmett–Teller (**BET**)

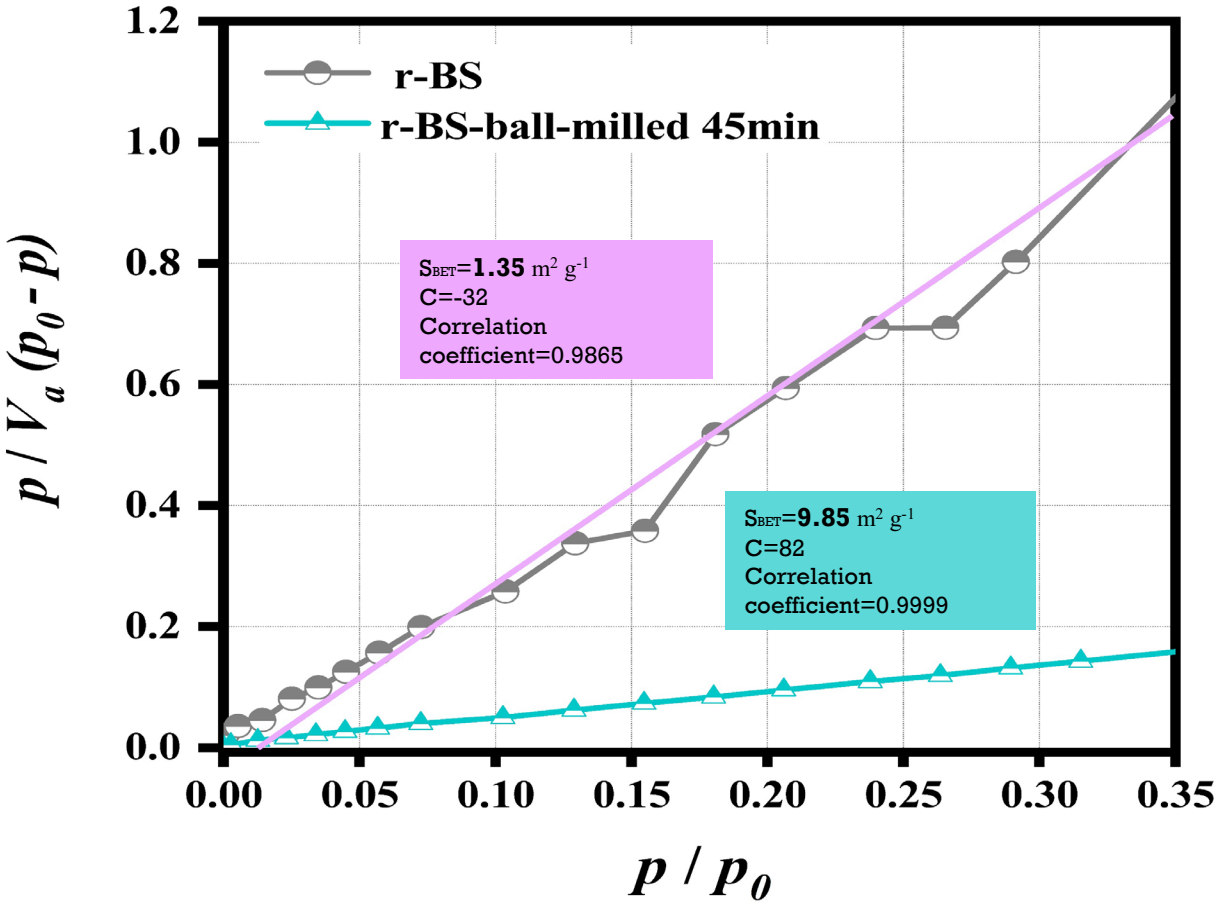

The crystal sizes are calculated based on the **Scherrer equation**.

The surface area was measured by **BET**.

After ball-milling for 45 min, the **crystallite size decreased**, whereas the **surface area increased**.

These results suggest a concomitant **increase in the area of exposed edges.**

In the case of r-BS for OER

experimentally evaluated the catalytic active sites by using ball-milling

XPS

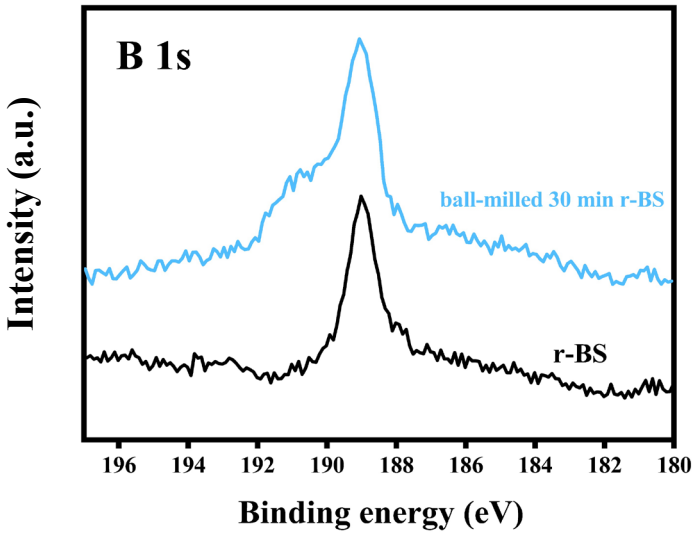

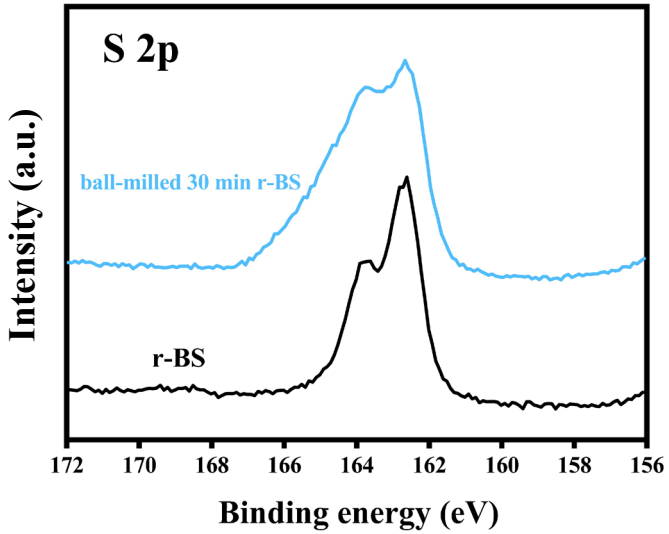

Additional peak components appeared in both the B 1s and S 2p regions at **higher energies** than the original peak energies, indicating that part of the surface and/or the exposed edges sites were slightly oxidised.

SEM

Ball-milled sample had a reduced particle size and increased area of edge sites compared to the original r-BS.

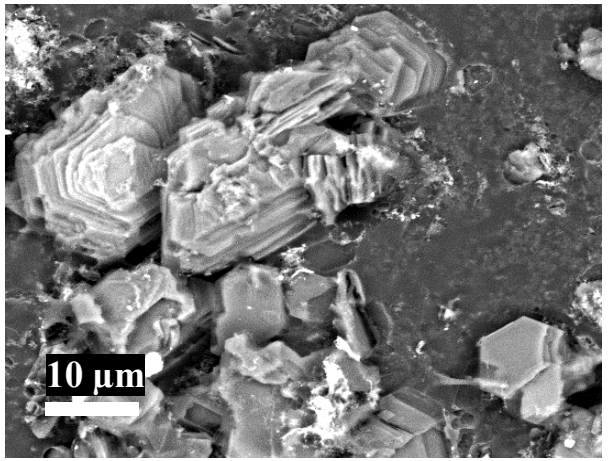

LSV

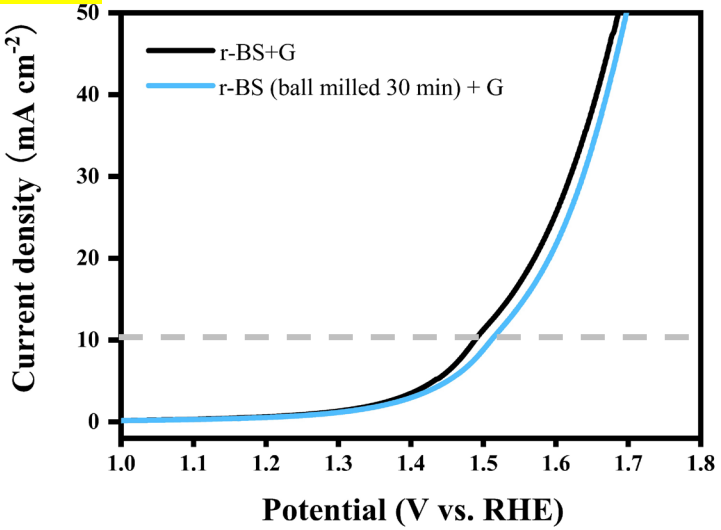

The performance was found to **deteriorate** when introducing ball-milling.

In the case of r-BS for OER

Continue ball-milling for longer time

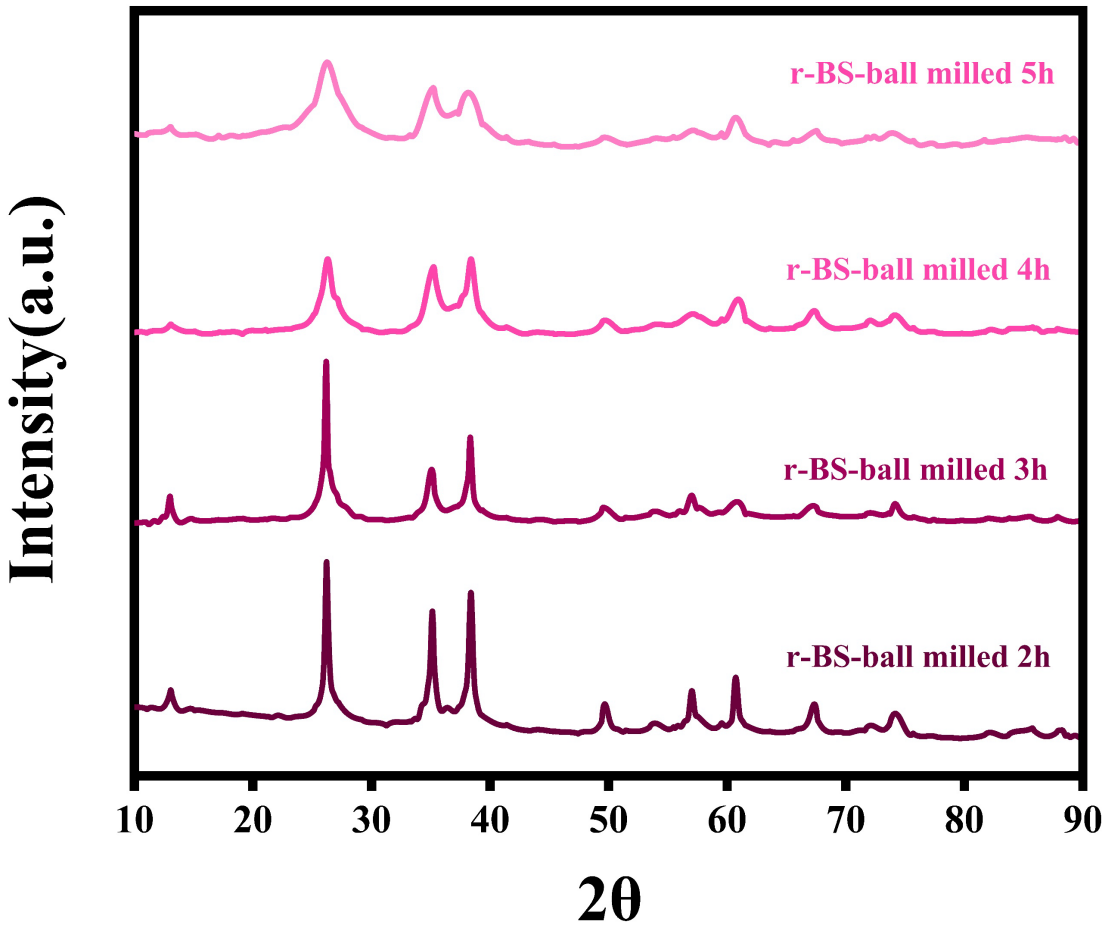

XRD peak positions and full widths at half-maxima (FWHMs) as well as calculated crystal sizes of ball-milled r-BS samples

Ball-milling time	2θ [°]	FWHM [°]	Size [nm]
2h	26.19	0.32	25
3h	26.15	1.26	6.5
4h	26.15	2.12	3.9
5h	26.17	2.37	3.4

After a longer ball-milled time,

the crystal size decreased a lot (34→3.4 nm).

In the case of r-BS for OER

Continue ball-milling for longer time

SEM

Original r-BS

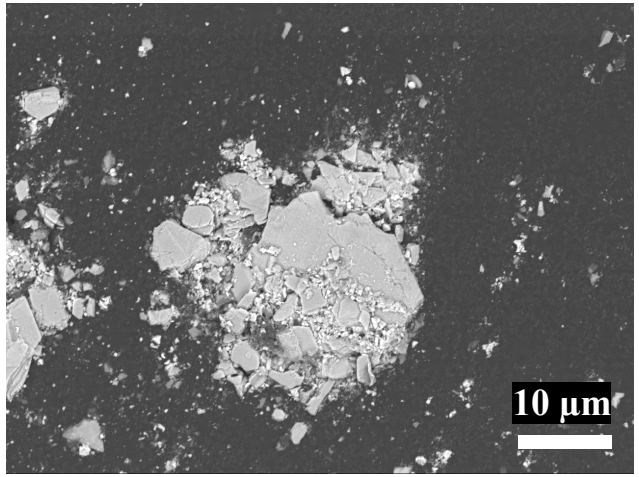

Ball-milled 2h r-BS

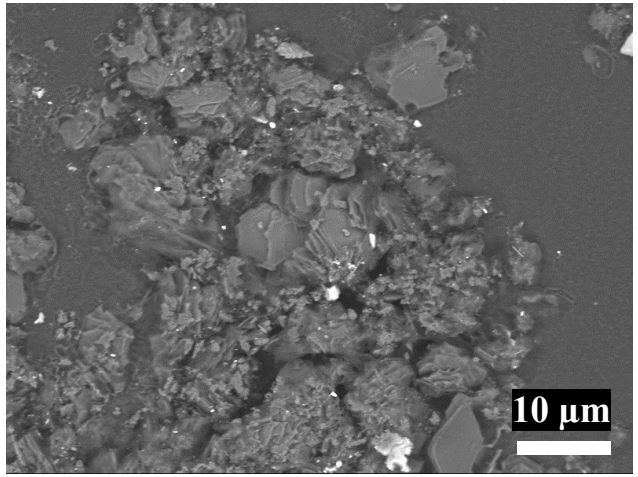

Ball-milled 5h r-BS

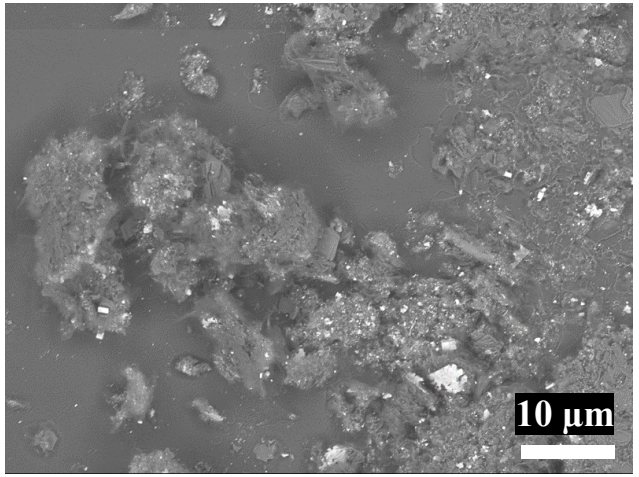

Element mapping

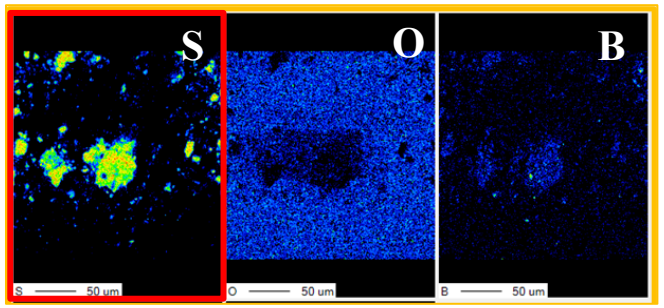

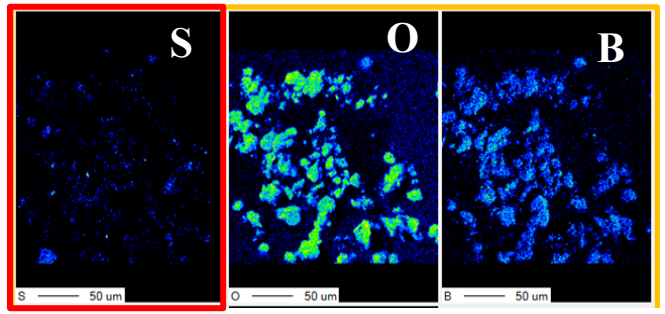

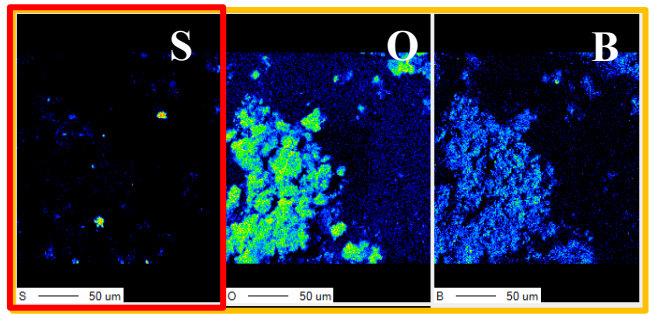

Sulfur lost after long-time ball-milling

Deep Exploration 3: Discussion about the active sites

Continue ball-milling for longer time

XPS

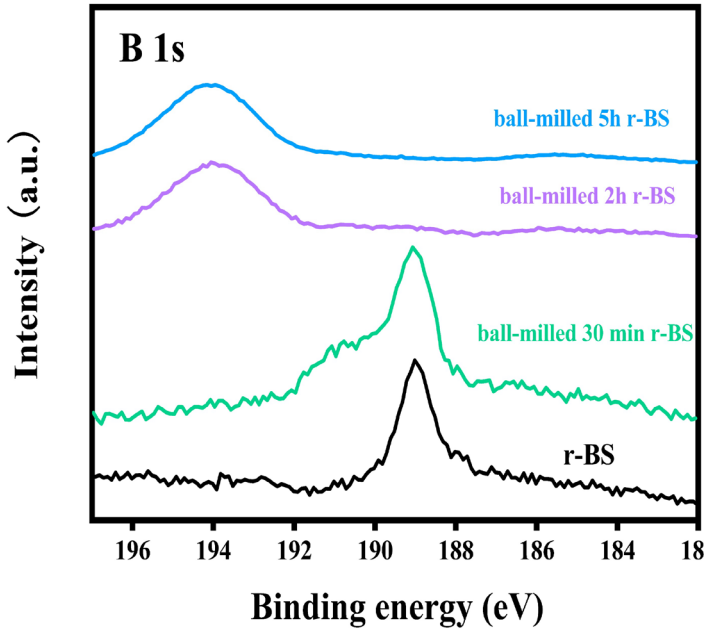

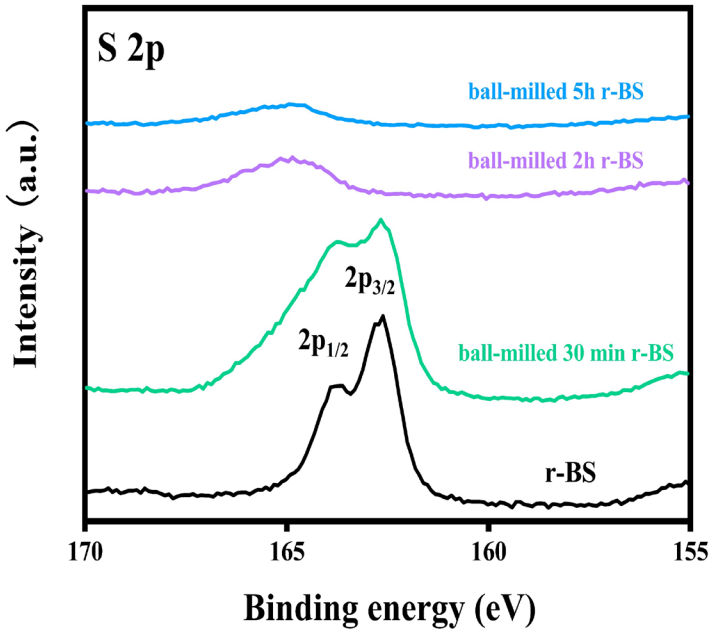

LSV

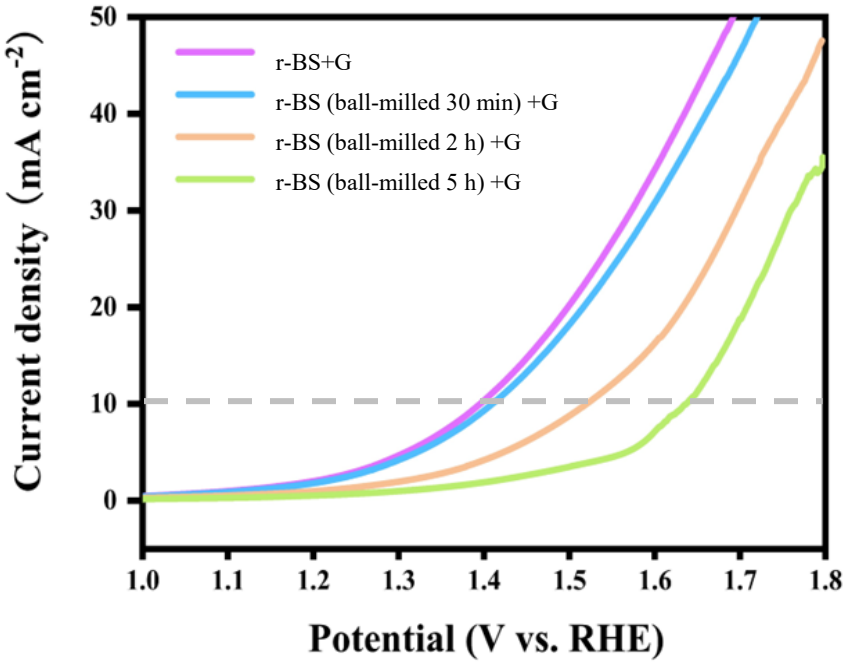

Original Boron and Sulfur peaks disappeared, and new oxide peaks appear after long-time ball-milling → **Activity decreased a lot**

In the case of r-BS for OER

experimentally evaluated the catalytic active sites by using heating

Method:
Firstly, 10 mg of r-BS and 20 mg of GNP were mixed together by grinding. Then **heat the mixture** (r-BS mixed G) at different temperatures for 2h. Finally, take 15 mg of the heated mixture sample for these measurements.

LSV

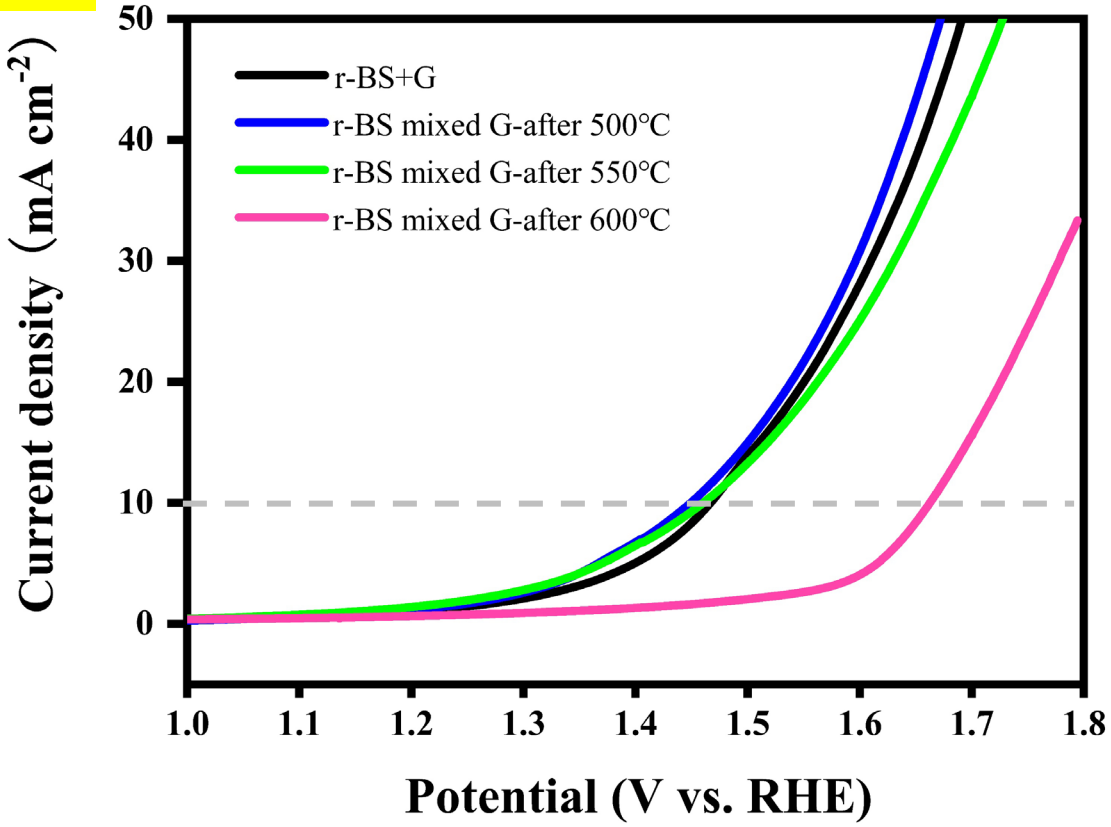

XRD

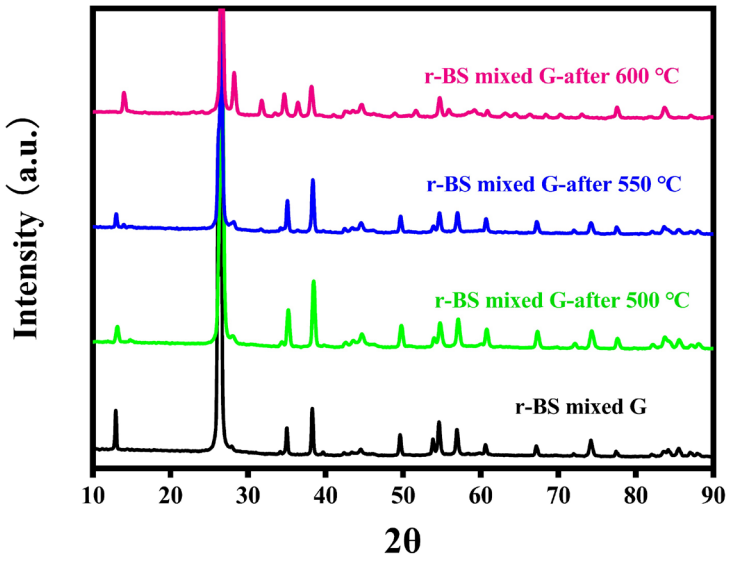

After heating, the activity decreased.
Especially after 600°C, the XRD already changed.

In the case of r-BS for OER

experimentally evaluated the catalytic active sites by using heating

Method:
Firstly, **heat the r-BS powder** at different temperatures for 2h, then mix the heated sample (5 mg) with 10 mg of GNP

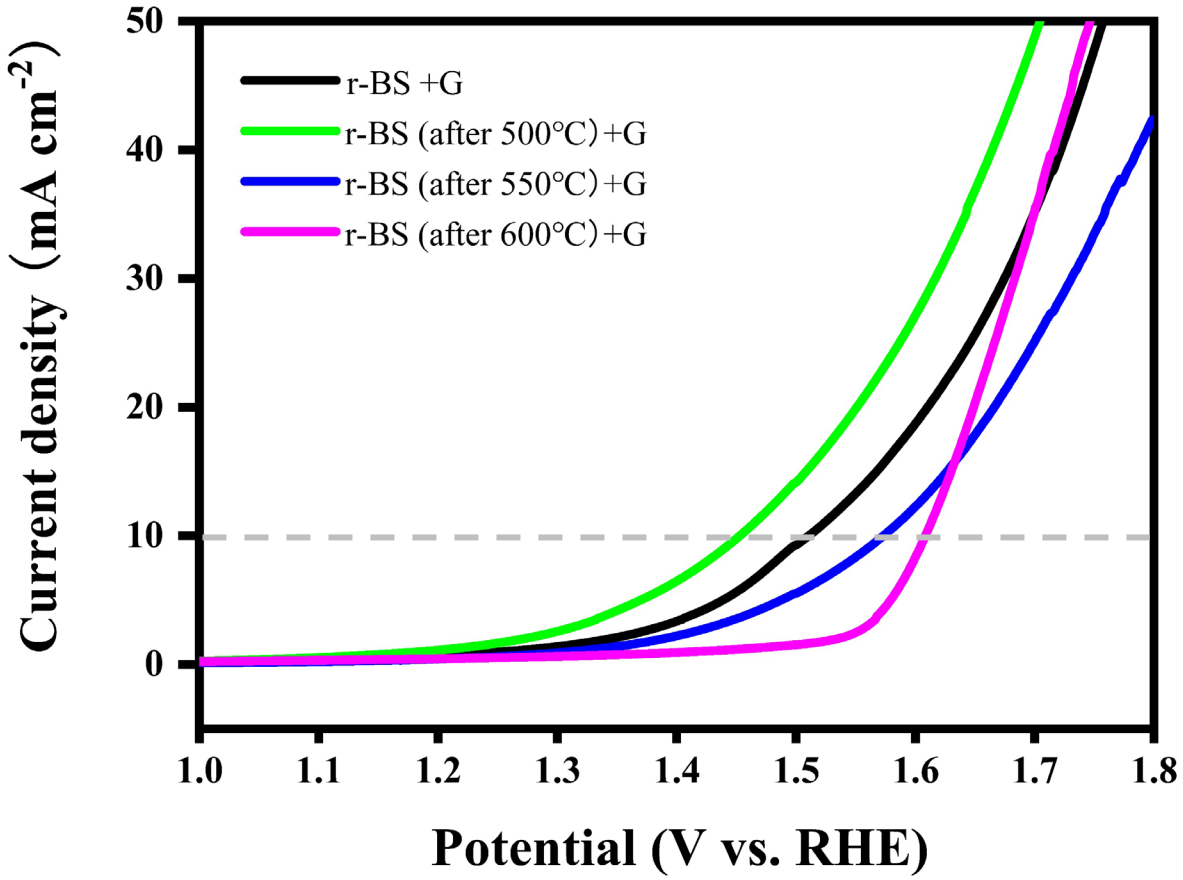

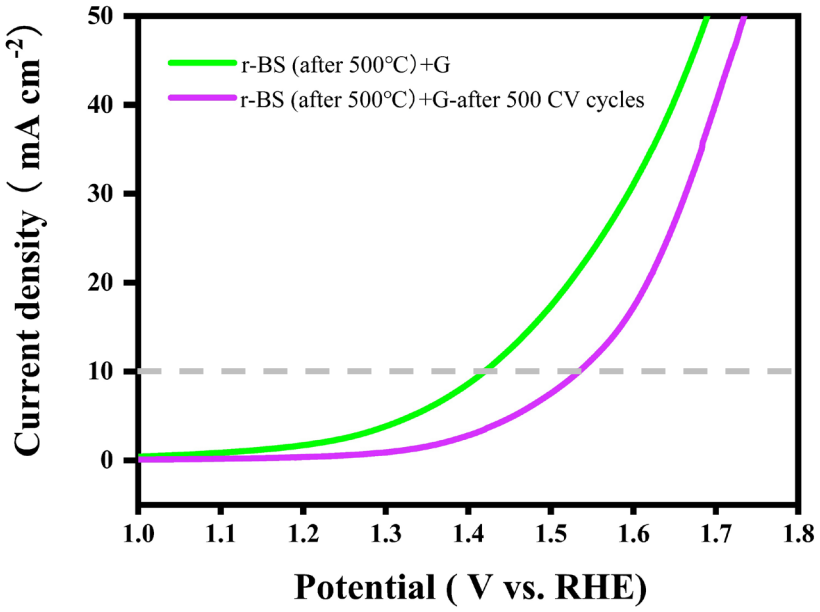

After heated r-BS at 500℃ then mixed with GNP, the activity increased, but the stability even worse, it means after heated sample become more unstable.

ACS APPLIED MATERIALS & INTERFACES

www.acsami.org Research Article

Electrocatalytic Mechanisms for an Oxygen Evolution Reaction at a Rhombohedral Boron Monosulfide Electrode/Alkaline Medium Interface

Satoshi Hagiwara,* Fumiaki Kuroda, Takahiro Kondo, and Minoru Otani*

Cite This: *ACS Appl. Mater. Interfaces* 2023, 15, 50174−50184 Read Online

Theoretically boron vacancy creates active site for OER!

ABSTRACT: Rhombohedral boron monosulfide (r-BS) with a layer stacking structure is a promising electrocatalyst for an oxygen evolution reaction (OER) within an alkaline solution. We investigated the catalytic mechanisms at the r-BS electrode/alkaline medium interface for an OER using hybrid solvation theory based on the first-principles method combined with classical solution theory. In this study, we elucidate the activities of the OER at the outermost r-BS sheet with and without various surface defects. The Gibbs free energies along the OER path indicate that the boron vacancies at the first and second layers of the r-BS surface (V_{B1} and V_{B2}) can promote the OER. However, we found that the V_{B1} is easily occupied by the oxygen atom during the OER, degrading its electrocatalytic performance. In contrast, V_{B2} is suitable for the active site of the OER due to its structure stability. Next, we applied a bias voltage with the OER potential to the r-BS electrode. The bias voltage incorporates the positive excess surface charge into pristine r-BS and V_{B2}, which can be understood by the relationship between the OER potential and potentials of zero charge at the r-BS electrode. Because the OH^- ions are the starting point of the OER, the positively charged surface is kinetically favorable for the electrocatalyst owing to the attractive interaction with the OH^- ions. Finally, we qualitatively discuss the flat-band potential at a semiconductor/alkaline solution interface. It suggests that p-type carrier doping could promote the catalytic performance of r-BS. These results explain the previous measurement of the OER performance with the r-BS-based electrode and provide valuable insights into developing a semiconductor electrode/water interface.

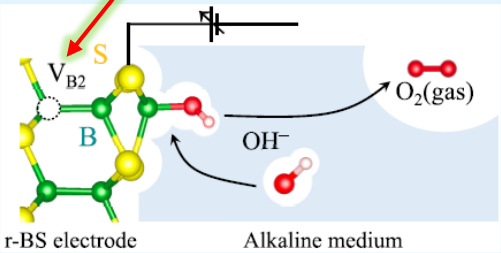

KEYWORDS: *rhombohedral boron monosulfide, oxygen evolution reaction, density functional theory, classical solution theory, semiconductor/water interface*

OER触媒性能向上の検討

・ホウ素欠陥の導入
・硫黄原子サイトへの置換型炭素ドープ

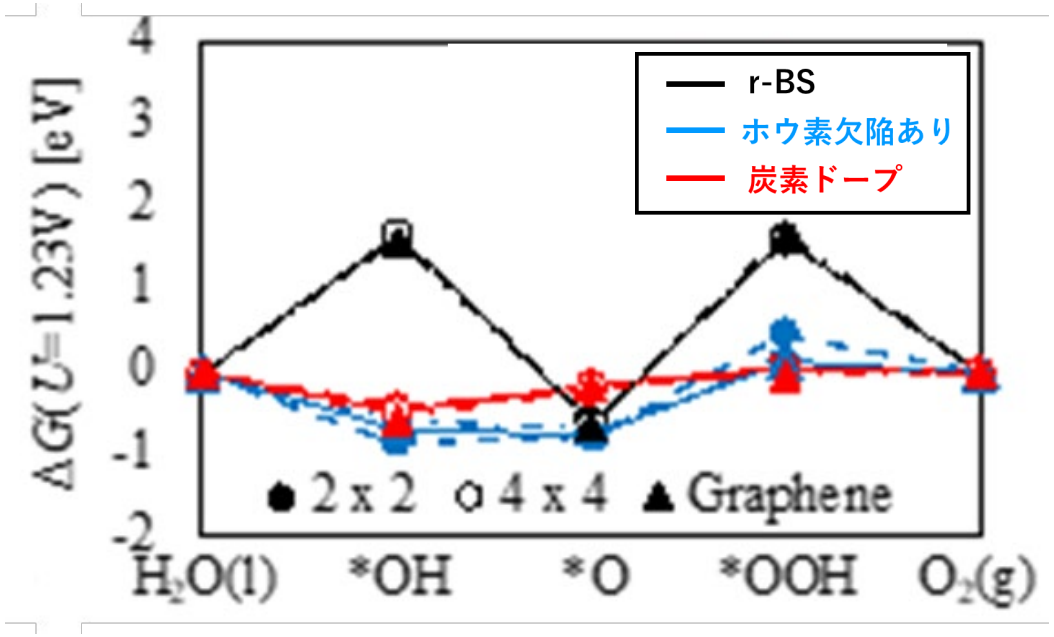

r-BS表面に吸着したOER中間体の
ギブズ自由エネルギー

r-BS

ホウ素欠陥あり

炭素ドープ

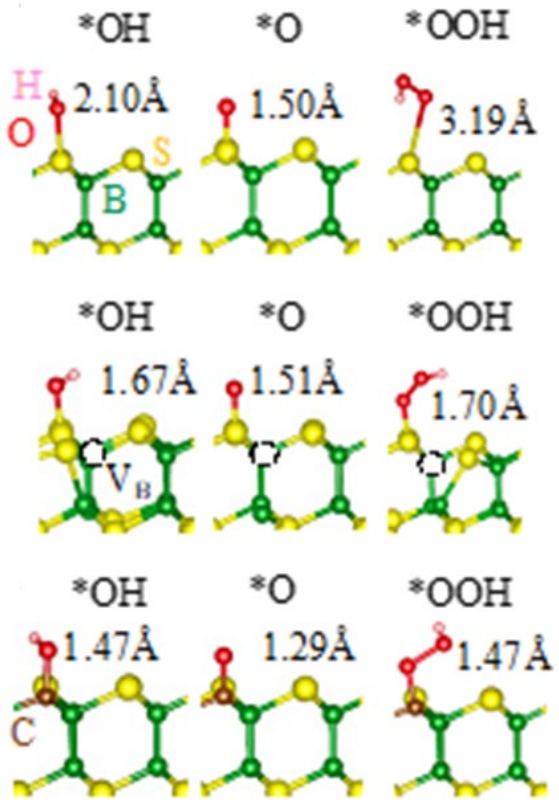

各状態のr-BS表面に吸着した
OER中間体の結合距離

r-BSにおいてホウ素欠陥や硫黄サイトへの炭素ドープがOER性能を向上させることが理論予測されている

S. Hagiwara, T. Kondo, M. Otani, et al., *ACS Appl. Mater. Interfaces* **15** (2023) 50174

B欠陥を導入したr-BS

r-BS合成原料の原子比をB:S=99:100として合成し、欠陥の導入を狙った

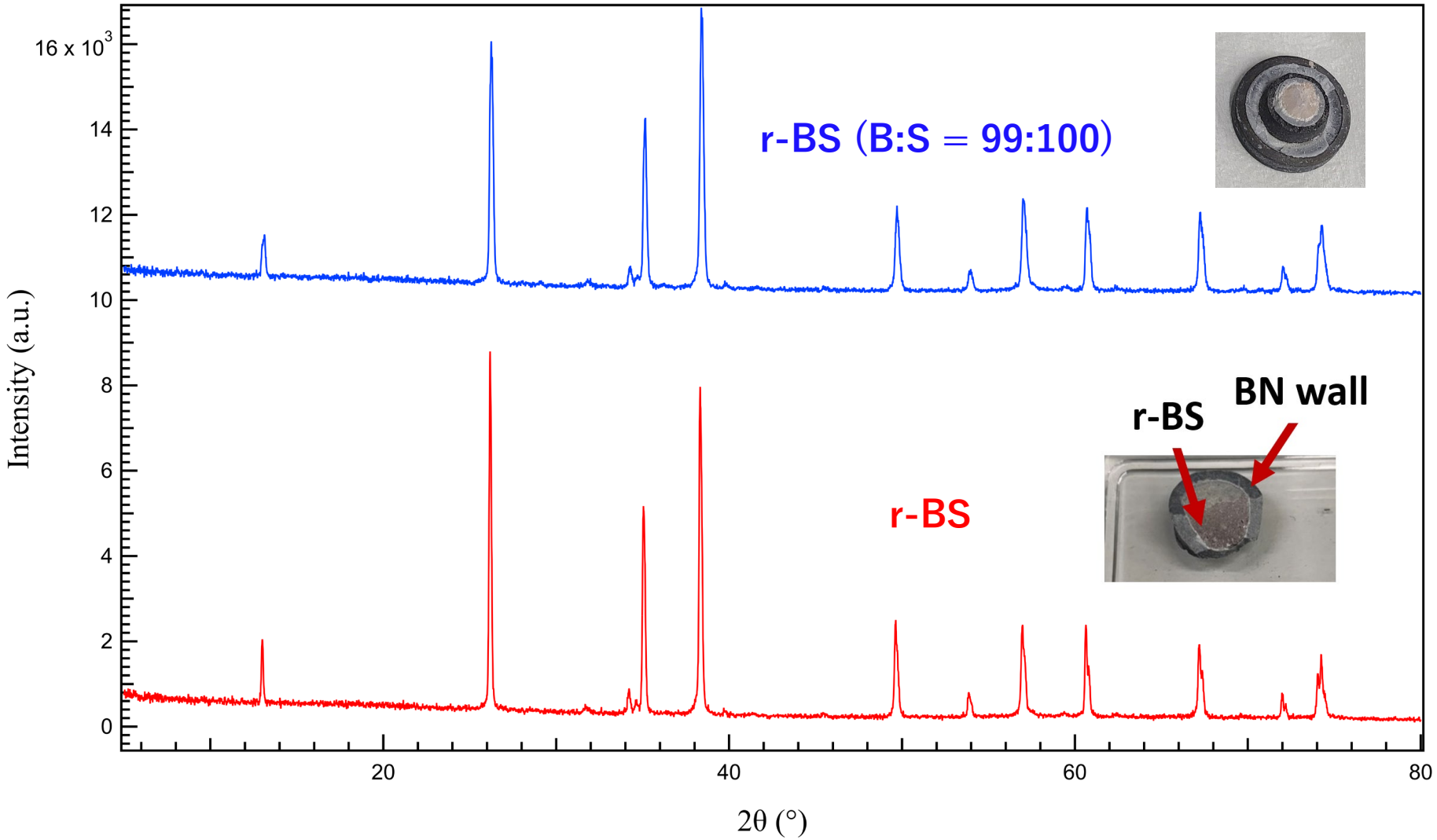

期待された構造イメージ

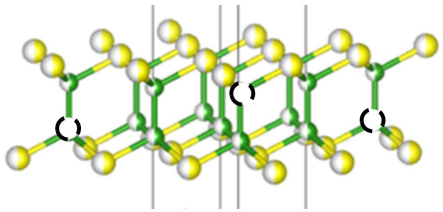

合成した試料ではr-BSの結晶構造のみが示された

B欠陥を導入したr-BSのOER触媒性能の評価

インクの調整: 5 mg r-BS（B:S=99:100）＋ 100 μL ナフィオン分散液 +1 mL エタノール

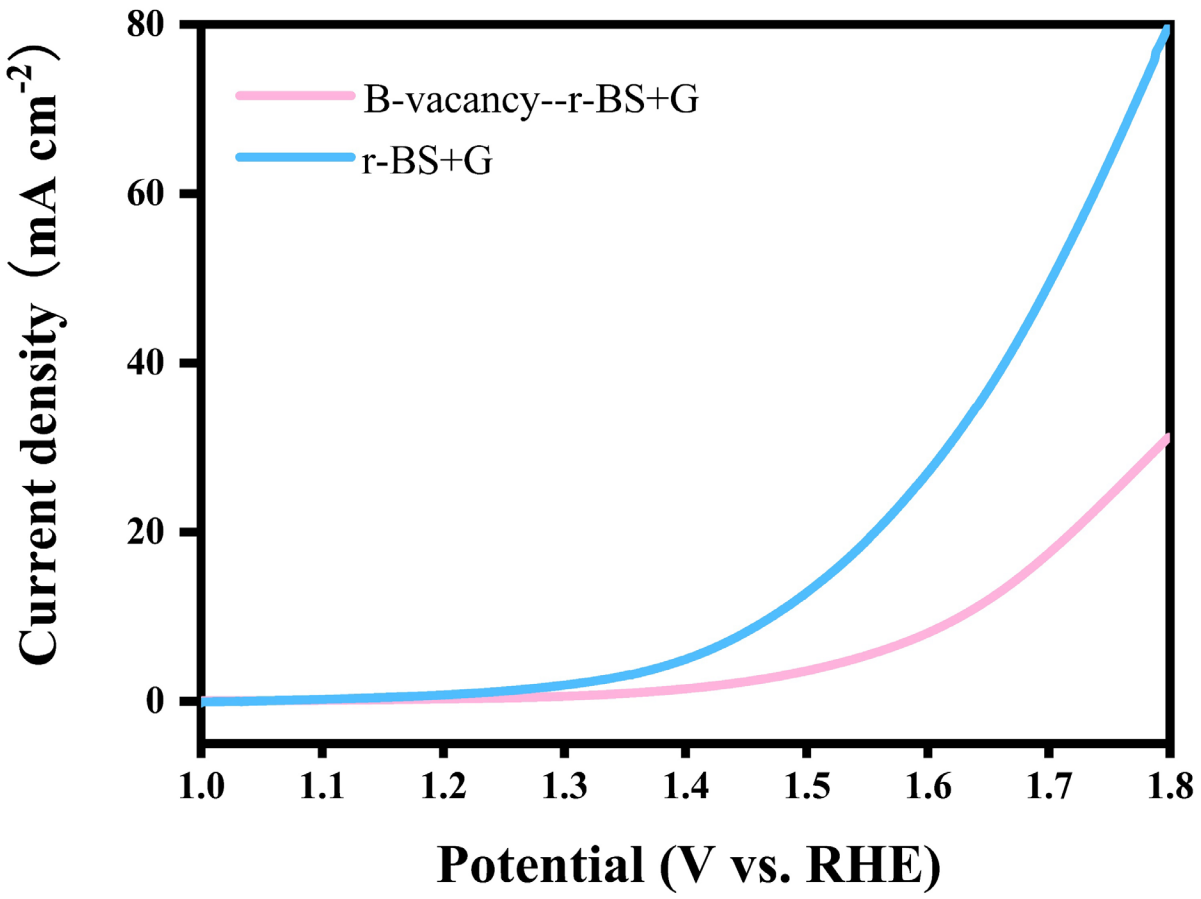

r-BSの結晶構造に変化がないにもかかわらずわずか1%のBを減らすだけで触媒活性が大きく変化

ホウ素原料の減少によりOER触媒としての性能は悪化した

なぜB欠陥を導入したr-BSでOER活性が劣化したか

B欠陥には2種類ある

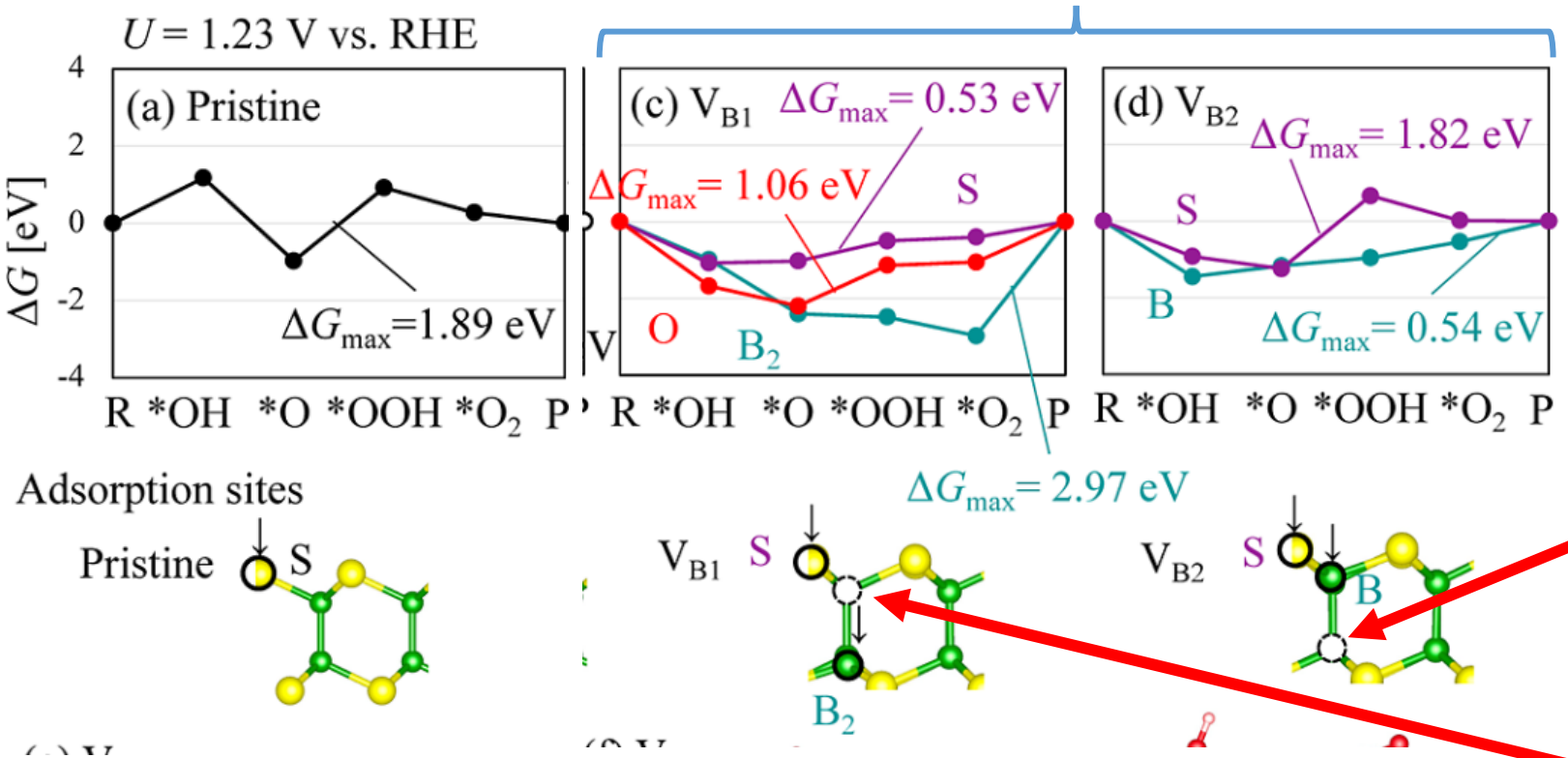

B2サイト(内部)の欠陥
→OER触媒の高活性サイト

B1サイト(表面)の欠陥
→O原子がサイトに入り反応
の進行を阻害する

B1サイトへの欠陥も導入されたことで性能向上が見られなかった可能性がある

S. Hagiwara, T. Kondo, M. Otani, et al., *ACS Appl. Mater. Interfaces* **15** (2023) 50174

Density Functional Theory (DFT) calculation

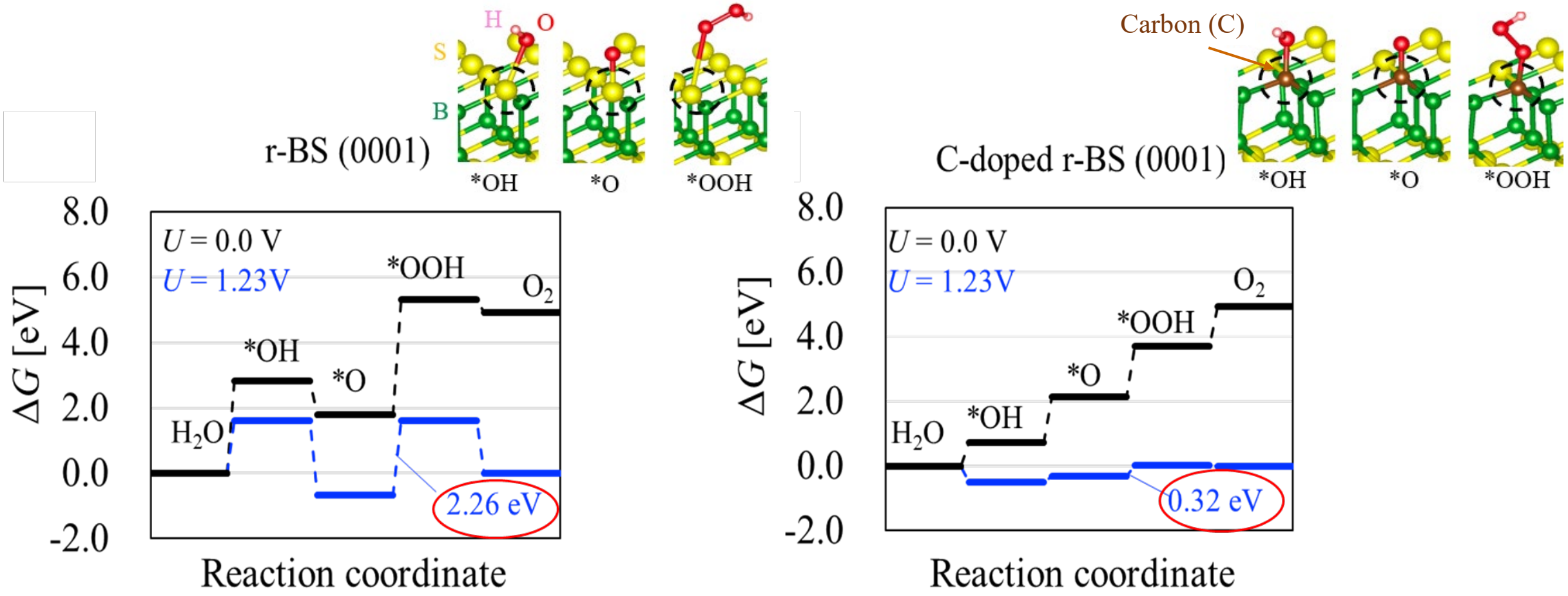

C-doped r-BSが高活性であるという理論予測

Why will the introduction of defects increase the activity?

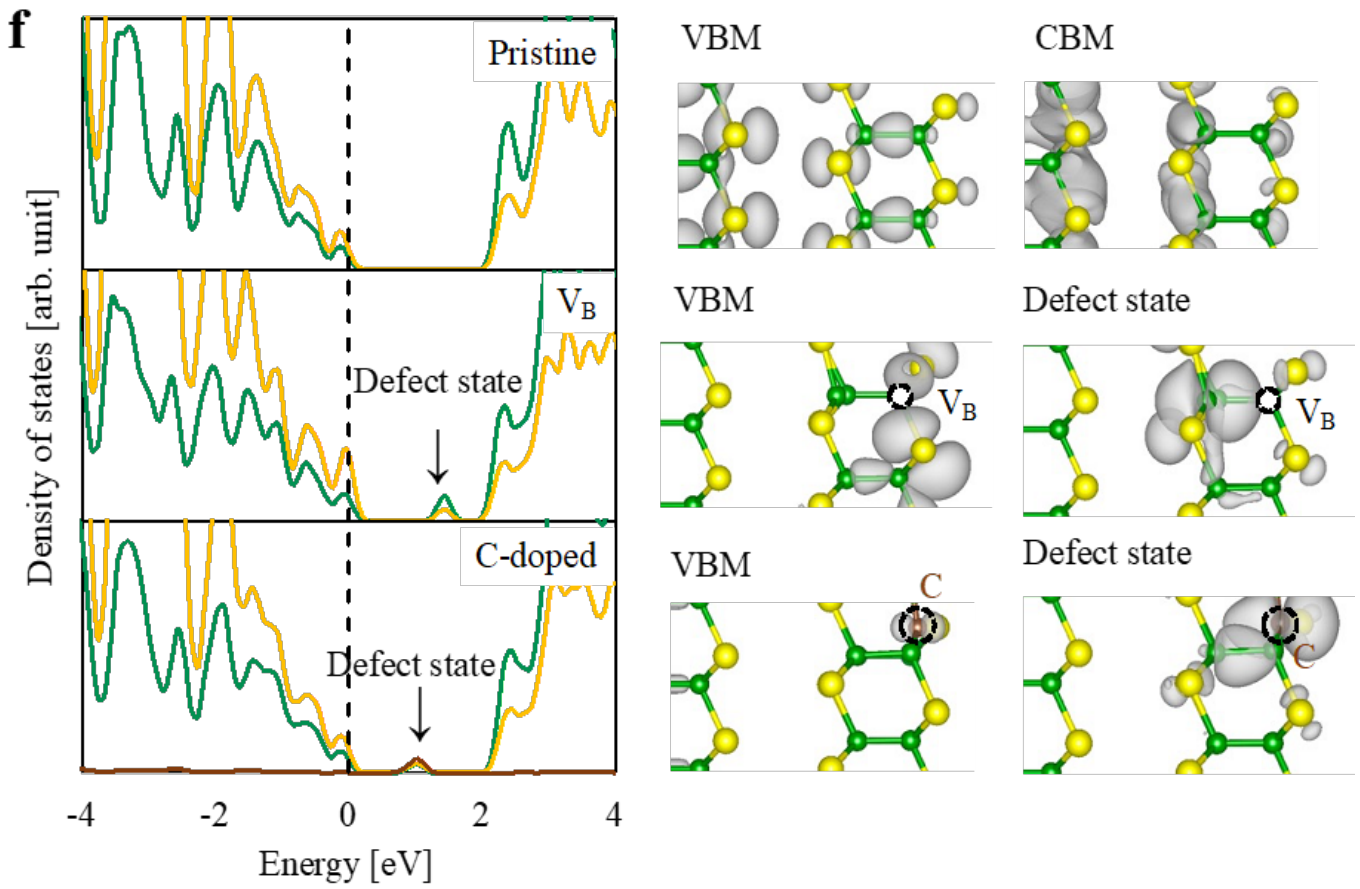

(**f**) Density of states and Kohn-Sham level densities at the valence band maximum (VBM) and conduction band minimum (CBM) (or defect states in the band gap) for the pristine (upper panel), V_B (middle panel), and C-doped surfaces (bottom panel), respectively.

Iso-values of KS level densities for the pristine, V_B and C-doped surfaces were set to 0.0001, 0.001, and 0.001 [au], respectively. The origin of the difference between pristine and defected r-BS can be qualitatively explained by the stabilities of *OH, *O, and *OOH intermediates. Panel (**c**) shows that the S–O bond length in the S–OH and S–OOH states equalled 2.10 and 3.19 Å, respectively, whereas that in the *O state was lower (1.50 Å) than those in the *OH and *OOH states. Thus, compared to *O, the *OH and *OOH intermediates have weaker bonding to pristine r-BS, which suggests that the formation of *OOH from *O is the limiting step. **After introducing V_B (carbon-atom doping), the S–OH (C–OH) and S–OOH (C–OOH) bonds become shorter than the S–OH and S–OOH bonds at the pristine surface, as shown in panel (d) and (e). Thus, both *OH and *OOH are reasonably stabilised, while *O also possesses sufficient stability, thereby aiding OER catalysis.**

C-doped r-BS

・原料の調製方法

炭素源：炭化ホウ素(B_4C)をr-BS原料に一定量混合した

薬品名	表記	分子式	純度	製造元
アモルファスホウ素	高純度アモルファスホウ素	B	99%	山本明保先生(東京農工大)
硫黄華	硫黄	S	99%	和光純薬工業(株)
炭化ホウ素	炭化硼素	B_4C	99%	(株)高純度化学研究所

B_4C

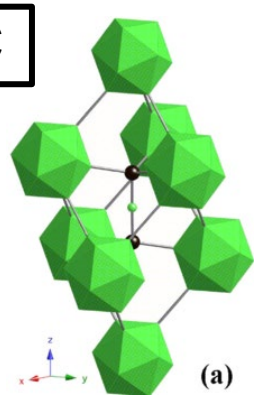

✓組成比は
- B:(S+C)=1:1 … S原子置換
- (B+C):S=1:1 … B原子置換

の2通り

・試料の合成方法

ベルト型高圧合成装置を用いて5.5 GPa, 1873 K, 40分間保持
(通常のr-BSと同様の温度圧力条件)

期待される構造イメージ

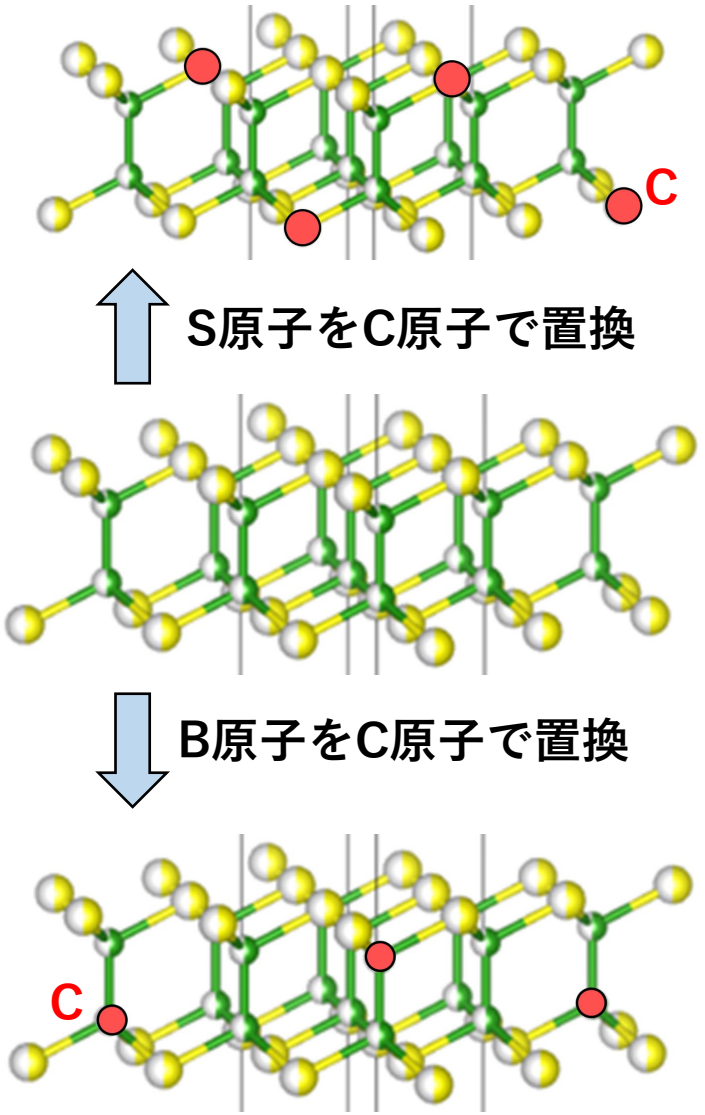

C-doped r-BS

・XRD

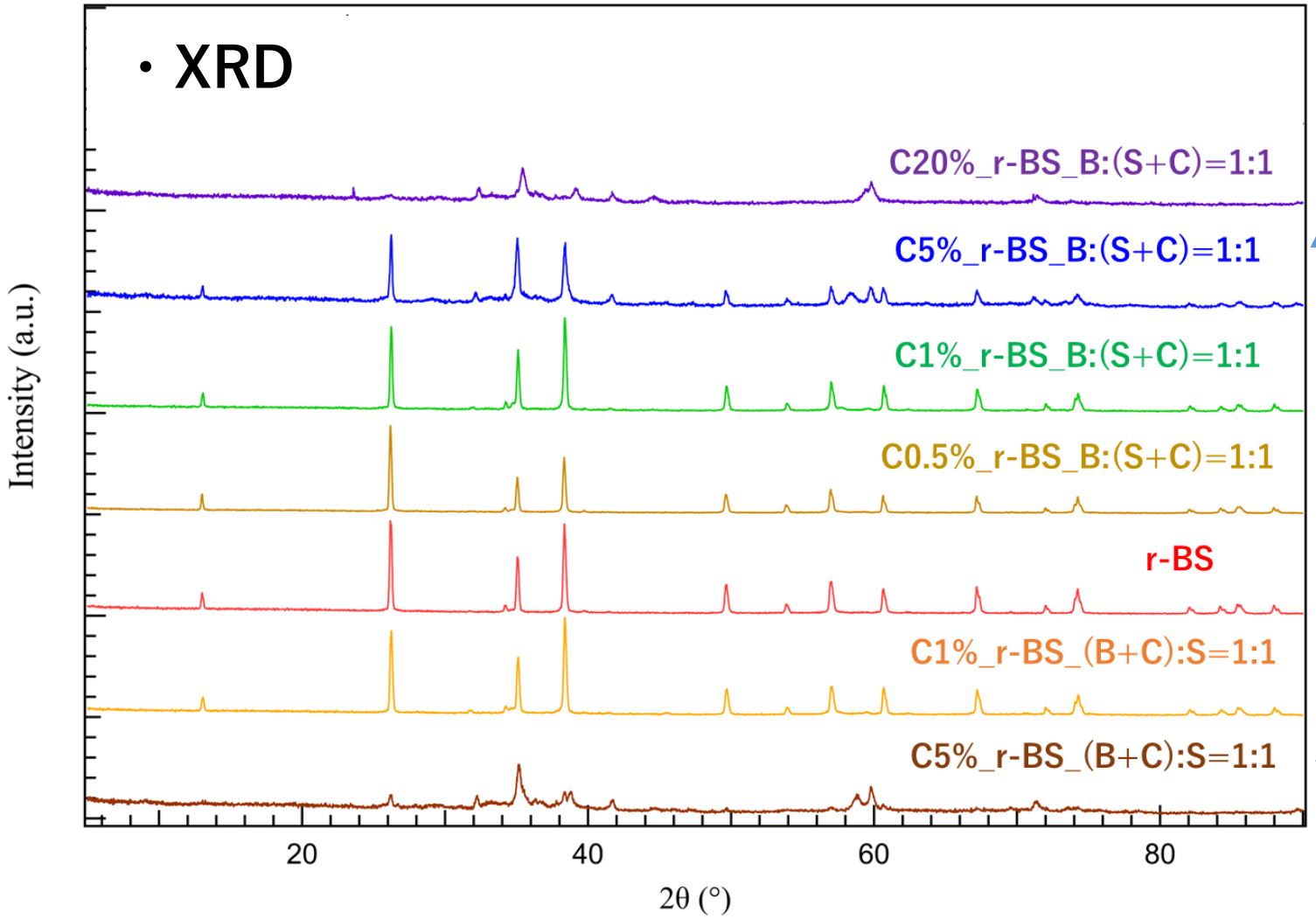

- S原子の置換を狙った試料では
  C5 at%までr-BSの構造が保たれた

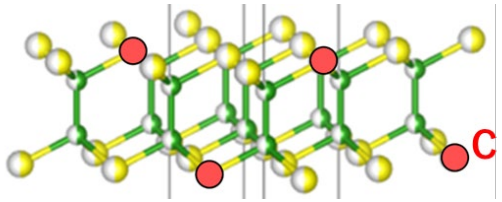

S置換

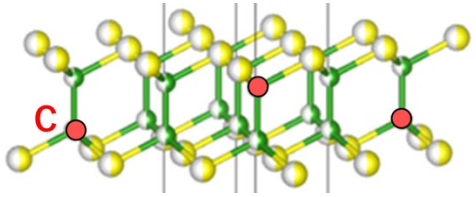

B置換

- B原子の置換を狙った試料では
  C1 at%までr-BSの構造が保たれた

- いずれの試料にも原料に見られるB_4Cのピークは確認されず、
  想定通り熱分解が起きて置換型ドープができたことが推測される

C-doped r-BS

・OER触媒性能

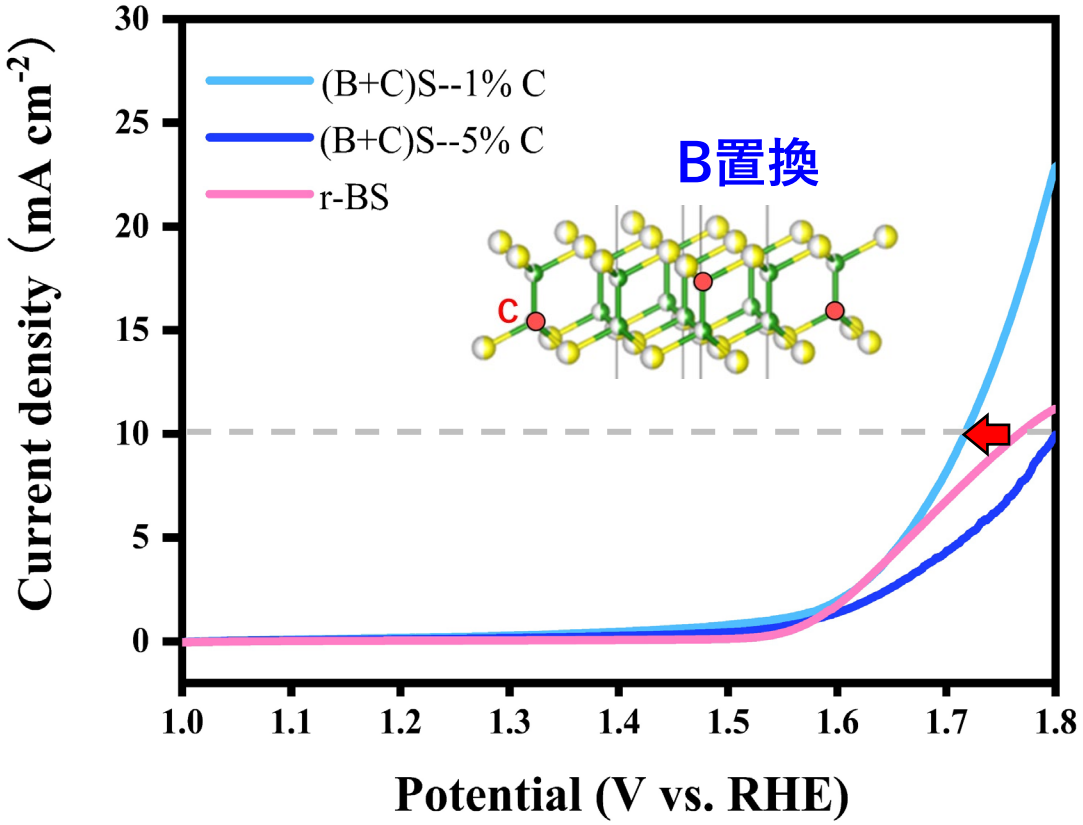

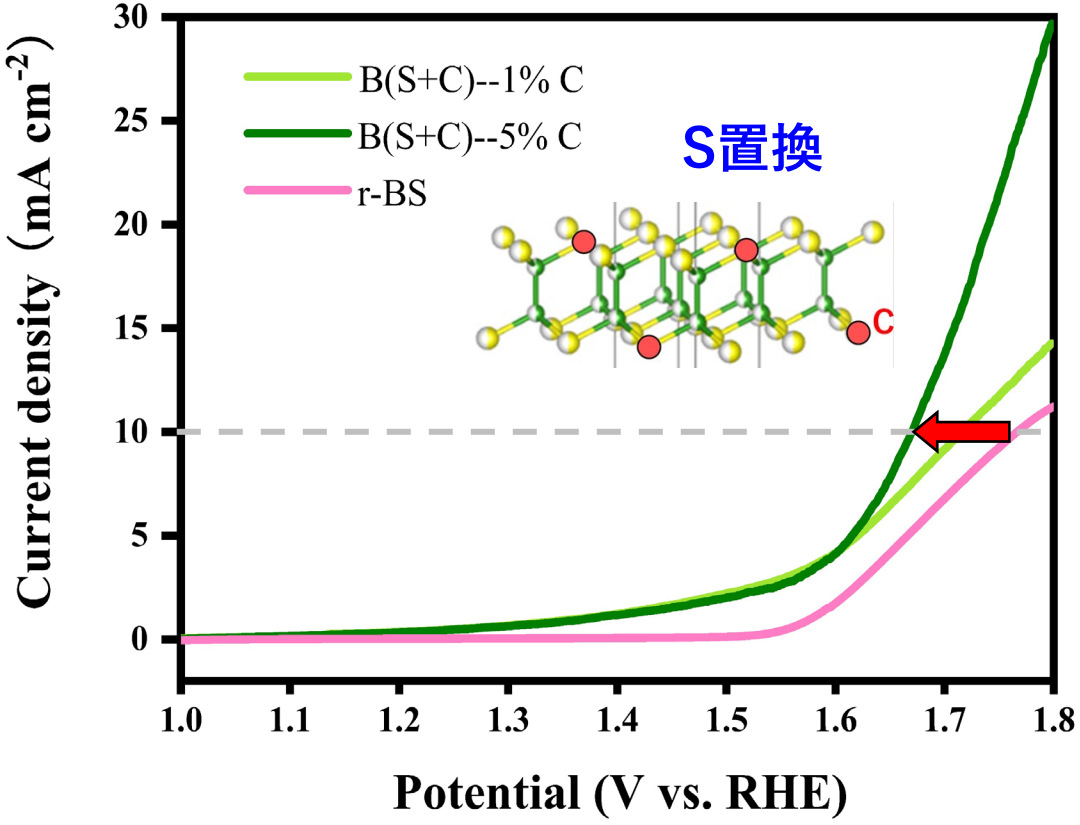

原料に炭素源を加えたr-BSではOER触媒性能の向上が見られた

C-doped r-BS＋G

Method:
mixed with GNP, keep 5 mg of C-doped r-BS mixed with 10 mg of GNP

Mixed with GNP

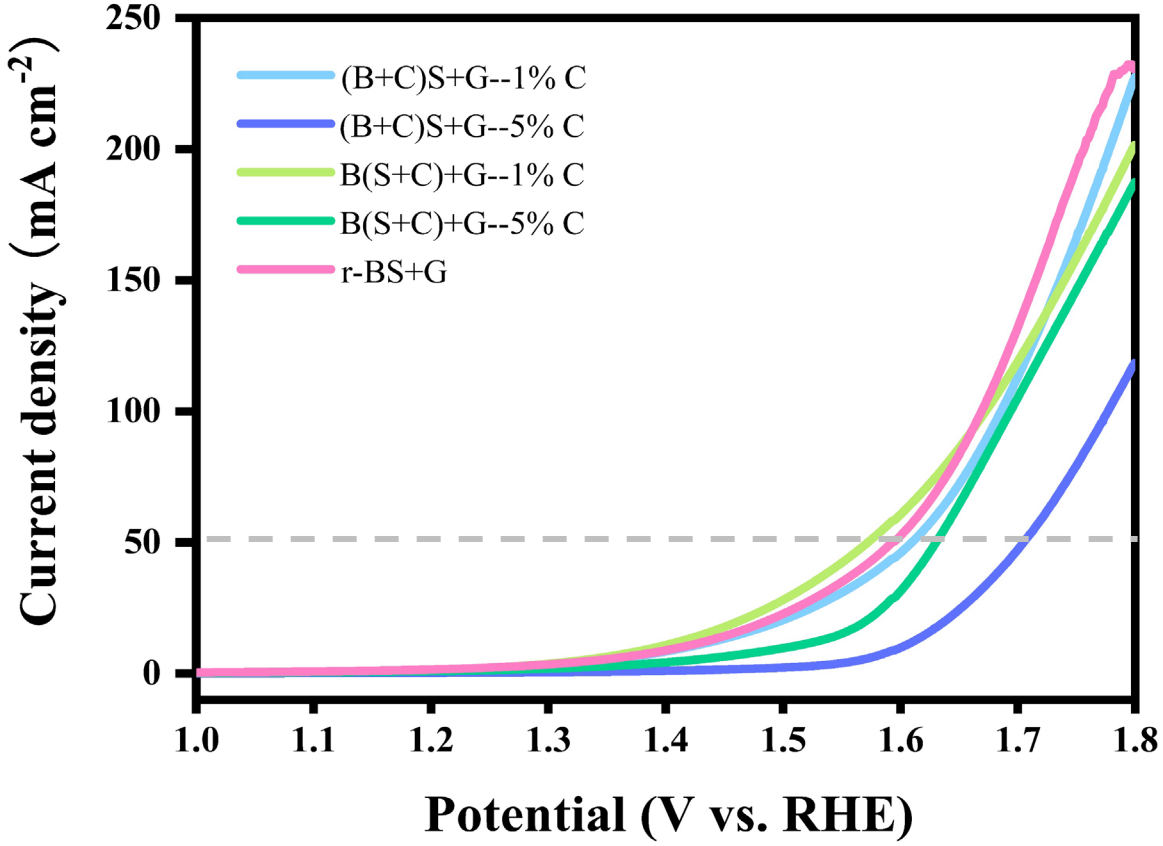

For original sample, the C-doped r-BS showed better activity,
but when mixed with GNP, C-doped r-BS+G performed worse

・C1 %_r-BS_S 置換

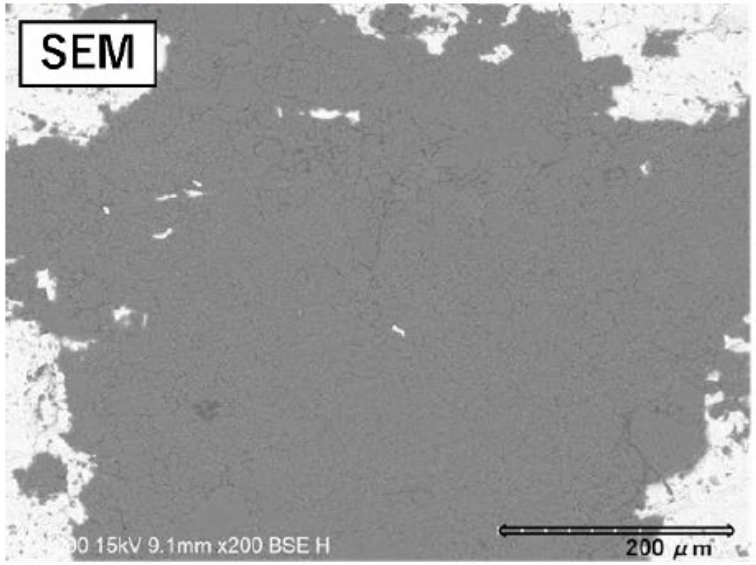

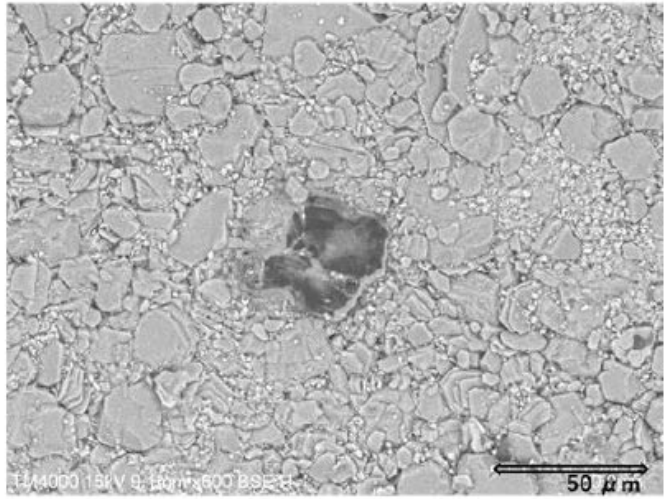

EDX

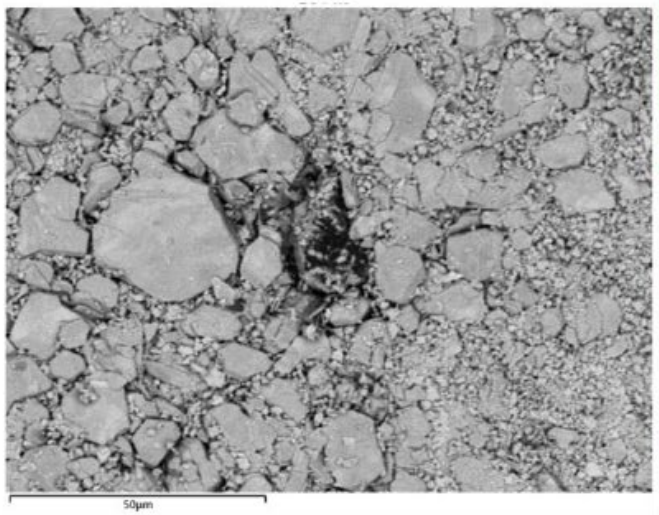

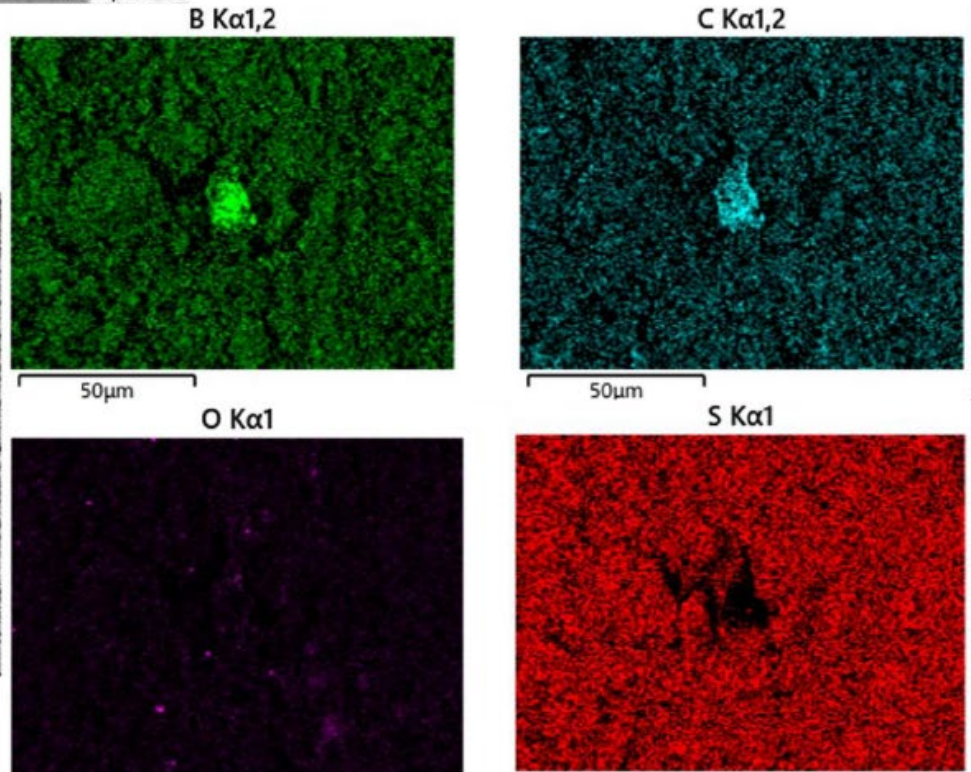

うまくSに置換型でドープされずホウ素と炭素の塊（おそらくC源のB_4C）が別に塊で存在している

うまくSに置換型でドープされず
ホウ素と炭素の塊（おそらくC源のB_4C）
が別に塊で存在している

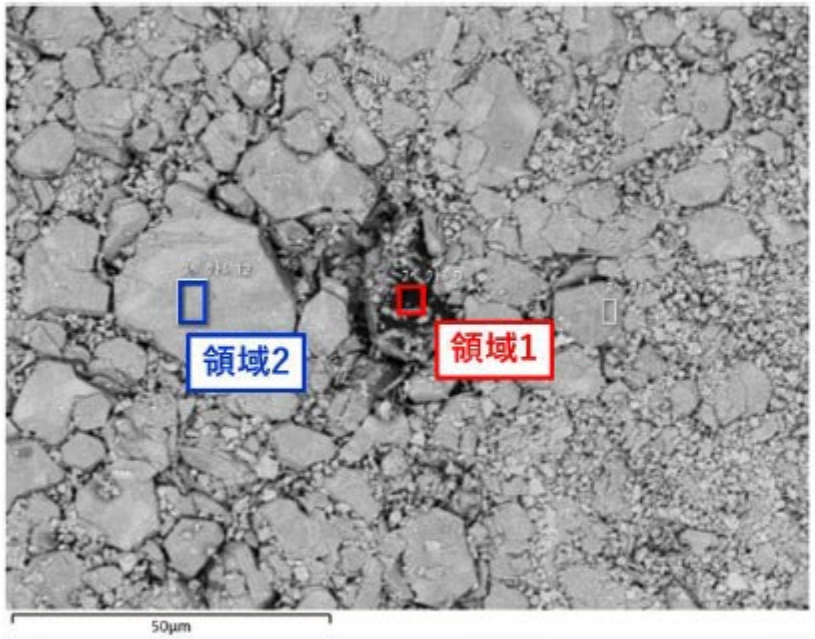

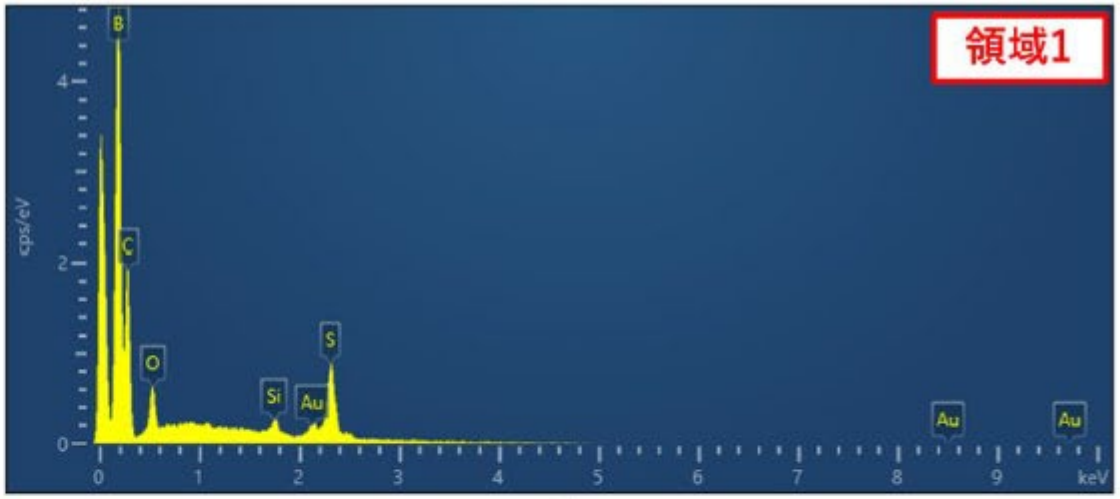

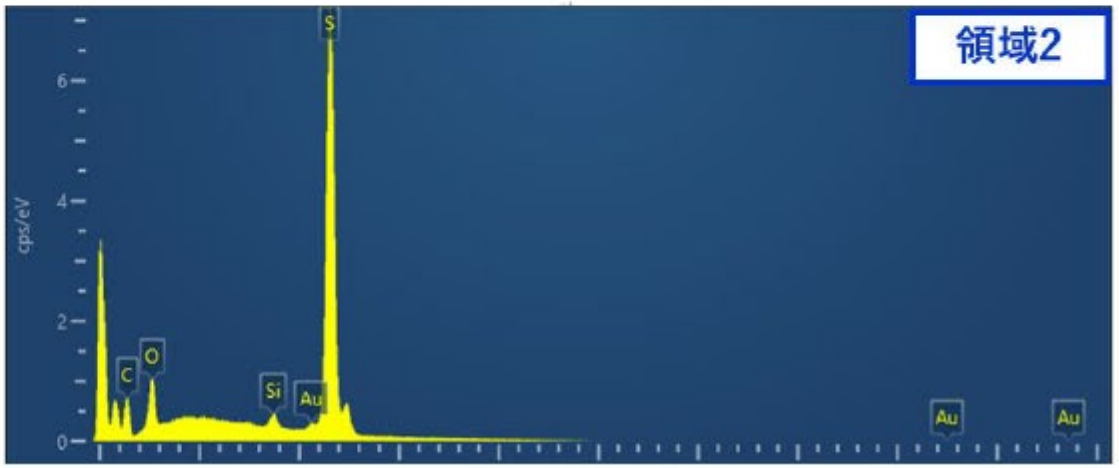

Summary

In summary, we have developed **a new metal-free electrocatalyst for OER**. Introducing the graphene nanoplates into the r-BS by a very simple method, the mixture (**r-BS+G**) exhibits high electronic performance.

We clarified that the electrochemical current of r-BS+G in the whole swept potential range mainly originated from the OER, and the Faradic efficiency is **98.8%**.

In the experiment, to determine the active sites in r-BS+G, future studies will involve atomic-scale microscopy and further spectroscopy studies on well-defined and defect-controlled model catalysts.

L. Li, T. Kondo, et al. ***Chem. Eng. J.*** 471, 144489. (2023).

Outline

1. 自己紹介

2. カーボンニュートラルの必要性と材料開発の重要性

3. 水素製造に貢献する材料開発
典型元素を利用した高活性アルカリ水電解触媒

(1) 硫化ホウ素(r-BS)の合成と評価

(2) r-BSとグラフェンの混合物が示す
高いOER触媒特性

(3) r-BSの活性点（MoS_2のHER活性点との比較）

(4) r-BS＋グラフェンOER触媒の高耐久性化

4. 水素利用に貢献する材料開発

5. 水素吸蔵に貢献する材料開発

Previous our results: r-BS+G is a promising OER electrocatalyst

L. Li, T. Kondo, et al. *Chem. Eng. J.* 471, 144489. (2023).

r-BS: rhombohedral boron monosulfide

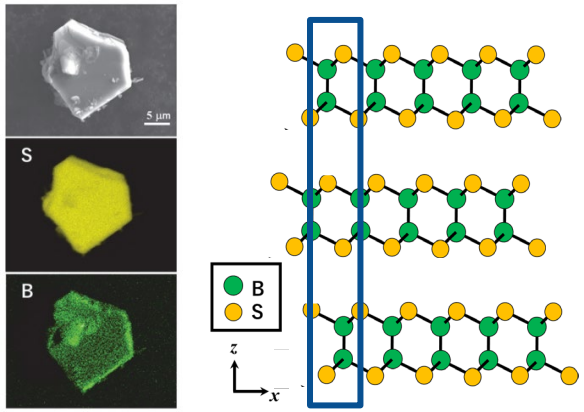

H. Kusaka, L. Li, T. Kondo, et al., *J. Mater. Chem. A,* 9, 24631 (2021).

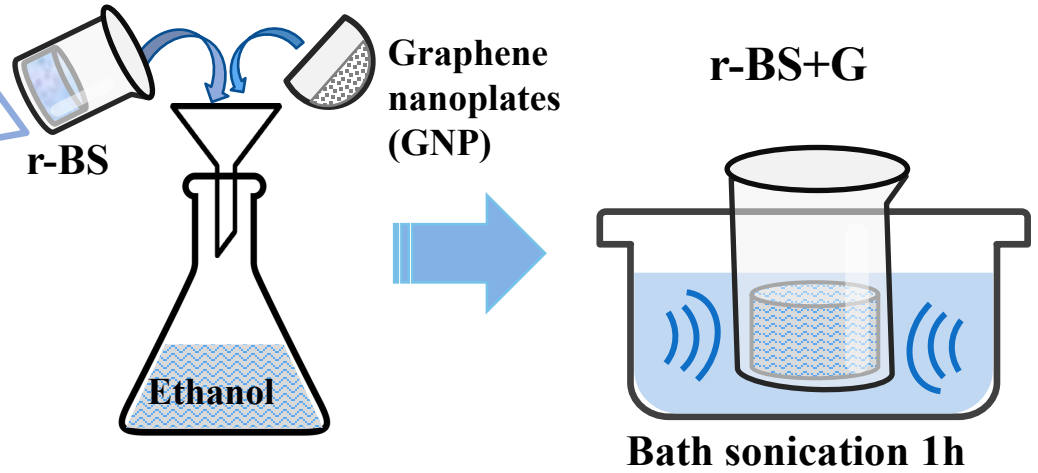

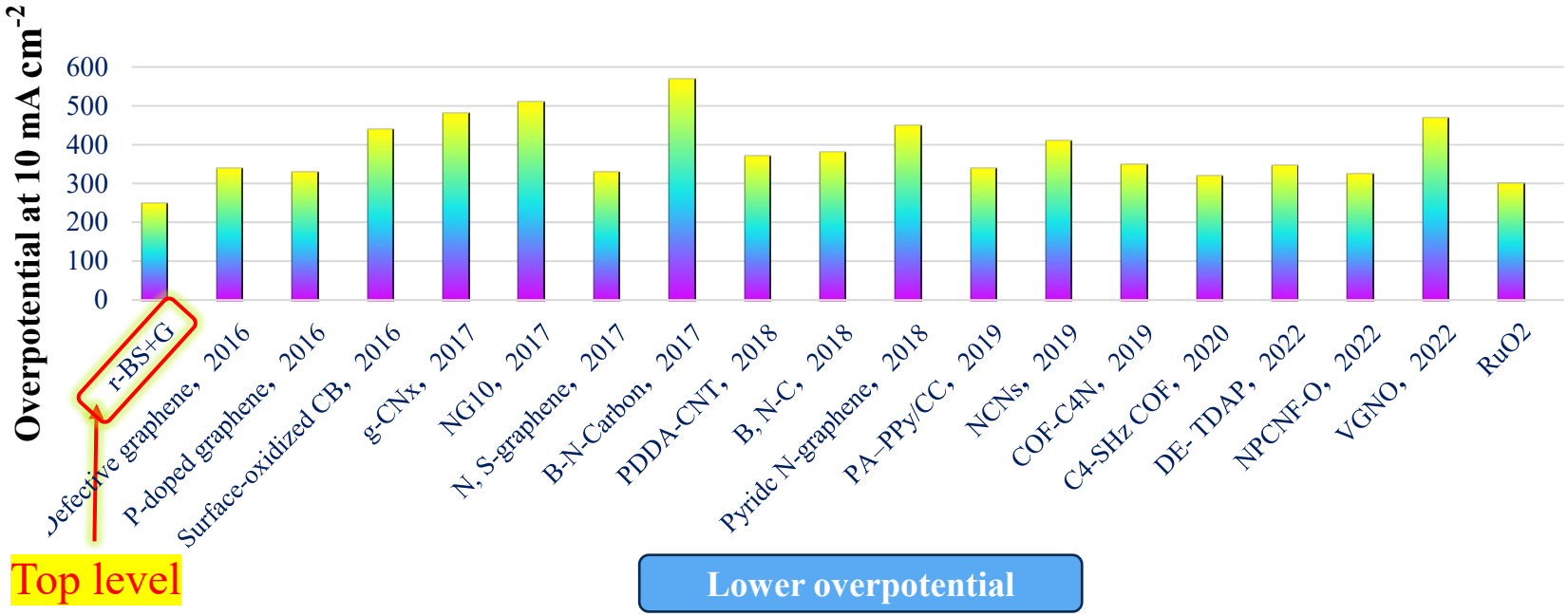

r-BS+G has superior activity to commercial RuO_2 and most reported metal-free catalyst !

Problem 1: electrochemical stability

The stability of r-BS+G was explored using cyclic voltammetry (CV)

The stability is very important for the wide application of electrocatalysts

LSV curves of r-BS+G after 500 CV and 2000 CV cycles between

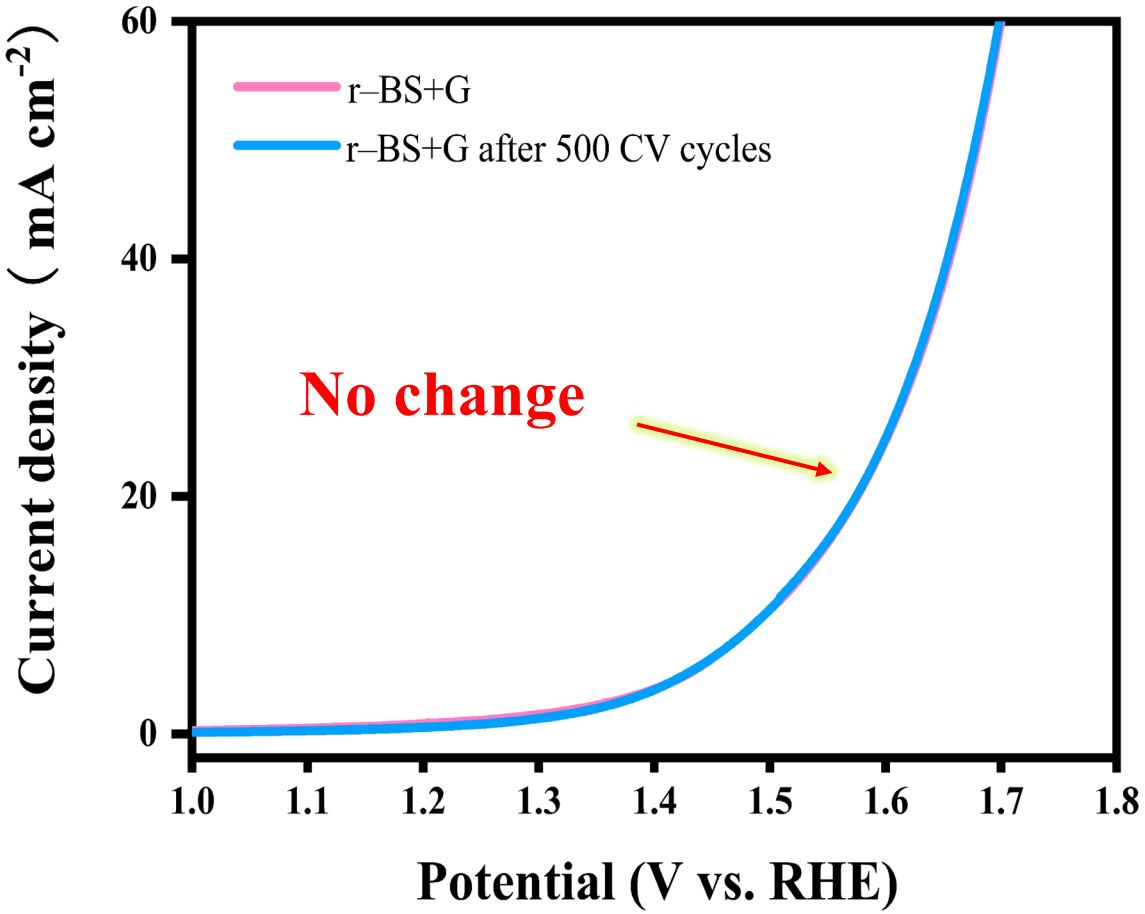

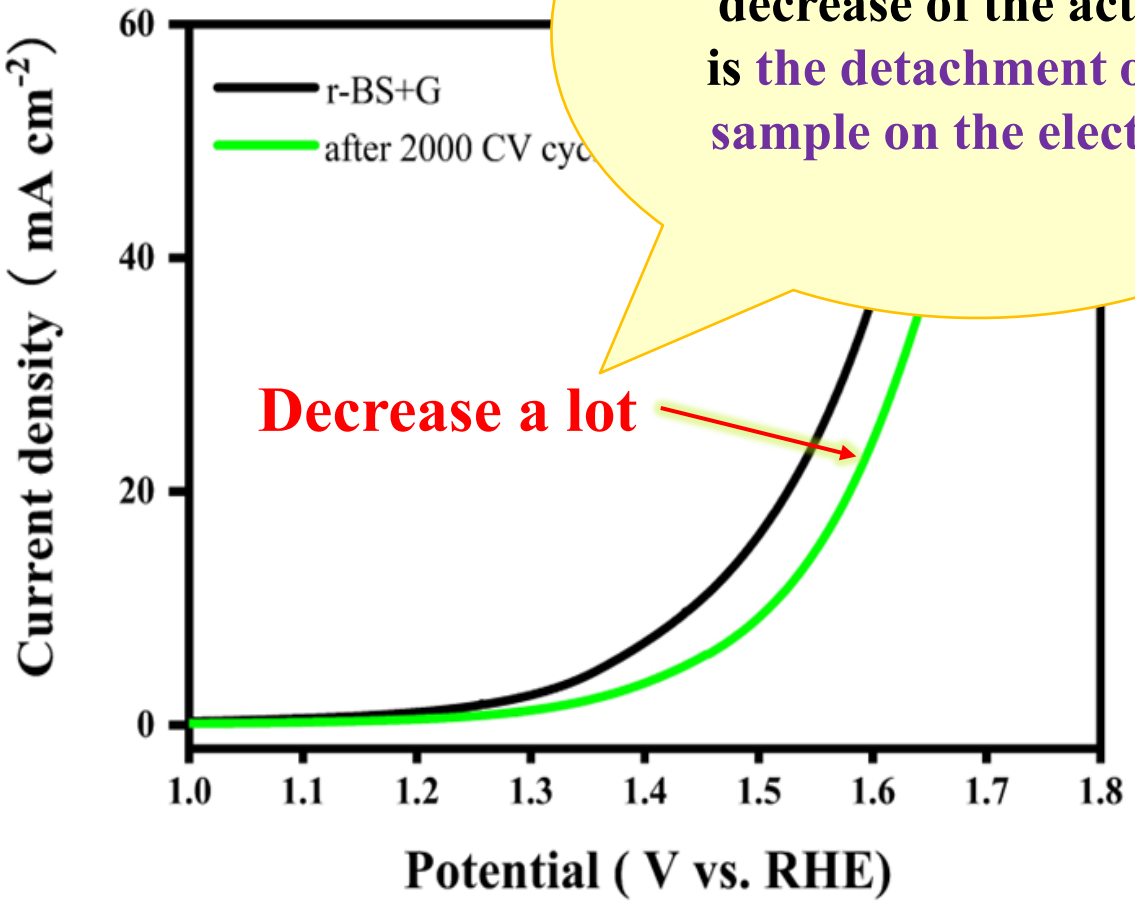

The reason for the decrease of the activity is the detachment of the sample on the electrode

Why did the activity decrease after 2000 CV cycles?

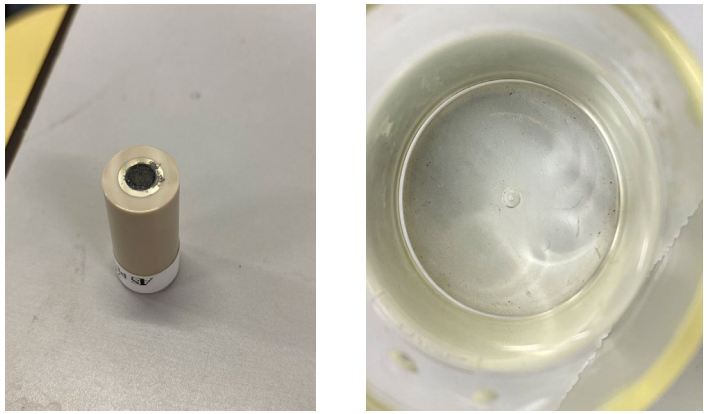

RRDE after 2000 CV cycles

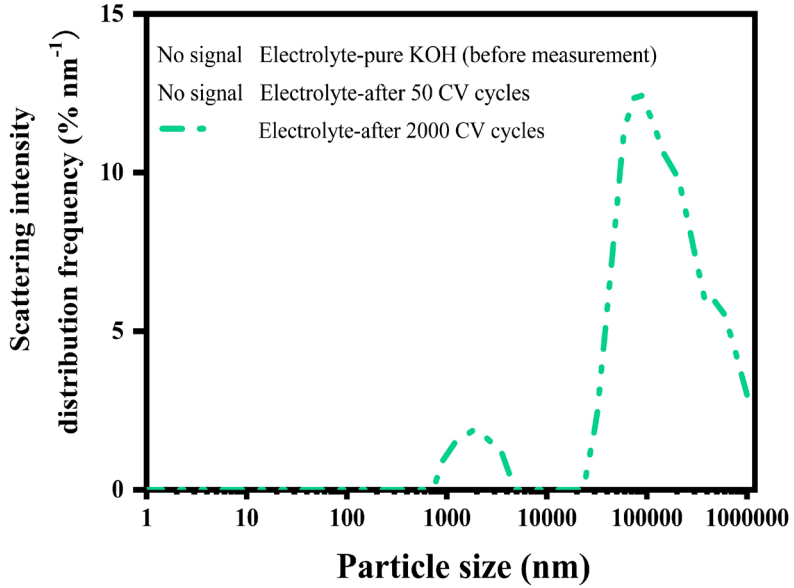

After 2000 CV cycles, some samples was **detached from the electrode**, causing the loss of the activity.

動的光散乱で粒子が検出される

Problem2 : Tafel slope

Tafel plots of different catalysts

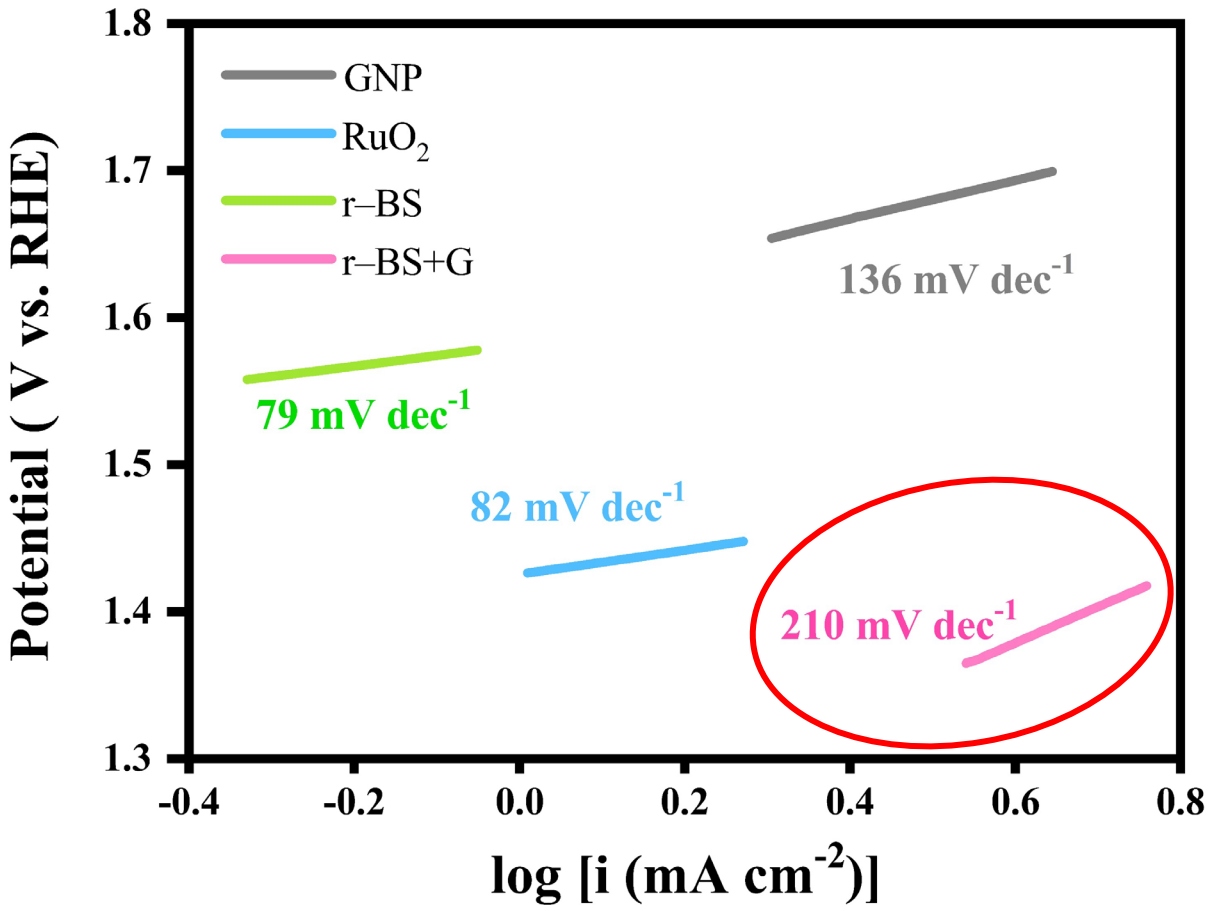

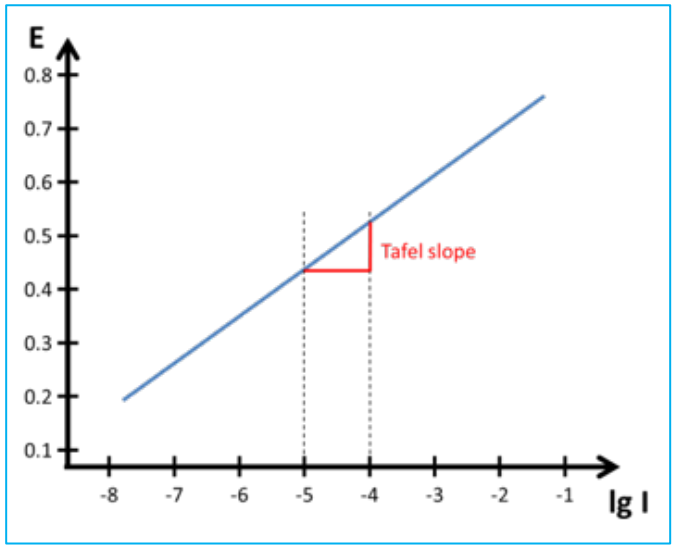

Tafel slope: a quantification of the additional voltage required to increase the catalytic current density by a decade.

Smaller Tafel slope, better performance.

The Tafel slope is large

Next step: Development of highly stable r-BS+G catalyst for OER

Unstable reason:

Generated O_2 bubbles cause detach of the catalyst in electrolyte

To solve:

Introducing the **self-supporting structure**.

The 3D **nickel foam (NF)** with high conductivity, large surface area and stability is a promising candidate as substrates.

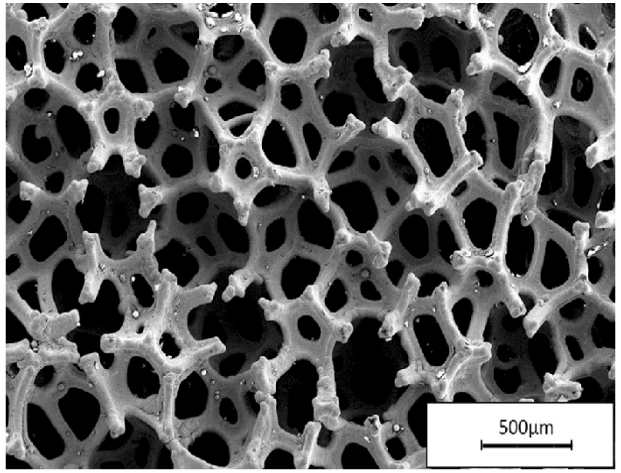

Nickel foam (NF)

We introduced the Nickel foam as the self-support electrode

L. Li and T.K.*, et al., ***Sci. Tech. Adv. Mater***. 24 (2023) 2277681.

Method

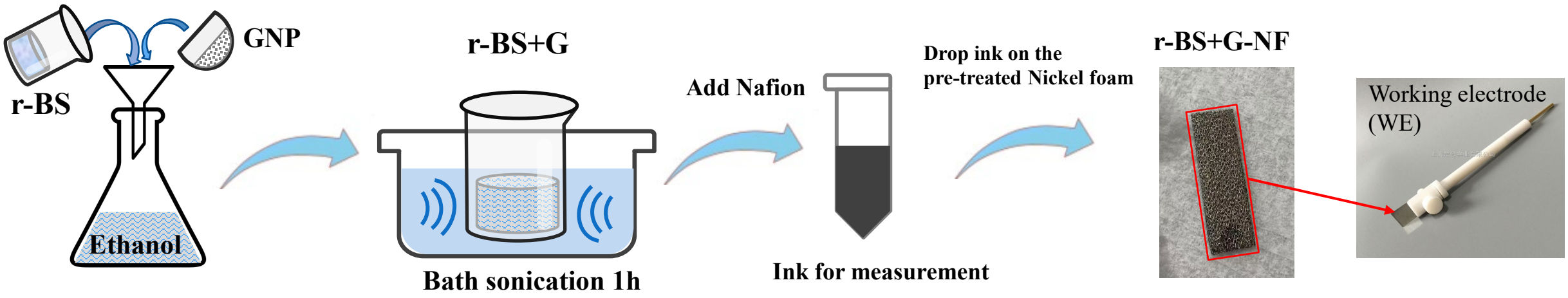

[r-BS-NF, graphene-NF, RuO_2-NF were prepared by the same method (drop same amount of catalyst on NF)]

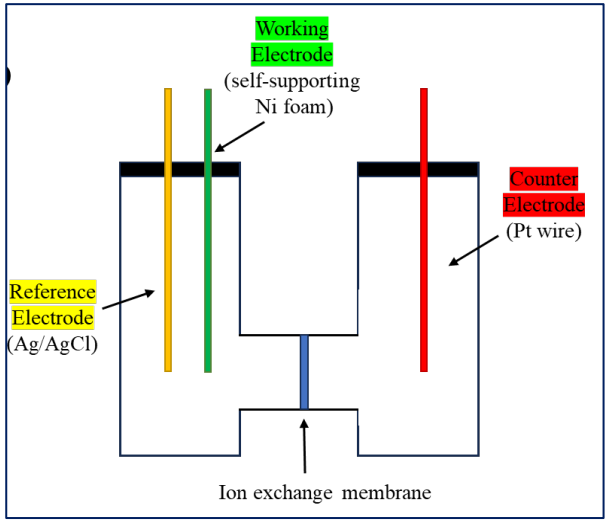

All electrochemical measurements were performed with a three-electrode system in 1 M aqueous KOH with an **H-type** electrolytic cell

Physical characterization

Scanning electron microscopy (**SEM**) of r-BS+G-NF

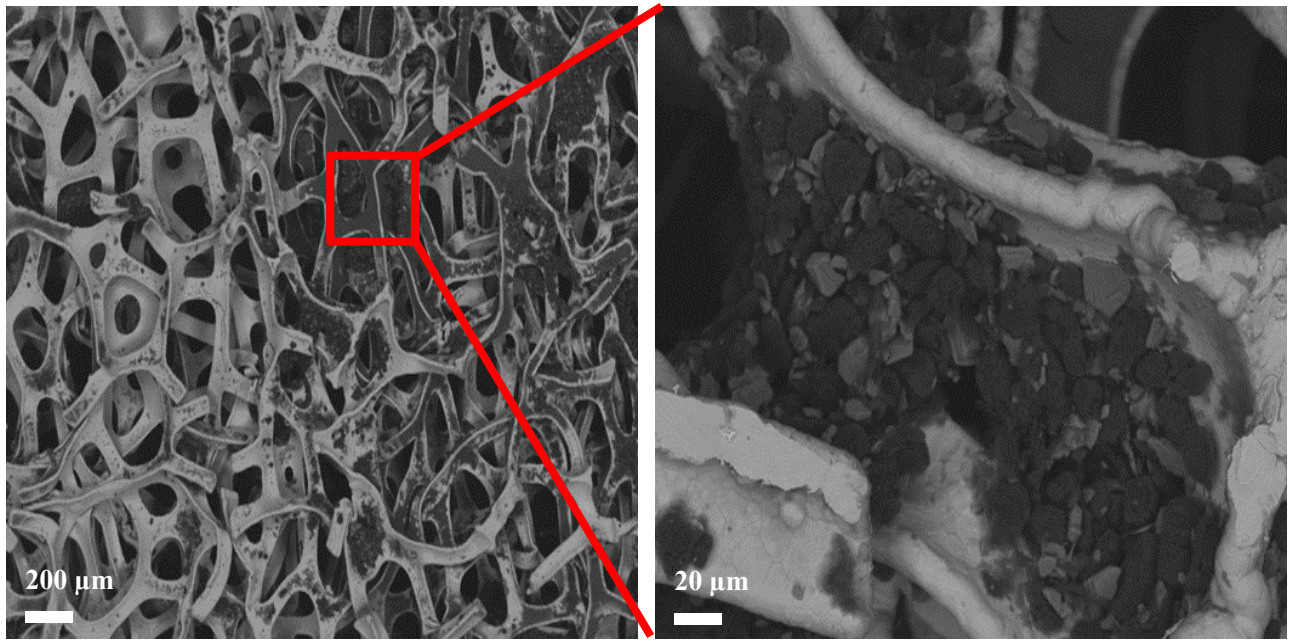

Electron probe microanalyzer (**EPMA**) image and element mapping of r-BS+G-NF

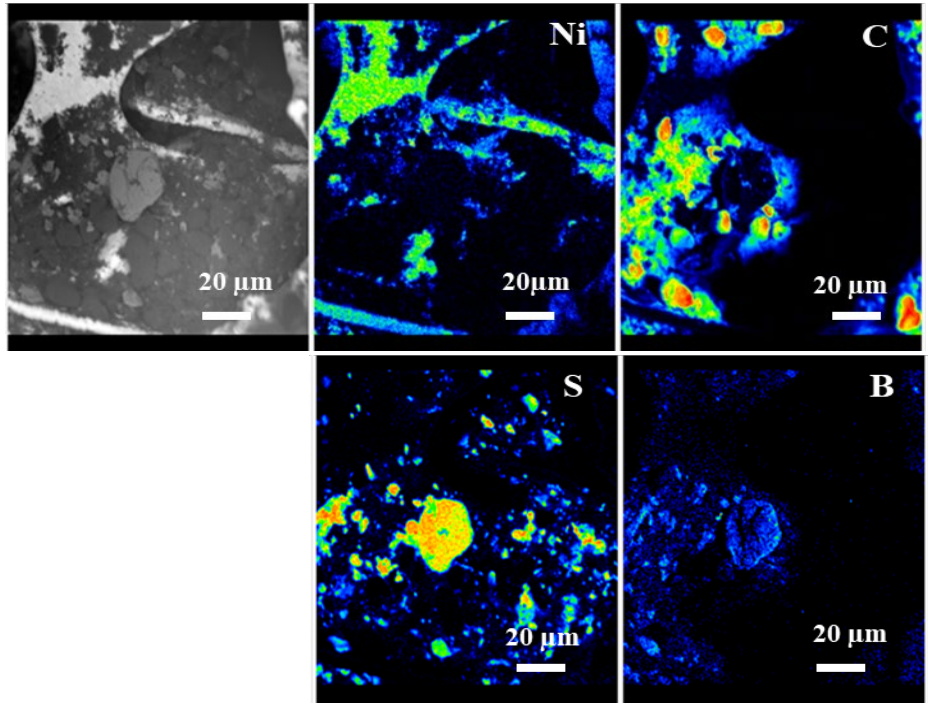

r-BS and graphene particles were well supported by the Ni foam

L. Li and T.K.*, et al., ***Sci. Tech. Adv. Mater***. 24 (2023) 2277681.

Excellent electrochemical activity of r-BS+G-NF

25°C
1 M KOH
RE: Hg/HgO
5 mV/s

LSV curves of NF-supported catalysts

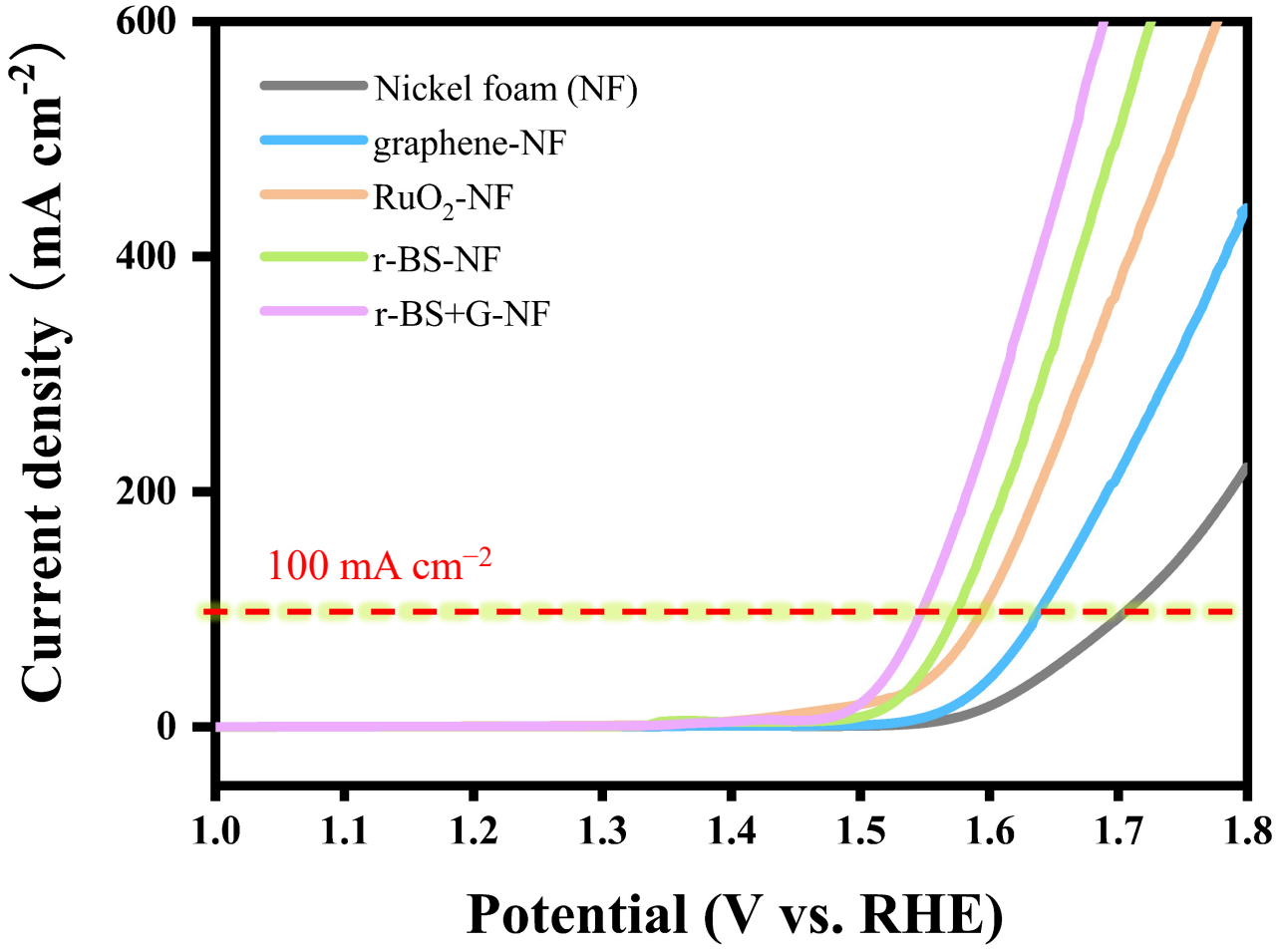

(overpotential = Abs (Experimental potential–thermodynamic(1.23V))potential.)

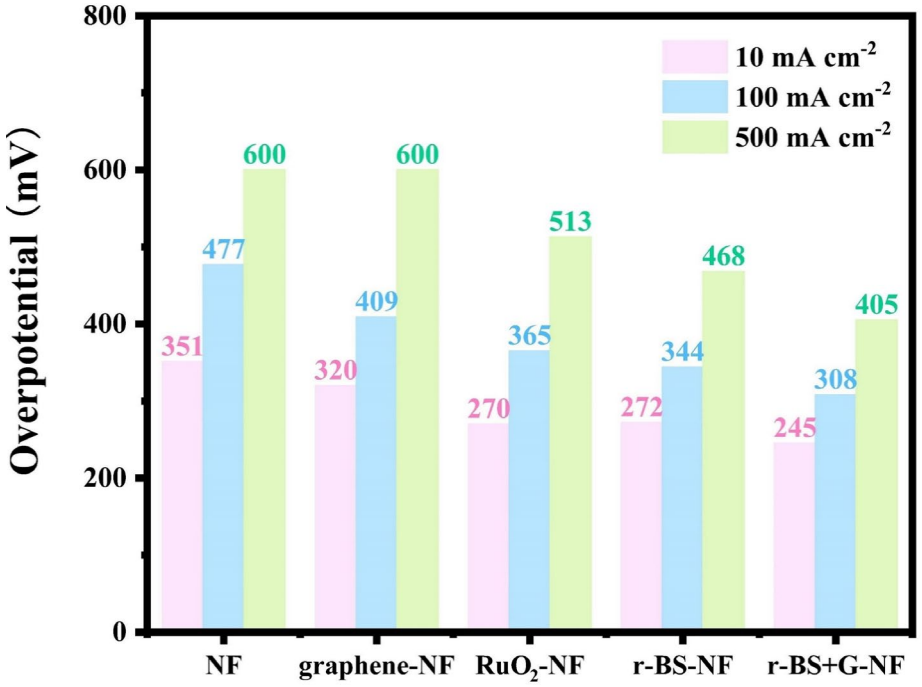

better than that of commercial RuO_2

Excellent stability of r-BS+G-NF

r−BS+G−NFの
クロノポテンショメトリー曲線　20 h at 100 mA cm^{-2}

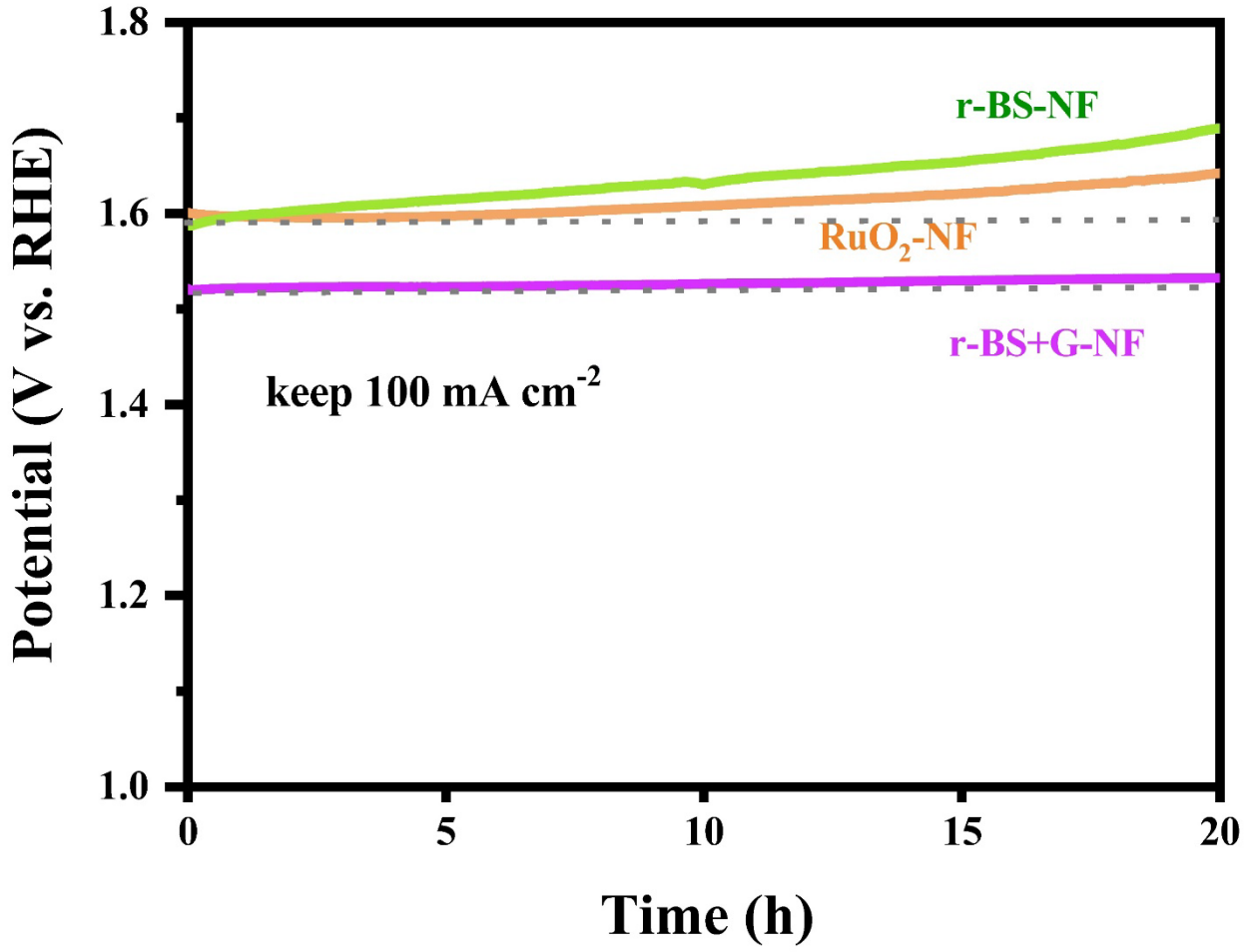

RuO_2-NF and r-BS-NF showed a trend of continuously increasing voltage (Unstable)

r-BS+G+NF: a negligible change (Stable)

These results further suggest that as a support material for effectively combining r-BS and NF, the **flexible graphene sheets played a critical role in stabilizing the electrocatalyst.**

L. Li and T.K.*, et al., ***Sci. Tech. Adv. Mater***. 24 (2023) 2277681.

Excellent stability of r-BS+G-NF

r−BS+G−NFの
クロノポテンショメトリー曲線
100 h at 100 mA cm^{-2}

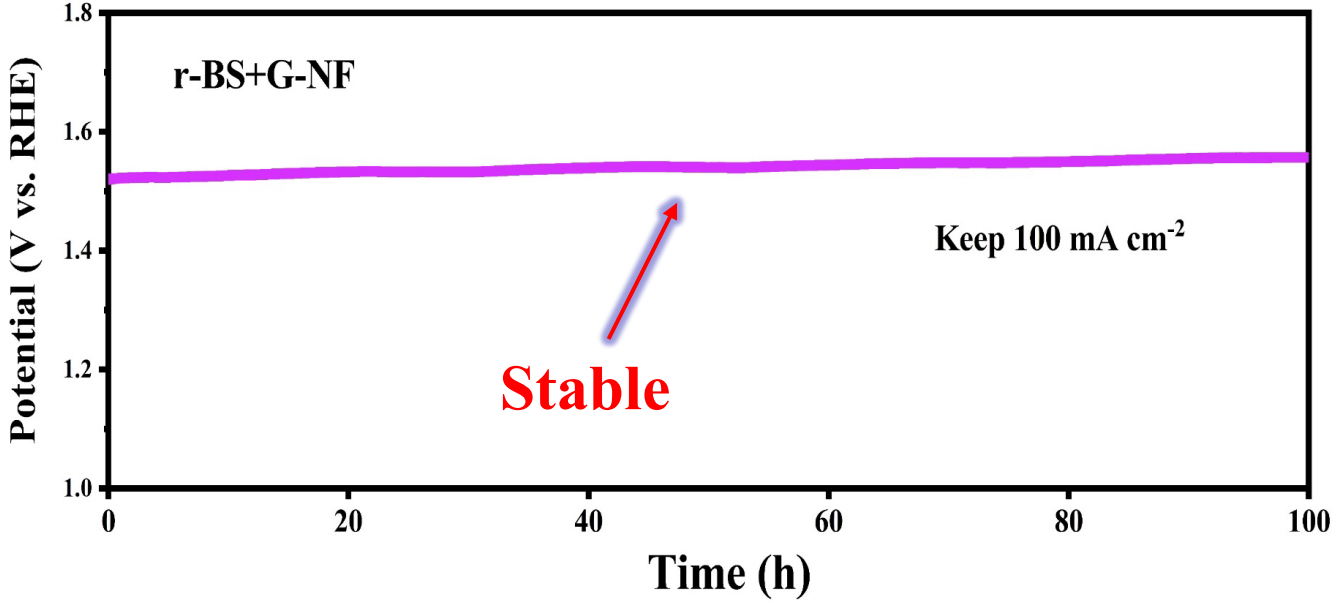

1.20 から 1.55 V の間の
2000 CV サイクル後の
r-BS+G-NF after RHEの関係

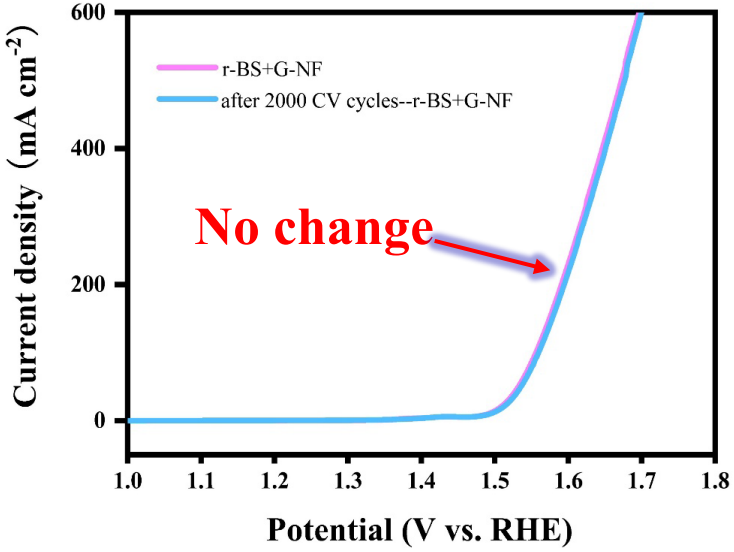

ニッケルフォーム（NF)で3次元化した
r-BS+G-NF は高い触媒安定性を示し、産業用途でさらに期待できる

L. Li and T.K.*, et al., ***Sci. Tech. Adv. Mater***. 24 (2023) 2277681.

Excellent electrochemical activity of r-BS+G-NF

Tafel plots of different catalysts

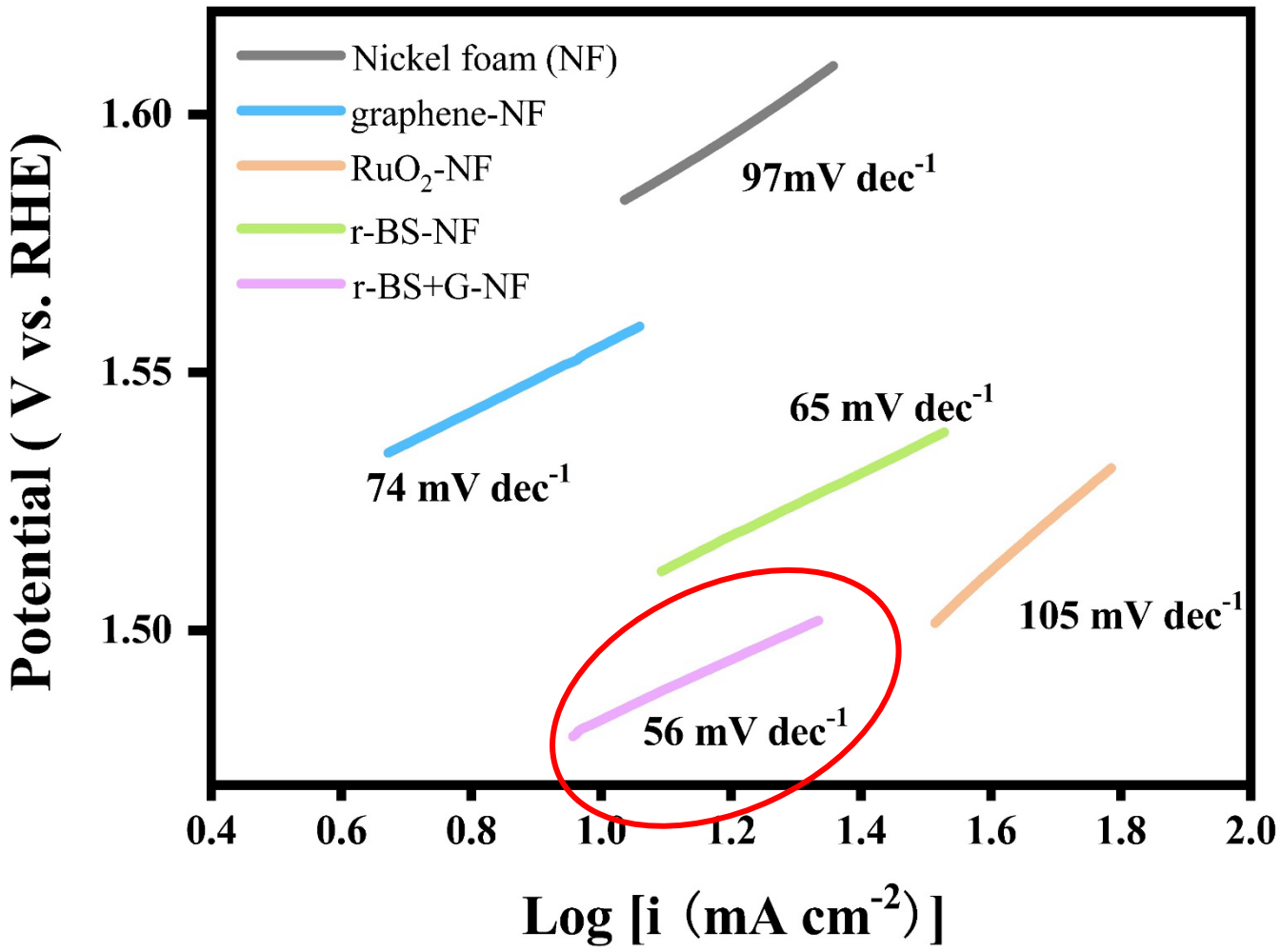

The Tafel slope is much smaller than without Ni-support catalyst– r-BS+G (210 mV dec^{-1}), and the smallest in all the measured catalysts

This indicates that the rate-determining steps differ and/or that different reactions occur.

L. Li and T.K.*, et al., ***Sci. Tech. Adv. Mater***. 24 (2023) 2277681.

r-BS+G-NFの相安定性（ラマン分光分析）

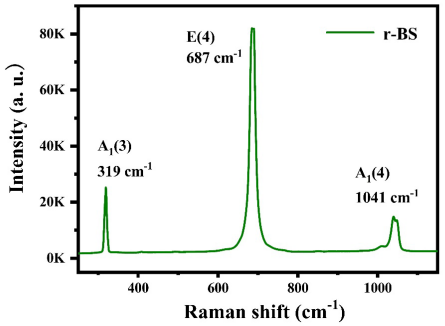

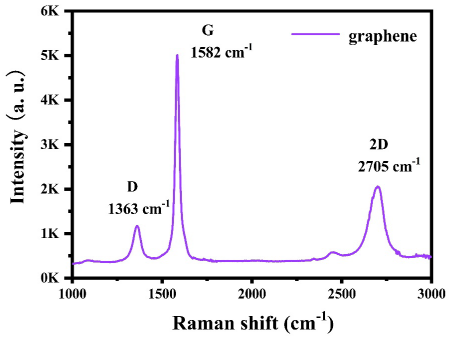

r-BSにフォーカス

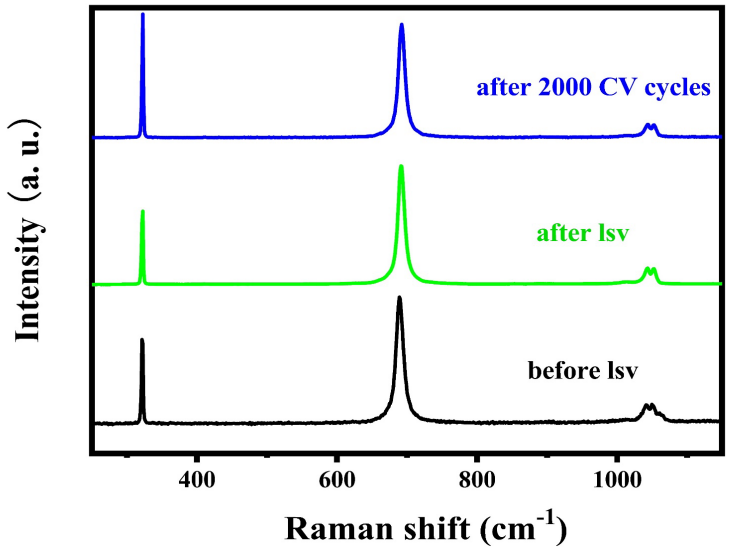

グラフェンにフォーカス

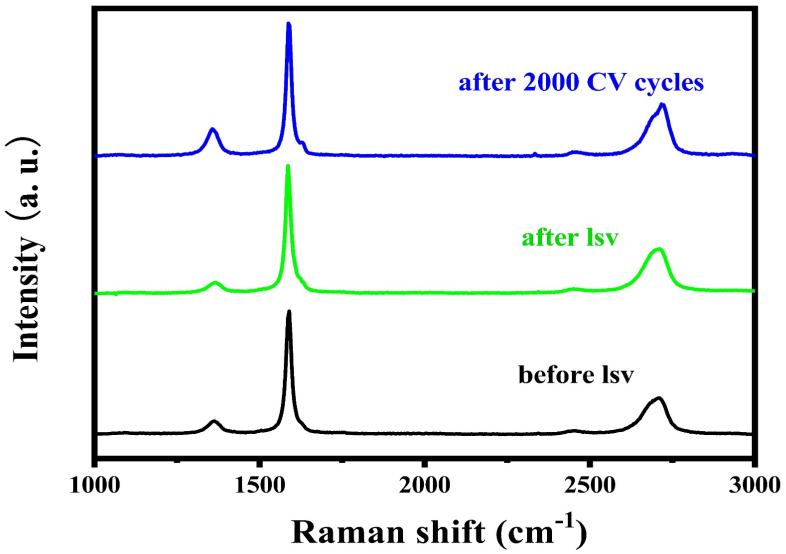

特別なスペクトル変化は見られない

The Kinetics of electrode reactions

Electrochemical impedance spectra (**EIS**) of different electrode materials under an applied potential of 1.6 V (*vs*. RHE)

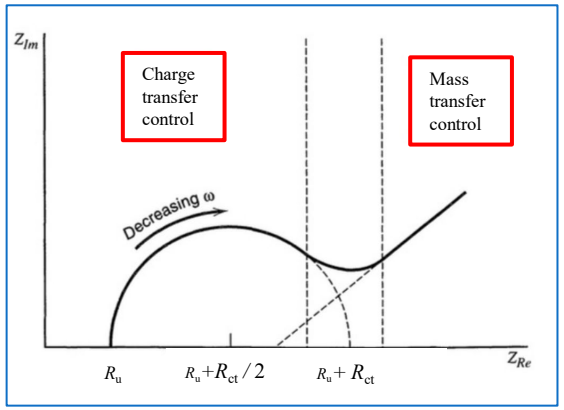

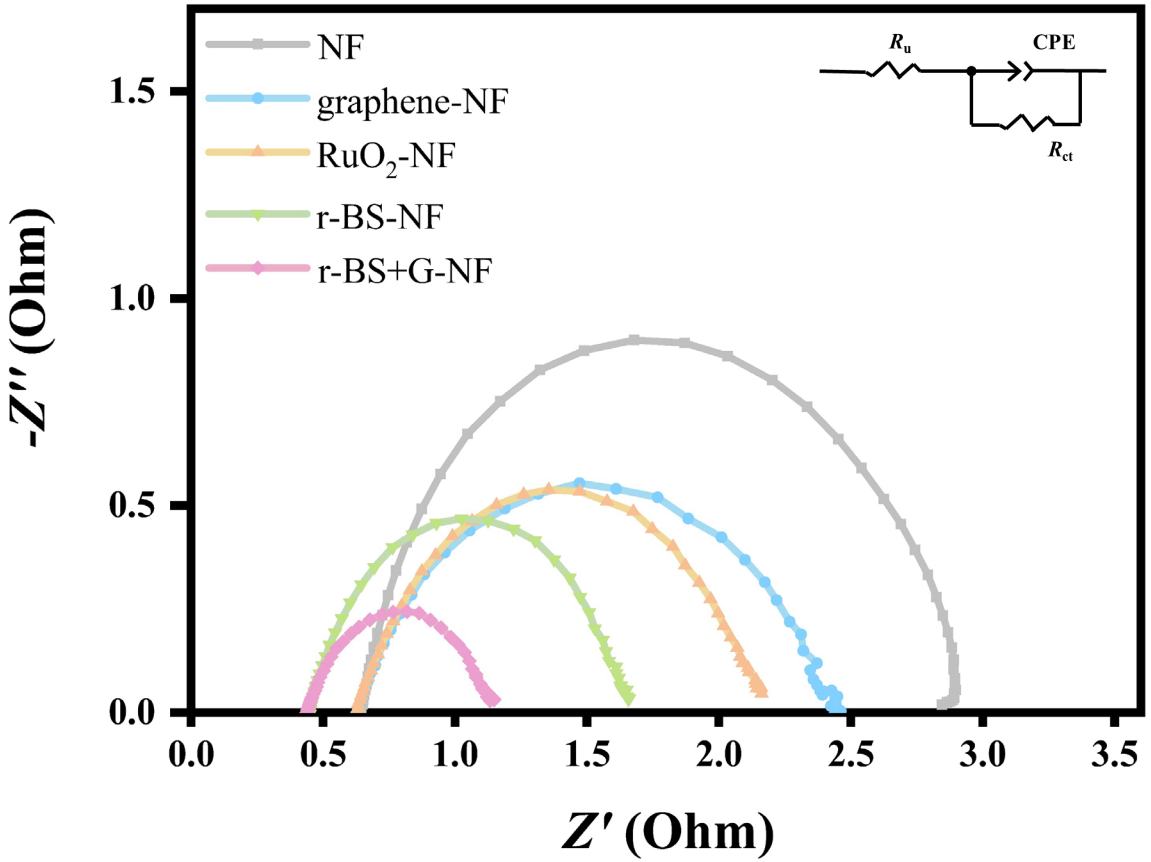

Samples	Solution series resistance (R_u /Ω)	Charge transfer resistance (R_{ct} /Ω)
r-BS+G-NF	0.43	0.72
r-BS-NF	0.45	1.22
RuO_2-NF	0.63	1.56
Graphene-NF	0.62	1.83
Bare NF	0.64	2.27

r-BS+G-NF exhibited the smallest R_{ct}, which implies increased electrochemical activity and/or an increased number of active sites.

Comparison of OER activity of NF-supported electrocatalysts

in alkaline electrolyte

Lower overpotential, smaller Tafel slope

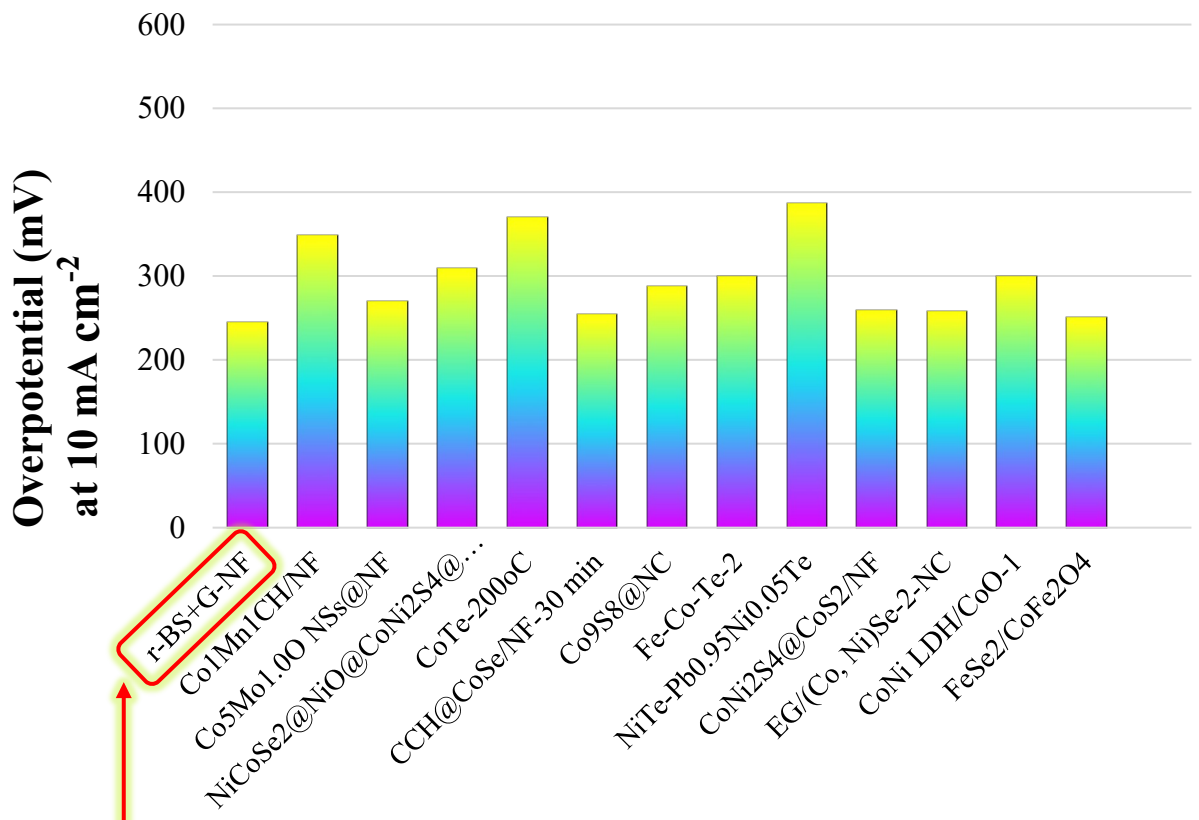

Top level
And Highly Stable

better than reported NF-supported OER electrocatalysts

Electrocatalysts	η_{10} (mV vs. RHE)	Tafel slops (mV dec^{-1})	Reference
r-BS+G-NF	245 345@η_{100}	56	This work
Co_1Mn_1CH/NF	349@η_{100}	—	2017
$Co_5Mo_{1.0}O$ NSs@NF	270	55	2018
$NiCoSe_2$@NiO@$CoNi_2S_4$ @CoS_2/NF	310 @η_{30}	159.1	2018
CoTe-200°C	370	—	2018
CCH@CoSe/NF-30 min	255	66.4	2019
Co_9S_8@NC	288	65	2019
Fe-Co-Te-2	300	45	2019
NiTe-$Pb_{0.95}Ni_{0.05}Te$	387	96	2019
$CoNi_2S_4$@CoS_2/NF	259	45	2019
EG/(Co, Ni)Se-2-NC	258	73.3	2019
CoNi LDH/CoO-1	300	123	2019
$FeSe_2$/$CoFe_2O_4$	251	88.76	2020

$\eta_{10/100}$: overpotential at 10 or 100 mA cm^{-2}

Summary

A freestanding high-efficiency electrocatalyst (**r-BS+G-NF**) was synthesized using a simple method. The electrocatalyst **exhibited lower overpotentials and high durability (100 h),** where **flexible graphene sheets were suggested to play an important role as a support for effectively combining r-BS.** Furthermore, it provides greater possibilities for future practical applications and also provides strategies for the modification of other materials.

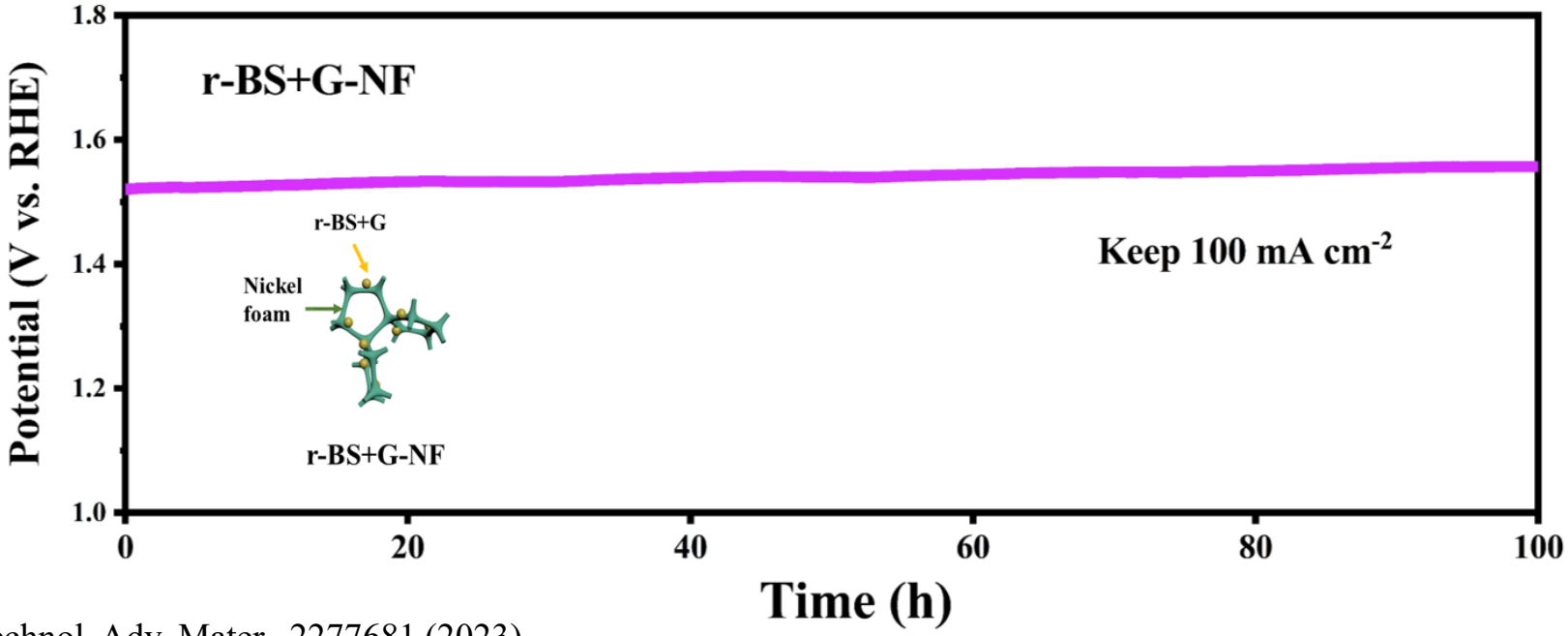

L. Li, T. Kondo, et al. Sci. Technol. Adv. Mater., 2277681 (2023).

Outline

1. 自己紹介

2. カーボンニュートラルの必要性と材料開発の重要性

3. 水素製造に貢献する材料開発
典型元素を利用した高活性アルカリ水電解触媒

(1) 硫化ホウ素(r-BS)の合成と評価

(2) r-BSとグラフェンの混合物が示す
高いOER触媒特性

(3) r-BSの活性点（MoS_2のHER活性点との比較）

(4) r-BS＋グラフェンOER触媒の高耐久性化

4. 水素利用に貢献する材料開発

5. 水素吸蔵に貢献する材料開発

水素利用

Stationary fuel cell

Fuel cell car

高価で希少な白金を代替する
触媒材料の開発が必要不可欠
窒素を含む炭素材料が
候補として世界中で開発競争

貴金属の白金が触媒材料として使用されている

酸素還元反応(ORR) 触媒機能に重要な部位について論争
ピリジン型窒素 or グラファイト型窒素

ピリジン型窒素

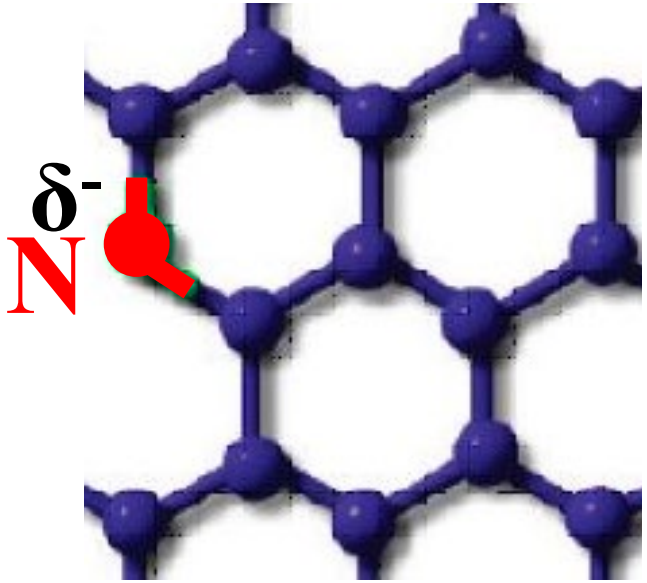

N is negatively charged

(1s core level: 398.5 eV)

Lone pair and larger electronegativity

グラファイト型窒素

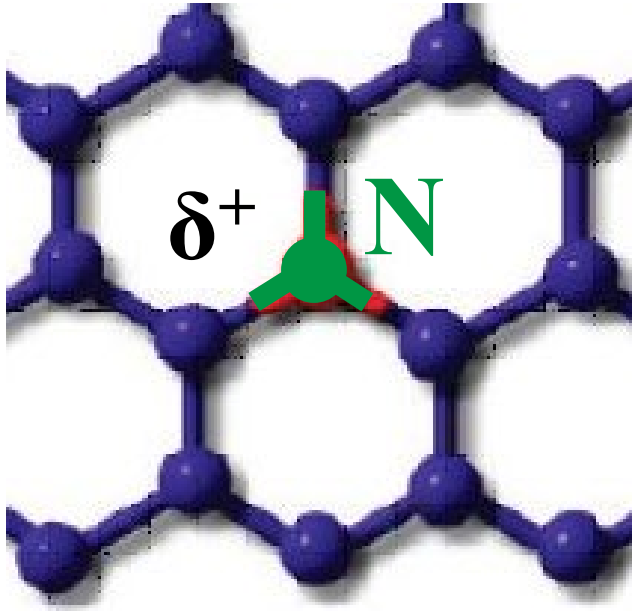

N is positively charged

(1s core level: 401.3 eV)

A valence electron flows into stable π-system

Our work: ピリジン型窒素 が重要な部位であることを特定

ELECTROCHEMISTRY

Active sites of nitrogen-doped carbon materials for oxygen reduction reaction clarified using model catalysts

Donghui Guo,[1] Riku Shibuya,[2] Chisato Akiba,[2] Shunsuke Saji,[2] Takahiro Kondo,[1*] Junji Nakamura[1*]

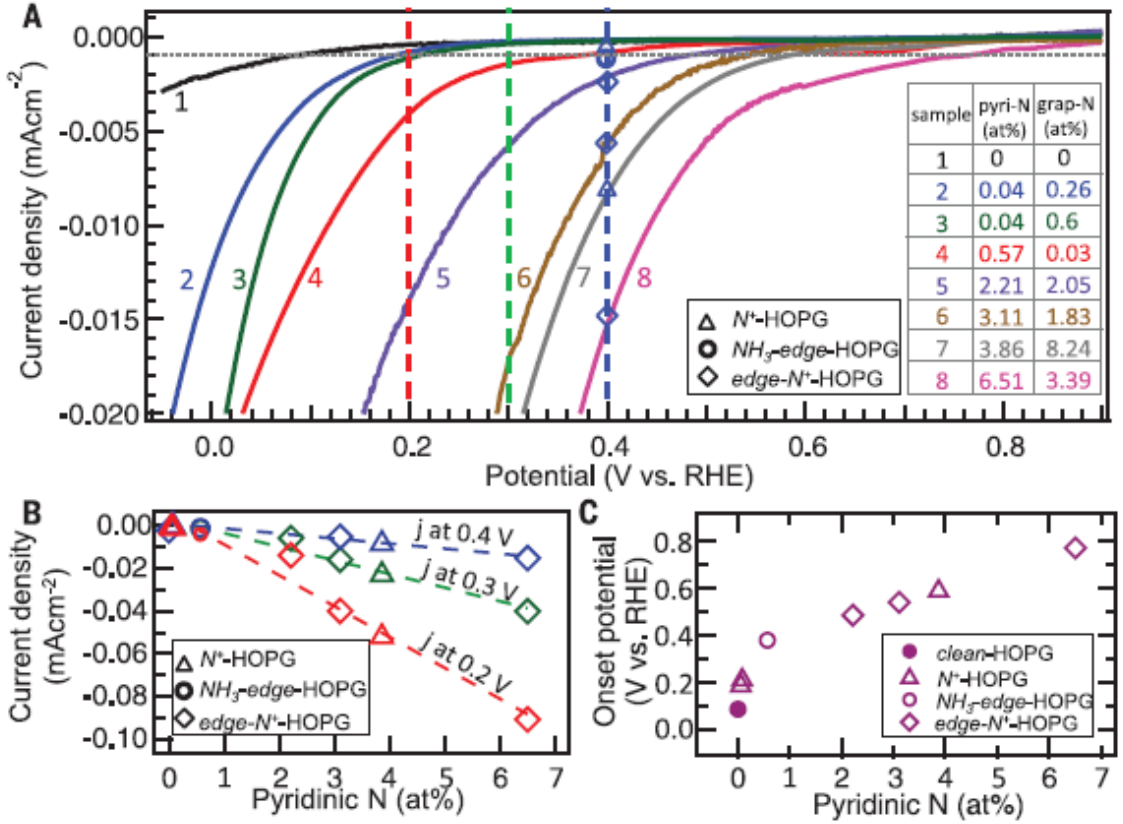

sample	pyri-N (at%)	grap-N (at%)
1	0	0
2	0.04	0.26
3	0.04	0.6
4	0.57	0.03
5	2.21	2.05
6	3.11	1.83
7	3.86	8.24
8	6.51	3.39

論争に終止符を打った

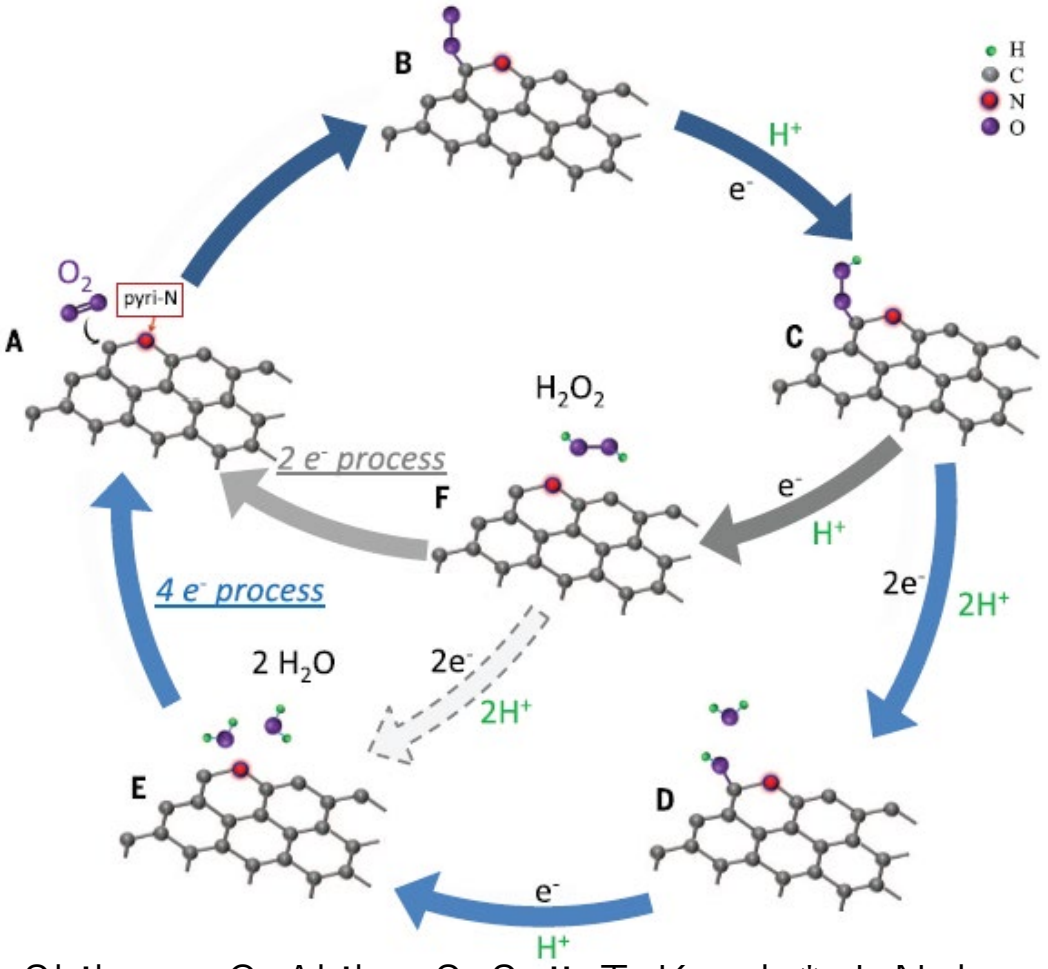

D. Guo, R. Shibuya, C. Akiba, S. Saji, T. Kondo*, J. Nakamura*
*:corresponding authors
Science 351 (2016) 361-365.

Clarivate English Products

Web of Science™ Search Sign In Register

Search › Results for Catalyst (All Fiel… › Results for Catalyst (All Fiel… › Refine results for Catalyst (… › Refine results for Catalyst (All Fields) and 2025 or 2024 or 2023 or 2019 or 20…

401,938 results from Web of Science Core Collection for:

Catalyst (All Fields) Copy query link

+ Add Keywords Quick add keywords: + oxygen reduction reaction + oxygen evolution reaction + hydrogen evolution reaction + electrocatalysis + catalyst

Refined By: Publication Years: 2025 or 2024 or 2023 or 2019 or 2020 or 2021 or 2022 or 2018 or 2017 or 2016 ✕ Document Types: Article ✕ Clear all

401,938 Documents You may also like... Analyze Results Citation Report Create Alert

Refine results Export Refine

Search within results...

Quick Filters

- Early Access 7,221
- Open Access 113,837
- Associated Data 15,858
- Enriched Cited References 117,418
- Open publisher-invited reviews 806

Publication Years

Show Final Publication Year

- 2025 3,537
- 2024 54,074

0/401,938 Add To Marked List Export Citations: highest first 1 of 2,000

1 **Active sites of nitrogen-doped carbon materials for oxygen reduction reaction clarified using model catalysts**

Guo, DH; Shibuya, R; (...); Nakamura, J

Jan 22 2016 | SCIENCE 351 (6271) , pp.361-365

Nitrogen (N)-doped carbon materials exhibit high electrocatalytic activity for the oxygen reduction reaction (ORR), which is essential for several renewable energy systems. However, the ORR active site (or sites) is unclear, which retards further developments of high-performance catalysts. Here, we characterized the ORR active site by using newl ... Show more

Tulips Linker Full Text at Publisher •••

3,517 Citations

21 References

Related records

2 **A review on g-C_3N_4-based photocatalysts**

Wen, JQ; Xie, J; (...); Li, X

2nd International Symposium on Energy and Environmental Photocatalytic Materials (EEPM2)

2,462 Citations

932 References

引用が多い順に表示

Catalystをキーワードで検索する：2016年以降のArticle（原著論文）で40万1938の論文中で我々の論文が最も引用数が多い（1位）！

Outline

1. 自己紹介

2. カーボンニュートラルの必要性と材料開発の重要性

3. 水素製造に貢献する材料開発
典型元素を利用した高活性アルカリ水電解触媒

(1) 硫化ホウ素(r-BS)の合成と評価

(2) r-BSとグラフェンの混合物が示す
高いOER触媒特性

(3) r-BSの活性点（MoS_2のHER活性点との比較）

(4) r-BS＋グラフェンOER触媒の高耐久性化

4. 水素利用に貢献する材料開発

5. 水素吸蔵に貢献する材料開発

水素吸蔵

HDV (Heavy Duty Vehicles) の高圧タンク

https://motor-fan.jp/mf/article/142385/

トヨタと日野が共同で開発した
燃料電池大型トラック

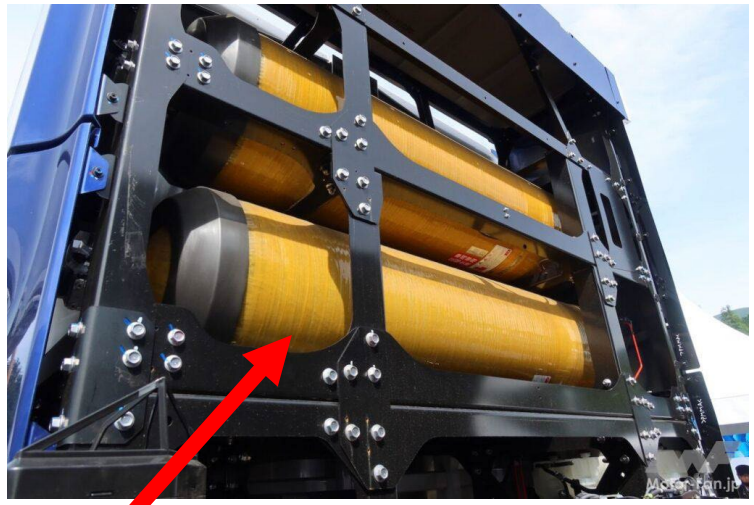

https://motor-fan.jp/mf/article/142385/

高圧水素タンク6本で
50kgの水素を搭載

ここにもっと水素が貯めるために
水素吸蔵材料を入れる案がある
良い水素吸蔵材料の開発が望まれている

新物質

我々はホウ素と水素で構成される新しい二次元状の物質 ボロファン（ホウ化水素）シートを世界で初めて合成

ホウ素が負に帯電し、水素が正に帯電しているため
“ホウ化水素（Hydrogen boride：HB）”と命名

At RT and ambient pressure
under N_2 atmosphere

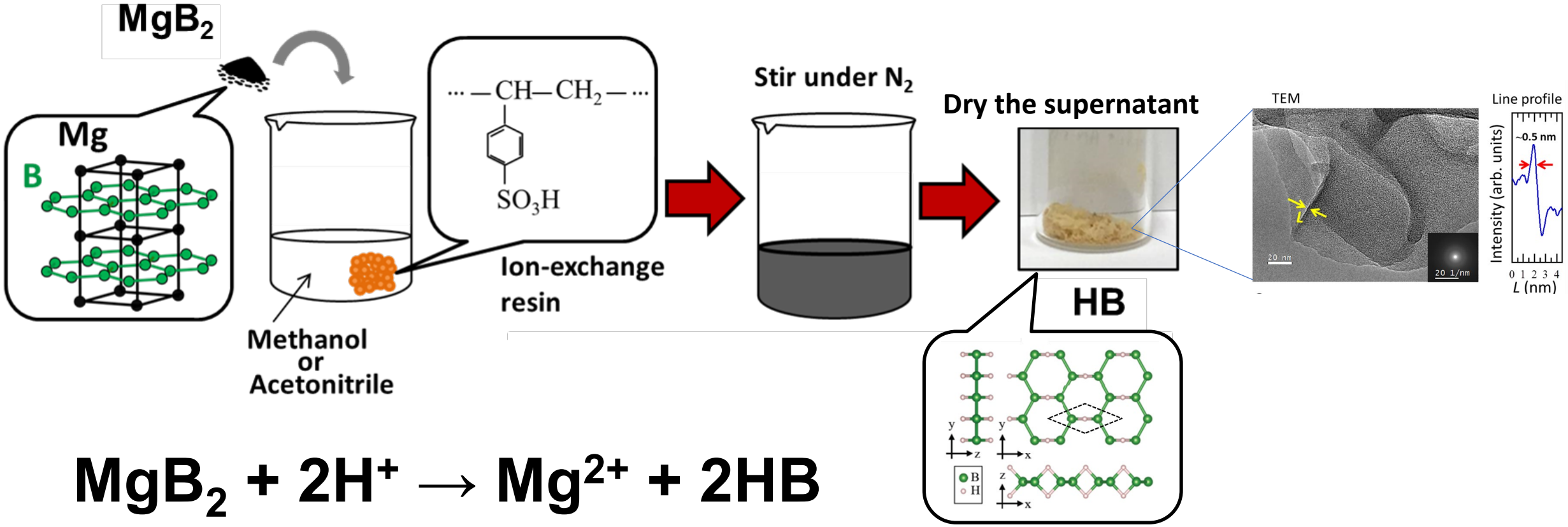

$$MgB_2 + 2H^+ \rightarrow Mg^{2+} + 2HB$$

Patent: US10781108 (T.K.*, et al.)
Patent: JP7057569 (T.K.*, et al.)

H. Nishino, T.K.*, et al., ***J. Am. Chem. Soc.*** 139 (2017) 13761-13769.

HもBも大陸地殻に豊富に存在する元素

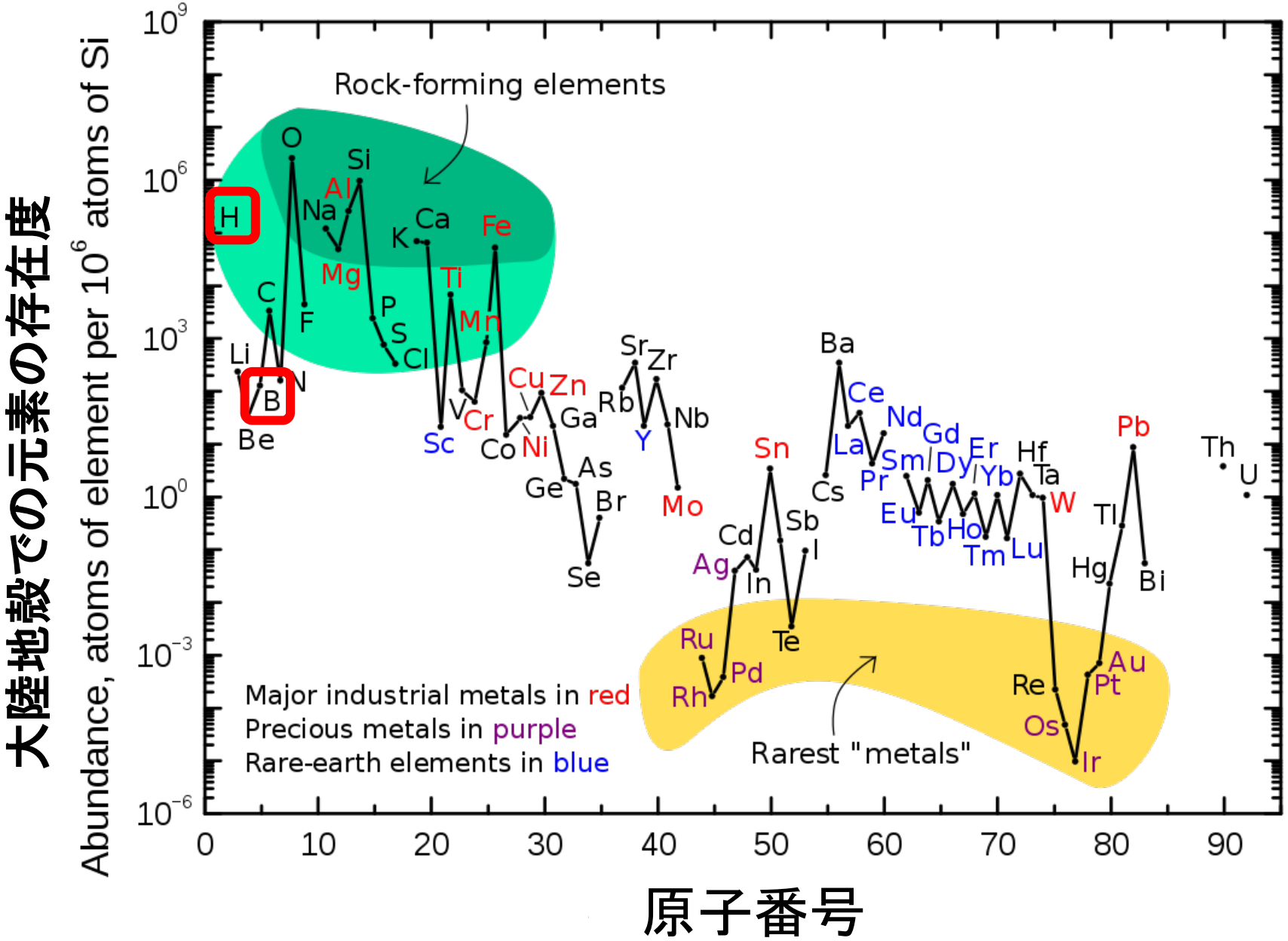

https://ja.wikipedia.org/wiki/地殻中の元素の存在度

ホウ化水素シートの外観と特徴の概略

Derived local structure

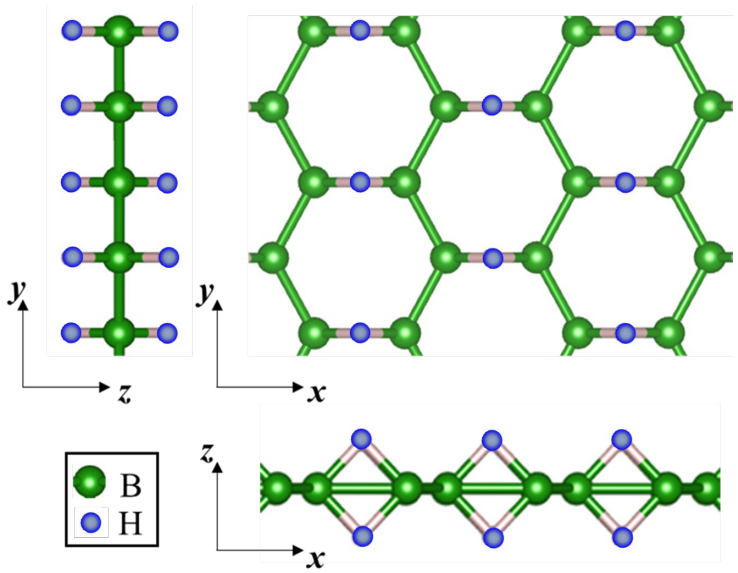

B : H = 1 : 1

- 水に安定
- 軽くてたくさんの水素を持つ物質

表面積（理論値）
4068 m^2/g
水素重量密度（実測値）
8.5 wt%

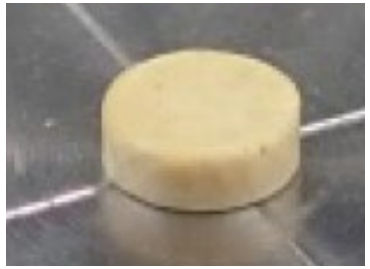

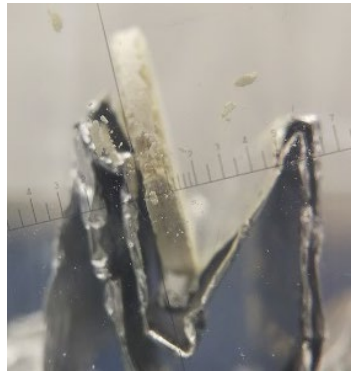

物質の体積密度: 1.29 g/cm^3
ペレットの質量：0.1012 g
直径: 10 mm
厚さ: 1.0 mm
$0.5 \times 0.5 \times \pi \times 0.10 = 0.0785\ cm^3$
$0.1012/0.0785 = 1.29\ g/cm^3$
体積水素密度
$1290 \times 1/(11.8*1) = 109.3\ kg/m^3$

S. Ito, T. K.* et al., *Phys. Chem. Chem. Phys*. 25 (2023) 15531.

2017-2024 Our reports for HB sheets

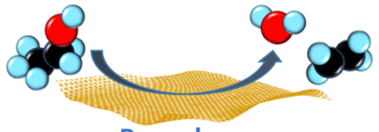

Borophane

$C_2H_5OH \rightarrow C_2H_4 + H_2O$

Excellent Solid Acid Catalyst

A. Fujino, T. K.* et al., *ACS Omega* 4 (2019) 14100. *Phys. Chem. Chem. Phys.* 23 (2021) 7724

Recently, 100% selectivity for HCOOH thermal conversion to CO by HB was discovered

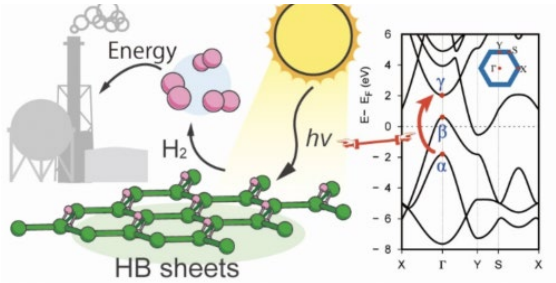

UV induced H_2 release

R. Kawamura, T. K.*, M. Miyauchi* et al., *Nature Commun.* 10 (2019) 4880.

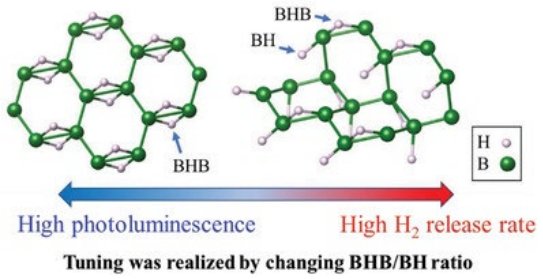

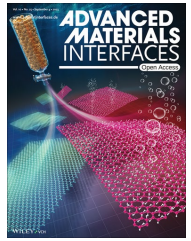

Front cover

Controlling H_2 release rate by bond tunning

M.Hikichi, M. Miyauchi*, T. K.*, et al., *Adv. Mate. Int.* 10 (2023) 2300414 .

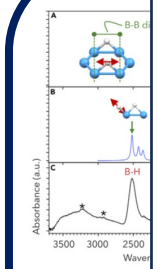

High s

S. To

Chem. 6 (2020) 406.

Featured article

NIMS 冨中博士

CO_2 adsorption・C-C co

T. Goto, I. Hamada*, T. K.*, et al., *Commun. Chem.* 5 (2022) 118.

Selected as collection

Chemically stable in H_2

KIM. Rojas, T. K.*, I. Hamada* et

Commun. Mate. 2 (2021) 81.

大阪大 濱田准教授

Specific reductant

S. Ito, M. Miyauchi*, T. K.* et al., *Chem. Lett.* 49 (2020) 789.

Editor's choice

Inside cover

Plasmon induced H_2 release

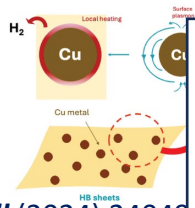

Small (2024) 24049

Visible light inc
release by dye a

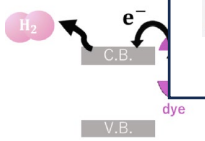

HB nanosheet

ACS Appl. Mater. Interfaces, 16 (2024) 35225.

東工大 宮内教授

Low voltage H_2 release

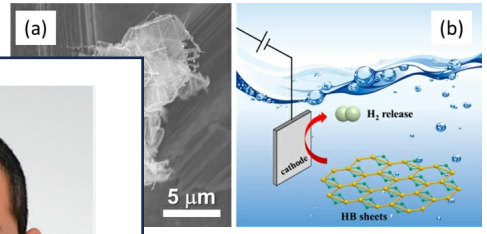

ura, T. K.*, M. Miyauchi*

mall 20 (2024) 231023.

g 1,10-phenanthroline
ble-light H_2 release site

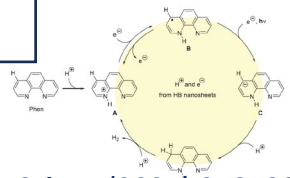

Adv. Sci. 11 (2024) 2405981.

東大 松田教授

(1) J. Am. Chem. Soc. 139 (2017) 13761.
(2) J. Phys. Chem. C 121 (2017) 10587.
(3) Sci. Technol. Adv. Mater. 18 (2017) 780.
(4) Phys. Rev. B 97 (2018) 075430.
(5) Phys. Rev. Materials 3 (2019) 024004.
(6) ACS Omega 4 (2019) 14100.
(7) Nature Communications 10 (2019) 4880.
(8) Chem 6 (2020) 406. (Featured article)
(9) Phys. Rev. B 101 (2020) 195412.
(10) Chem. Lett. 49 (2020) 789. (Editor's choice)
(11) Chem. Lett. 49 (2020) 1194.
(12) ChemPhysCh
(13) Phys. Chem.
(14) 2D Boron (202
(15) Communicati
(16) Phys. Rev. Ma
(17) Molecules 26
(18) J. Phys. Chem
(19) Communicati
(Collection)
(20) Molecules 27
(21) Molecules 28
(22) Phys. Chem.
(23) Chem. Lett. 52
(24) Adv. Mate. Int. 10 (2023) 2300414 (Front cover).
(25) Small 20 (2024) 2310239.
(26) ACS Appl. Mater. Interfaces, 16 (2024) 35225.
(27) Phys. Rev. Materials 8 (2024) 074005.
(28) J. Phys. Chem. Lett. 15 (2024) 9349.
(29) Adv. Science 11 (2024) 2405981.
(30) Small (2024) 2404986 (in press)
(31) J. Phys. Chem. Lett. 15 (2024) 10965.

ホウ化水素（HB）シートの特徴

- 高い質量水素密度（8.5 wt% 実測 [1]）
- 高い体積水素密度（109.3 g/L以上 実測 [2]）
- 高い理論表面積：4068 m^2/g（理論 [1]）
- 水に安定（禁水ではない）[3]

米国エネルギー省（DOE）の最終ターゲットを超える水素保持量(＊自身の水素を繰り返し出し入れできるかは検証中)

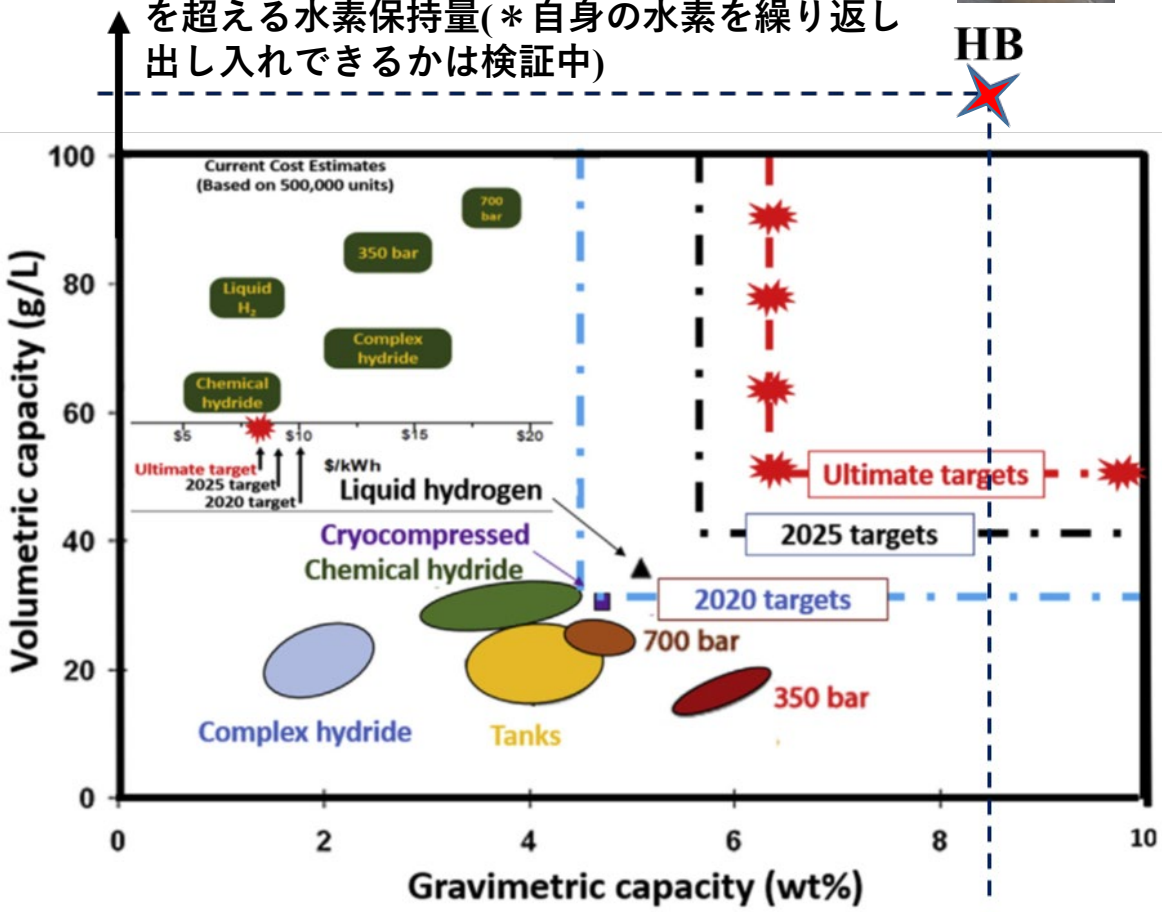

気体の水素と違い固体であるため体積が非常に小さく、安全に簡単に大量の水素運搬が可能！

HB自身の水素ではなく高圧で水素分子を吸蔵する場合の理論予測 [4]：LiデコレートHBシートだと 3.27 wt% (0.3 MPa, 100°C), 11.57 wt% (3 MPa, 25°C) 8.3 wt%の出し入れ可能：

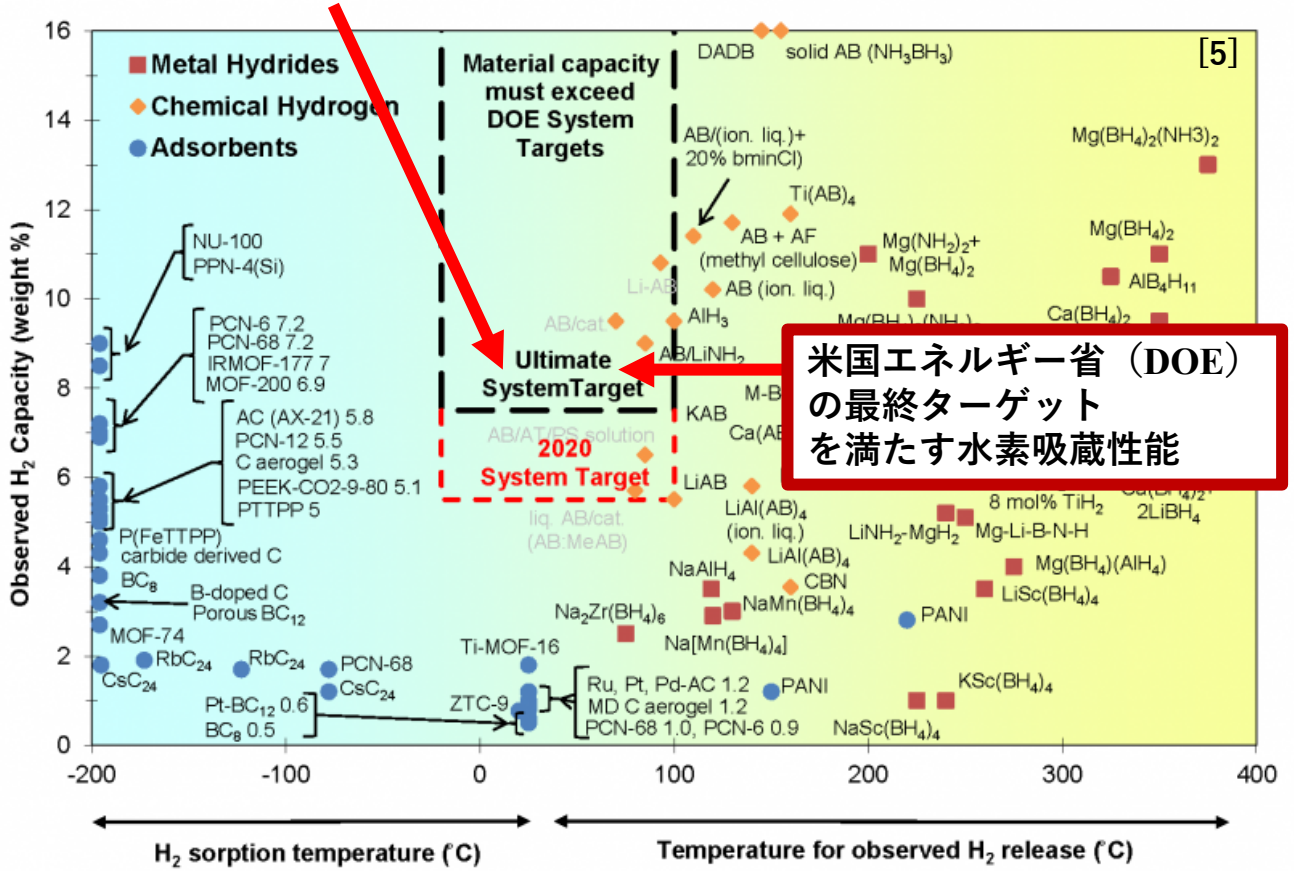

[1] H. Nishino, T.K.*, et al., *J. Am. Chem. Soc.* 139 (2017) 13761.
Patent: US10781108 (T.K.*, et al.) , JP7057569 (T.K.*, et al.)
[2] S. Ito T.K.*, et al., *Phys. Chem. Chem. Phys*. 25 (2023) 15531.
[3] KIM. Rojas, T.K.*, I. Hamada* et al., *Commun. Mate.* 2 (2021) 81.
[4] L. Chen, et al., *Phys. Chem. Chem. Phys*. 20 (2018) 30304.
[5] HP of US DOE (https://www.energy.gov/eere/fuelcells/materials-based-hydrogen-storage)

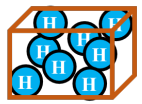

水素貯蔵材料が鍵

安価で安全に高密度の貯蔵ができる材料が必要

From other groups

Similar research of HB as reductant was reported as an application for superior fuel cell Pt/B-C catalyst synthesis from Chinese group.

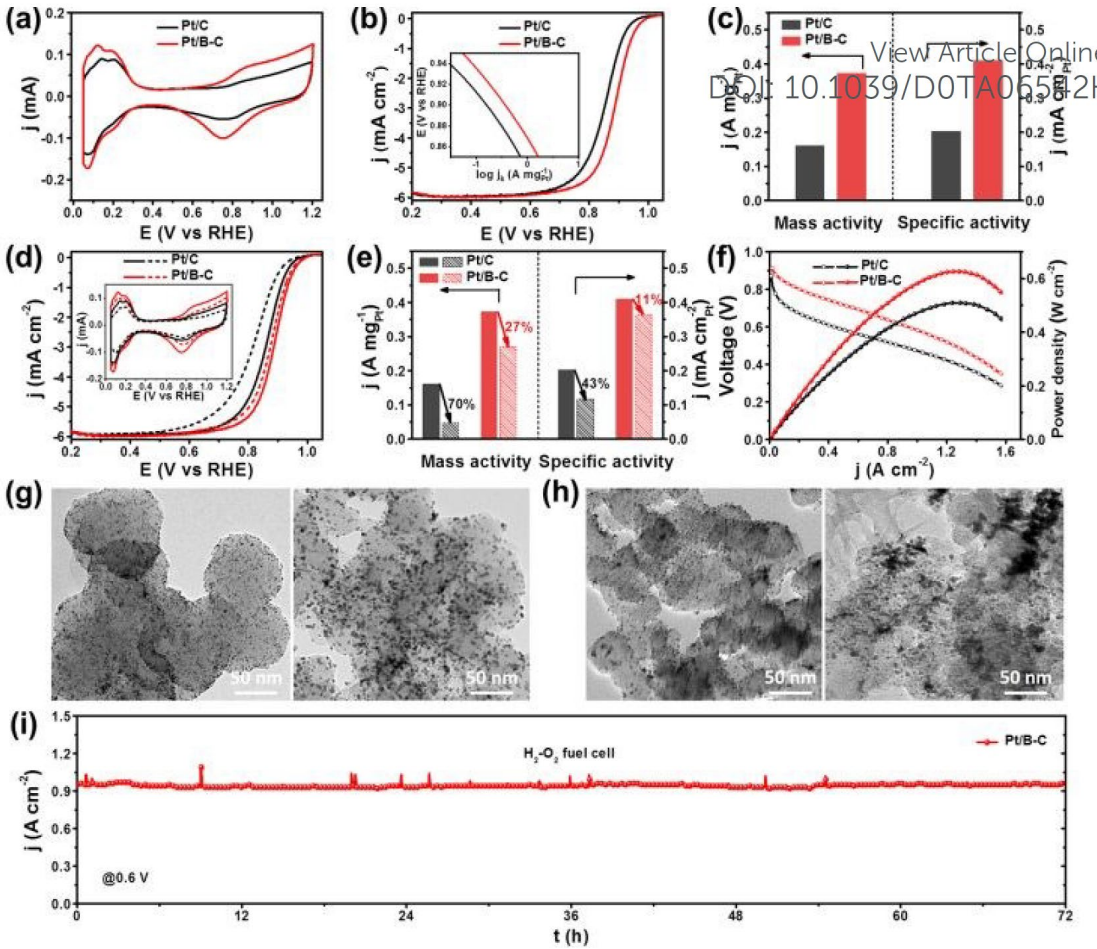

View Article Online
DOI: 10.1039/D0TA06542K

ARTICLE

2D Hydrogenated Boride as Reductant and Stabilizer for in-situ Synthesis of Ultrafine and Surfactant-Free Carbon Supported Noble Metal Electrocatalysts with Enhanced Activity and Stability

Received 00th January 20xx,
Accepted 00th January 20xx

DOI: 10.1039/x0xx00000x

Saisai Gao,[a] Yang Zhang,[a] Jinglei Bi,[a] Bin Wang,[a*] Chao Li,[b] Jiamei Liu,[b] Chuncai Kong,[a] Sen Yang[a] and Shengchun Yang[ac*]

The common issues of carbon-supported noble metal catalysts, which are the most widely used catalysts in scientific and commercial cases, are the poor dispersion and stability, large particle size of noble metal. Herein, we uncover the reducibility of 2D hydrogenated boride (HB) toward noble metal ions, such as $PtCl_4^{2-}$, $PdCl_4^{2-}$ and $AuCl_4^-$, for synthesizing ultrafine and surfactant-free noble metal nanoparticles. Furthermore, inspired by such results, the carbon supported noble metal nanoparticle electrocatalysts (M/B-C, M = Pt, Pd and Au) with ultrafine size (2-3 nm) and high dispersion are prepared through a simply mixing-stirring-filtering (MSF) method at room temperature, even the noble metal loading amount reaches as high as 52.9 wt.%. There are no organic surfactants and other reductants involved in the whole preparation process. In light of ultrafine size and clean surface, the M/B-C catalysts exhibit surpassing activity relative to the commercial counterparts. The theoretical calculations indicate that the as-formed noble metal nanoparticles (NPs) present much stronger interaction with the HB hydrolysate, i.e., 2D boron sheet, than that with carbon black, contributing to the excellent catalytic durability of M/B-C. This work provides a new strategy for synthesizing carbon-supported noble metal electrocatalysts with enhanced activity and durability.

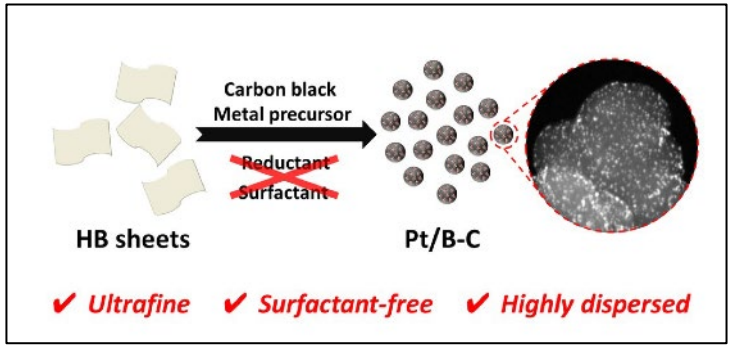

Article information

https://doi.org/10.1039/D0TA06542K

Submitted	04 Jul 2020
Accepted	19 Aug 2020
First published	19 Aug 2020
Citation	*J. Mater. Chem. A*, 2020,

ACS APPLIED MATERIALS & INTERFACES

www.acsami.org Research Article

Hydrogenated Boride-Assisted Gram-Scale Production of Platinum–Palladium Alloy Nanoparticles on Carbon Black for PEMFC Cathodes: A Study from a Practical Standpoint

Saisai Gao,[#] Haidong Zhao,[#] Pengfei Gao,[#] Jinglei Bi, Dan Liu, Daolong Zhu, Bin Wang,* and Shengchun Yang*

Cite This: *ACS Appl. Mater. Interfaces* 2022, 14, 34750–34760

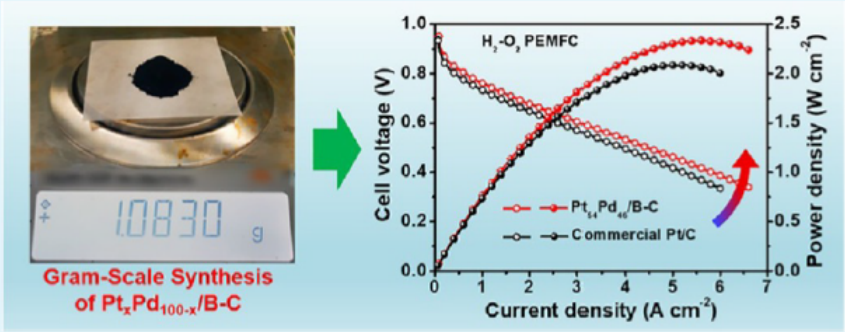

ABSTRACT: Platinum–palladium (PtPd) alloy catalysts with high durability are viable substituents to commercial Pt/C for proton exchange membrane fuel cells (PEMFCs). Herein, a facile approach for gram-scale preparation of Pt_xPd_{100-x} alloy nanoparticles on carbon black is developed. The optimized $Pt_{54}Pd_{46}$/B–C catalyst shows a mass activity (MA) of 0.549 A mg_{Pt}^{-1} and a specific activity (SA) of 0.463 mA cm^{-2} at the rotating disk electrode (RDE) level, which are 3.4 and 1.9 times those of commercial Pt/C, respectively. In H_2/O_2 and H_2/air PEMFCs, the membrane electrode assembly (MEA) with $Pt_{54}Pd_{46}$/B–C achieves peak power densities of 2.33 and 1.04 W cm^{-2}, respectively, and shows negligible performance degradation after 100 h of running in H_2/O_2 conditions. Moreover, the MA of MEA with $Pt_{54}Pd_{46}$/B–C in H_2/O_2 PEMFC reaches 0.978 A mg_{Pt+Pd}^{-1} beyond the 2020 target of the Department of Energy (DOE) of 0.44 A mg_{Pt}^{-1}. After 30k cyclic voltammetry cycles in PEMFC, the MA loss and cell voltage loss of MEA with $Pt_{54}Pd_{46}$/B–C are well within the DOE 2020 target. Density functional theory calculations reveal that the PtPd(111) surface can weaken the adsorption of *OOH and *OH compared to the Pt(111) surface, indicating that $Pt_{54}Pd_{46}$/B–C is more energetically favorable for the oxygen reduction reaction (ORR) than commercial Pt/C. This study offers a new approach for batch preparation of PtPd alloy-based catalysts for PEMFCs.

KEYWORDS: *PtPd alloy, gram-scale production, oxygen reduction reaction, membrane electrode assembly, PEMFC*

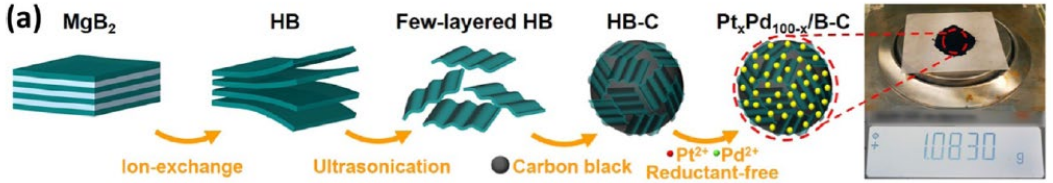

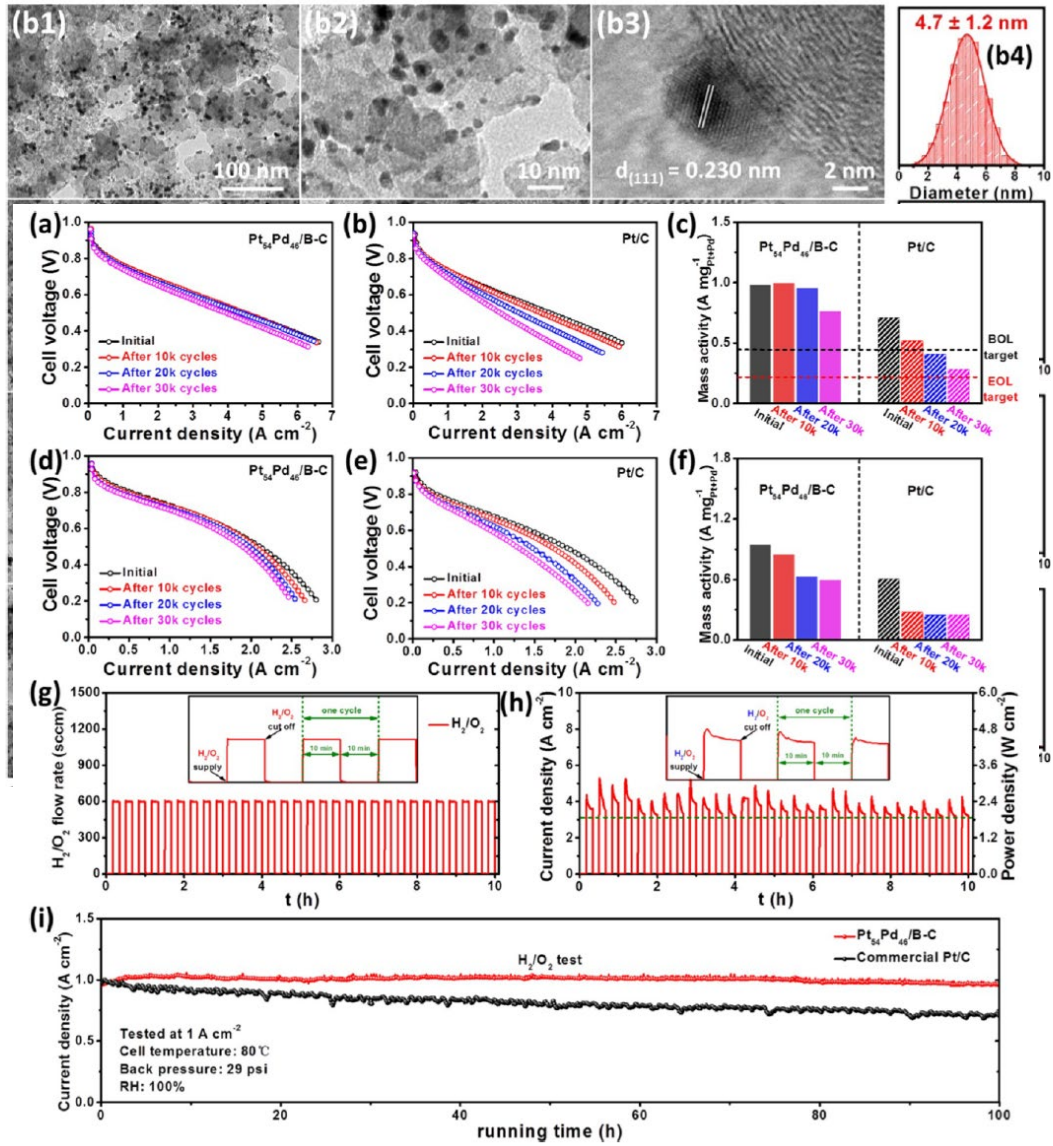

nature communications

Article

https://doi.org/10.1038/s41467-023-43294-z

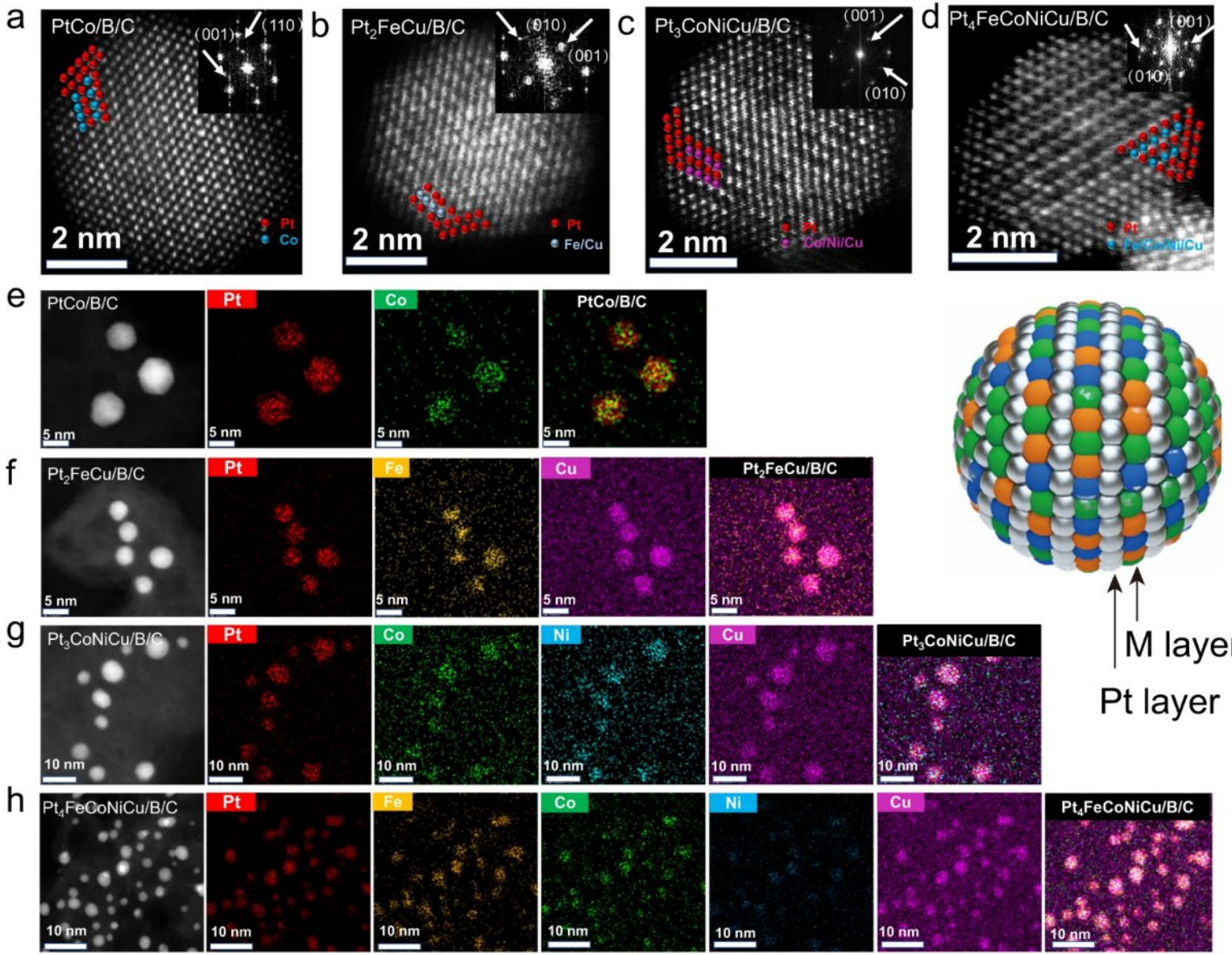

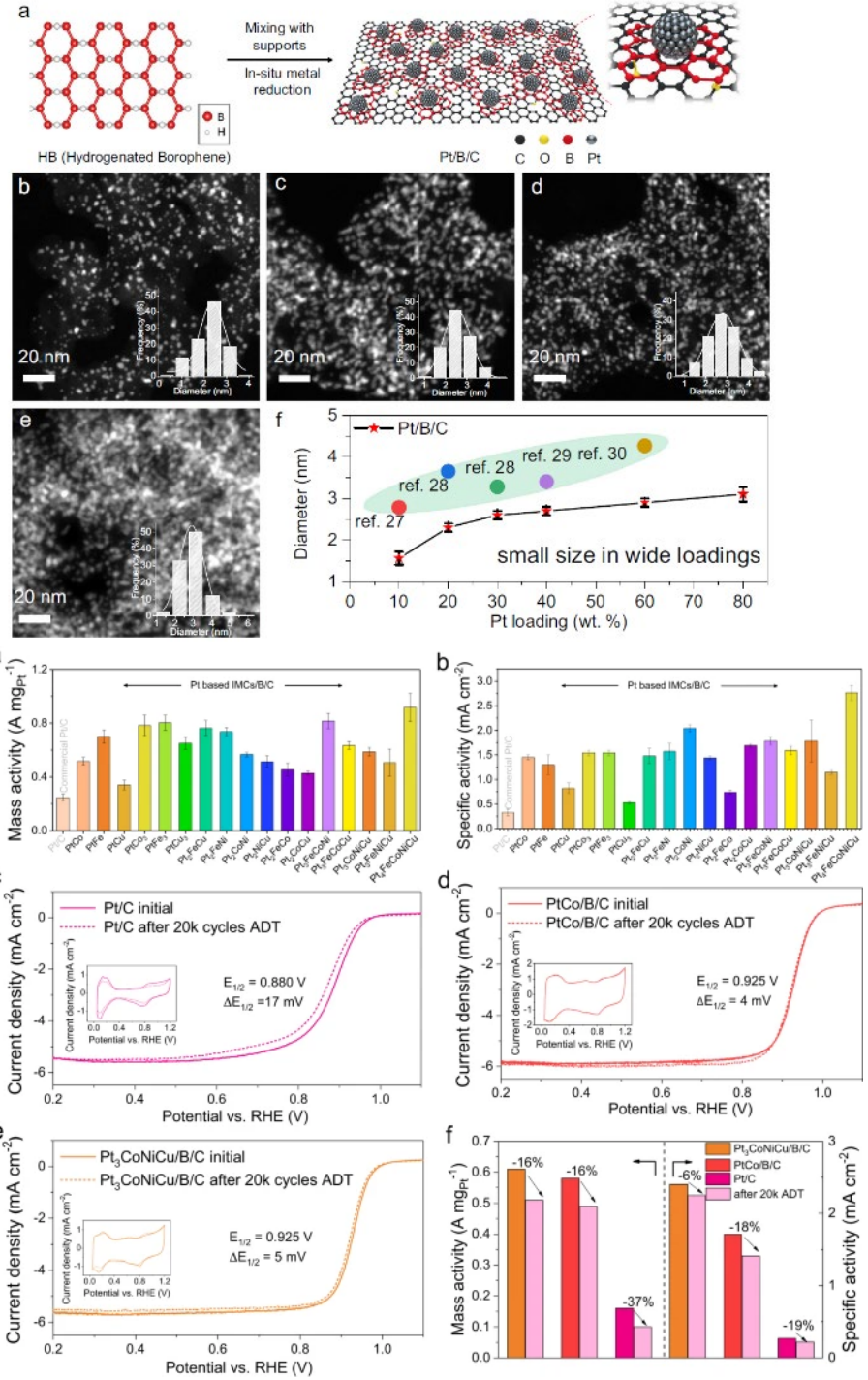

From other groups

HB nanosheets were used for Ag reduction and product composite with Co_3O_4-Ag@B show great OER property

Applied Catalysis B: Environmental 298 (2021) 120529

Contents lists available at ScienceDirect

Applied Catalysis B: Environmental

journal homepage: www.elsevier.com/locate/apcatb

Ag nanoparticles modified crumpled borophene supported Co_3O_4 catalyst showing superior oxygen evolution reaction (OER) performance

Ali Saad [a], Dongqing Liu [b], Yuchen Wu [a], Zhaoqi Song [a], Ying Li [a], Tayyaba Najam [a], Kai Zong [a], Panagiotis Tsiakaras [c,d,e,*], Xingke Cai [a,*]

[a] Institute for Advanced Study, Shenzhen University, Shenzhen, China
[b] College of Mechatronics and Control Engineering, Shenzhen University, Shenzhen, China
[c] Laboratory of Alternative Energy Conversion Systems, Department of Mechanical Engineering, School of Engineering, University of Thessaly, 1 Sekeri Str., Pedion Areos, 38834, Greece
[d] Laboratory of Materials and Devices for Clean Energy, Department of Technology of Electrochemical Processes, Ural Federal University, 19 Mira Str., Yekaterinburg, 620002, Russian Federation
[e] Laboratory of Electrochemical Devices Based on Solid Oxide Proton Electrolytes, Institute of High Temperature Electrochemistry (RAS), Yekaterinburg, 620990, Russian

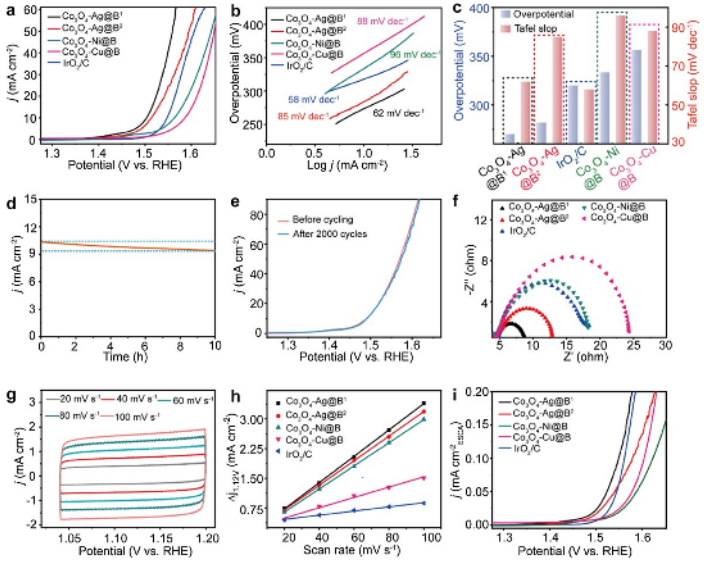

A. Saad et al. *Applied Catalysis B: Environmental 298 (2021) 120529*

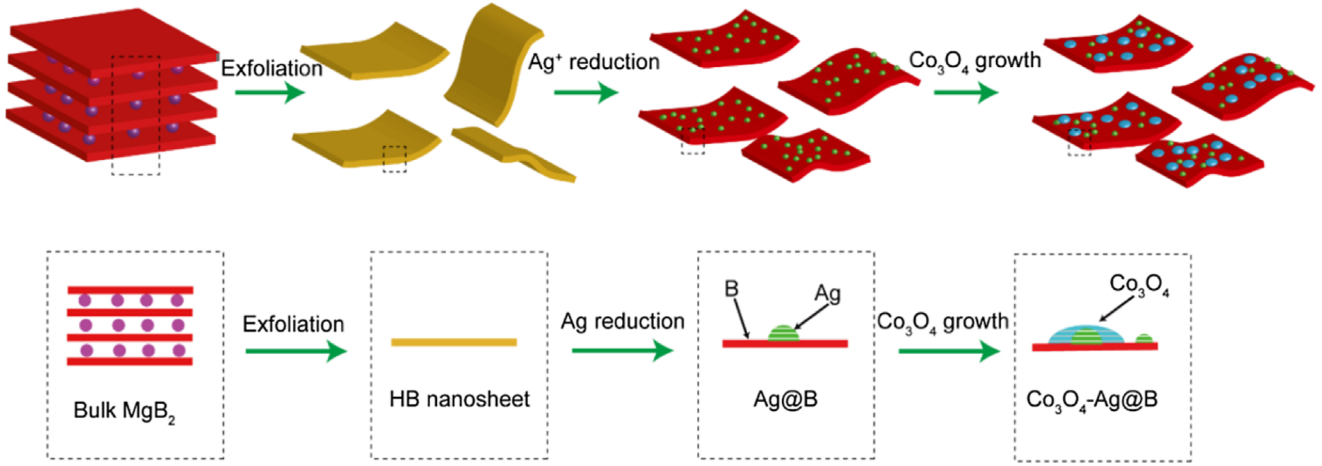

Scheme 1. Schematic illustration for the preparation of Co_3O_4-Ag@B. (Up: 3D structure, bottom: cross section structure in the dash box of the up scheme).

Summary

1. 自己紹介

2. カーボンニュートラルの必要性と材料開発の重要性

3. 水素製造に貢献する材料開発
典型元素を利用した高活性アルカリ水電解触媒

(1) 硫化ホウ素(r-BS)の合成と評価

(2) r-BSとグラフェンの混合物が示す
高いOER触媒特性

(3) r-BSの活性点（MoS_2のHER活性点との比較）

(4) r-BS＋グラフェンOER触媒の高耐久性化

4. 水素利用に貢献する材料開発

5. 水素吸蔵に貢献する材料開発